Identification and validation of target pathways influencing outcome after traumatic brain injury

Thesis

IDENTIFICATION AND VALIDATION OF TARGET PATHWAYS INFLUENCING OUTCOME AFTER TRAUMATIC BRAIN INJURY

BY

SCOTT ALLEN FERGUSON

This thesis is being submitted for a degree in Doctor in Philosophy in the discipline of Neuroscience

Primary supervisors: Drs. Fiona Crawford and Gogce Crynen
Additional supervisors: Professor Mike Rowan

Affiliated Research Center
Roskamp Institute
2040 Whitfield Ave
Sarasota, FL 34234

The Open University
Department of Life and Biomolecular Sciences
Walton Hall
Milton Keynes
MK76 AA, UK

DATE OF SUBMISSION: July 6th 2012

DATE OF AWARD: 2 OCTOBER 2012

This thesis is dedicated to all who wear the uniform of free nations.
Your sacrifice is not forgotten.

ACKNOWLEDGMENTS

First and foremost I would like to thank my Ph.D. supervisor Dr. Fiona Crawford, without whom this thesis would not have been possible. Her patience, support, knowledge, and wisdom cannot be over-stated. I am extremely fortunate to have had her as my guide on this journey and I could not have made it here without her support.

I also cannot over-state the support given by my secondary Ph.D. supervisor, Dr. Gogce Crynen. Her support was equally indispensable, and always available. Both of my supervisors have gone above and beyond the call of duty in order to help make this possible, and I am forever in their debt.

I would also like to thank all of my co-workers who have all at some point contributed to this research. In particular, I would like to thank Alex Bishop, who went out of his way to assist me, far beyond what was required of him, on more occasions than I can count. I am also indebted to Benoit Mouzon, whose steady hands worked tirelessly to perform the surgeries needed to carry out this work. I would also like to thank Jon Reed, whose mastery of analytical chemistry and scientific rigor raised the bar on the level of work done in our lab and made our proteomics platform what it is today. Likewise, I would like to thank Dr. Olubunmi Ojo and Myles Mullan, who have provided invaluable assistance in conducting the pathological analysis of the tissue generated in these experiments. Most of the research I've done for the last several years is also thanks to the outstanding work of Dr. Daniel Paris and Dr. Chao Jin, who work at the cutting edge of drug discovery.

Thanks also go to Dr. Michael Mullan, whose insight and vision provide the leadership needed to keep us on the path, always seeking discoveries that will have clinical utility and improve the human condition. I am also forever grateful to Robert and Diane Roskamp, our philanthropic benefactors whose generosity founded our institution and made it possible for us to do the research that what we do.

I would also like to thank my entire family, in particular my parents who never stopped believing in me, and have always supported me in pursuing this dream. Thanks also go to my brother, who proudly serves his country and defends my freedom to pursue my dream, and to my daughter, whose precious smile gives me hope for the future.

TABLE OF CONTENTS

page

LIST OF TABLES

LIST OF FIGURES

LIST OF ABBREVIATIONS

AD Alzheimer's Disease

ALS amyotrophic lateral sclerosis

ANOVA Analysis of variance

APC antigen presenting cells

APOE Apolipoprotein E

APP Amyloid precursor protein

Aβ amyloid β

BACE-1 Beta-secretase 1

BCA bicinchoninic acid

BM Barnes Maze

CBF cerebral blood flow

CCI controlled cortical impact

CD40L CD40 ligand

CHI closed head injury

CID collision induced dissociation

CVLT California Verbal Learning Test

ELISA enzyme-linked immunosorbent assays

ESI electrospray ionization

GCS Glasgow Coma Scale

GFAP Glial fibrillary acidic protein

GOAT Galveston Orientation and Amnesia Test

GOS Glasgow Outcome Scale

IL-1B interleukin-1B

IL-6 interleukin-6

IPA Ingenuity Pathway Analysis

iTRAQ Isobaric tags for relative and absolute quantitation

MCAO middle cerebral artery occlusion

MCP-1 monocyte chemotactic protein-1

MWM Morris water maze

NF-κB nuclear factor kappa-light-chain-enhancer of activated B cells

NMDA N-methyl-D-aspartate

OEF Operation Enduring Freedom

OIF Operation Iraqi freedom

RPM revolutions per minute

TBI Traumatic brain injury

TNF-Alpha Tumor necrosis factor-alpha

ABSTRACT

Traumatic brain injury (TBI) involves both an initial primary insult to the brain and a delayed secondary injury in the hours and days thereafter. The delayed nature of secondary brain injury leaves open the possibility for a window of therapeutic intervention to prevent neurodegeneration. As there are currently no approved drugs for the treatment and prevention of secondary injury after TBI, my approach has been to first identify molecular pathways associated with a

differential outcome from injury, followed by validation of these pathways by targeting them with a variety of therapeutic strategies ranging from genetic manipulation to novel drug compounds, and dietary supplementation. The Apolipoprotein E (APOE) gene has three major alleles, APOE2, APOE3 and APOE4, the latter of which confers risk for poor outcome following TBI. Using quantitative Liquid Chromatography-Mass Spectrometry, large proteomic datasets can be generated, and the difference in protein expression in response to TBI between transgenic mice expressing APOE3 or APOE4 can reveal changes that reflect a "better" or "worse" outcome, respectively. Analyzing such datasets from APOE3 and APOE4 transgenic mice at a wide range of time points, we examined the differential response to TBI and identified several protein pathways of interest, including: CD40 signaling, NF-kB signaling, and APP related proteins. Optimizing several behavioral testing paradigms (Rotarod, Morris Water Maze, and Barnes Maze), we characterized spatial memory and motor function deficits resulting from TBI in order to quantify a "good" or "poor" response. Using a variety of targeted intervention strategies (CD40L knockout, administration of (-)-Nilvadipine, or anatabine) to modulate the protein pathways of interest, we showed improvement in response to TBI. Overall, these experiments provide demonstrate the effectiveness of using a systems biology approach to find potential targets for therapeutic intervention.

CHAPTER 1
AN OVERVIEW OF TRAUMATIC BRAIN INJURY

Traumatic Brain Injury

Traumatic brain injury (TBI) is any damage to the brain caused by an external force. There are a nearly limitless number of possible sources of the injurious force, but some of the most common that result in emergency room visits include falling (35.2%), motor vehicle accidents (17.3%), and being struck in the head by an object or striking one's head against an object (16.5%) (Faul et al., 2010). Other causes of TBI may not result in ordinary emergency room visits, but may be as injurious as any of the aforementioned causes. These include injuries sustained in sporting events as well as blast and shrapnel exposure on the battlefield. These injuries can result in changes and deficits in motor coordination, mood, speech, word retrieval and memory. TBI severity is assessed shortly after injury by neurological measures such as the Glasgow Coma Scale (GCS), which ranks patients with scores of 3-18 based on their verbal, visual, and motor responsiveness to commands and stimuli. Scores less than 8 are classified as severe TBI, 9-12 are classified as moderate head injury, and 13-15 are classified as mild TBI (Teasdale and Jennett, 1976). Just as GCS classifies the neurological state immediately after TBI, the Glasgow Outcome Scale (GOS) classifies the outcome from a TBI into categories of death, vegetative state, severe disability, moderate disability, and good recovery (Jennett and Bond, 1975). The Rancho Los Amigos Level of Cognitive Functioning is another outcome measure that contains 8 levels ranging from no response to purposeful, appropriate, based on the extent of memory deficits, coherence, living skills, attention and self awareness (Gouvier et al., 1987).

These deficits are persistent and can place a great deal of strain not only on the victim but also the victim's family, in terms of the need for support, and the

changing dynamics of inter-personal relationships that can be brought about by the injury. Unfortunately for the patient and their family, there are no pharmacological treatments currently approved for use in TBI regardless of the cause.

Prevalence of TBI

A minimum of 1.4 million people sustain a TBI in the United States each year, contributing to 30.5% of the injury-related fatalities in the US (Faul et al., 2010). TBI is also a growing problem within the military population. The annual incidence of TBI within the military has more than doubled since the year 2000 with a total of 178,876 known cases from 2000 to early 2010. This represents a significant fraction of the 1.1 million troops deployed to Afghanistan and Iraq during Operation Enduring Freedom (OEF) and Operation Iraqi freedom (OIF) since 2001 (after accounting for the 37% that were deployed at least twice) (Fischer, 2010). Though it is anticipated that the number of soldiers deployed to Middle East conflicts (where most of these injuries were sustained) will be decreasing in the coming years, those who were affected will continue to experience the consequences of their injuries. The sequelae of TBI persist long after the initial insult to the brain, and an estimated 5.3 million people in the US are currently living with the long-term effects from injury (Langlois et al., 2006). This number is likely to increase since approximately 35% of hospitalized TBI survivors are expected to be afflicted with long-term disabilities (Brooks et al., 1997).

In England the TBI prevalence in 2001-2002 was 229 per 100,000, with 112,718 patients admitted with this diagnosis (Tennant, 2005). Of those, 31% were aged 0-15 years, 56% were 16-74 years old, and the remaining 13% were aged 75+ years. It is noteworthy that these age groups accounted for 20%, 72% and 8% of the population respectively (Tennant, 2005), highlighting the fact that TBI disproportionately affects the young and old of society. TBI thus primarily

affects those who will spend the longest time coping with the consequences, and those who are vulnerable to the most severe consequences following a given severity of injury. A UK report from 2002 stated that 280 out of 100,000 children spend one or more days in the hospital for TBI each year, more than 10% of those having moderate or severe injuries which carry the most severe consequences (Hawley et al., 2002). Children permanently affected by a TBI will spend most of their lives coping with the consequences and the costs, both financial and emotional.

Across Europe, the incident rate from TBI, whether fatal or not, is approximately 235 per 100,000 based on research reports from 23 European nations spanning 1980 to 2003 (Tagliaferri et al., 2006). The mortality rate from TBI within the United States has decreased since 1980, now only 15 per 100,000, and therefore most of these patients will need care, possibly long term, to recover from the consequences of TBI. Rising healthcare costs are becoming an increasing concern for nations already burdened by debt, and the cost of care is extremely high for those living with the consequences of TBI (Thurman, 1999). The cost of TBI in the United States is $48.3 billion annually (Lewin, 1992), which does not include indirect costs such as lost earnings and productivity for both the victim and the victim's family. Direct and indirect costs combined add up to an estimated $76.5 billion/year in the US as of the year 2000 (Finkelstein et al., 2006). The cost of caring for a single individual with TBI can be as high as $1,875,000 over that person's lifetime (Brain, 1999). By comparison, cancer treatment, which has the highest per person cost of any medical condition in the US, resulted in direct costs of $95.5 billion in 2000 (Marchione, 2012.). Although cancer treatment costs are a frequent topic when discussing the rising cost of health care within the United States, traumatic brain injury is not dramatically far behind.

A study of 6484 TBI patients in the UK showed an average treatment cost of £15,462 per patient. 51% of the cost was contributed by the length of stay in critical care while another 38% was contributed by the length of stay in regular care (Morris et al., 2008). Costs were highest in patients with motor vehicle injuries, due to the severe nature of the injury as well as polytrauma. Mortality was negatively correlated with cost, so as survival rates improve due to better care and safety mechanisms in motor vehicles, the costs of healthcare will also increase. Until an effective treatment can be found to improve outcome and reduce the damage that results from TBI, costs are unlikely to decrease.

Cognitive Problems after Traumatic Brain Injury

Traumatic brain injury can induce a number of cognitive impairments that can severely affect the quality of life of the affected individual. These include deficits in motor function, working memory and amnesia. Even a mild TBI can induce deficits in motor function, correlating to the extent of cognitive impairment (Sosnoff et al., 2008). Working memory is impaired after TBI, with central executive functioning primarily impacted (Van der Linden et al., 1992, Allain et al., 2001). Amnesia after TBI can involve both retrograde amnesia, memory loss which affects recall of events that took place prior to the injury, and anterograde amnesia, dysfunction in the ability to create new memories after the injury.

Motor function after TBI has been found to correlate with cognitive function (Sosnoff et al., 2008), possibly due to the fact that both functional impairments originate from the same source, the initial TBI. Damage to the white matter tracts assessed by fractional anisotropy in diffusion tensor imaging has also been noted as correlating with the extent of motor impairment (Caeyenberghs et al., 2011). This correlation has also been noted in cognitive impairments, with region-specific results. For instance, subjects with greater impairments in executive function have

been noted to have a greater amount of white matter damage in their frontal lobes (Kinnunen et al., 2011).

The central executive portion of working memory is impaired after TBI and is thought to be the primary impairment seen in working memory (Van der Linden et al., 1992, Allain et al., 2001) as assessed by problems with dual-task processing, particularly when the task is complicated (Brouwer et al., 1989, Veltman and Gaillard, 1996, McDowell et al., 1997, Park et al., 1999, Mangels et al., 2002). Common tests of central executive functioning include the Brown-Peterson paradigm, which tests the ability to store information in short-term memory while simultaneously performing a second cognitive task. The task involves arithmetic and reading spans, the former of which requires the subjects to perform a simple calculation given audibly and remember the results and their order, and the latter requires subjects to read several sentences out loud and remember a word from each sentence at a given position within the sentence (first or last word, for instance). A TBI patient may be able to read aloud and perform basic arithmetic, but when combined with time pressures and memorization, they begin to show deficits compared to healthy controls.

Amnesia after TBI can be temporary in the case of mild injuries, with retrograde amnesia usually rectifying itself prior to anterograde amnesia during the post-traumatic period (Cantu, 2001). Severe injuries, however, can produce prolonged periods of anterograde or retrograde amnesia, even months after the insult (Markowitsch et al., 1993, Levine et al., 1998, Demery et al., 2001). The Galveston Orientation and Amnesia Test (GOAT) was designed to assess post-traumatic amnesia and orientation to location and time in the post-traumatic recovery period. Serial measurements with the GOAT have been shown to be predictive of the long-term outcome (Levin et al., 1979). The GOAT asks questions of patients such as the last thing they remember before and after the injury

occurred as well as their current location and city of birth. Depending on the injury severity, they may have memory loss from the time immediately surrounding the accident, but still be able to recall their current location and hometown, or if they have sustained a more severe injury they will have a greater extent of amnesia and be unable to give the correct answer to any of the questions.

Review of Molecular Events Following Primary Injury

Traumatic brain injury is characterized by both primary and secondary injuries. The primary injury results from the initial trauma to the brain, which can occur with or without penetration of the skull. Within the military, common causes of TBI include blast from improvised explosive devices and head wounds from shrapnel and bullets. Blast waves from explosions can induce head injury even without the person being initially aware of the damage (Shanker, 2007). Within the civilian population, common causes are motor vehicle accidents, falling and objects striking the head (Guerrero et al., 2000). Primary injury is generally subdivided into penetrating and closed categories. A penetrating head wound is always severe in nature with severity increasing as a function of the velocity of the penetrating object, but a closed head injury can be mild, moderate, or severe. Within the realm of closed head injuries, there are two sub-types, coup and contrecoup. The former is caused by the initial impact, while the latter is caused by the brain rebounding within the skull after the initial impact, injuring the region of the brain opposite of the impact (Horn and Zasler, 1996). A moderate or severe head injury can induce post-traumatic hematomas within the dura and surrounding structures, compressing the brain and potentially impacting cerebral oxygen metabolism (Valadka et al., 2000).

Following primary injury to the brain, there are very acute molecular consequences that start a chain of events leading to further damage collectively known as secondary brain injury. Secondary injury occurs in the hours and days

following the initial insult and can even affect neurons distal to site of the primary injury. Secondary injury is mediated by such factors as extracellular glutamate and aspartate levels near the site of injury (Faden et al., 1989), neuroinflammation (Morganti-Kossmann et al., 2001), oxidative stress from free radicals (Ates et al., 2006), and calcium influx causing calpain activation and inhibition of mitochondrial respiratory chain-linked electron transfer (McIntosh et al., 1997, Xiong et al., 1997). Excitotoxicity causes the generation of reactive oxygen species such as hydrogen peroxide, superoxides, and peroxynitrite which overwhelm the endogenous antioxidant system leading to oxidative stress and damage via protein oxidation and interruption of the mitochondrial electron transport chain (Werner and Engelhard, 2007). Oxygen radicals in turn induce expression of pro-inflammatory genes (Crack et al., 2009)and Nuclear Factor-kappa B (NF-kB) activation (Sun et al., 1993). NF-kB is a transcription factor, and once dissociated from inhibitory IkB proteins it translocates to the nucleus and can induce the transcription of inflammatory cytokines such as interleukin-1 beta (IL-1B), interleukin-6 (IL-6), and tumor necrosis factor alpha (TNF-Alpha) (Tak and Firestein, 2001). NF-kB can remain activated for at least one year after injury in the region of expanding ventricles as discovered in a rat model of TBI (Nonaka et al., 1999a).

NF-kB activation following TBI induces inflammatory cytokines such as IL-1B,IL-6, and TNF-alpha. Up-regulation of chemokine and adhesion molecule results in infiltration of immune cells in injured tissue (Werner and Engelhard, 2007). As a result of inflammatory damage following TBI, the pericontusional area of the cortex will experience a spreading depression of electrical silencing caused by disrupted ion homeostasis, interrupting cortical function (Fabricius et al., 2006). The disruption of ion homeostasis and cortical depression can lead to microglial activation (Gehrmann et al., 1993) which may persist in patients of severe TBI for

at least 11 months after injury (Ramlackhansingh et al., 2011). This activation was found to begin 72 hours after injury in a penetrating rat model of TBI and is thought to involve CD40 signaling (Williams et al., 2007). By comparison, pro-inflammatory cytokines such as IL-1B, IL-6, and TNF-Alpha are up-regulated within hours of injury, but the inflammatory process is both progressive and persistent. Because there is a delay between the primary injury and the onset of secondary injury, there may be an opportunity for therapeutic intervention to interrupt this sequence and prevent further neuronal loss.

Risk Factors for Poor Outcome after TBI

Genetic factors have been shown to influence outcome after TBI. In this regard the Apolipoprotein E (APOE) gene which confers risk for Alzheimer's Disease has been the most widely investigated. Apolipoprotein E is a lipid-binding protein that is involved in the catabolism of triglycerides and contributes to cholesterol and triglyceride homeostasis with three major isoforms, APOE2, APOE3, and APOE4 (Kypreos et al., 2001). Many studies have now shown that the APOE4 allele (E4) is not only associated with increased risk for AD but is also associated with a risk for poor outcome following TBI (Friedman et al., 1999, Crawford et al., 2002, Smith et al., 2006). Of the many studies of APOE influence on TBI, a few have failed to demonstrate risk (Ashman et al., 2008, Rapoport et al., 2008, Hiekkanen et al., 2009), however in a meta-analysis of 14 studies Zhou and colleagues found that although APOE4 is not a risk factor for worse initial outcome immediately after TBI, it did correlate with worse outcome six months after TBI (Zhou et al., 2008). This is consistent with the conclusions of Ponsford and colleagues who did not see APOE genotype dependent differences in acute outcome as measured by GCS scores or the length of post-traumatic amnesia (Ponsford et al., 2011), but suggest that the E4 allele determines long-term outcome after TBI. A study by Isoniemi and colleagues found that 30 years after

TBI, APOE4 carriers were at risk of greater cognitive decline than non-carriers, leading to dementia (Isoniemi et al., 2006).

Not only does APOE genotype influence the clinical outcome from TBI, it may also affect or even inhibit attempts at therapeutic intervention. In preclinical studies Wang et al. found that an ApoE mimetic peptide improved the histological and functional outcome of APOE2 and APOE3 transgenic mice after TBI but not APOE4(Wang, Durham et al. 2007). In human clinical trials, APOE genotype has also been shown to influence the effectiveness of Alzheimer's disease therapeutics. Cholinergic enhancers, reelin, rosiglitazone, and even combination therapies are all negatively impacted in the APOE4/4 genotype (Cacabelos, 2007, 2008, Cacabelos and Martinez-Bouza, 2011). A retrospective analysis of a failed phase-II AD clinical trial of the bapineuzumab antibody against the Alzheimer's Aβ peptide (see below) showed efficacy, but only for non-carriers of E4 (Salloway et al., 2009).

Relationship Between TBI and Alzheimer's Disease

Epidemiological studies have shown that TBI is a risk factor for the development of AD later in life (Rasmusson et al., 1995, Nemetz et al., 1999). The primary pathological molecules of AD are the beta amyloid peptide (amyloid β (Aβ)) deposited as amyloid plaques, and hyperphosphorylated tau protein which accumulates as paired helical filaments that in turn aggregate into neurofibrillary tangles. Autopsies of TBI patients have revealed the presence of Aβ plaques in 30% of victims with survival times as short as four hours (Graham et al., 1995). Patients who have sustained severe TBI and undergone decompressive craniectomy have been found to have amyloid plaques present in their brains. A study of 19 severe closed head injury patients was conducted by DeKosky and colleagues in 2007 and showed that patients positive for Aβ plaques had a higher percentage of APOE4 carriers (50% vs 10%), as well as a significantly higher ratio

of the longer, more toxic form of Aβ (42 amino acids in length, compared to the most common 40 amino acid peptide) (DeKosky et al., 2007). The Aβ40 level was similar in both groups, only the Aβ42 level differed significantly ($p<.009$). These results may implicate Aβ production, particularly Aβ42, as a mechanism driving the differential response to injury between APOE3 and APOE4 carriers. As mentioned above, APOE genotype confers risk for AD, with the APOE4 allele precipitating an earlier age of onset (Corder et al., 1993, Coon et al., 2007, Sandberg et al., 2012). The same allele is a risk factor for worse outcome after TBI (Bergem and Lannfelt, 1997, Cruz-Sanchez et al., 2000, Cui et al., 2000, Jellinger et al., 2001, Kay et al., 2003, Small et al., 2004). Christensen and colleagues (Christensen et al., 2010) have shown that the possession of an APOE4 allele is associated with an accumulation of Aβ intraneuronally. Because ApoE4 is associated with increased intraneuronal Aβ levels, it might help explain why APOE4 carriers are at risk for a worse neurological outcome following TBI.

In addition to amyloid plaques, neurofibrillary tangles have also been demonstrated in human TBI pathology (Ikonomovic et al., 2004, DeKosky et al., 2007). Repetitive TBI can lead to progressive accumulation of Tau-immunoreactive tangles and dementia known as chronic traumatic encephalopathy, commonly known as dementia pugilistica. This is characterized by memory impairments, motor and speech problems, and Parkinsonian tremors (McKee et al., 2009, Gavett et al., 2010). Additionally, total tau in the cerebrospinal fluid (CSF) has also been shown to correlate with TBI and outcome from TBI (Franz et al., 2003, Ost et al., 2006). TBI, in particular repetitive TBI, is increasingly recognized to be a risk factor for other neurodegenerative diseases as well, such as Parkinson's and amyotrophic lateral sclerosis (ALS) (Tortarolo et al., 2003, Goldman et al., 2006, Gohar et al., 2009, McKee et al., 2009, Gavett et al., 2010).

Animal Models of TBI

Due to the complex and diverse nature of TBI, we need to be able to model it within a laboratory setting where we control variables that range from age, time after injury, injury severity, and genetic factors. However, modeling TBI presents a challenge because different mechanisms and extents of primary injury can lead to different patterns of secondary injury and pathological outcomes. Blast injury, for example, induces diffuse damage that is dependent on the physics of the shockwave reaching the skull (Cernak et al., 2011), and is frequently accompanied by polytrauma from burns and lung injury to the patient (Cernak et al., 1999, Kochanek et al., 2009). Animal models of blast injury generally utilize shock tubes (Long et al., 2009), but blast injury models are still under development (Saljo et al., 2000, Cernak et al., 2001). Due to the unique nature of this injury, the results from these models may not be directly comparable to more generalized models of TBI.

Closed head injury (CHI) models simulate a physical impact to the head and are designed to create a diffuse injury leading to diffuse axonal injury with a blow to the head that does not fracture the skull. Traditionally this method has been performed using a weight dropped from a fixed height over the intact skull (Whiting et al., 2006). This results in diffuse axonal injury, edema formation, and hypertension (Foda and Marmarou, 1994). We utilized an electromagnetic impactor (Brody et al., 2007) in order to deliver a more controlled hit in a new model of CHI being developed and characterized in-house (for more information, see chapter 3).

An alternative method is to perform a craniectomy in order to directly access the dura and impact the brain directly. In the fluid percussion injury (FPI) procedure a cannula is surgically attached through the cranial window and fluid pressure is applied directly to the brain to induce an injury. The injury can be administered centrally or laterally from the midline, and results in hemorrhaging,

cavitation, traumatic axonal injury, and cell death (Dixon et al., 1987, McIntosh et al., 1989, Carbonell et al., 1998, Whiting et al., 2006). Controlled cortical impact (CCI) also involves a craniectomy followed by an impact over the intact dura, but employs an impactor rather than fluid pressure in order to deliver an impact at a fixed speed and depth. This offers superior precision and accuracy of the impact velocity and force delivered (Lighthall, 1988, Dixon et al., 1991, Hamm et al., 1992, Hall et al., 2005).

A role for Aβ, tau and APOE in TBI has also been demonstrated in laboratory models of TBI. Aβ is known to induce inflammation in the brain through p38MAPK signal transduction in rats (Giovannini et al., 2002), and mice over-expressing a mutant form of the amyloid precursor protein (PDAPP mutation) show a drastic increase in Aβ as well as neuronal death within the hippocampus after TBI (Gong et al., 1995, Smith et al., 1998, Smith et al., 2003). Genomic studies of mutant APP (Swedish mutation APP, APPsw) mice who received CCI also show drastic differences from the wild type response, most significantly with genes related to inflammation, immune response, and cell death (Crawford et al., 2007).

Tau hyperphosphorylation is also known to occur after TBI in triple transgenic mice (3xTg-AD) (Tran et al., 2011). These mice develop both plaques and tangles since they are transgenic for the M146V mutation of Presenilin 1 (PS1), APPsw, and the P301L mutation of tau. Tau hyperphosphorylation also occurs in wild type mice transiently after CHI, peaking at 4 hours after injury and subsiding by 24 hours. APOE knockout mice, by contrast, showed tau hyperphosphorylation prior to injury, but not 4 hours after injury, only returning at longer timepoints but not to the extent seen in the wild type controls' transient expression (Genis et al., 2000).

APOE knockout mice have worse cognitive and motor impairment after brain injury than wild type mice as well as increased blood-brain barrier permeability

even in the absence of brain injury (Chen et al., 1997, Methia et al., 2001). ApoE's receptor binding domain is known to decrease tau phosphorylation *in vitro* (Hoe et al., 2006), thus wild type APOE appears to be actively beneficial in a manner that is not compensated for by other apolipoproteins in the absence of APOE. In an animal model of type 2 diabetes treated with pioglitazone, APOE3 mice showed differentially reduced tau phosphorylation where APOE4 mice showed no reduction in tau phosphorylation compared to APOE knockout and murine APOE mice (To et al., 2011). APOE genotype also has an effect on Aβ after TBI; mice transgenic for both PDAPP and E3, E4, or knocked out for APOE were analyzed by pathology 3 months after a cortical impact. APOE4 transgenic mice showed a greater number of amyloid deposits and only E4 showed the presence of thioflavine-S-positive Aβ in the dentate gyrus of the hippocampus. Neither the E3 nor E4 mice showed amyloid deposition at that age (9-10 weeks) in the absence of TBI. E4 mice as well as APOE knockout mice also suffer from a significantly greater mortality rate after closed head injury than E3 mice (Sabo et al., 2000).

Therapeutic Intervention Strategies

There are currently no approved treatments for TBI, though a number of approaches have been attempted. Glutamate NMDA receptor antagonists such as selfotel, aptiganel, and eliprodil were used unsuccessfully in an attempt to prevent excitotoxicity after TBI and/or stroke and avert downstream oxidative stress and inflammation. Instead of simply preventing excitotoxicity, the blockade of synaptic transmission may have inadvertently reduced neuronal survival. Selfotel was the first such drug to enter phase III clinical trials, but the TBI clinical trial was aborted when a concomitant trial of Selfotel in stroke began to show increased mortality in the treated group. The drug also was never shown to be capable of out-competing glutamate at high glutamate concentrations, nor was the drug's concentration in the brain measured (Narayan et al., 2002). Aptiganel was also halted in a nested

phase II/III clinical trial for stroke after the treated group showed less improvement than placebo and showed a higher mortality rate in the high dose group (Albers et al., 2001). Eliprodil also failed to show a significant benefit after TBI in phase III clinical trials (Maas et al., 2008). Although glutamate is initially involved in excitotoxicity acutely after injury, it rapidly returns to normal levels and is important for cell survival (Ikonomidou and Turski, 2002).

Another intervention strategy currently being evaluated is erythropoietin (EPO) to restore cerebral blood flow (CBF) after TBI. Both focal and diffuse injuries lead to reduced CBF and hypoperfusion in regionally-specific manners [Kim, 2010 #84]. It was found that treatment with EPO provided benefits including reduced contusion volume and hippocampal cell loss when administered within 6 hours of CCI injury in rats (Kim et al., 2010). It has also been shown to improve spatial memory and increase neurogenesis in rats when administered for 2 weeks after injury (Lu et al., 2005), however chronic treatment with EPO after mild TBI has been found to increase the risk of post-injury seizures, cerebral hematoma and intracerebral hemorrhage in rats (Evans and Persinger, 2010). Preliminary results indicate that erythropoiesis stimulating agents reduce mortality after severe TBI in human trials, so they may be efficacious (Talving et al., 2010), however most of the mortality occurred within the window of time where treatment was administered and raises questions as to the cause of improvement seen in the treated group.

Research Approach to Traumatic Brain Injury

Our approach at the Roskamp Institute has been to develop appropriate animal models in order to characterize the neurobehavioral, molecular, and pathological profile of TBI in controlled experiments. Although *in vitro* stretch models of axonal injury exist, due to the complexity of TBI it is not possible to fully model in an *in vitro* system. Our most utilized model has been the controlled

cortical impact (CCI) model of TBI in both wild type and transgenic mouse models. CCI involves performing a craniectomy under anesthesia followed by an impact from an electromagnetic impactor at a controlled velocity and depth over the intact dura in the right hemisphere. Sham operated controls only receive anesthesia and a craniectomy. Staff at the Roskamp Institute have recently developed a model of mild closed head injury (CHI). This model also employs the electromagnetic impactor for precise control of the impact force, but the TBI is administered on intact skin directly over the midline. This model produces a mild injury without fracturing the skull and can be repeated in order to model repetitive TBI. In the course of this research, after receiving TBI using one of these two models of injury, mice are profiled using neurobehavioral techniques in order to examine their motor functions and memory and quantify the deficits present in the injured mice compared to controls. At euthanasia, tissue samples are collected for biochemical (including proteomic and genomic) and neuropathological analyses, and plasma samples are collected for biomarker analyses by targeted antibody-based approaches or proteomic/lipidomic interrogation.

We took a systems biology approach to identify potential target pathways for modulation in order to change the outcome of TBI. Proteomic analysis of dissected brain tissue generates profiles of large numbers of proteins, and a comparison of the profile of injured compared to sham control mice reveals significant TBI-dependent modulation of proteins, allowing us to generate datasets of the molecular pathways associated with neurodegeneration following TBI. The response to injury is also dependent on severity of injury, time post injury and the brain region being analyzed. Furthermore, in order to identify molecular pathways that are associated with a favorable or unfavorable outcome after TBI, we refined the datasets by utilizing mice genetically modified to model human risk of favorable or poor outcome after TBI; namely transgenic mice expressing either the

APOE3 or APOE4 alleles of the human apolipoprotein E (APOE) transgenic mice following CCI. Molecular pathways found to be important in this transgenic mouse model of differential outcome from TBI were subsequently targeted using genetic modulation, pharmaceutical treatment and dietary supplementation. These strategies were evaluated using a series of neurobehavioral tests that I had honed for use in TBI laboratory models. Although pathological and molecular analyses showed confounding results in some approaches, neurobehavioral analysis using the paradigms that I optimized and implemented revealed beneficial effects of modulating these pathways in order to alter the outcome from TBI(figure 1.1). This shows we have a very effective platform with which to conduct pre-clinical research into effective therapies for TBI.

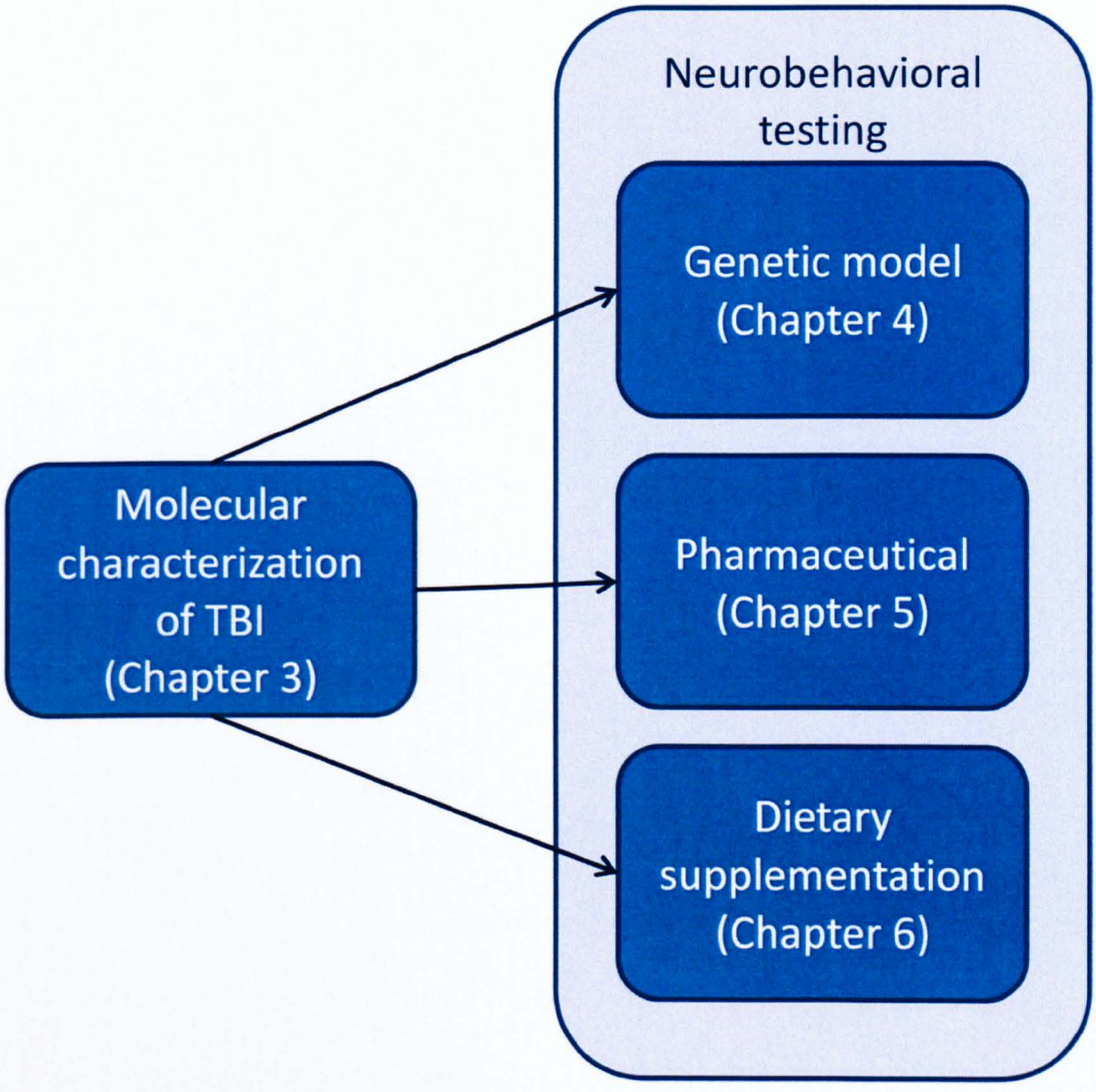

Figure 1-1. Experimental Outline Flowchart.

CHAPTER 2
NEUROBEHAVIORAL EVALUATION OF TRAUMATIC BRAIN INJURY

Introduction

Traumatic brain injury is a very complex phenomenon owing to the many possible sources and mechanisms of primary injury and the wide cascade of events that follows primary injury (Giza and Hovda, 2001). Animal models of TBI are required to recapitulate the full complexity of events following TBI; even within animal models, the complexity of the TBI being modeled is reduced by the level of control exerted on the variables, such as using inbred mouse strains and focusing on a single sex (Cernak, 2005). As outlined in chapter 1, several different animal models of TBI have been developed over the years, and until very recently the CCI model was the one most widely used at the Roskamp Institute. CCI produces time-dependent neurodegeneration distal to the cortical site of injury with silver staining showing maximal neurodegeneration within the hippocampus 48 hours after injury, but with degeneration still present in the mossy fiber projections at least 7 days after injury (Hall et al., 2005). Initial TBI research at the Roskamp Institute focused on genomic analyses (Crawford et al., 2007, Crawford et al., 2009), but it became clear that there was a need to be able to correlate molecular and pathological changes with functional outcome measures in order to identify the consequences of TBI that might be amenable to therapeutic intervention. Neurobehavioral testing of rats subjected to a moderate CCI injury show spatial memory deficits at both short and long timepoints after injury (11-15 days and 30-34 days respectively) as seen by Hamm et al (Hamm et al., 1992). The CA1 and CA3 of the hippocampus show dystrophic neurons up to 2 weeks after injury followed by cell death (Colicos et al., 1996). This is consistent with studies of human TBI showing hippocampal volume loss after TBI corresponds with impairments of memory and executive functioning (Bigler et al., 1997, Himanen et

al., 2005, Tasker et al., 2005). By studying these effects in an animal model of TBI, we can evaluate potential therapeutic approaches in a controlled environment. Therefore we chose this model of TBI in order to evaluate and refine a series of neurobehavioral tests that would allow us to quantify impairments in motor function and memory resulting from TBI.

Motor coordination impairment is a major problem following TBI in humans, and practicing the use of motor skills can result in their improvement over time (Neistadt, 1994). The Rotarod provides a rapid test of motor coordination by providing a task of increasing difficulty over time in order to quantify dysfunction. The Rotarod test consists of a rotating beam notched with grooves to enable a mouse to grip the beam and walk with it as it rotates beneath the mouse at a programmable speed. 5 slots are divided with plastic barriers so that each mouse is isolated and cannot see any of the neighboring mice during the test. Previous studies have shown that the Rotarod is a more sensitive test of motor function impairment than other alternatives such as the balance beam and beam walk tests (Hamm et al., 1994). Rotarod performance is negatively impacted by TBI where an initial drop in performance is seen, followed by gradual improvement as the mice adapt to their impairment. A significant improvement in Rotarod performance corresponding to a therapeutic may suggest its usefulness in improving motor coordination after TBI, particularly when combined with rehabilitation therapy.

In addition to motor coordination impairments, memory loss is another main consequence of TBI. One way to quantify memory impairment in rodents is to utilize tests of spatial memory. The Morris Water Maze (MWM) is a test of hippocampus-dependent spatial learning and memory (Morris, 1984). The MWM consists of a pool filled with transparent (for pre-testing) or opaque water (for acquisition and probe testing) containing a platform submerged just below the surface of the water. Mice are naturally averse to water and immediately seek to

escape from the pool. This is particularly important for the mouse strain we utilized for all of our experiments, C57BL/6J. This strain of mouse is well characterized and has been shown to exhibit reduced exploratory activity after previous handling and testing has occurred, thus the aversion to water provides an important motivator for the mice to search for an escape from the maze (Võikar, Vasar et al. 2004). Mice are introduced into the pool at randomly selected cardinal starting locations along the outer perimeter of the pool and are given a short period of time to locate the platform using spatial cues along each wall of the testing room to orient themselves. If they fail to find the platform they are guided to it by hand and are required to remain there for a short period of time before being returned to their cage. Poor performance in the water maze indicates spatial memory loss and is known to occur after CCI (Scheff et al., 1997, Fox et al., 1998a). Given the known effects of TBI on the hippocampus both in the CCI model of TBI and in human TBI, we chose MWM to study spatial memory impairments induced by TBI.

The Barnes Maze (BM) is an alternative test of spatial memory performed by placing the mice on a 1.2 meter circular table with 18 holes around its perimeter. A goal box is affixed underneath one of the holes, and as with the water maze, spatial cues of various shapes and sizes are placed around the walls of the room. In order to encourage the mice to seek a way out of the maze, provided by the goal box, halogen flood lamps were aimed at the walls of two diametrically opposed corners of the room in order to drastically increase the lighting level of the room through indirect lighting. Mice naturally prefer a dark environment to a bright one and will tend to seek escape from the bright open space of the maze into the goal box. If they fail to find or enter the goal box they are guided to it by hand and required to enter the box for a short period of time before being returned to their cage. Like MWM, poor performance on the BM is indicative of an impairment of

spatial learning and memory (Fox et al., 1998b). The ability to measure impairments in spatial learning and memory is vital to understanding the effectiveness of potential therapeutic strategies as well as the correlation between changes in molecular pathways in response to injury and clinical outcome.

My goal was to establish a neurobehavioral platform with which to evaluate outcome after TBI in mouse models. I evaluated neurobehavioral tests, including MWM, that were being used at the time in the Roskamp Institute for observing behavioral differences in models of neurodegenerative diseases such as Alzheimer's disease. I then introduced two new testing paradigms to the Roskamp Institute, Rotarod and Barnes maze, which I adapted in order to characterize the consequences of TBI under a variety of injury conditions and time points. Neurobehavioral confirmation of functional deficits after TBI supports our contention that the molecular differences between injured and uninjured mouse models (Chapter 3) reflect pathogenic consequences of TBI that directly relate to their outcome.

Materials and Methods

Animals

For the TBI severity study, we utilized male and female APOE knockout mice (APOE-deficient on a C57BL/6J background) 20-50 weeks old (with one at 104 weeks old) (n=7-8).

For the APOE study, we used transgenic mice (n=8-12) expressing different human ApoE isoforms (ApoE3 or ApoE4) with human APOE regulatory sequences on a murine-APOE deficient background (APOE-def) with C57BL/6J as the background strain (Xu et al., 1996, Crawford et al., 2009, Ferguson et al., 2010). These mice exhibit behavior similar to their C57BL/6J background strain, but exhibit difficulties during breeding including small liter size and frequent cannibalization of the young. All APOE transgenic mice (originally obtained

through Dr. Crawford's collaboration with Dr. Allen Roses (Duke University) and bred in-house) were hemizygous for the human APOE transgene (either APOE3 or APOE4) and homozygous for mouse APOE deficiency. We have previously evaluated brain expression levels of ApoE by ELISA (MBL International) in both of these mouse APOE genotypes and found no genotype-, injury-, or genotype*injury-dependent differences in cortex, hippocampus or cerebellum ($p>0.19$ in all analyses), demonstrating that any differential effects of TBI seen between mice of different APOE genotypes is not due to differences in levels of expression of ApoE.

For optimization of the Barnes maze, female C57BL/6J wild type mice were utilized (for pilot study, n=10 for the 4 day study at 28 weeks old, n=4 for the 7 day study at 39 weeks old). These mice received no TBI.

All procedures involving mice were carried out under IACUC approval and in accordance with the National Institute of Health Guide for the Care and Use of Laboratory Animals.

Administration of TBI by CCI

For the administration of TBI, mice were anaesthetized with 1liter/min O_2; 4% isofluorane; once anesthetized, the isofluorane was reduced to 2% and the animal mounted in a stereotaxic frame in a prone position secured by ear and incisor bars. Temperature was monitored throughout the surgery using a rectal probe. Following a midline incision and reflection of the soft tissues, a 5mm craniectomy was performed adjacent to the central suture, midway between lambda and bregma. The dura was kept intact over the cortex. Injury was administered as previously described (Crawford et al., 2009) by impacting the right cortex with a 2 mm diameter tip at a rate of 5 m/s and depth of either 1.3mm, 1.8 mm, or 2.0mm using an electromagnetic impactor (MyNeuroLab) (Diagram 2-1). Sham mice for

the CCI procedure received craniectomy without injury. After surgery, mice were singly housed and monitored closely for adverse events until reacquisition of their righting reflex. Food and water were provided in a dish for direct access by the mice. Adverse event monitoring continued throughout the course of the experiments. For the severity study mice received either a 1.3mm or a 2.0mm CCI or sham injury; for the APOE transgenic study mice received a 1.8mm CCI or sham injury.

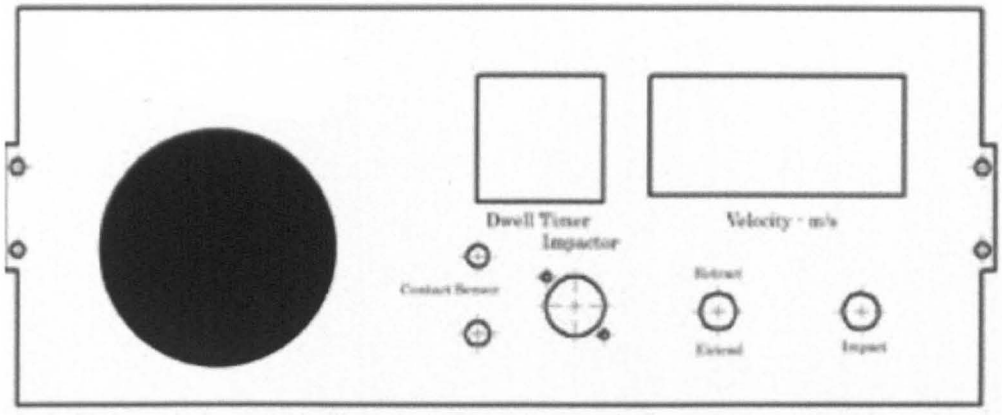

Diagram 2-1: Electromagnetic Impactor (MyNeuroLab)

Rotarod

Three days prior (unless otherwise noted) to the administration of a CCI, mice were pre-trained and baseline tested for Rotarod performance. All mice were given 3 trials to walk on the Rotarod at a constant speed of 5 revolutions per minute (RPM). Mice were returned to the Rotarod bar after each fall for a period of 3 minutes followed by a 3 minute rest period. After pre-training, the mice were given a minimum of 30 minutes to fully recover before beginning their first baseline test. For all subsequent tests, the Rotarod was set to an accelerating speed of 5-50 RPM over a period of 5 minutes. 3 trials were given with a 3 minute rest period between trials. Latency to fall and the speed of the Rotarod at the moment of the fall were recorded. Clinging to the Rotarod without walking was penalized by terminating that mouse's trial if the clinging occurred for 5 consecutive rotations of the bar. This is because the primary purpose of the test is to measure motor function, coordination, balance, and a small degree of learning; clinging to the bar only indicates grip strength.

On the day following the third day of Rotarod baseline testing, mice were given a craniectomy followed by a CCI (excepting sham controls) and were then tested every other day after surgery starting on day 1 and ending on days 5 or 7. Post-surgery testing occurred at an accelerating speed of 5-50 RPM over a period of 5 minutes. 3 trials were given with a 3 minute rest period between trials. Latency to fall and the speed of the Rotarod at the moment of the fall were recorded. As before, clinging to the Rotarod for 5 consecutive rotations ended that mouse's trial.

Morris Water Maze

A 1.8 meter pool was filled with opaque water and a platform was hidden 1.5 mm below the surface of the water. Mice were introduced into the pool near the wall and could escape by finding and remaining on the hidden platform for a period of 30 seconds, at which time the trial was ended and the mouse was retrieved from the pool. Spatial cues of various shapes, designs, and colors/brightness were placed around the walls of the room and small strips of tape were placed along the inside wall of the pool to enable the mice to orient themselves and find the platform without seeing it. Each mouse's movement during each trial was recorded and analyzed using Noldus Ethovision XT software.

All mice received pre-testing for three days prior to the start of acquisition trials. Pre-testing consisted of using clear water so that the platform would be visible to the mice. Each mouse was tested in sequence, and each received a total of 4 trials, each trial starting from a different randomly selected cardinal point. If a mouse failed to find the platform within 60 seconds, they were guided to it by hand and kept there for 30 seconds, preventing them from reentering the water. After three days of pre-testing, the water was filled and stirred with non-toxic white tempera paint to hide the location of the platform. Trials resumed as before, but now each mouse was given 1.5 minutes to find the hidden platform before being guided to it. On the 9^{th} day of acquisition testing, a probe trial was given. The hidden platform was removed from the pool and each mouse was given one 60 second trial starting from a novel position. The time spent in the quadrant containing the hidden platform location, the latency to find the hidden platform location, and the path length of each mouse's total movement were extracted from the data.

Barnes Maze

Mice were introduced into the Barnes Maze using a PVC tube and brought into the room covered in a towel; this prevented them from seeing any of the maze or spatial cues before the start of the trial. When the trial began the PVC tube was lifted straight up and away and the experimenter then left the room. Each mouse was given 1.5 minutes to explore the maze and enter the goal box. If they entered the goal box the trial was terminated and 30 seconds were allowed to elapse before retrieving the goal box and returning the mouse to the home cage. The mouse was placed into the goal box directly and left there to acclimate for 30 seconds if they had not already entered it on their own by the end of the trial period. Each mouse received 4 trials starting in front of each of 4 randomly selected cardinal holes for a period of 6 days. On the 7th day the goal box was removed and the mouse was introduced into the maze at a novel position in the center of the table. This probe trial was only given once to each mouse and lasted for 60 seconds. Each mouse's orientation and movement was recorded by Noldus Ethovision XT software. The number of pokes into each hole, average distance of the nose from the target hole, and average time spent with the nose in the target hole during the probe trial were extracted from the data.

Results

Severity Study

We initially explored different levels of injury in the CCI model using the Rotarod as a measure of the functional outcome. Injury depth was set to either 1.3mm or 2.0mm and mice were tested on days 1, 3 and 5 after surgery. Rotarod showed a significant effect of injury, but only a non-significant trend towards the 2.0 mm depth injury being more severe than the 1.3mm depth injury. Figure 2-1. The results of this study led to two changes in our approach. Firstly, we decided to extend Rotarod testing to 7 days as the results of this test pointed to an

increasing difference in performance between injury groups over time and we wished to further explore this divergence. Secondly, we found that the 2.0mm depth injury produced a mortality rate of approximately 25%. Since our interest is in studying the long term consequences of TBI survival, not mechanisms of mortality, this was an unacceptably high mortality rate. We subsequently reduced the depth of injury for the "severe" paradigm to a depth of 1.8mm in order to consistently achieve 100% survival.

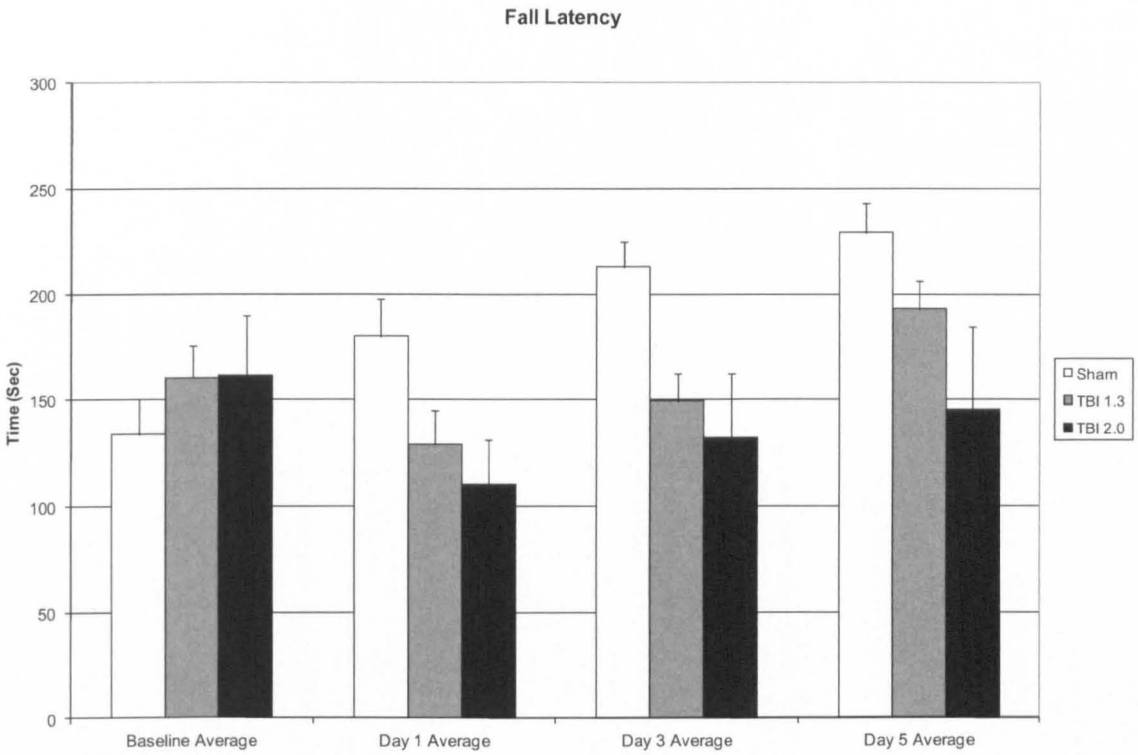

Figure 2-1Fall latency during the Rotarod in Severity Study. Injury was signififcant by ANOVA repeated measures ($p<0.05$). Error bars represent standard error.

Effects of APOE genotype on Rotarod performance after CCI

Rotarod results from the APOE cohort were analyzed by expressing each mouse's average fall latency as a percentage of their baseline fall latency average.. APOE3 mice showed a trend for superior performance compared to APOE4 mice. Raw fall latency showed a significantly higher fall latency in TBI APOE3 mice than TBI APOE4 mice ($p<0.05$) (Figure 2-2). This effect was not present when normalizing the data to baseline performance. APOE3 mice also recovered to their baseline performance level by day 5 after injury and recovered to sham performance by day 7. APOE4 mice failed to recover to either their baseline or sham levels within the first week after injury, and when tested again at 3 months, immediately prior to MWM testing (see below) they required 3 days of testing in order to recover to sham levels. This supports previous studies in the literature showing that APOE4 is a risk factor for worse outcome following TBI.

As this is primarily a test of motor function, it does not indicate that the level of secondary injury sustained in the hippocampus following TBI was necessarily worse in the APOE4 mice than the APOE3 mice. 3 months after surgery, the mice were given 3 additional days of testing with one rest day between each testing day. The results showed that motor performance of all TBI mice regardless of genotype returned to E3 sham levels within the three day testing period three months after injury.

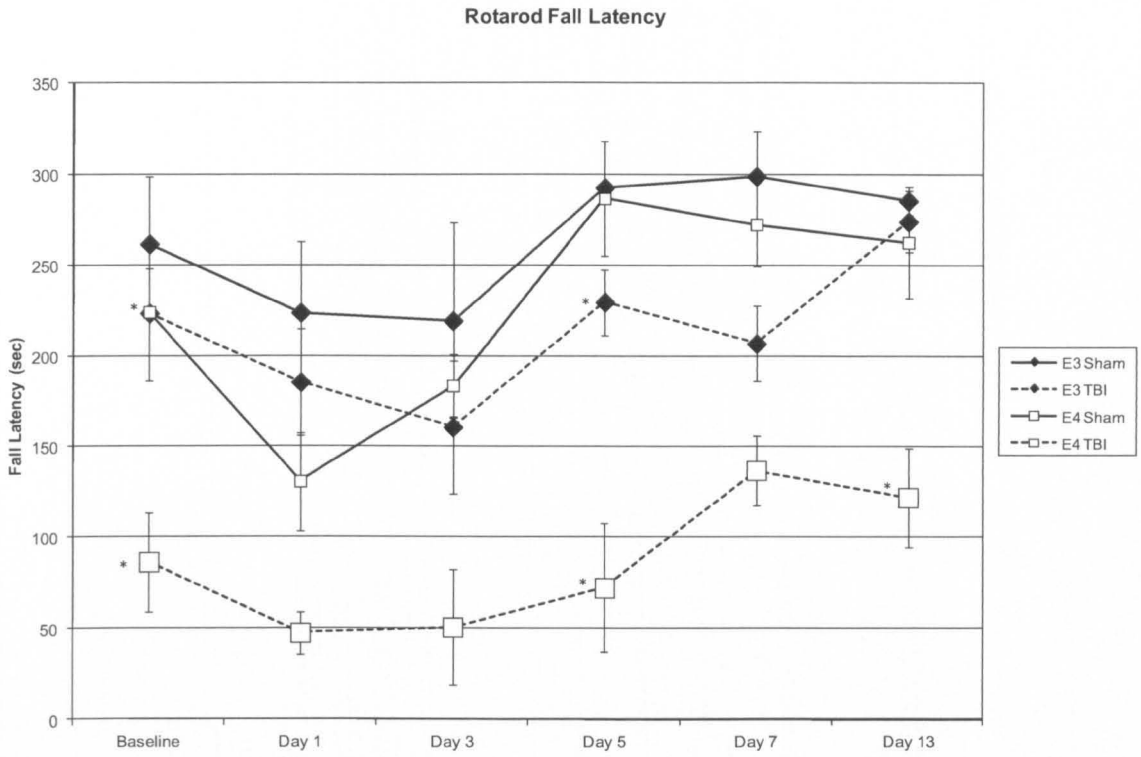

Figure 2-2. Rotarod Fall Latency. TBI E4 mice performed significantly worse than TBI E3 mice (globally) by student's T-test ($p<0.05$) but not after normalizing the data to baseline performance. Error bars represent standard error. * indicates significance relative to the corresponding sham by T-test ($p<0.05$).

Morris Water Maze

In the APOE transgenic mouse cohort, Morris Water Maze testing began 3 months after TBI, immediately after the second period of Rotarod testing described above, in order to study the long term consequences of TBI on memory and the effect of APOE genotype on the outcome from injury. Interestingly, our MWM results not only failed to indicate a significant impact of genotype on the level of injury to the hippocampus, they also failed to indicate a significant impact of injury on spatial memory associated with the function of the hippocampus (figure 2-3, figure 2-4, figure 2-5 and Appendix A: the Morris water maze chapter of the supplementary DVD). This is inconsistent with our Rotarod results discussed above, which show APOE4 mice generally performing worse than their APOE3 counterparts in both the sham and injury groups. In the Rotarod, APOE4 TBI mice performed worse on the first day of testing 3 months after injury, only recovering to E3 sham levels (and never to its corresponding sham) by the third day of testing, showing that TBI-induced deficits persist 3 months after injury.

Our MWM results showed no statistically significant effect of genotype ($p>0.05$), but the trend shows E4 mice outperforming E3 mice in terms of time spent in the quadrant containing the target platform and in terms of the path length (which is expected to decrease as mice learn more direct ways to find the target platform) over the course of the testing period. Not only was genotype an insignificant factor, but so was the injury effect itself. Injury was only significant in the pre-testing trials, when the platform was visible and spatial memory was not required to locate it. A significant effect only during the pre-testing trials indicates a motor or motivation deficiency in the TBI mice, but not a difference in spatial memory.

Given that the TBI was severe, the hippocampus was expected to be deeply injured and a severe impairment of spatial memory compared to either sham group. Although no effects were seen in the MWM, the Rotarod data showed a significant effect of injury and a trend for worse performance in APOE4 mice than the APOE3 mice. This prompted me to introduce and optimize an alternative method of measuring spatial learning and memory.

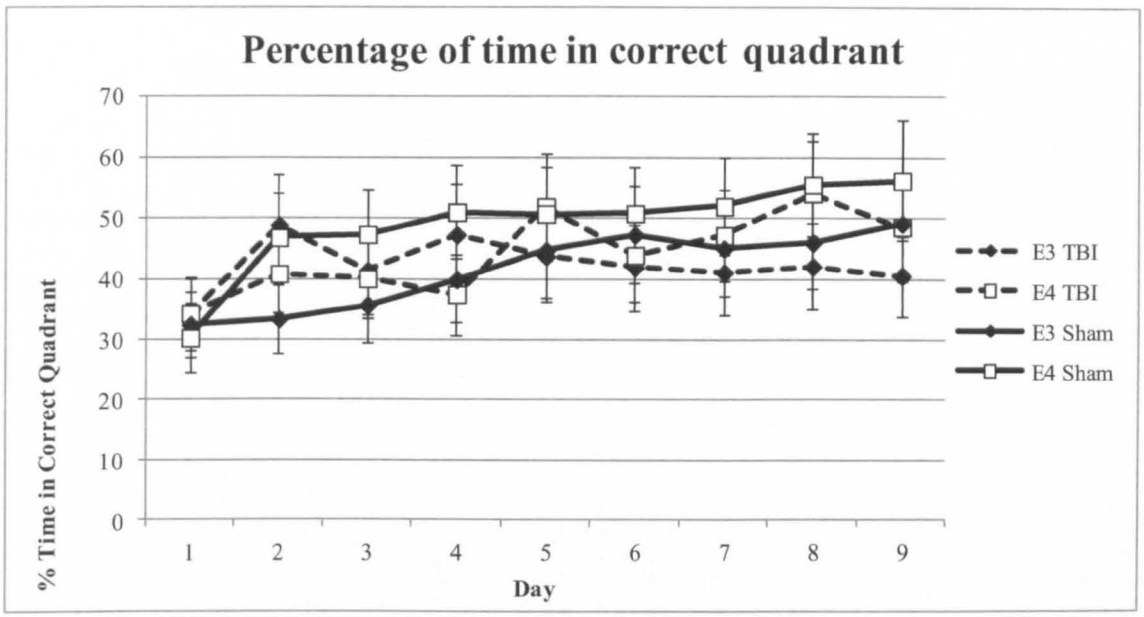

Figure 2-3. Percentage of time spent in the correct quadrant during the MWM by the APOE cohort. No statistical significance. Error bars represent standard error.

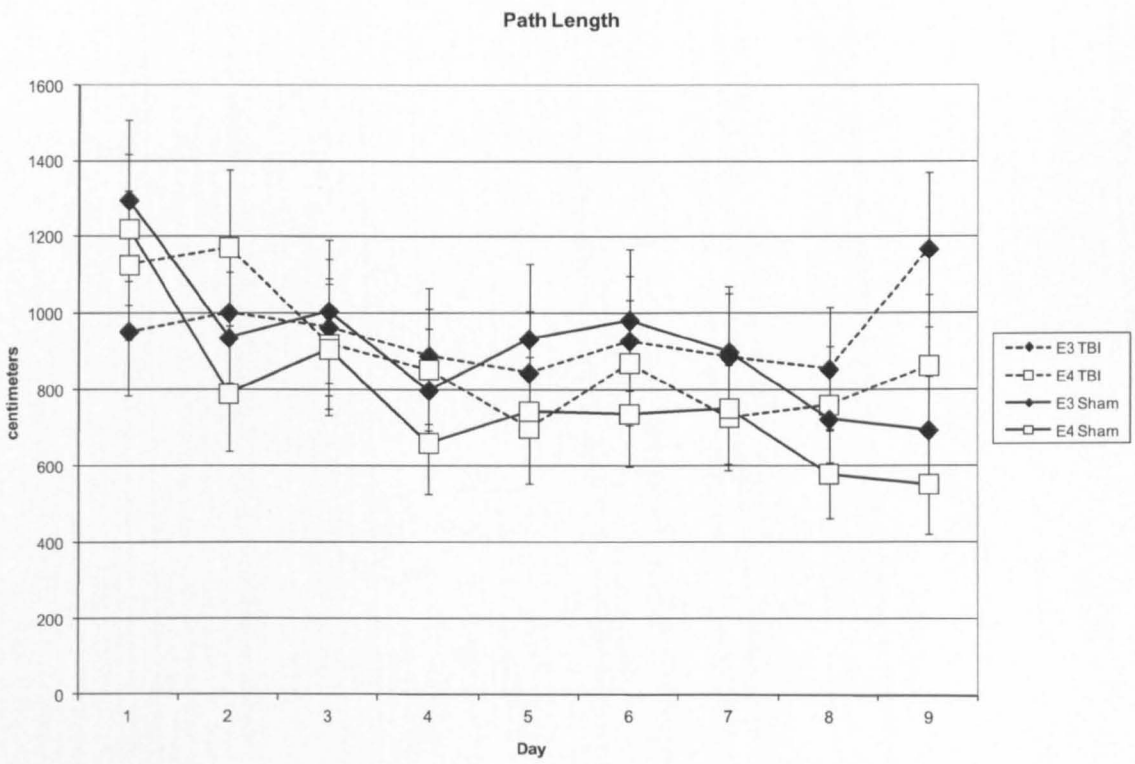

Figure 2-4. Path length during the MWM by the APOE cohort. No statistical significance. Error bars represent standard error.

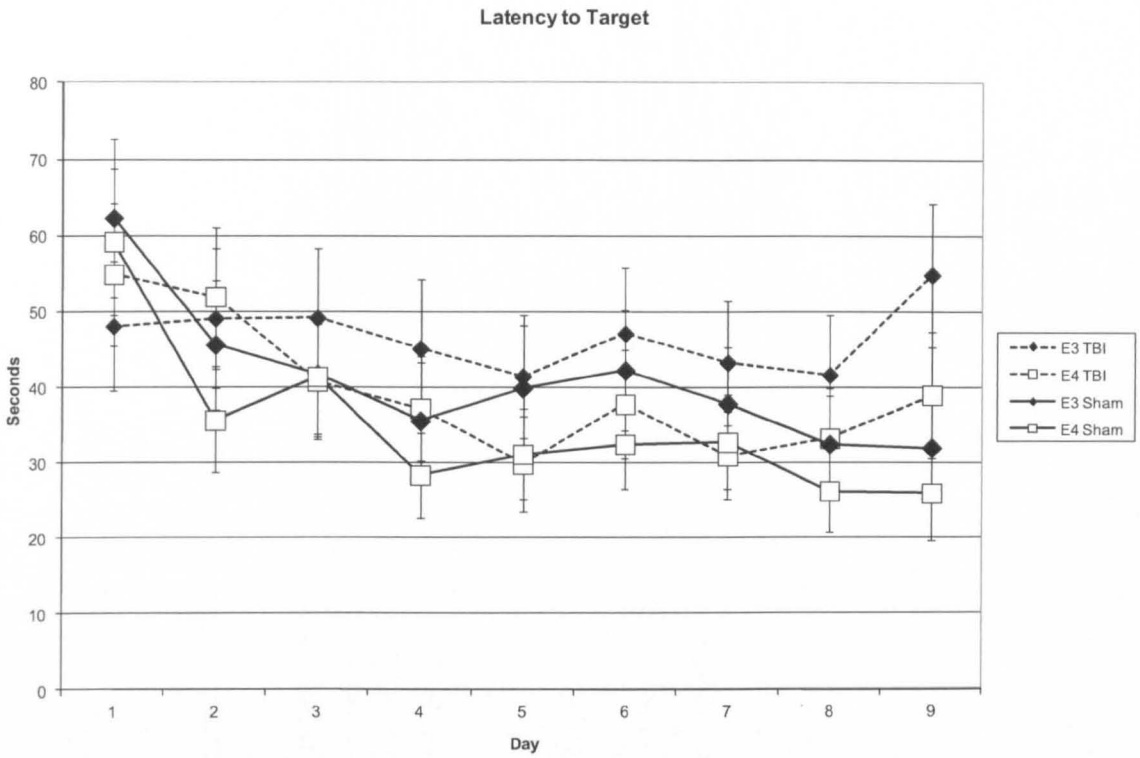

Figure 2-5. Latency to the target platform during the MWM by the APOE cohort. No statistical significance. Error bars represent standard error.

Barnes Maze Optimization Pilot Cohort

I chose the Barnes maze as an alternative to the MWM because this particular strain of mouse (C57BL/6J) shows a preference for less stressful paradigms (Harrison et al., 2009), and this was the background strain of choice as the APOE transgenic mice and other mouse models of interest to us are on the C57BL/6J background. To optimize the Barnes maze, C57BL/6J wild type mice were tested for a range of times to determine the minimum acquisition period required. Previous work has shown the ability of this strain of mouse to develop spatial memory in this paradigm within 4 days of acquisition testing (Koopmans et al., 2003), so we began with 3 days of acquisition testing with a probe trial on the fourth day. In a second cohort we also conducted acquisition testing for 6 days before performing a probe trial on day 7. 6 days of acquisition trials resulted in a smaller average distance of the nose of the mouse from the target hole during the probe trial. figure 2-6. This showed that the mice continued to develop spatial memory on the last 3 days of acquisition testing. Given these results, future tests using the Barnes maze would involve 6 days of acquisition trials followed by a probe trial on the 7^{th} day.

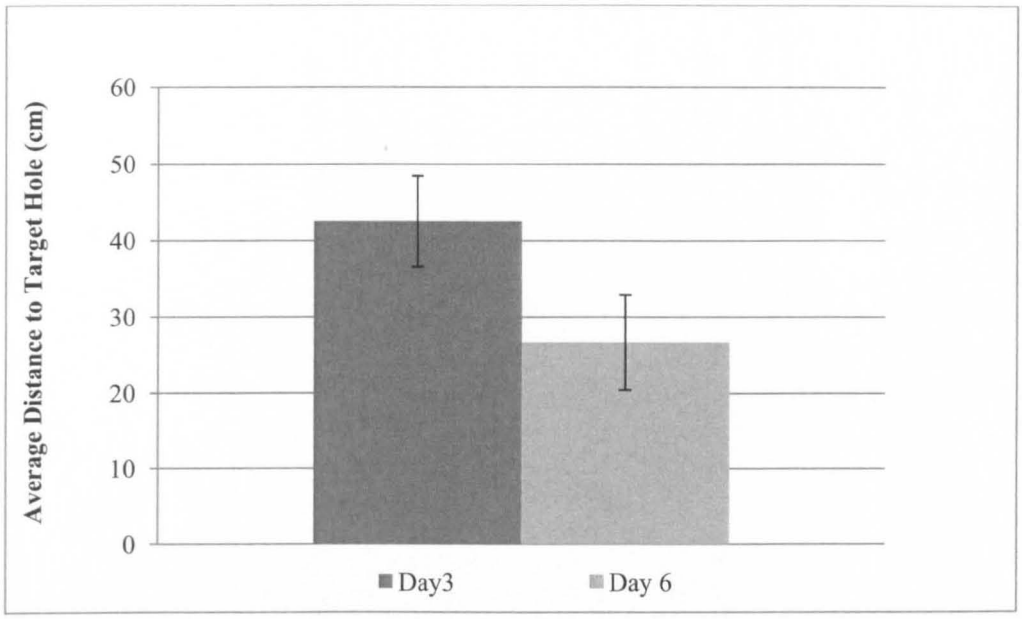

Figure 2-6. Average distance to the target hole during the probe trial of the Barnes maze optimization study. Error bars represent standard error. No statistical significance,

Discussion

Overall, our model of TBI demonstrates impairments in motor coordination and memory that are consistent with the symptoms of TBI seen in human clinical situations. Not every neurobehavioral paradigm utilized showed the expected effect, but we optimized alternative methods designed to assess the same impairments and here we demonstrate their success not only at showing effective learning in these mice, but significant impairments resulting from TBI. Rotarod, Morris water maze, and Barnes maze all require optimization and not every test is appropriate for every strain of mouse, but when properly applied allow us to quantify the level of impairment present after traumatic brain injury. With the TBI severity study, we did not see a significant difference between the 1.3mm and 2.0mm depth injury, but that particular experiment lead to further optimization of our Rotarod protocol and because it was a pilot study it involved the use of mice from a wide range of ages which is a confounding factor in these mice (Serradj and Jamon, 2007). Future cohorts would continue to not only show the Rotarod's ability to distinguish CCI injury from sham, but also its ability to discriminate genotype and treatment differences as well (see chapters 4 and 5).

Rotarod testing performed on our APOE cohort showed a non-significant trend for APOE4 performance to be worse than APOE3, whether they received TBI or a sham surgery. Injured APOE3 transgenic mice recovered to sham performance levels by day 7 after TBI, while APOE4 transgenic mice showed a trend for worse performance even 3 months after TBI. Though our results were not statistically significant, they were consistent with the hypothesis that APOE4 predisposed the mice to a worse outcome from injury. The number of mice in each group ranged from 8-12, and it is possible that increasing the number of mice

to 12 per group consistently as well as confining the age and gender of the mice would have allowed the trends to become statistically significant.

MWM of the APOE mice not only failed to indicate a significant impact of genotype on spatial memory, they also failed to indicate a significant impact of injury. Injury was only significant in the pre-testing trials, when the platform was visible and spatial memory was not required to locate it. A significant effect only during the pre-testing trials indicates a motor or motivation deficiency in the TBI mice, but not a difference in spatial memory. This may be due to stress, particularly once the platform is hidden by opaque water during the acquisition trials; Harrison and colleagues demonstrated that C57BL/6J mice show a significant correlation of stress level with maze performance in the water maze (Harrison et al., 2009). The CCI model of TBI employed here should have shown significant effects on spatial learning and memory (Fox et al., 1998b). The results not only contradict the findings of other experimenters studying the CCI model, but they also directly contradict our Rotarod data discussed above, which show a significant effect of injury and a trending lower percentage of baseline performance in the APOE4 mice than the APOE3 mice. Even 3 months after injury, our E4 mice initially showed impairments relative to sham mice that did not resolve until the third day of testing.

The difficulties encountered with the Morris Water Maze were not unique to this particular experiment; another pilot study showed differences between treatment groups on days 1 and 9, but the overall trend did not show any difference between the two (see chapter 5). That particular pilot study did not include sham mice for controls.

Spatial memory testing is a vital tool for studying the neurobehavioral consequences of traumatic brain injury within a controlled animal model. Although MWM is frequently utilized in assessing the consequences of TBI (Hanell et al.,

2010, Singleton et al., 2010, Zhu et al., 2010), previous groups have shown a mouse strain-dependent effect on neurobehavioral testing. Strain dependent effects have been noted in the Morris water maze as well as the Barnes maze; in contrast to our C57BL/6J mice, CD1 mice have been reported to show superior performance in the Morris water maze, but poorer performance on the Barnes maze than C57BL/6J (Patil et al., 2009). C57BL/6J serves as the background strain for mice carrying the human APOE transgene relevant to the study of traumatic brain injury, as well as countless other transgenes used in other models of disease (Hartman et al., 2002, Crawford et al., 2009, Ferguson et al., 2010, Jiang et al., 2010, Yao et al., 2010), and therefore using a test suitable for that strain is appropriate.

Our Rotarod results indicated a pronounced effect of injury in every cohort of mice tested, yet as previously mentioned, MWM was unable to show a significant effect of TBI three months after the initial insult. An examination of the video recordings of each trial showed a failure of sham mice to utilize spatial strategies, with most mice using systematic strategies at best to locate the platform (See Appendix A). Videos of the Barnes maze testing would later show sham mice utilizing spatial strategies to directly locate the target hole, while TBI mice would use systematic strategies of searching hole by hole until the correct hole was located (See chapter 5 and Appendix A, the Barnes maze chapter in the supplementary DVD). TBI mice in the Morris water maze similarly failed to use spatial strategies, but the difference between their performance and that of sham mice was evidently minimized as seen by examining both the acquisition and probe trial data. Time was statistically significant over the acquisition period, indicating that learning was occurring, but this may have been driven more by goal-oriented learning than spatial memory learning. Goal-oriented learning drives the non-spatial component of both the water maze and Barnes maze; the mice

must learn and remember to find and remain in the target box or target platform. Goal-oriented learning and memory is independent of dorsal hippocampal functioning, but is moderately impacted by damage to the ventral hippocampus. Spatial-memory, unlike goal-oriented memory, is dependent on the functioning of the dorsal hippocampus (Levita and Muzzio, 2010). Early in the acquisition testing mice had not yet learned the non-spatial goal portion of the task; that the hidden platform was the only way to escape the pool, so they did not remain on the platform for the required 3 seconds even when accidentally encountering it.

Harrison et al, demonstrated that this strain of mouse, C57BL/6J, show water maze performance that is significantly inversely correlated to stress as measured by corticosterone levels. Corticosterone levels were most elevated during water maze testing, but were also evaluated during the Barnes maze and although still significantly elevated (though to a lesser extent than in MWM) and were not correlated with performance (Harrison et al., 2009).

If stress is the main driver of Morris water maze performance in this strain of mouse, then it may be masking other spatial memory impairments such as TBI. We optimized the Barnes maze as a test of spatial memory by performing acquisition testing for 3 days followed by a probe trial on day 4 and compared this to 6 days of acquisition testing followed by a probe trial on day 7. Due to limited numbers of mice available for the 7 day comparison study, we only had an n of 4 and the mice were 11 weeks older than the mice used for the 4 day study. In spite of these limitations, both groups showed similar standard error and the mice from the 7 day study had a smaller average distance from the target hole. Though the results were not statistically significant due to the small n of the 7 day group, the consistency shown and the relatively small amount of standard error was a remarkable result, particularly compared to our previous MWM results. This gave us confidence in the power of the Barnes maze to discriminate between groups

with different levels of spatial memory. The probe trial of the Barnes maze is performed after approximately 20 hours have elapsed from the final day of acquisition testing (day 6), making it a much better indicator of long term spatial memory retention (Appendix A, the Barnes maze chapter of the supplementary DVD). This shows that the Barnes maze is capable of discriminating injury and long term spatial memory loss as well as spatial memory learning. The dramatic differences seen between the Barnes maze and Morris water maze outcomes confirm previous studies showing that high stress levels experienced during Morris water maze testing negatively impact C57BL/6J performance. For our purposes therefore, in modeling TBI in the laboratory, the Barnes maze is more suitable for this strain of mouse and produces results that correlate with hippocampus-dependent spatial memory functioning. With the Rotarod and Barnes maze tests, we can now properly quantify the neurobehavioral outcome from injury, and the large differences seen between TBI and sham groups provides sufficient power to discriminate between treated and untreated TBI mice showing any evidence of improved outcome after injury.

CHAPTER 3
MOLECULAR CHARACTERIZATION OF TRAUMATIC BRAIN INJURY AT ACUTE AND LONG TERM TIMEPOINTS

Introduction

As previously discussed in chapter 1, traumatic brain injury consists of both a primary injury directly caused by the forces acting on the brain, as well as a secondary delayed injury caused by conditions and processes within the brain in the hours and days after the primary insult. The delay between the primary insult and secondary injury involves a cascade of events where intervention may be capable of reducing or preventing additional neuronal damage. Unfortunately, the exact mechanisms of secondary injury are not fully understood, in particular what processes occurring within secondary injury result in a better or worse patient outcome. In order to elucidate mechanisms of secondary injury important to determining outcome and thereby identify potential targets for therapy, the Roskamp Institute Proteomic Core Lab utilized high throughput proteomics to profile proteome-wide changes occurring after TBI in APOE3 and APOE4 transgenic mice. As described in chapter 1, the presence of at least one APOE4 allele is associated with worse outcome from traumatic brain injury in humans and mice (Friedman et al., 1999, Sabo et al., 2000, Crawford et al., 2002, Smith et al., 2006). Because APOE genotype influences outcome from TBI, differential proteomic responses in mice transgenic for human APOE3 and APOE4 over a null mouse APOE background may reveal molecular pathways involved in determining the relative outcome from TBI. I analyzed the data generated from our proteomic analysis in order to find molecular pathways that were associated with the differential response of APOE3 and APOE4 transgenic mice to TBI.

In order to study molecular changes occurring after TBI in an unbiased manner, we utilized a state of the art proteomic platform suitable for analysis of complex biomatrices (i.e. hippocampal and cortical brain tissue). Traditionally

proteomic analyses was performed using two-dimensional gel electrophoresis, separating proteins first by their isoelectric point, then by their molecular mass. Separated proteins are then resolved as discrete spots on the gel and densitometry is used to compare their relative amounts. The individual spots may then be extracted from the gel and analyzed by mass spectrometry in order to identify the protein. This technique is imited, however, as low abundance proteins are lost and proteins with extremes of charge or mass are not resolved (Gygi et al., 2000). To overcome these limitations, the preferred contemporary approach utilize multidimensional liquid chromatography combined with mass spectrometry to separate proteins in a liquid phase without losses from gel transfers and limited gel resolution (Link et al., 1999). Though this improves resolution and the ability to detect lower abundance proteins, there are still limitations; because this is not a fixed array such as a gene chip with pre-defined probes for specific proteins, you do not detect the same set of proteins each time. Nevertheless, this technique provides superior separation to gel techniques. Liquid chromatography/mass spectrometry (LC/MS) techniques are currently employed by the Roskamp Institute Proteomic Core lab in order to separate complex mixtures of proteins from a diverse range of sources including human and mouse plasma, cell culture and dissected brain tissue from mouse models of human conditions, including our mouse modes of TBI.

The proteomic pipeline begins with the isolation of soluble and insoluble fractions from the protein sample, and digestion with an appropriate protease, typically trypsin. Tryptically digested peptides are then separated through multidimensional liquid chromatography before elution into the MS instrument. Mass spectrometric analysis and identification of proteins begins by receiving tryptically digested peptides as they elute from liquid chromatography, followed by electrospray ionization (ESI). Mass spectrometry works by measuring the mass to

charge ratio of each ion (*m/z*), forming a spectra of ions with differing abundances and *m/z* ratios. As peptides are isolated by MS based on their *m/z* ratio in the full scan, they are then fragmented by high energy collision with gas (collision induced dissociation or CID) and then the *m/z* spectrum of the fragmented peptide is generated in a second MS scan (MS/MS). The CID spectra are then compared using an algorithm for matching not only the CID spectra, but also the full scan spectra against the known spectra of tryptically digested peptides (for review, see (Aebersold and Mann, 2003)). The ability to separate and identify many different peptides present in our samples allowed us to take a very broad look at a wide portion of the proteome in each sample studied. Not only does this technique identify the peptide, but the CID spectra also contain the abundances of reporter ions that each have *m/z* ratios unique to the sample they originated from.

For quantitative proteomics we use a method termed Isobaric Tagging for Relative and Absolute Quantitation (iTRAQ) (Ross et al., 2004). iTRAQ uses covalent labels to tag peptides for simultaneous identification and quantitation of samples in a multiplexing manner. Because the samples are labeled in an isobaric manner, the fragmentation spectra for identification form single peaks from all samples. Each sample to be compared is labeled with one tag with a specific *m/z* ratio, allowing for the comparison of 4, 6, or even 8 samples simultaneously. Fragmentation releases the reporter ions, which have masses unique to each sample, allowing for quantitation of each sample simultaneously (Wu et al., 2005). Combined with the separation and identification power of LC-MS/MS methods, this approach enabled in depth proteomic analyses of APOE3 and APOE4 transgenic mice after TBI at multiple timepoints and severities.

We utilized the CCI animal model of TBI (as described in Chapter 2) at different injury depths to induce what we termed for the purposes of this experiment a "mild" and "severe" injury, though both injuries model a penetrating

head wound and are more severe than a non-penetrating head injury. The "mild" injury used a 1.3mm depth while the "severe" injury used a 1.8mm depth level to examine the differences in the proteomic response between different primary injury severities. Since secondary injury is also a delayed and prolonged process, we profiled the proteomic response over time in order to examine temporal changes in molecular profiles. Molecular response to injury was investigated in cortex and hippocampus of the ipsilateral hemisphere at 24 hours, 1 month, and 3 months in severely injured mice, and at 24 hours and 1 month in mildly injured mice with both APOE3 and APOE4 mice for a total of 10 datasets (See flow chart figure 3-1). To the best of our knowledge, no one has yet carried out such a detailed characterization of the consequences of TBI in an animal model, let alone including differential outcome as an additional variable. The long-term clinical consequences for TBI in human APOE4 carriers relative to non-E4 carriers are known (Friedman et al., 1999, Crawford et al., 2002, Smith et al., 2006), and similar observations have been made in APOE mouse models (Sabo et al., 2000, Hartman et al., 2002); thus the underlying hypothesis is that proteomic profiles of APOE4 mice after injury correlate with unfavorable outcome compared to APOE3.

Analysis of our proteomic data revealed many different injury-dependent cellular responses, as well as responses that were significantly different in APOE3 versus APOE4 mice. Among these, the importance of nuclear factor kappa B (NF-kB) related proteins after TBI was evident, as well as cellular inflammation. In order to identify early markers of later outcome, particularly at timepoints more acute than 24 hours, we focused on potential early responders from inflammatory mechanisms and examined mouse brain tissue at 1, 6, 12, 24, 48 hours after injury. Because NF-kB itself is such a fast responder to TBI and previous groups have shown that it has already peaked in response in 4 hours or less after TBI (Sanz et al., 2002), we targeted cytokines downstream of NF-kB including

interleukin-6 (IL-6), interleukin-1B (IL-1B), and monocyte chemotactic protein-1 (MCP-1) expecting that these inflammatory molecules would be up-regulated at acute timepoints after TBI and provide a rapid panel of markers that could be correlated to outcome at later timepoints. Previous studies have shown that these markers can become elevated very quickly after TBI (Morganti-Kossmann, Cristinia et al. 2002) IL-6 expression is activated by NF-kB in cooperation with c-Jun (Xiao et al. 2004) and its concentration in serum is thought to correlate with the severity of injury (Kalabalikis et al., 1999). NF-kB also induces transcription of IL-1B (Cogswell et al., 1994) and studies have shown that reducing IL-1B after TBI may be neuroprotective (Clausen et al., 2011). MCP-1 is also regulated by NF-kB (Donadelli et al., 2000) and is involved in macrophage recruitment in TBI (Semple et al., 2009). In this acute study, in addition to the CCI and sham controls we also included a CHI model recently developed in-house, as a model of mild TBI/concussion as this is increasingly recognized to be a major health concern.

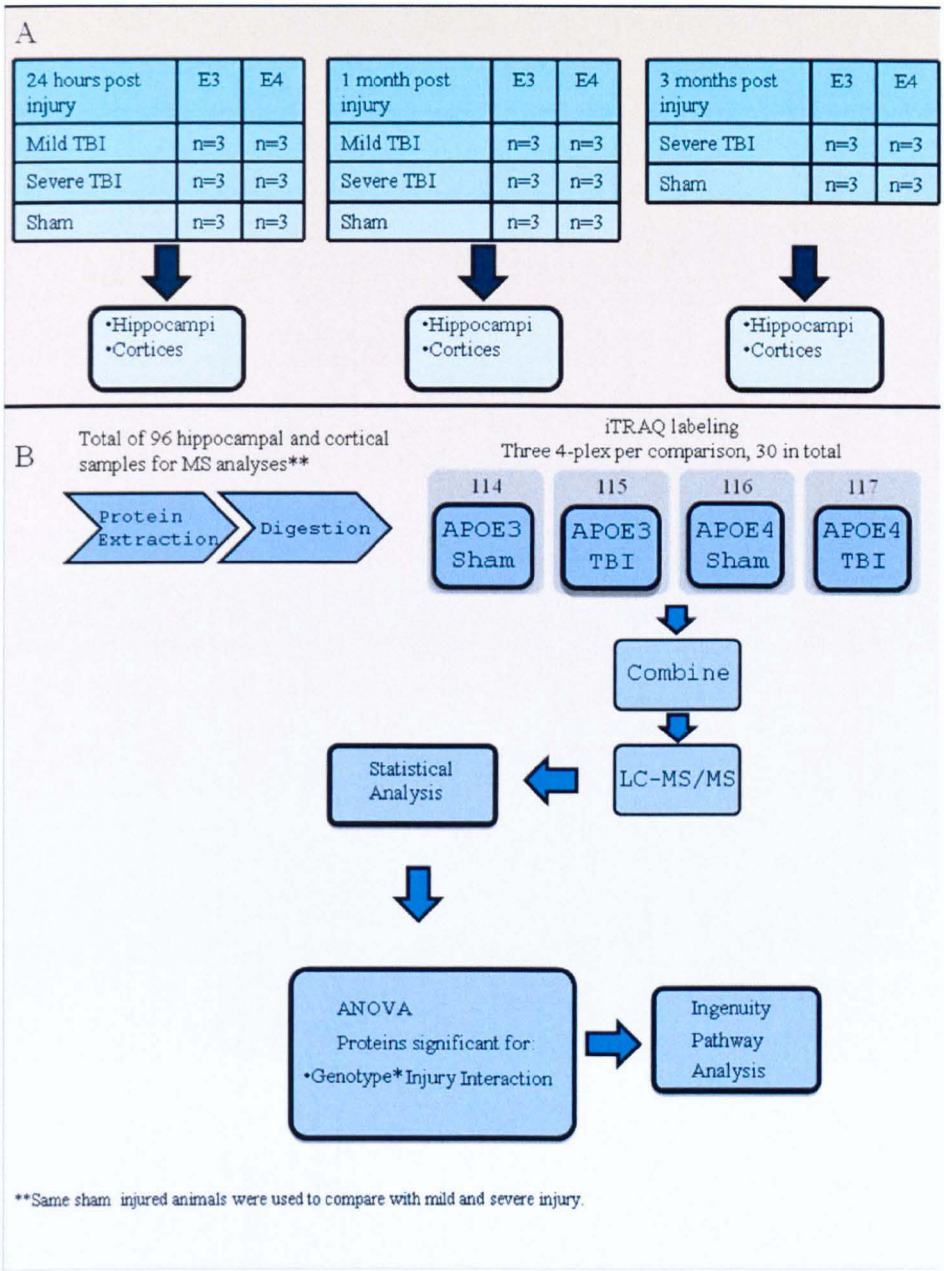

Figure 3-1. Proteomic analysis outline flowchart.

Time	Tissue	TBI	Number of significantly modulated proteins				Number of significantly modulated canonical pathways	
			Injury	Genotype	Interaction	Total	Injury	Interaction
24 hours	Cortex	Mild	131	23	20	156	37	2
1 Month	Cortex	Mild	31	25	31	69	3	29
24 hours	Hippocampus	Mild	47	17	23	62	38	30
1 Month	Hippocampus	Mild	15	10	18	36	4	14
24 hours	Cortex	Severe	27	15	11	42	8	8
1 Month	Cortex	Severe	35	51	32	91	21	12
24 hours	Hippocampus	Severe	24	19	19	46	10	10
1 Month	Hippocampus	Severe	34	24	40	75	61	26
3 Months	Cortex	Severe	10	10	9	19	9	22
3 Months	Hippocampus	Severe	19	15	24	42	10	15

Table 3- 1 Breakdown of significantly modulated proteins within the proteomic datasets

Materials and Methods

In order to elucidate the mechanisms driving the APOE-genotype dependent response to TBI, a mild or severe (n = 3 per group) controlled cortical impact (CCI) or sham injury was administered to APOE3 and APOE4 hemizygous transgenic mice (described in Xu et al 1996) as described in chapter 2. Mice were then euthanized at 24 hours, 1 month, or 3 months (severe only) after injury for proteomic and immunohistochemical analysis of dissected regions of the brain, including the cortex and hippocampus. Mice were euthanized by isoflourane followed by intracardial PBS perfusion. For the ELISA studies, mice were euthanized at 1, 6, 12, 24, or 48 hours after CCI using the same protocol.

Sample Preparation for iTRAQ

At euthanasia, mouse brains were perfused with chilled 1X PBS. Brains were dissected into hemispheres, then cortices, hippocampi and cerebella at 4°C, and snapfrozen in liquid nitrogen (cerebellar and contralateral samples have been stored for future analyses). The entire hippocampus and cerebrocortex from the

ipsilateral hemisphere were dissected for analyses; not a specific region relative to the injury impact site. For all mice, soluble proteins from the ipsilateral hippocampi and cortices were extracted by sonication of tissue samples in 500µl chilled 1X PBS, supplemented with a protease inhibitor cocktail (Roche) and centrifugation at 100,000 x g (adapted from the methodology employed in (Abdullah et al., 2011)). The soluble fraction was quantified using the BCA assay, and verified by SDS-PAGE. There were a total of 96 samples to analyze – with 3 mice per group, 2 genotypes (APOE3, APOE4); 3 types of injury (sham, mild, severe); 3 timepoints (24hr and 1 month for all three injuries; 3 month for sham and severe) and 2 brain regions (cortex and hippocampus). For further details see appendices B and C.

Mass Spectrometry

Mass spectrometry analyses were carried out by the Roskamp Institute Proteomics Core Team. We used 4-plex iTRAQ with each plex containing one APOE3 sham, one APOE4 sham, one APOE3 TBI and one APOE4 TBI sample for direct comparison. Thus with three biological replicates per group there were three 4-plex for each comparison. Within each plex samples were from one brain region and one timepoint. The sham samples from each timepoint provided the control samples for both mild and severe injury samples. A total of 30 plexes were run in order to complete this experiment Samples were analyzed by LC-MS/MS methods with iTRAQ quantitation as described in Crawford (2012) or appendices B and C.

iTRAQ Data Analysis

LC- MS/MS data were analyzed using the SEQUEST search algorithm and datasets were generated by the Roskamp Institute Statistical Analysis and Data Management Core lab for all proteins for which the variable interactive term of "Genotype*Injury" was statistically significant according to ANOVA. The ratios of

E3 TBI/ E3 Sham and E4 TBI/ E4 Sham were calculated for each peptide and the arithmetic means of these ratios were reported for each protein. For further details see appendices B and C.

Data Analysis

LC- MS/MS data (*.raw) files were transferred to Bioworks 3.3.1 (Thermo Electron) to identify peptides using the SEQUEST search algorithm. The spectra were searched against the IPI.MOUSE.v3.59 database using the following search criteria: maximum allowed missed cleavages for trypsin, 2; fixed modifications of +57.02146 for IAA-modified cysteine residues; and variable modifications of +144Da for iTRAQ-labeled peptide N-termini and lysine side chains, and +15.99491 for oxidized methionine. The resulting Bioworks .SRF files were then converted to .OUT and .DTA files in order to import the results into the Trans Proteomic Pipeline (TPP) v 4.2 where peptides (and their corresponding proteins) were quantified using the Libra feature of the TPP software, where the reference ions are set as 114.1, 115.1, 116.1, and 117.1. The PeptideProphet feature of TPP was used to calculate a probability value for each peptide and these probabilities were used to set a false discovery rate (FDR) of 0.05. Peptides with a probability value equal to or higher than this cutoff value were exported to Excel. The Excel files were imported to JMP (SAS) 8.0.2 for data cleaning and statistical analysis. Ions counts below 20 were zeroed, peptides that did not yield any ion count for any of the iTRAQ labels were deleted. Proteins identified with 2 or more peptides were used for the quantitative analysis, but proteins identified by a single peptide were only included in the analysis if the same peptide was identified in multiple biological replications.

Reporter ion peaks extracted from the mass spectra in this study were analyzed by ANOVA using models adapted from (Hill et al., 2008) that were

crafted specifically for iTRAQ experiments. All reporter ion peak intensities were ln transformed to make intensity data additive, and the loading bias was removed by mean normalization on each replication and label.

$$ymijklh=\mu+rm+bi+pj+fk(j))+gl+sh+g*sl(h)+emijklh \quad (1)$$

where: μ is the population mean; r_m is the fixed effect of the iTRAQ plex; b_i is the mouse ~NID(0,σ^2_b), i=1 to 3; p_j is the random variable protein incomplete block ~NID(0,σ^2_p); $f_{k(j)}$ is the random variable peptide incomplete block ~NID(0,σ^2_f); g_l is the fixed variable Genotype; s_h is the fixed variable Injury; $g*s_{l(h)}$ is the fixed variable Genotype*Injury interaction ~NID(0,σ^2_{g*s}); e_{mijklh} is the random variable error within the experiment ~NID(0,σ^2_e). This linear model was used to analyze each TBI severity and time point post-TBI combination dataset separately. Due to the transformation and normalization of the experiments, effect sizes are usually lower than other quantitative approaches such as microarray. Since the effect sizes that we are detecting are small, iTRAQ-based proteomic approaches would necessitate much larger numbers of mice than the N of 3 mice per group possible in this study, thus potentially some important protein responses will have been missed.

We also assessed the coherence of protein expression across biological replicates and found that on average across all experiments proteins were identified in all 3 samples 55% of the time, and in 2 or more samples more than 87% of the time.

Datasets were thus generated for all proteins showing response to TBI, and ANOVA of these quantitative datasets identified proteins for which the variable "Injury" and/or the interactive term of "Genotype*Injury" was statistically significant. Proteins that were significantly regulated with respect to Genotype alone will form the basis of separate analyses and reports. The ratios of E3 TBI/ E3 Sham and

E4 TBI/ E4 Sham were calculated for each peptide and the arithmetic means of these ratios were reported for each protein.

Ingenuity Pathway Analysis

Our datasets containing the list of proteins statistically significant for the interaction of "Genotype*Injury" were uploaded to Ingenuity® Pathways Analysis (IPA). Each protein was mapped to its corresponding object in the Ingenuity® Knowledge Base. The "Network Eligible" molecules, were overlaid onto a global Ingenuity Systems molecular network developed from information contained in the Ingenuity Knowledge Base, containing 1,510,000 biological and chemical concepts spanning genes, proteins, and molecular and cellular processes. Over 19,600 human, 14,700 mouse, and 8,000 rat genes are currently represented in the knowledgebase. Networks of "Network Eligible" molecules were then algorithmically generated based on their connectivity, based on interactions curated from the literature. IPA generates biological networks, canonical pathways and functional groups based on known interactions and relationships. A right-tailed Fisher's exact test is used to calculate a p-value determining the probability that each biological function assigned to a given pathway or functional group is due to chance alone. P-values lower than 0.05 were considered significant.

The custom pathways represented in figures 2, 3 and 4 of this chapter are graphical representations of the molecular relationships between molecules. Molecules are represented as nodes, and the biological relationship between two nodes is represented as a line. All connections are supported by at least one reference from the literature, from a textbook, or from canonical information stored in the Ingenuity Knowledge Base. A bar graph beside each node indicates the degree of up- (red) or down- (green) regulation. Nodes are displayed using various shapes that represent the functional class of the gene product. Lines are displayed

with various labels that describe the nature of the relationship between the nodes (e.g., P for phosphorylation, T for transcription).

Custom pathways were created by seeding to find all the proteins within our datasets that have direct or indirect interactions with CD40/CD40L, NF-kB or APP. The aforementioned molecules acted as the seed point, from there each dataset was queried to expand the network over two iterations using only molecules present in those datasets. Custom pathway creation allows for the exploration of pathways of interest within a dataset (Yaspan and Veatch, 2011).

Tissue preparation for ELISA

For the acute inflammatory cytokine analysis, dissected cortical tissue was homogenized in 500ul M-PER and 1x Halt Protease/Phosphatase Inhibitors, followed by centrifugation at 20,000 g for 20 minutes, then splitting into aliquots and then storage at -80° C. Protein concentration was determined by BCA assay and confirmed by check gel with SYPRO Ruby staining.

Acute Timepoint ELISA Analysis

IL-6 and MCP-1 ELISA kits from Invitrogen were run according to manufacturer's directions, with the exception that each of the primary incubations of the samples were performed overnight at 4 degrees Celsius to minimize non-specific binding. A porcine sample was included in each assay to validate the specificity of the kit. 150 µg of protein were loaded into each well for each ELISA. Samples and standards were run in triplicate. Data are expressed as pg of protein per ml.

Statistical analysis

Reporter ion peaks were analyzed by mixed-model ANOVA to reveal proteins that were significantly different by injury, genotype, and by injury x genotype (interaction). See Crawford (2012). Student's T-Test was also used for

direct comparisons of ELISA results. All statistical analyses were performed using JMP 8.02 (SAS).

Results

A number of proteins (227 total across all 10 datasets; see http://www.rfdn.org/publication-suppl/2011/brain for the full list), were significant for the interactive effect of injury*genotype within each dataset (Table 3-1), and are likely to be important in determining the differential outcome of APOE3 and APOE4 mice. Further analysis by Ingenuity Pathways Analysis (IPA) specifically targeted at these "interactive" proteins showed that they modulate a large number of different cellular functions which we assume to be critical in outcome determination. IPA functional groups showed a number of functions that were regulated across all timepoints and within both the mild and severe injury. These included amino acid metabolism, cellular growth, proliferation, and development, neurotransmitters and nervous system signaling, disease-specific pathways, lipid metabolism and cellular immune response. Pathways such as amino acid metabolism and disease-specific development did not present any targets that would be easily modulated for our studies, and others such as cellular growth, proliferation, and development may be indicative of reparative processes occurring after TBI. Neurotransmitters and nervous system signaling may be indicative of differential excitotoxicity, but given the heavy focus already paid to that aspect of TBI (Palmer et al., 1993, Gong et al., 1995, Obrenovitch and Urenjak, 1997, Raghavendra Rao et al., 2001, Muir and Teal, 2005), we decided to focus our efforts elsewhere. Based on in-house expertise and resources, we decided to focus on cellular immune response and related pathways in order to find potential treatments. IPA canonical pathways also showed NF-kB- to be significantly regulated at 1 month in the cortex in the mild injury ($p<0.05$). Given these results I created custom functional pathways based on NF-kB, APP, and CD40/CD40L

related molecules within our datasets (Yaspan and Veatch, 2011). The datasets themselves were used to seed these pathways, with each of the 10 being used to build the network through direct or indirect effects on each of the starting molecules over two iterations. This allowed me to examine the direct and indirect response of molecules related to CD40/CD40L, NF-kB, and APP, if any, with the caveat of potential biasing towards these particular pathways at the exclusion of others.

Table 3-2 Custom functional pathways at various timepoints.

Timepoint	Tissue	TBI	Number of proteins significant for injury * genotype	Number of CD40/CD40L related proteins	Percent of CD40 related to total	Number of NF-kB related proteins	Percent of NF-kB related to total	Number of APP related proteins	Percent of APP related to total
24hr	Cortex	Mild	20	6	30%	4	20%	6	30%
24hr	Cortex	Severe	11	2	18%	2	18%	7	64%
24hr	Hippocampus	Mild	23	3	13%	3	13%	12	52%
24hr	Hippocampus	Severe	19	6	32%	8	42%	9	47%
1 month	Cortex	Mild	31	9	29%	9	29%	15	48%
1 month	Cortex	Severe	32	8	25%	9	28%	13	41%
1 month	Hippocampus	Mild	18	8	44%	7	39%	11	61%
1 month	Hippocampus	Severe	40	7	18%	7	18%	16	40%
3 months	Cortex	Severe	9	5	56%	6	67%	6	67%
3 months	Hippocampus	Severe	24	11	46%	11	46%	18	75%

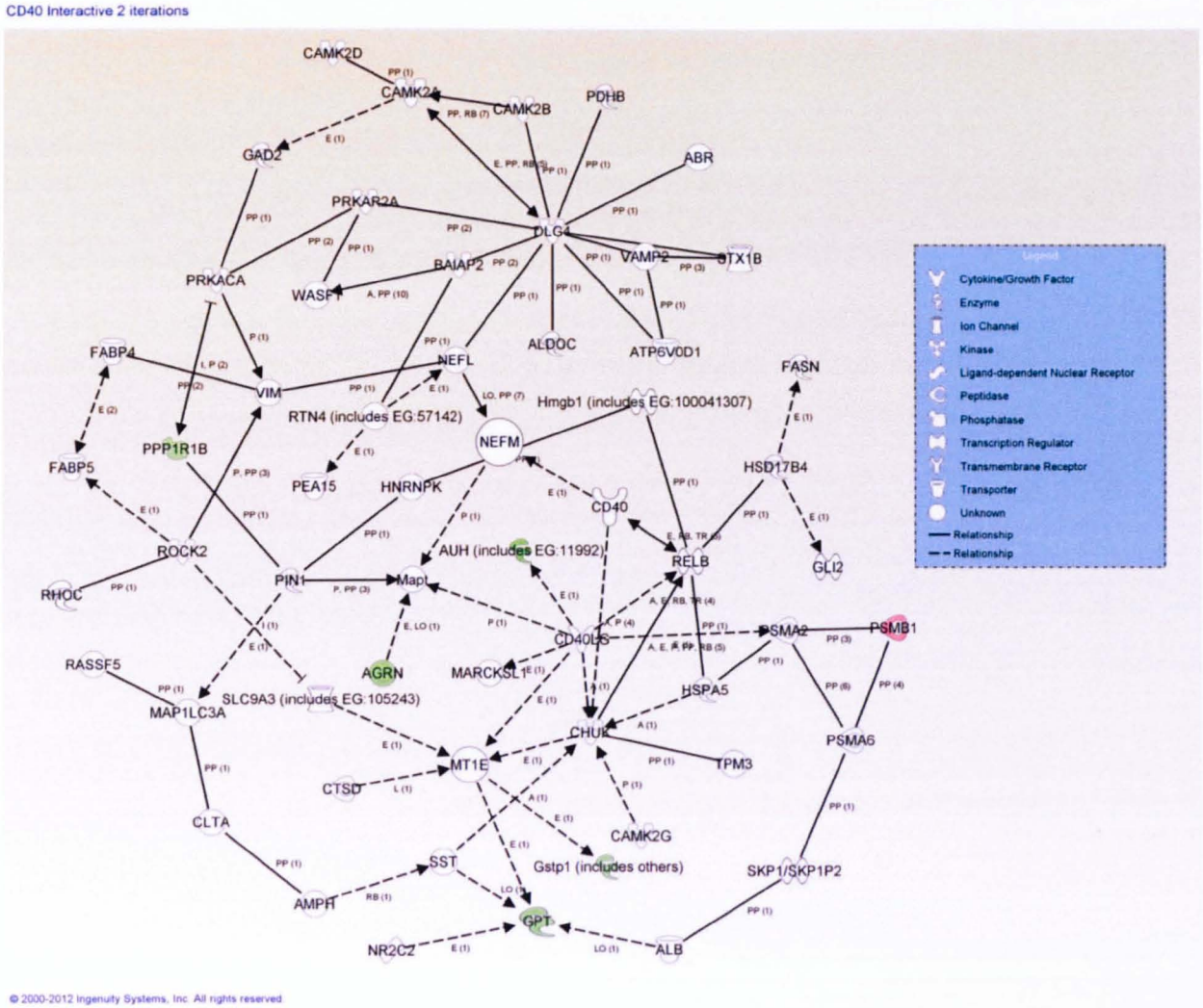

Figure 3-1A. CD40/CD40L related protein pathway overlayed with protein changes in cortical tissue 24 hour after-mild injury from an E4 mouse

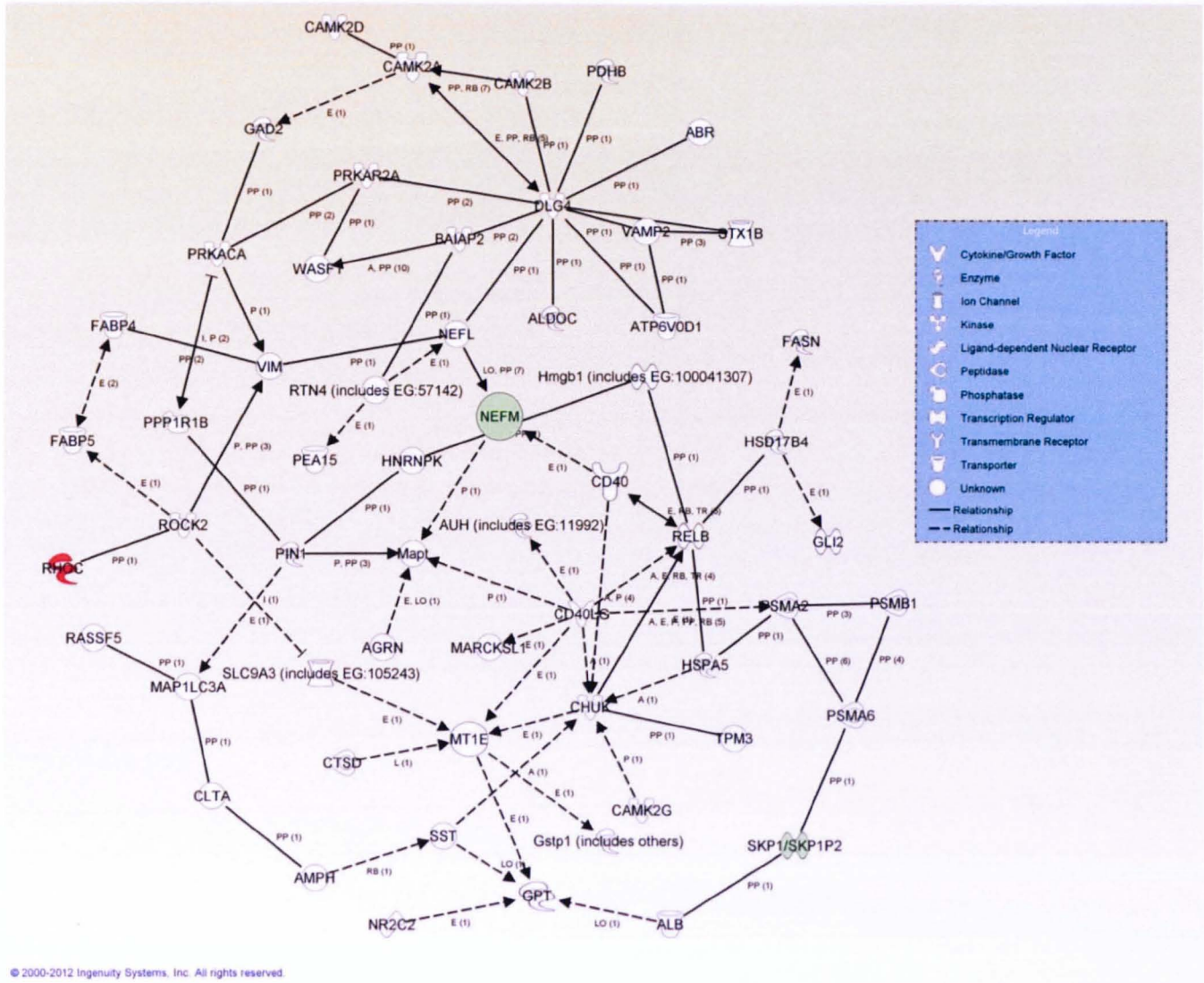

Figure 3-1B -CD40/CD40L related protein pathway overlayed with protein changes in hippocampus tissue 24 hour after a -mild injury from an E4 mouse.

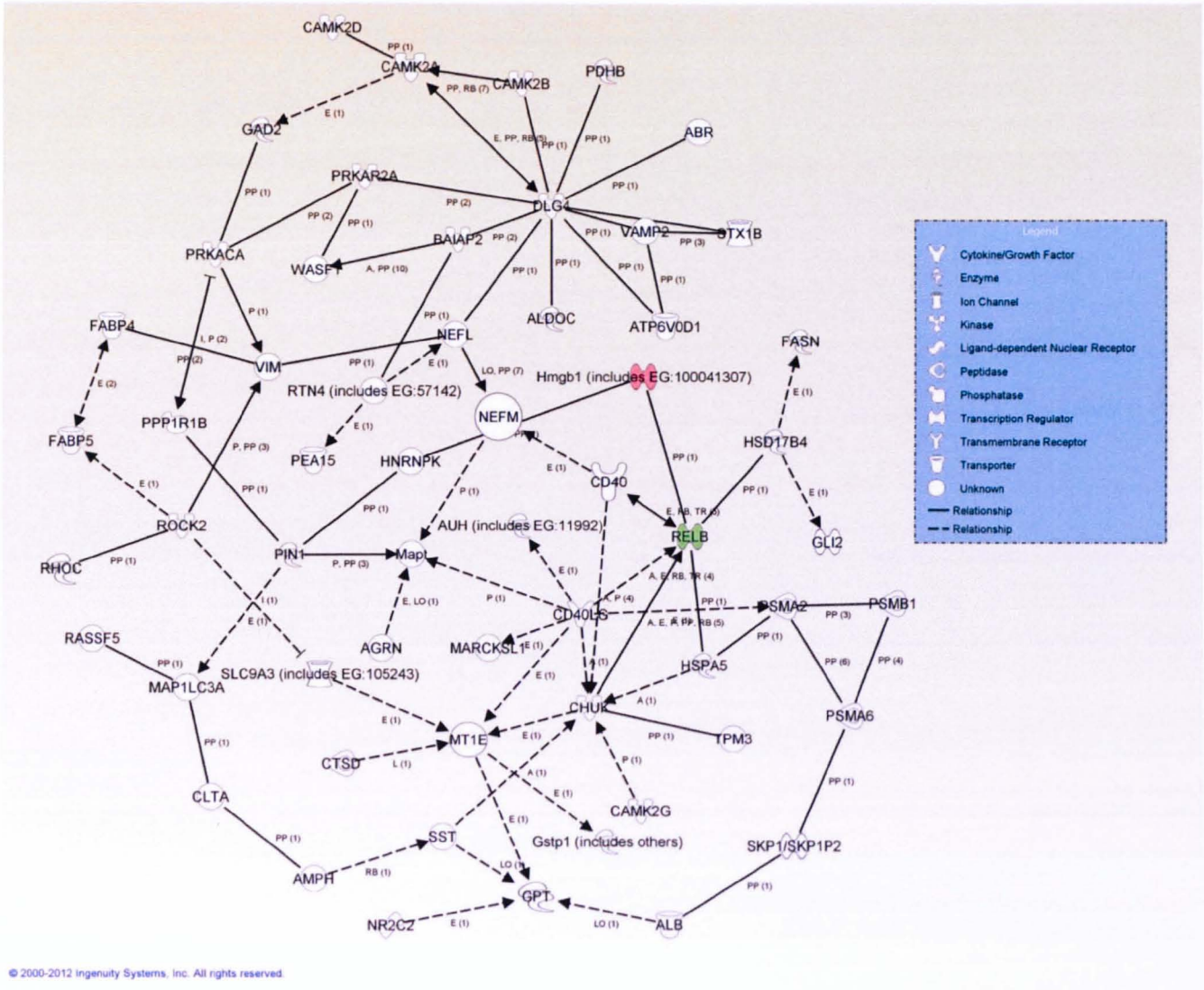

Figure 3-1C -CD40/CD40L related protein pathway overlayed with protein changes in cortical tissue 24 hours after a severe injury in an E4 mouse.

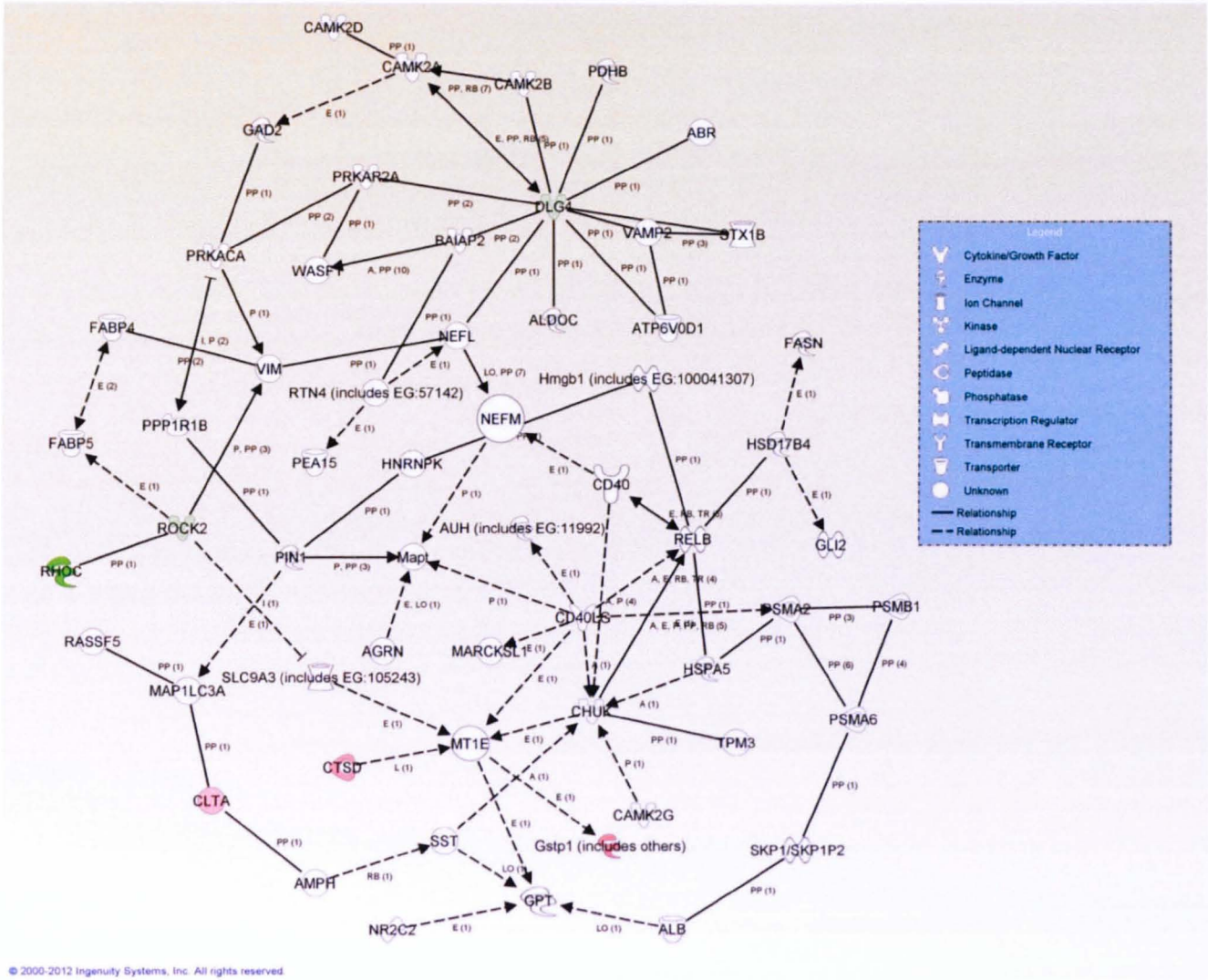

Figure 3-1D -CD40/CD40L related protein pathway overlayed with protein changes in hippocampus tissue 24 hours after severe injury from an E4 mouse.

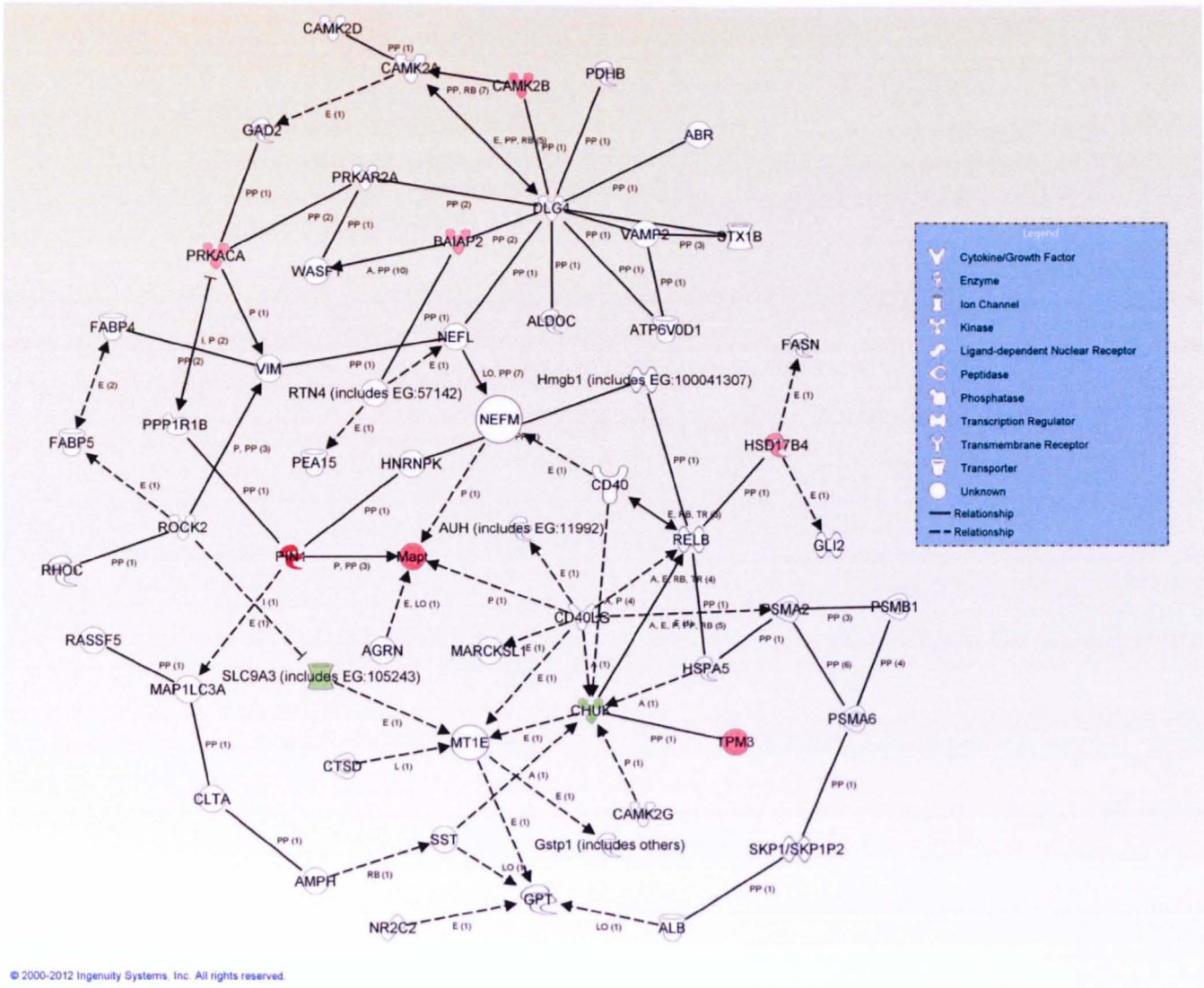

Figure 3-1E -CD40/CD40L related protein pathway overlayed with protein changes in cortical tissue 1 month after mild injury from an E4 mouse.

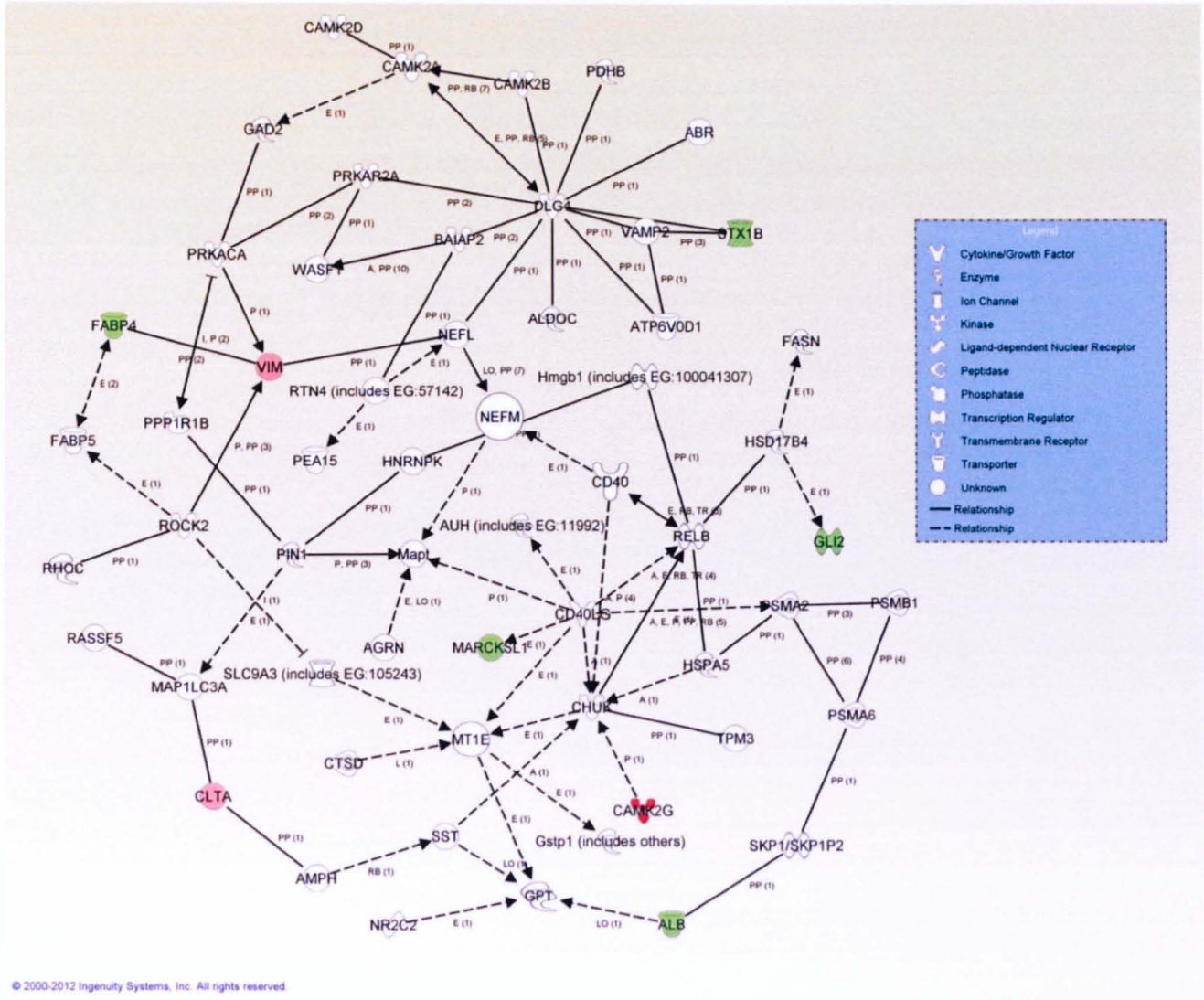

Figure 3-1F -CD40/CD40L related protein pathway overlayed with protein changes in hippocampus tissue 1 month after severe injury from an E4 mouse.

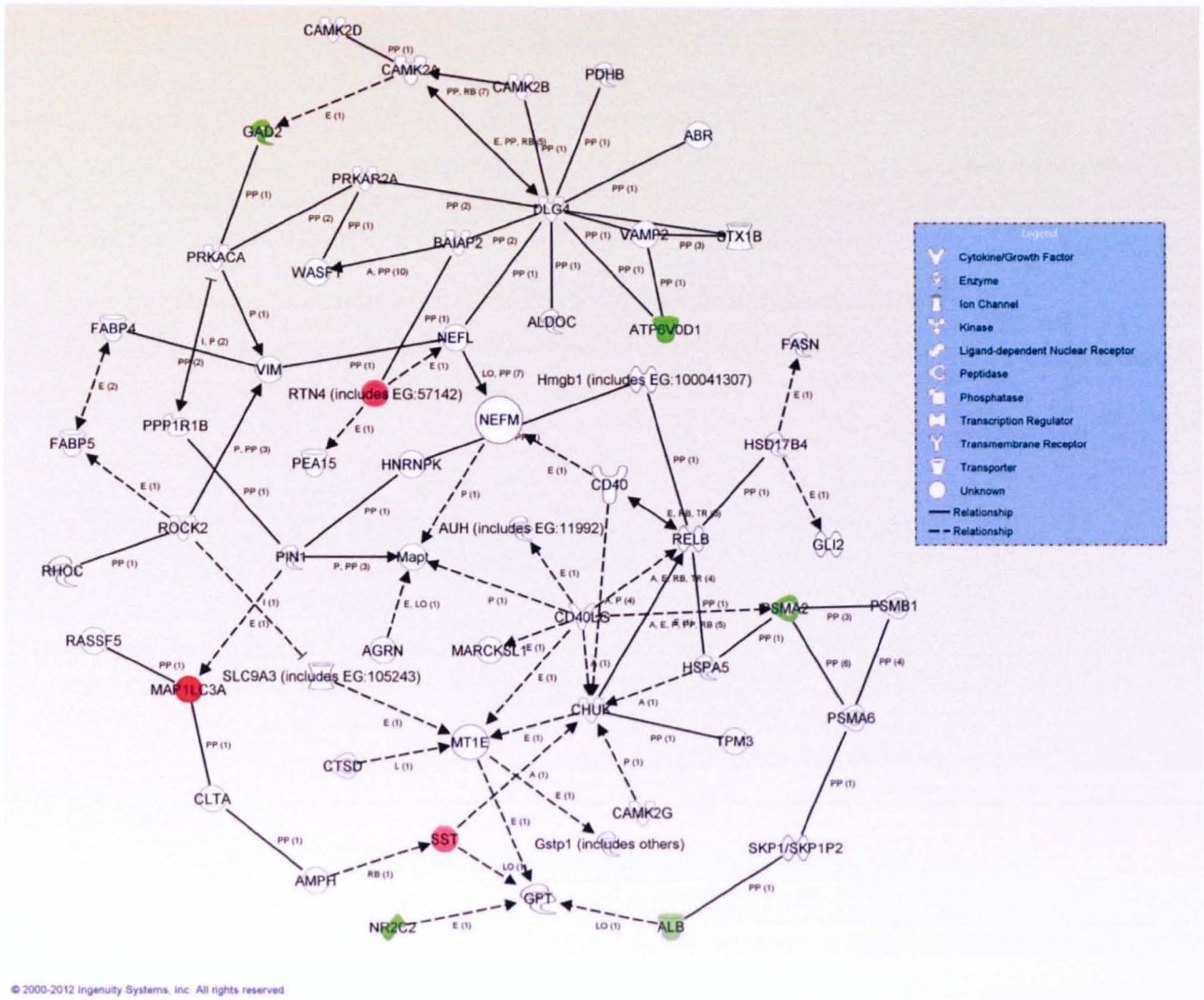

Figure 3-1G -CD40/CD40L related protein pathway overlayed with protein changes in cortical tissue 1 month after severe injury in an E4 mouse.

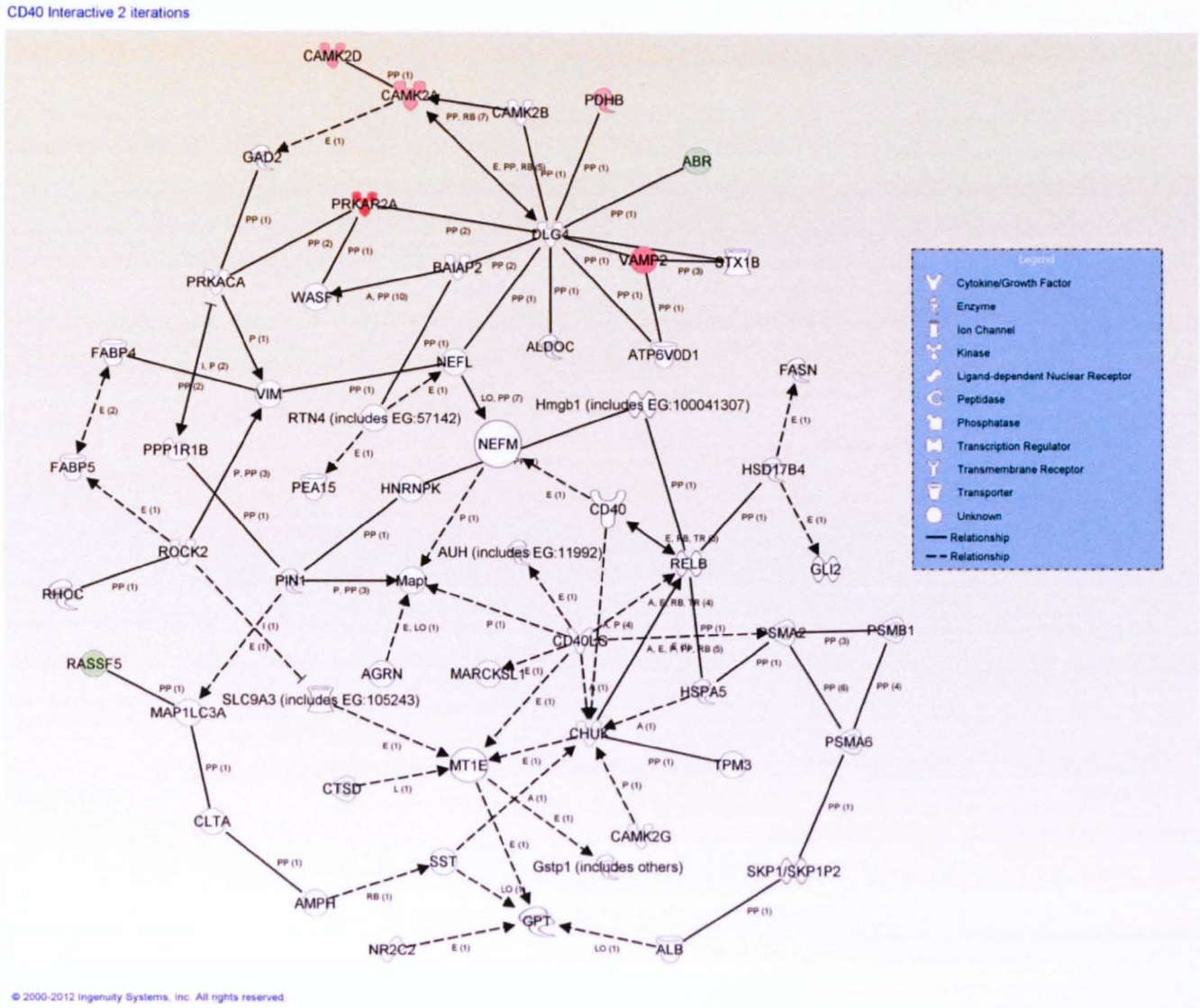

Figure 3-1H -CD40/CD40L related protein pathway overlayed with protein changes in hippocampus tissue 1 month after severe injury from an E4 mouse.

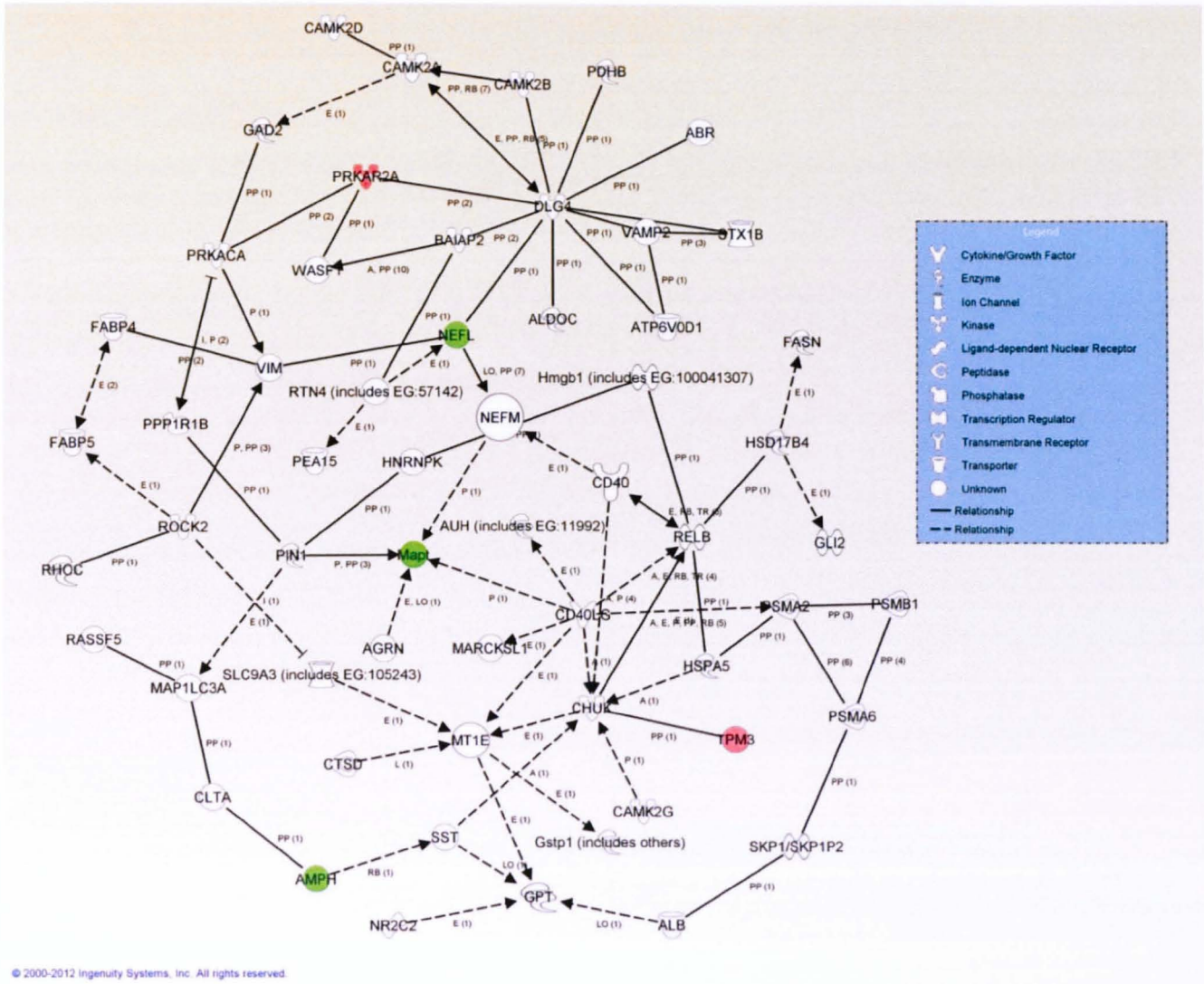

Figure 3-1I -CD40/CD40L related protein pathway overlayed with protein changes in cortical tissue 3 months after severe injury from an E4 mouse.

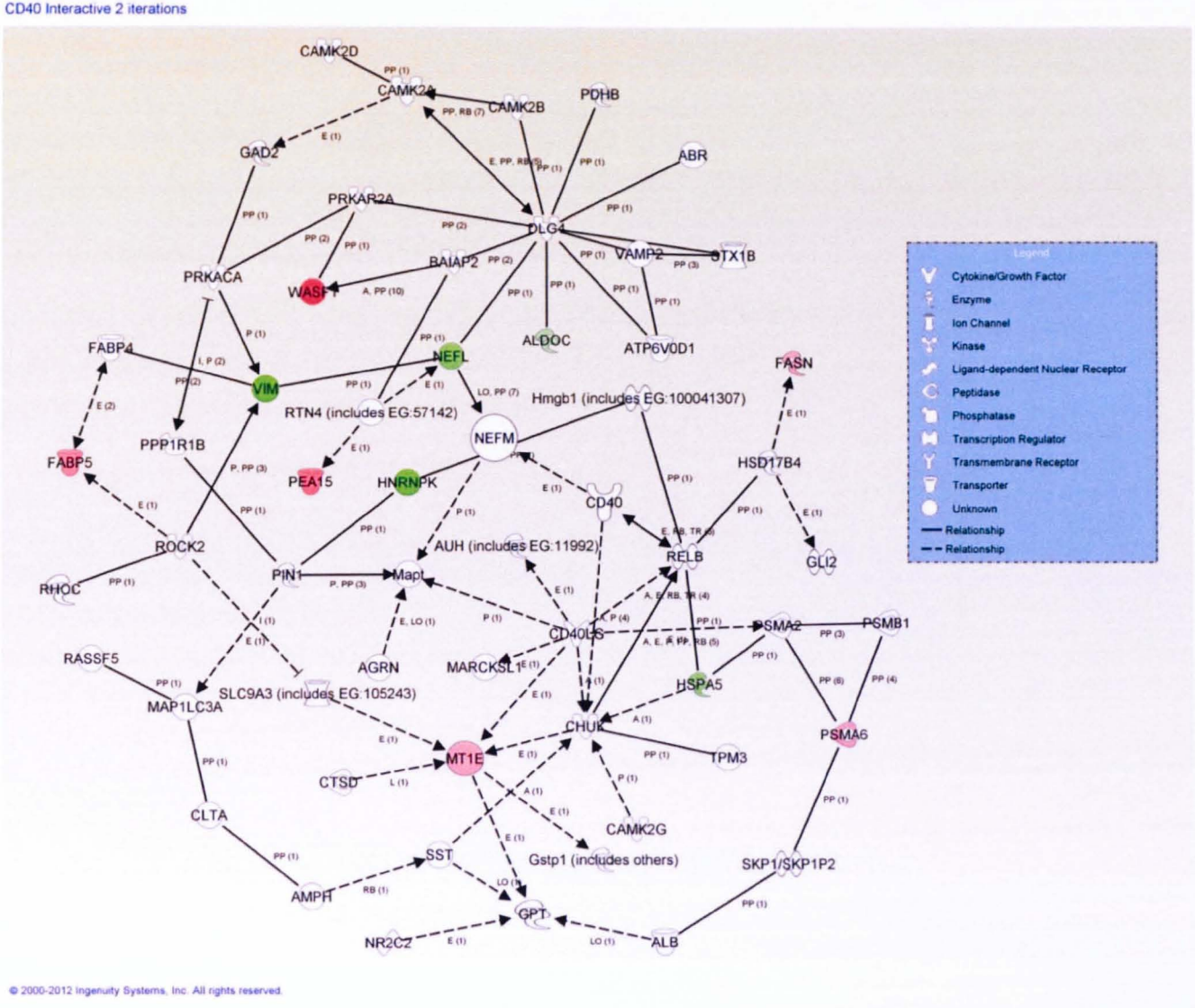

Figure 3-1J -CD40/CD40L related protein pathway overlayed with protein changes in hippocampus tissue 3 months after severe injury from an E4 mouse.

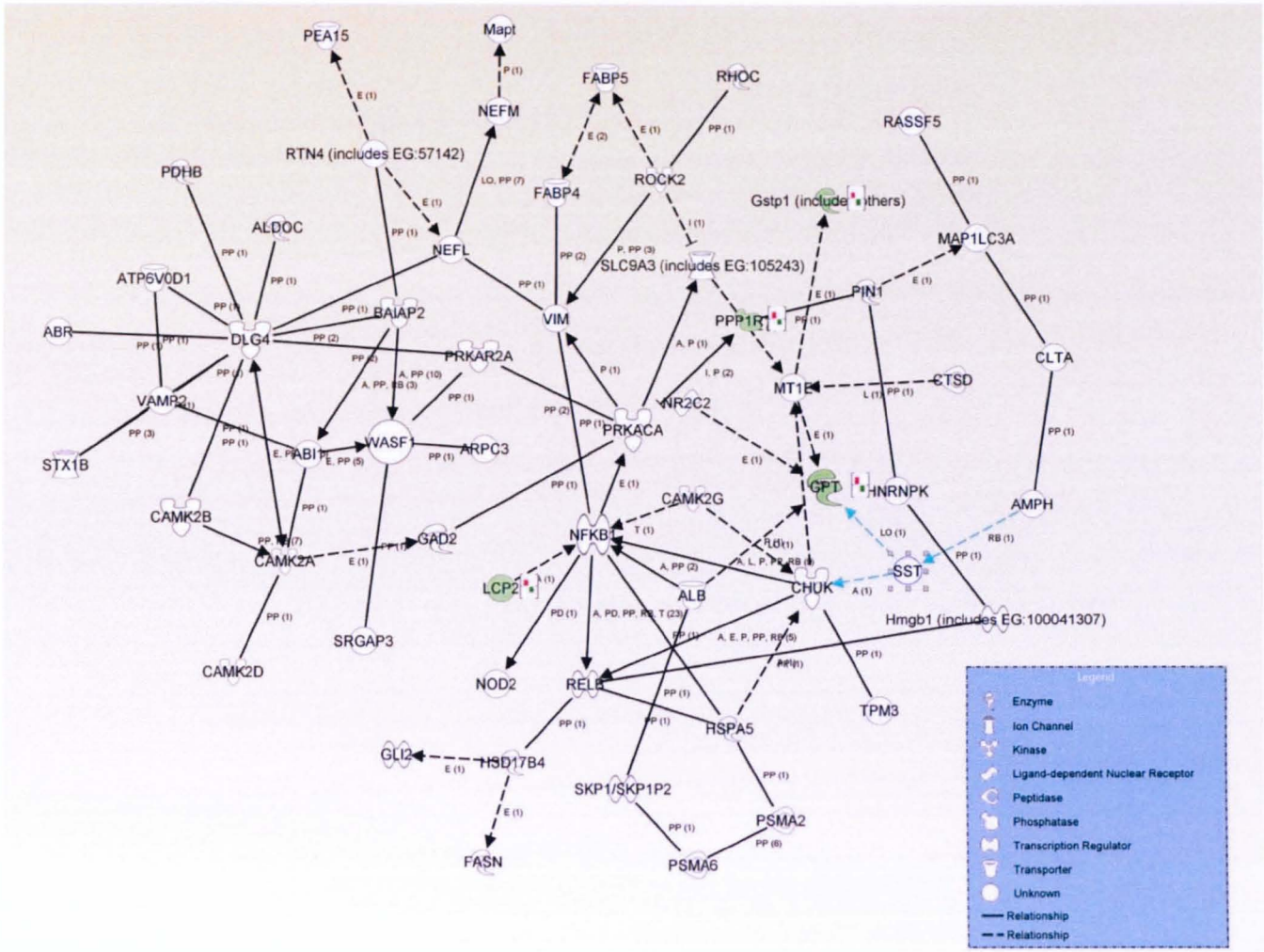

Figure 3-2A -NF-kB related protein pathway overlayed with protein changes in cortical tissue 24 hours after mild injury in an E4 mouse.

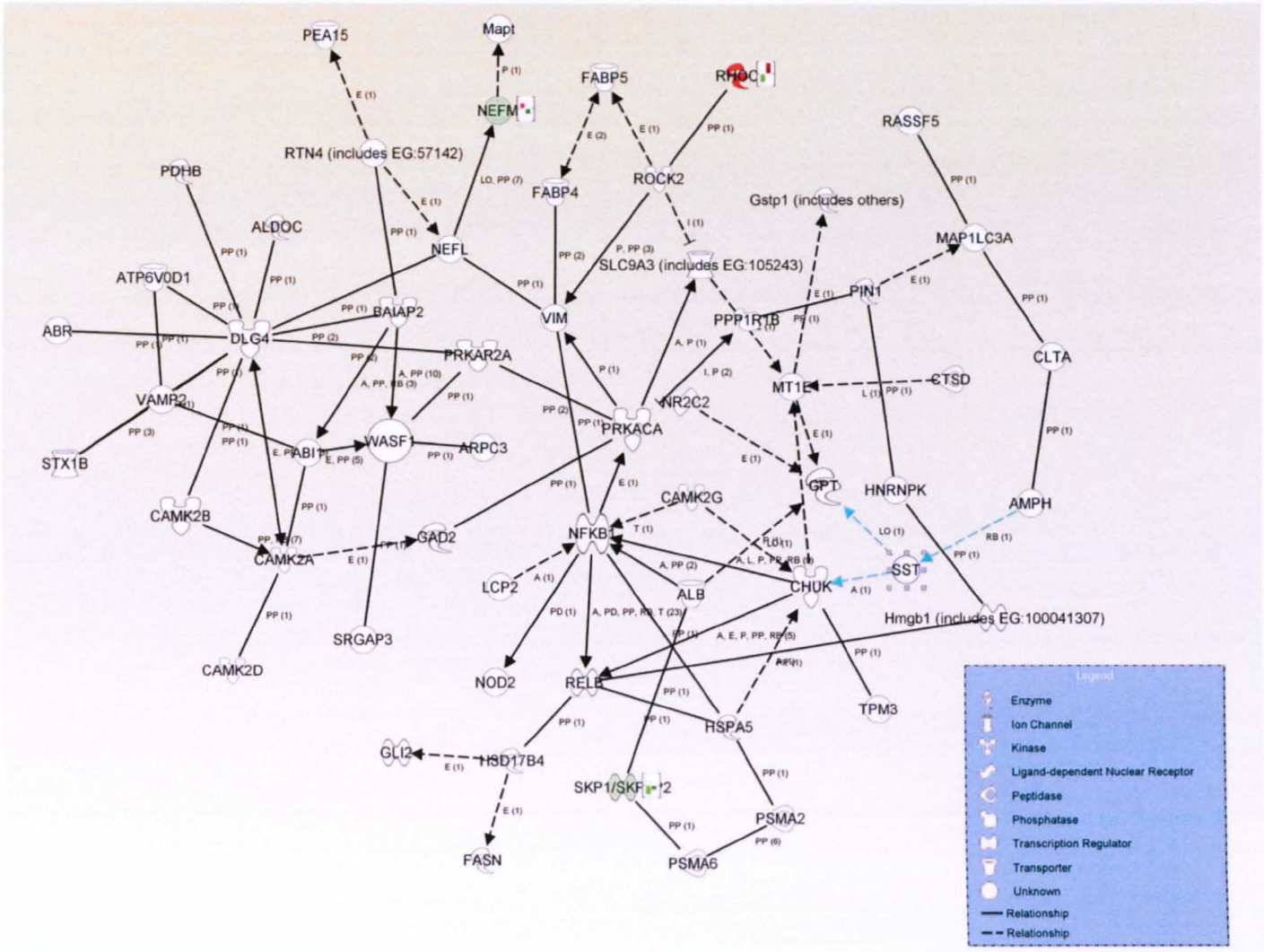

Figure 3-2B -NF-kB related protein pathway overlayed with protein changes in hippocampus tissue 24 hours after mild injury from and E4 mouse.

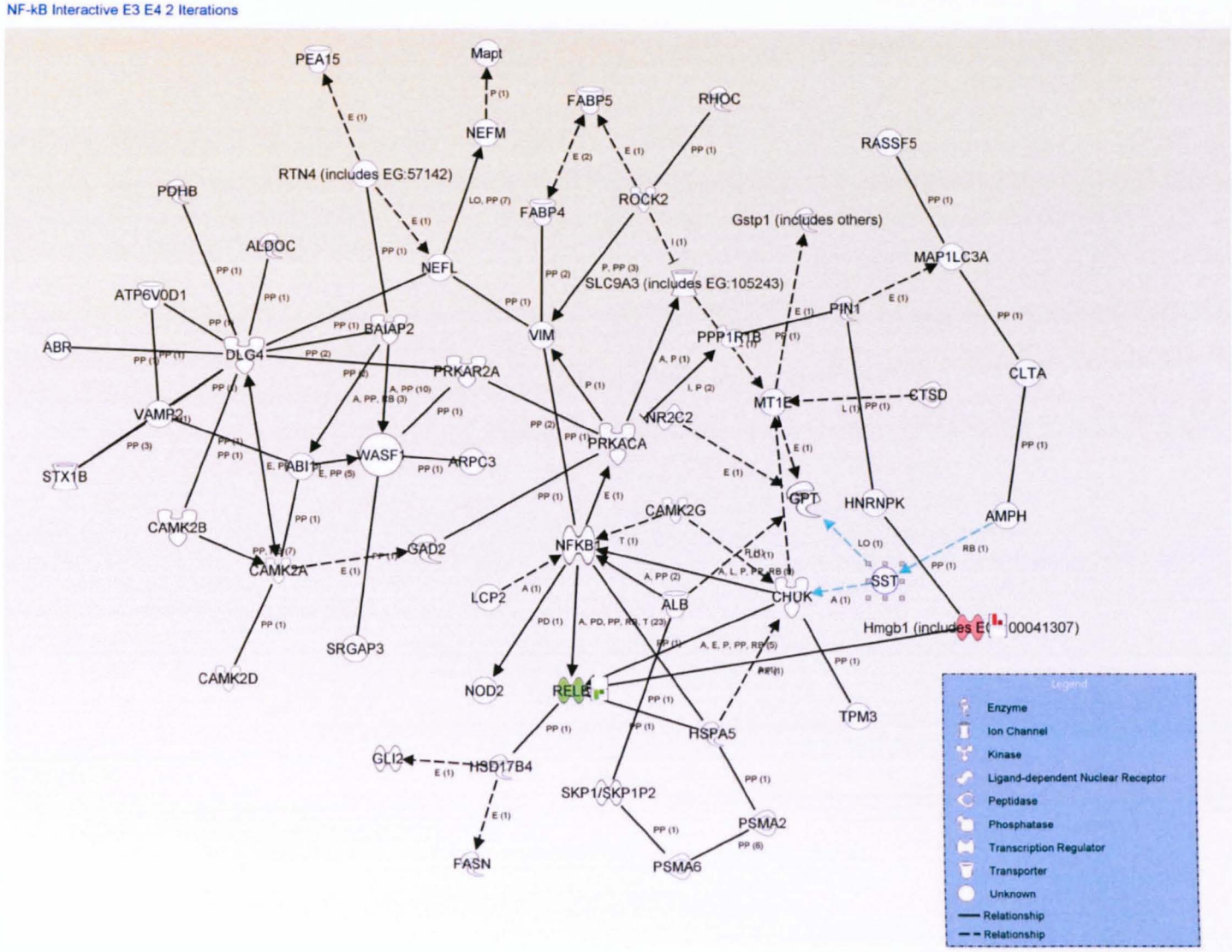

Figure 3-2C -NF-kB related protein pathway overlayed with protein changes in cortical tissue 24 hours after severe injury from an E4 mouse.

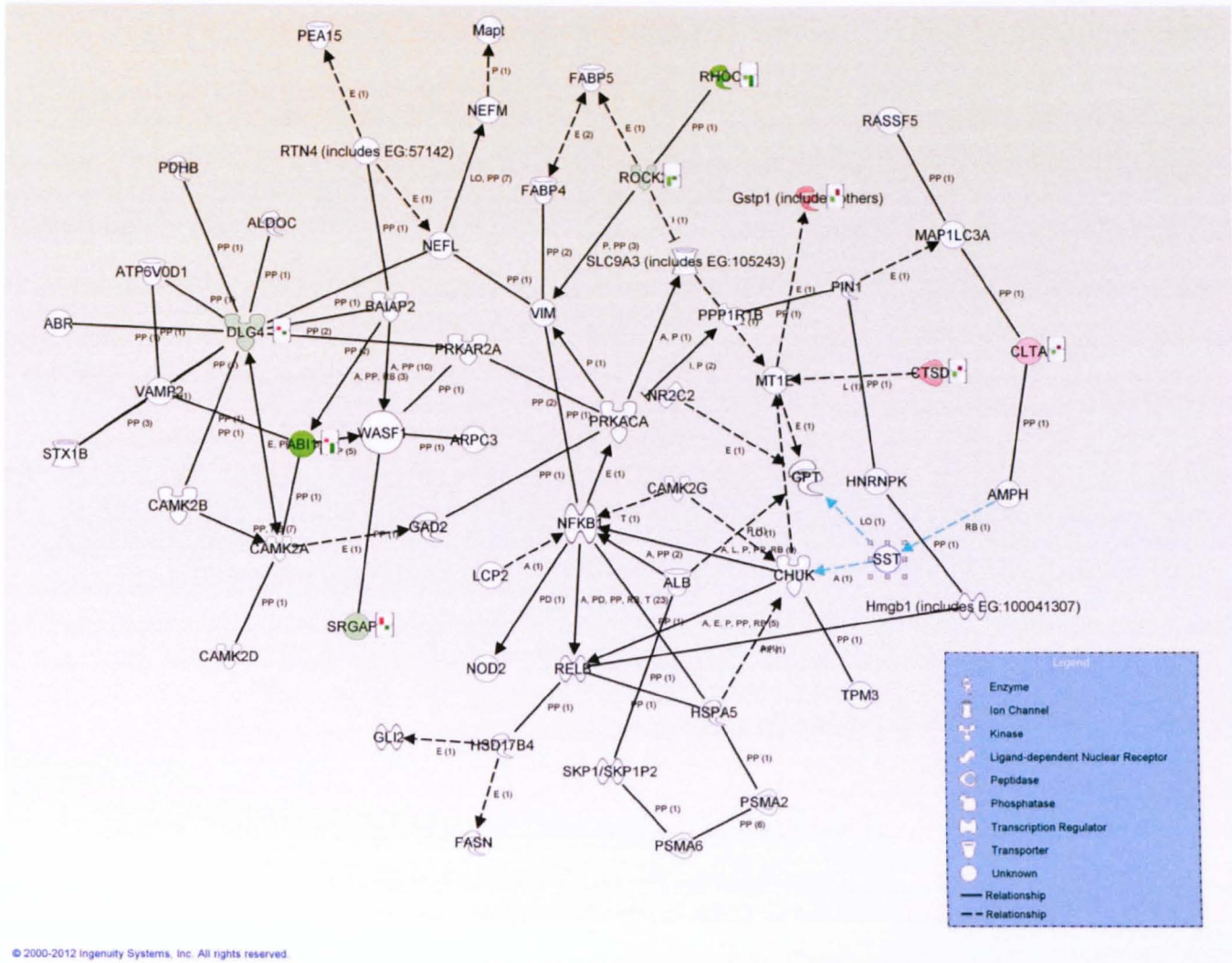

Figure 3-2D -NF-kB related protein pathway overlayed with protein changes in hippocampus tissue 24 hours after severe injury from an E4 mouse.

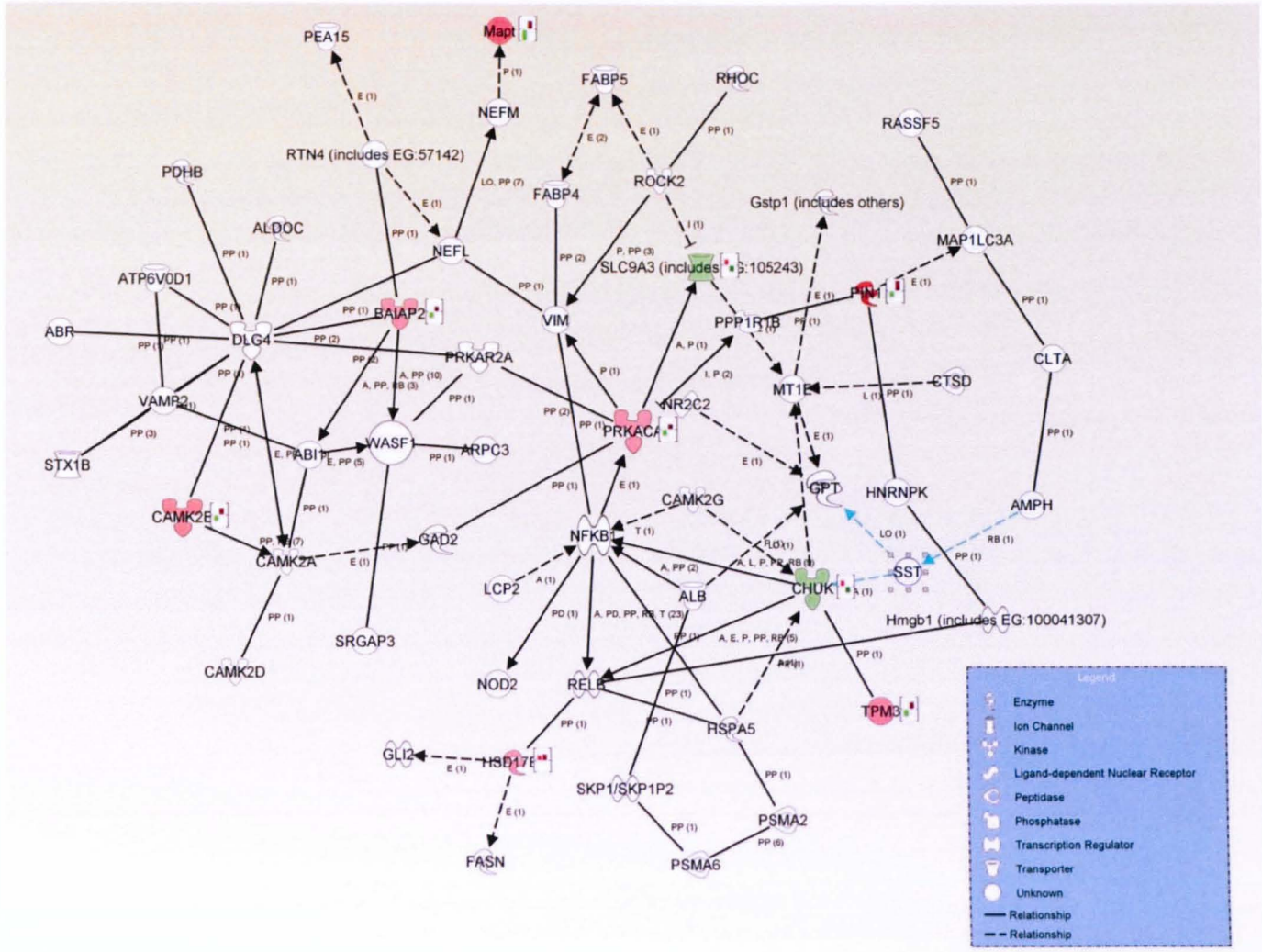

Figure 3-2E -NF-kB related protein pathway overlayed with protein changes in cortical tissue 1 month after mild injury from an E4 mouse.

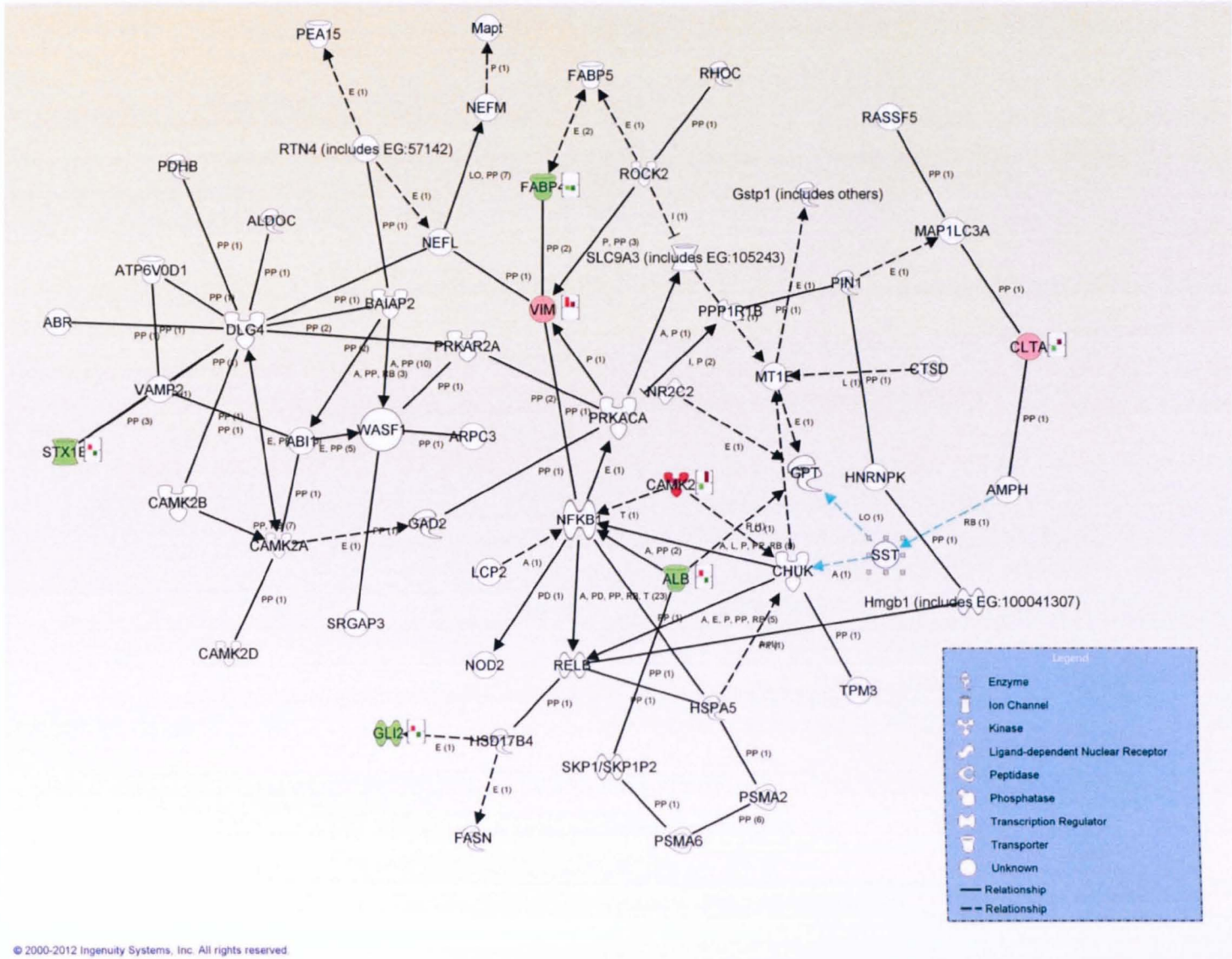

Figure 3-2F -NF-kB related protein pathway overlayed with protein changes in hippocampus tissue 1 month after mild injury from an E4 mouse.

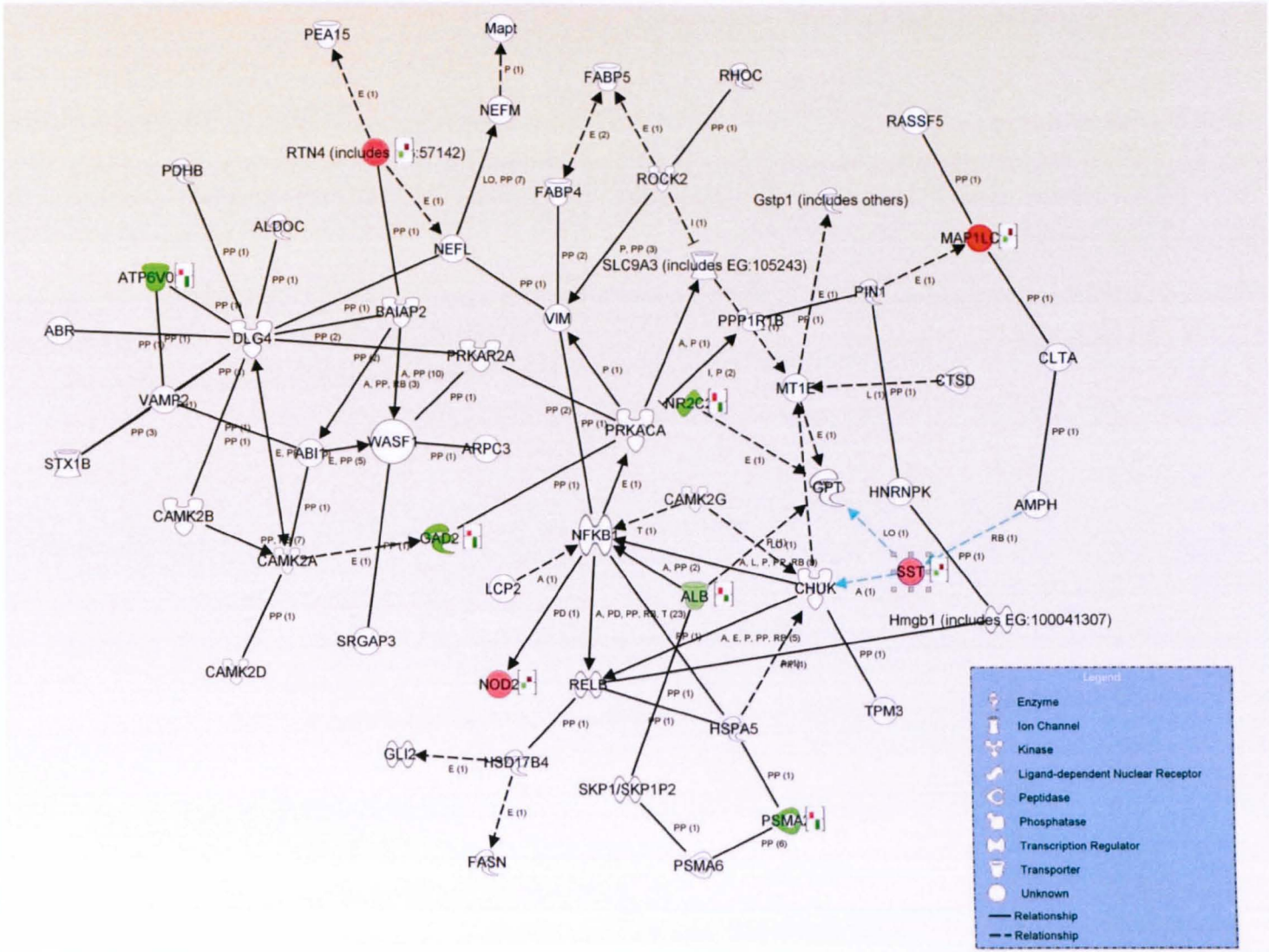

Figure 3-2G -NF-kB related protein pathway overlayed with protein changes in cortical tissue 1 month after severe injury from an E4 mouse.

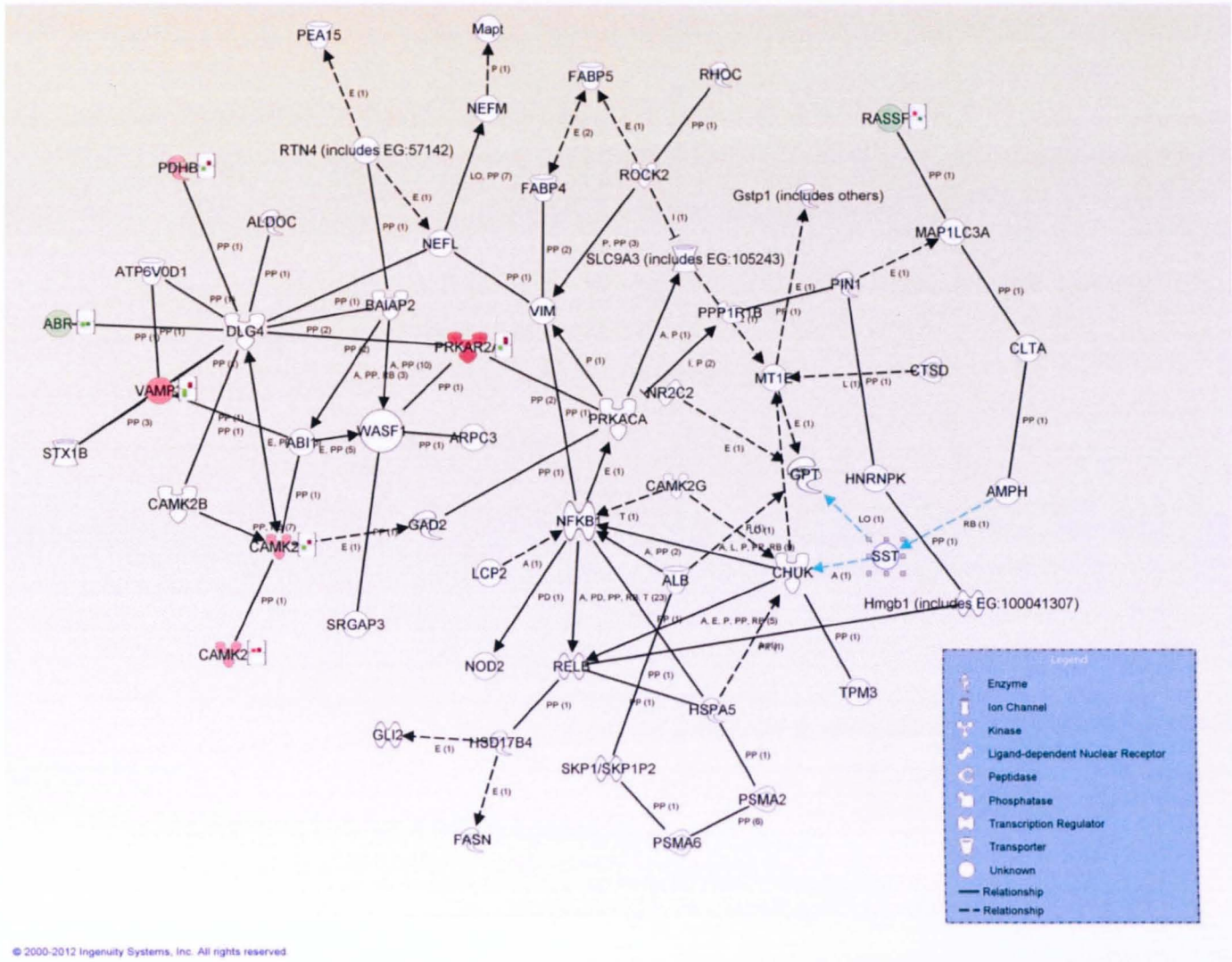

Figure 3 2H -NF-kB related protein pathway overlayed with protein changes in hippocampus tissue 1 month after severe injury from an E4 mouse.

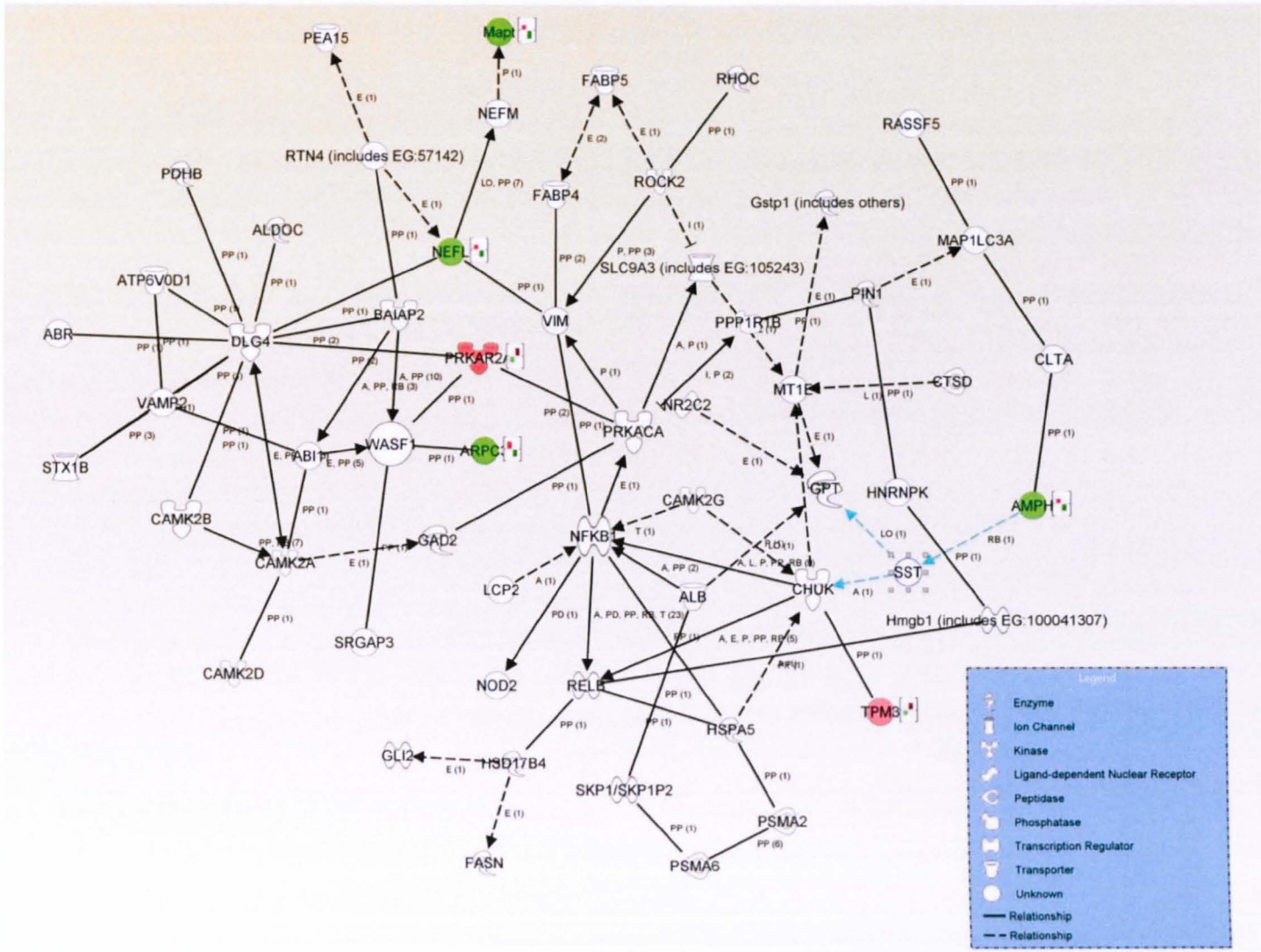

Figure 3-2I -NF-kB related protein pathway overlayed with protein changes in cortical tissue 3 months after severe injury from an E4 mouse.

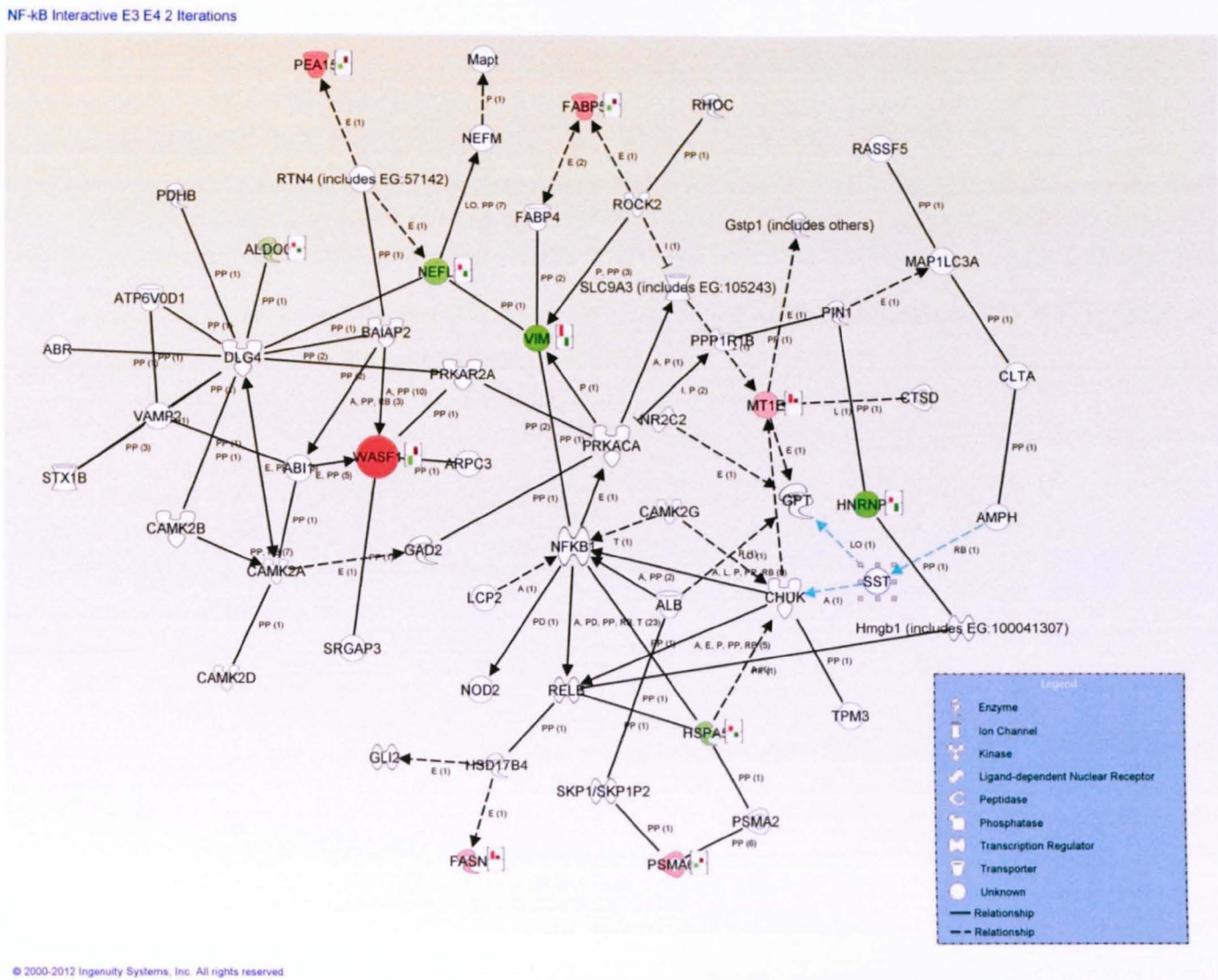

Figure 3-2J -NF-kB related protein pathway overlayed with protein changes in hippocampus tissue 3 months after severe injury from an E4 mouse.

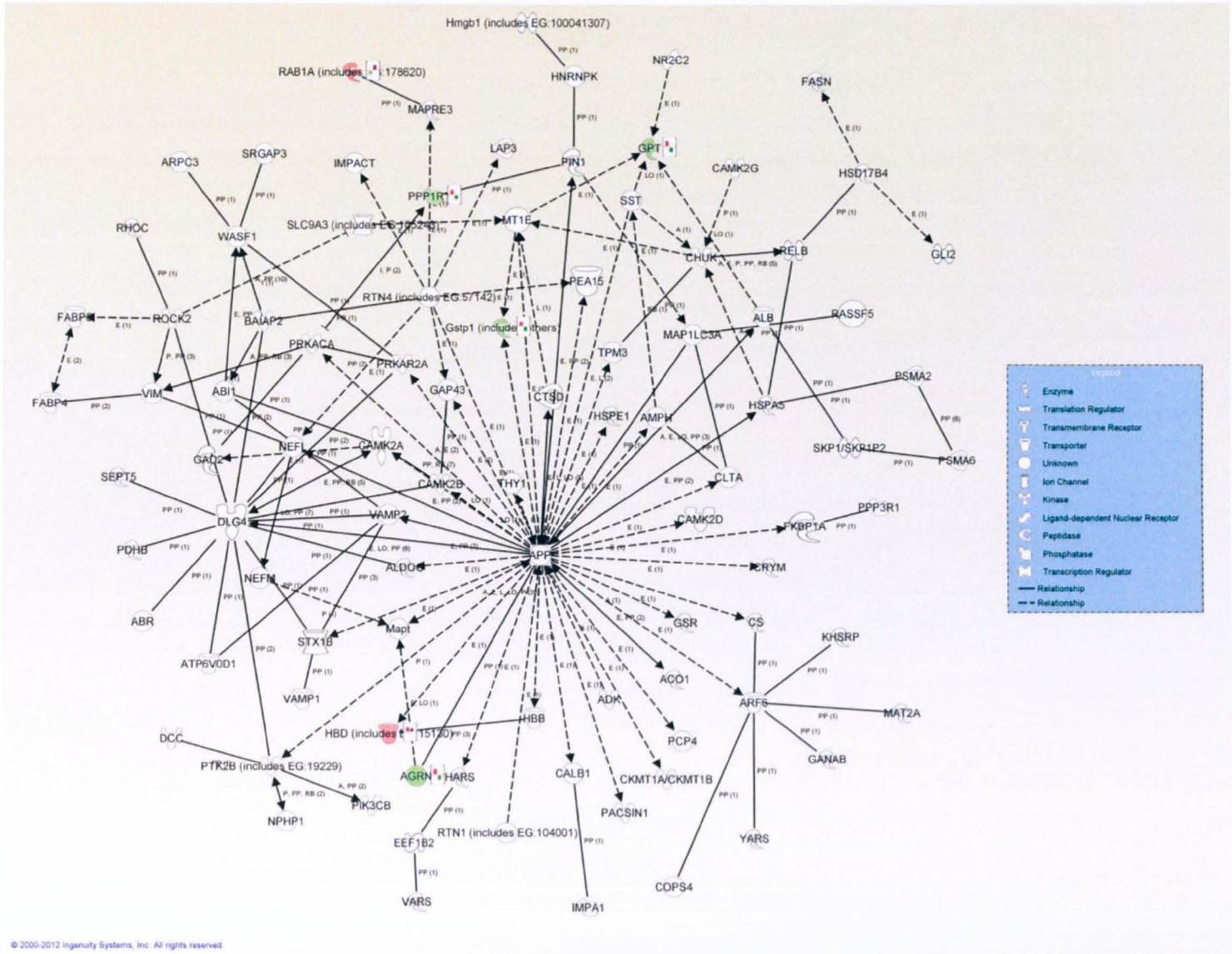

Figure 3-3A -APP related protein pathway overlayed with protein changes in cortical tissue 24 hours after mild injury from an E4 mouse.

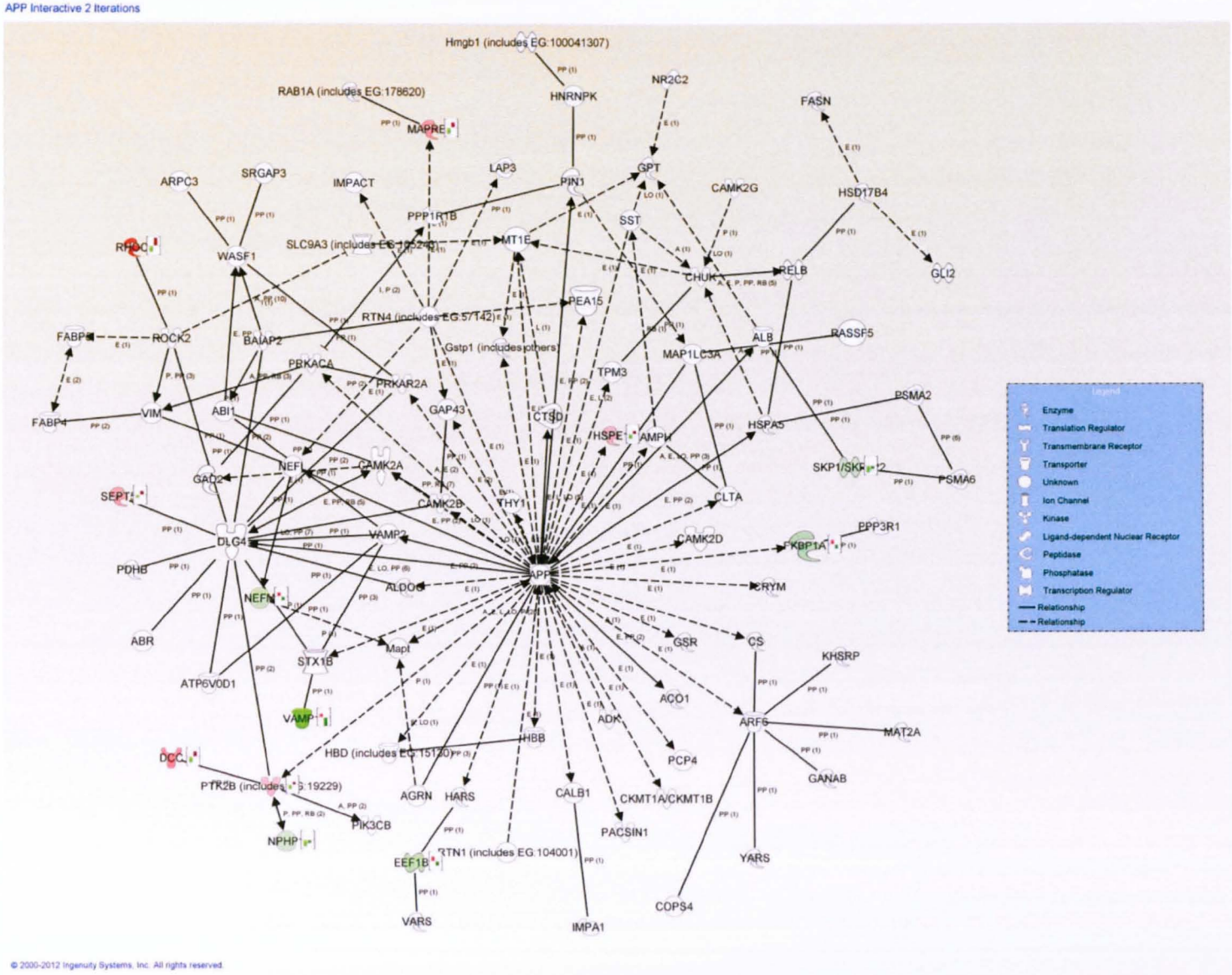

Figure 3-3B -APP related protein pathway overlayed with protein changes in hippocampus tissue 24 hours after mild injury in an E4 mouse.

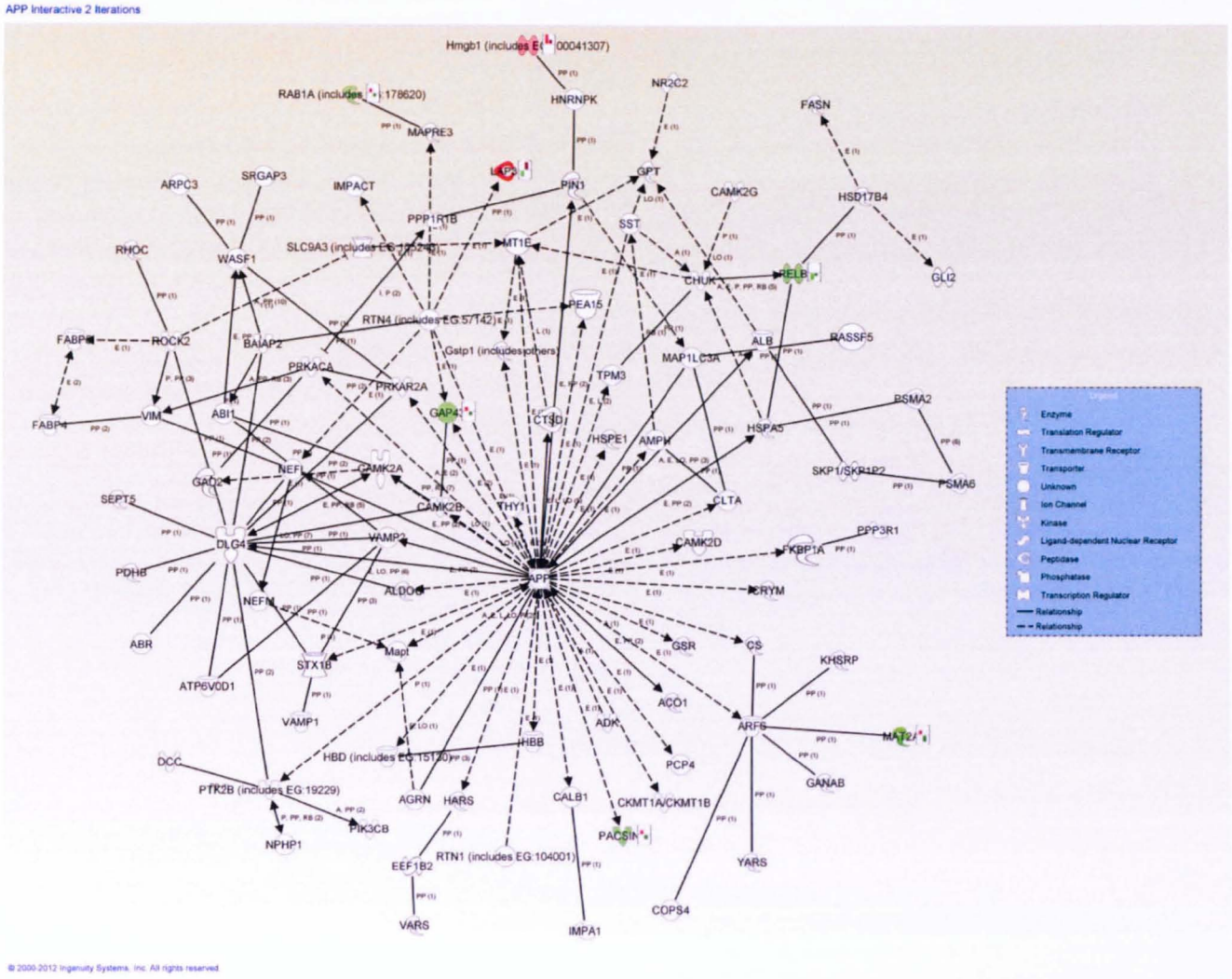

Figure 3-3C -APP related protein pathway overlayed with protein changes in cortical tissue 24 hours after severe injury from an E4 mouse.

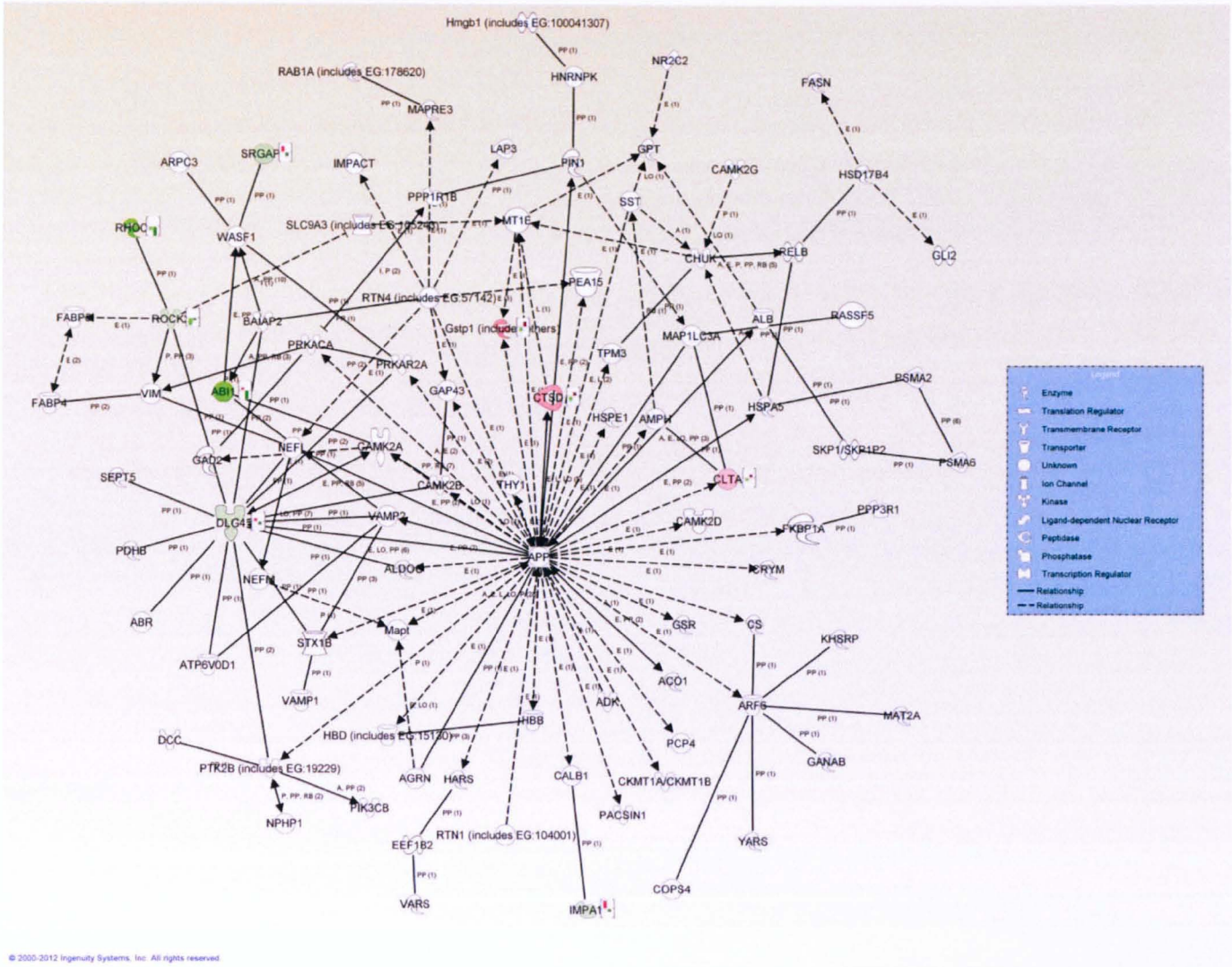

Figure 3-3D -APP related protein pathway overlayed with protein changes in hippocampus tissue 24 hours after severe injury from an E4 mouse.

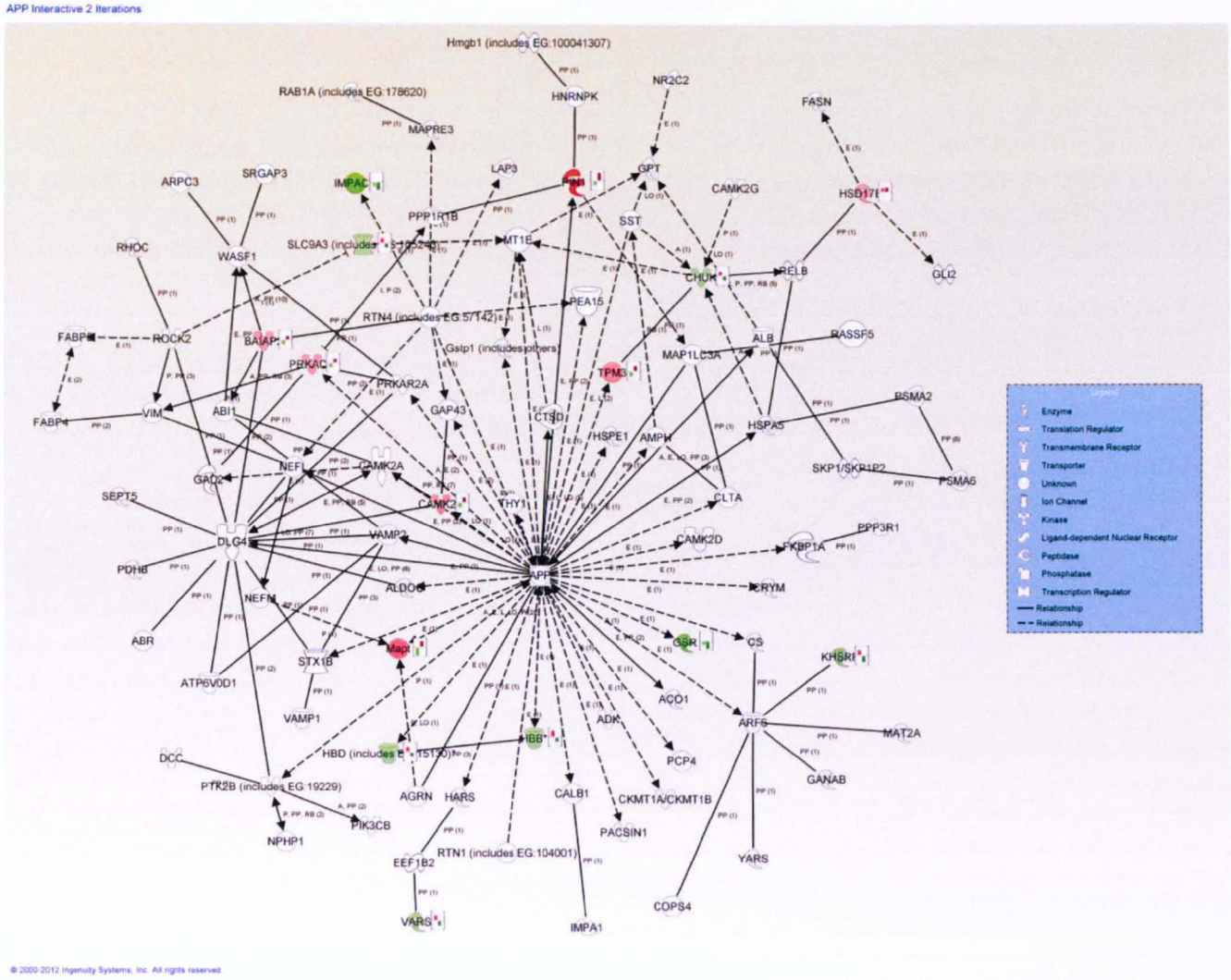

Figure 3-3E -APP related protein pathway overlayed with protein changes in cortical tissue 1 month after injury in an E4 mouse.

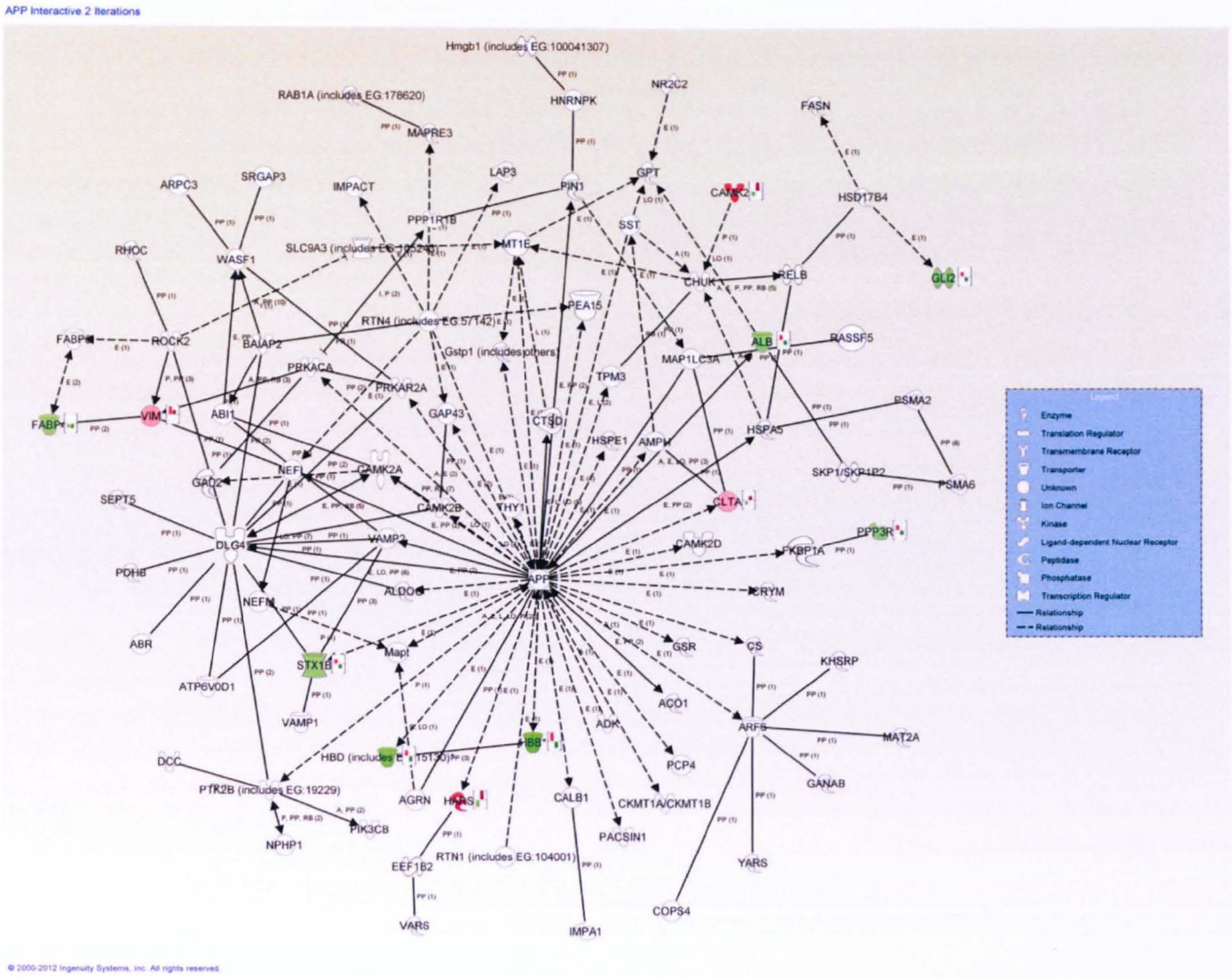

Figure 3-3F -APP related protein pathway overlayed with protein changes in hippocampus tissue 1 month after mild injury in an E4 mouse.

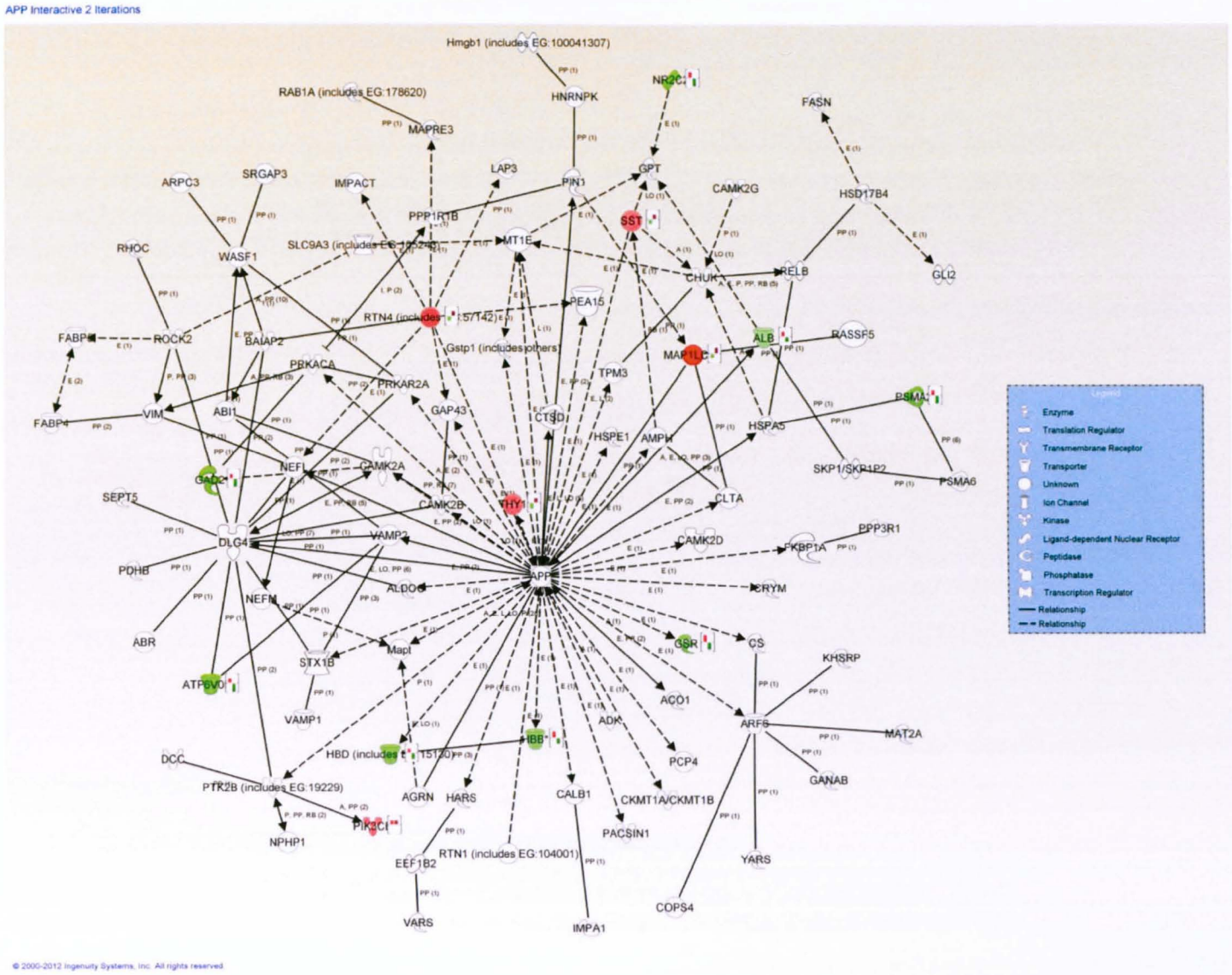

Figure 3-3G -APP related protein pathway overlayed with protein changes in cortical tissue 1 month after severe injury from an E4 mouse.

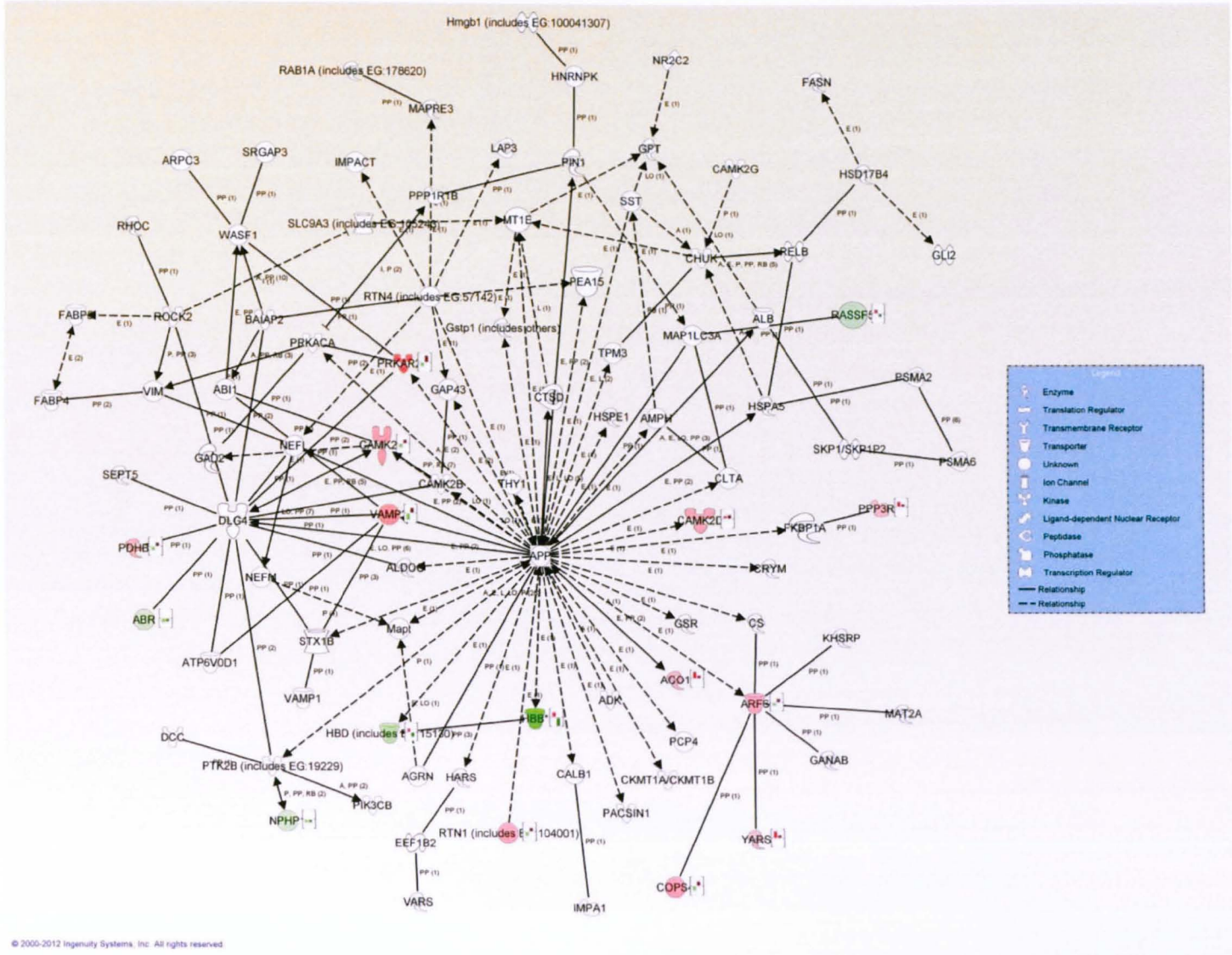

Figure 3-3H -APP related protein pathway overlayed with protein changes in hippocampus tissue 1 month after severe injury from an E4 mouse.

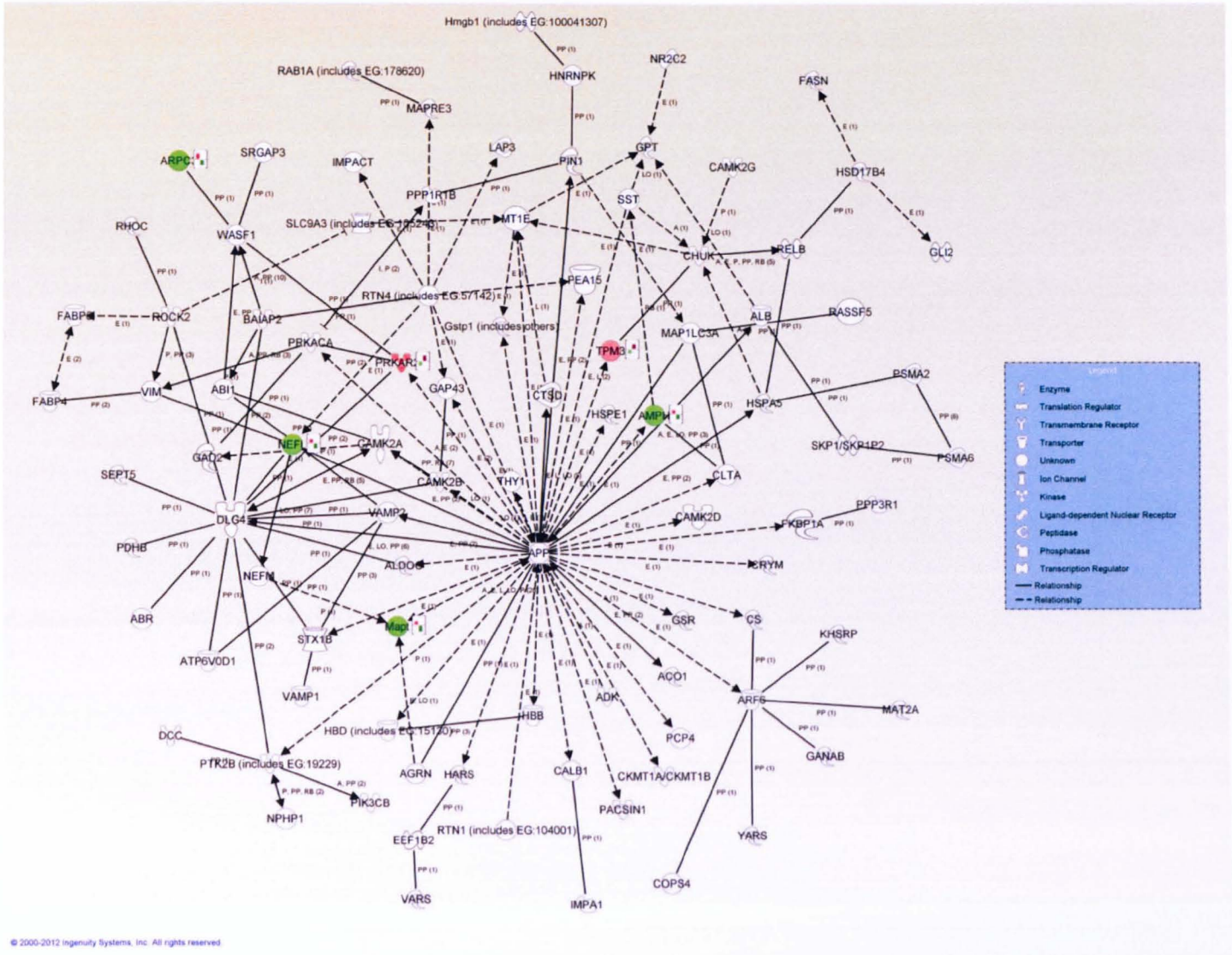

Figure 3-3l -APP related protein pathway overlayed with protein changes in cortical tissue 3 months after injury from an E4 mouse.

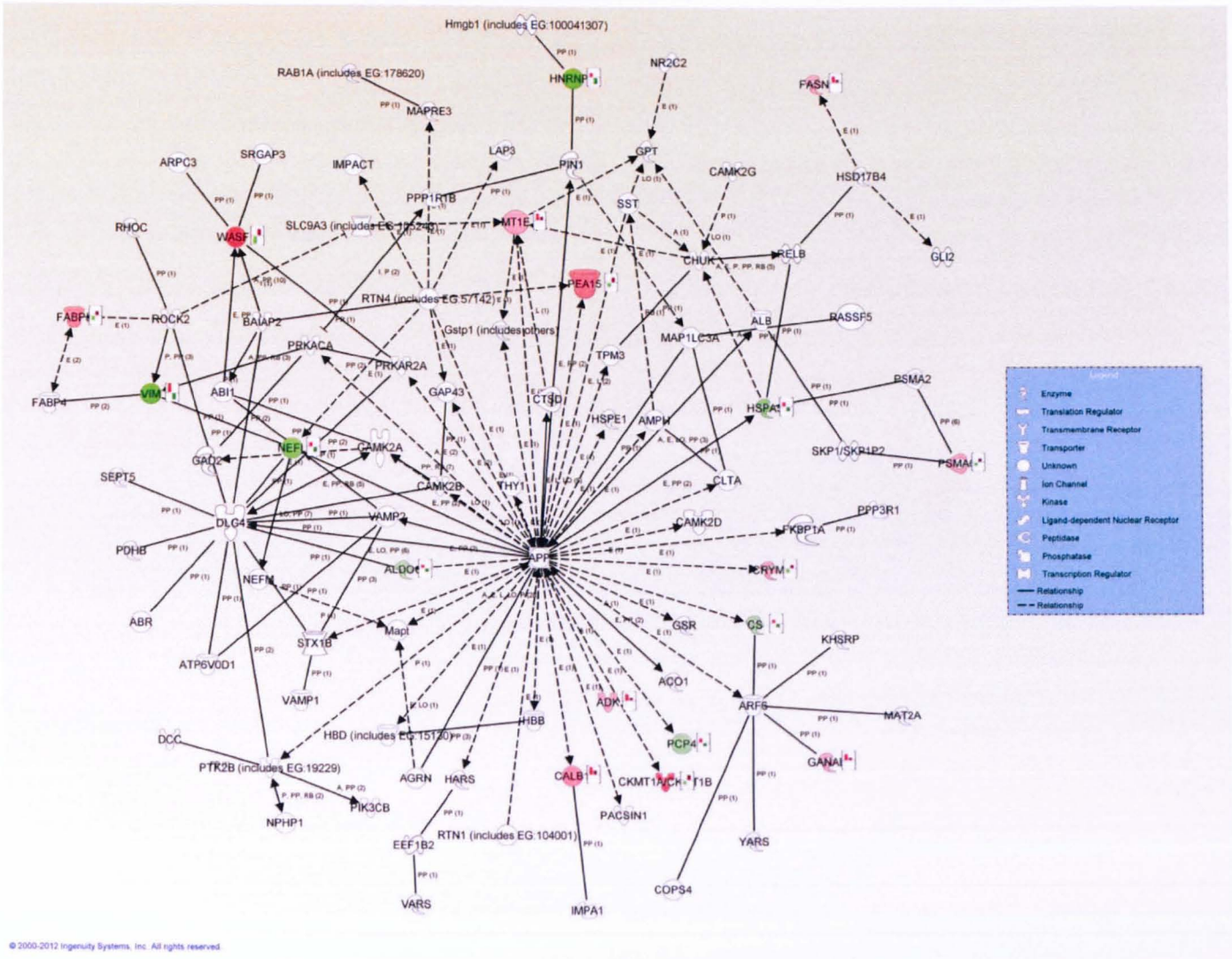

Figure 3-3J -APP related protein pathway overlayed with protein changes in hippocampus tissue 3 months after severe injury from an E4 mouse.

Table 3-3 CD40L Pathway Protein List

CD40L Pathway List	Full Name
ABR	Active BCR-related
AGRN	Agrin
ALB	Albumin
ALDOC	Aldoase C, fructose-bisphosphate aldolase
AMPH	Amphiphysin
ATP6V0D1	ATPase, H+ transporting, lysosomal 38kDa, V0 subunit d1
AUH	AU RNA binding protein/enoyl CoA hydratase
BAIAP2	BAI1-associated protein 2
CAMK2A	Calcium/calmodulin-dependent protein kinase II alpha
CAMK2B	Calcium/calmodulin-dependent protein kinase II beta
CAMK2D	Calcium/calmoudlin-dependent protein kinase II delta
CAMK2G	Calcium/calmoudlin-dependent protein kinase II gamma
CD40	CD40 molecule, TNF receptor superfamily member 5
CD40LG	CD40 ligand
CHUK	Conserved helix-loop-helix ubiquitous kinase
CLTA	Clathrin, light chain A
CTSD	Cathepsin D
DLG4	Discs, large homolog 4
FABP4	Fatty acid binding protein 4
FABP5	Fatty acid binding protein 5
FASN	Fatty acid synthase
GAD2	Glutamate decarboxylase 2
GLI2	GLI family zinc finger 2
GPT	Glutamic-pyruvate transaminase (alanine aminotransferase)
Gstp1	Glutathione S-transferase pi 1
Hmg1l1	High-mobility group (nonhistone chromosomal) protein 1-like 1
HNRNPK	Heterogenous nuclear ribonucleoprotein K
HSD17B4	Hydroxysteroid (17-beta) dehydrogenase 4
HSPA5	Heat shock 70kDa protein 5
MAP1LC3A	Microtubule-associated protein 1 light chain 3 alpha
MAPT	Microtubule-associated protein tau
MARCKSL1	MARCKS-like 1
MT1E	Metallothionein 1E
NEFL	Neurofilament, light polypeptide
NEFM	Neurofilament, medium polypeptide
NR2C2	Nuclear receptor subfamily 2, group C, member 2
PDHB	Pyruvate dehydrogenase (lipoamide) beta
PEA15	Phosphoprotein enriched in astrocytes 15
PIN1	Peptidyl cis/trans isomerase, NIMA-interacting 1
PPP1R1B	Protein phosphatase inhibitor 1, regulatory (inhibitor) subunit 1B
PRKACA	Protein kinase, cAMP-dependent catalytic, alpha
PRKAR2A	Protein kinase, cAMP-dependent, regulatory, type II, alpha
PSMA2	Proteasome (prosome, macropain) subunit, alpha type, 2
PSMA6	Proteasome (prosome, macropain) subunit, alpha type, 6
PSMB1	Proteasome (prosome, macropain) subunit, beta type, 1
RASSF5	Ras association (RalGDS/AF-6) domain family member 5
RELB	V-rel reticuloendotheliosis viral oncogene homolog B
RHOC	Ras homolog family member C
ROCK2	Rho-associated, coiled-coil containing protein kinase 2
RTN4	Reticulon 4
SKP1/SKP1P2	S-phase kinase-associated protein 1

SLC9A3	Solute carrier family 9, subfamily A (NHE3, cation proton antiporter 3), member 3
SST	Somatostatin
STX1B	Syntaxin 1B
TPM3	Tropomyosin 3
VAMP2	Vesicle-associated membrane protein 2 (synaptobrevin 2)
VIM	Vimentin
WASF1	WAS protein family, member 1

Table 3-4 NF-kB Protein Pathway List

NF-kB Pathway List	Full Name
ABI1	Abelson-interactor 1
ABR	Active BCR-related
ALB	Albumin
ALDOC	Aldoase C, fructose-bisphosphate aldolase
AMPH	Amphiphysin
ARPC3	Actin related protein 2/3 complex, subunit 3, 21kDa
ATP6V0D1	ATPase, H+ transporting, lysosomal 38kDa, V0 subunit d1
BAIAP2	BAI1-associated protein 2
CAMK2A	Calcium/calmodulin-dependent protein kinase II alpha
CAMK2B	Calcium/calmodulin-dependent protein kinase II beta
CAMK2D	Calcium/calmoudlin-dependent protein kinase II delta
CAMK2G	Calcium/calmoudlin-dependent protein kinase II gamma
CHUK	Conserved helix-loop-helix ubiquitous kinase
CLTA	Clathrin, light chain A
CTSD	Cathepsin D
DLG4	Discs, large homolog 4
FABP4	Fatty acid binding protein 4
FABP5	Fatty acid binding protein 5
FASN	Fatty acid synthase
GAD2	Glutamate decarboxylase 2
GLI2	GLI family zinc finger 2
GPT	Glutamic-pyruvate transaminase (alanine aminotransferase)
Gstp1	Glutathione S-transferase pi 1
Hmg1l1	High-mobility group (nonhistone chromosomal) protein 1-like 1
HNRNPK	Heterogenous nuclear ribonucleoprotein K
HSD17B4	Hydroxysteroid (17-beta) dehydrogenase 4
HSPA5	Heat shock 70kDa protein 5
LCP2	Lymphocyte cytosolic protein 2 (SH2 domain containing leukocyte protein of 76kDa)
MAP1LC3A	Microtubule-associated protein 1 light chain 3 alpha
MAPT	Microtubule-associated protein tau
MT1E	Metallothionein 1E
NEFL	Neurofilament, light polypeptide
NEFM	Neurofilament, medium polypeptide
NFKB1	Nuclear factor of kappa light polypeptide gene enhancer in B-cells 1
NOD2	Nucleotide-binding oligomerization domain containing 2

NR2C2	Nuclear receptor subfamily 2, group C, member 2
PDHB	Pyruvate dehydrogenase (lipoamide) beta
PEA15	Phosphoprotein enriched in astrocytes 15
PIN1	Peptidyl cis/trans isomerase, NIMA-interacting 1
PPP1R1B	Protein phosphatase inhibitor 1, regulatory (inhibitor) subunit 1B
PRKACA	Protein kinase, cAMP-dependent catalytic, alpha
PRKAR2A	Protein kinase, cAMP-dependent, regulatory, type II, alpha
PSMA2	Proteasome (prosome, macropain) subunit, alpha type, 2
PSMA6	Proteasome (prosome, macropain) subunit, alpha type, 6
RASSF5	Ras association (RalGDS/AF-6) domain family member 5
RELB	V-rel reticuloendotheliosis viral oncogene homolog B
RHOC	Ras homolog family member C
ROCK2	Rho-associated, coiled-coil containing protein kinase 2
RTN4	Reticulon 4
SKP1/SKP1P2	S-phase kinase-associated protein 1
SLC9A3	Solute carrier family 9, subfamily A (NHE3, cation proton antiporter 3), member 3
SRGAP3	SLIT-ROBO Rho GTPase activating protein 3
SST	Somatostatin
STX1B	Syntaxin 1B
TPM3	Tropomyosin 3
VAMP2	Vesicle-associated membrane protein 2 (synaptobrevin 2)
VIM	Vimentin
WASF1	WAS protein family, member 1

Table 3-5 APP Pathway Protein List

APP Pathway List	Full Name
ABI1	Abelson-interactor 1
ABR	Active BCR-related
ACO1	Aconitase 1
ADK	Adenosine kinase
AGRN	Agrin
ALB	Albumin
ALDOC	Aldoase C, fructose-bisphosphate aldolase
AMPH	Amphiphysin
APP	Amyloid beta precursor protein
ARF6	ADP-ribosylation factor 6
ARPC3	Actin related protein 2/3 complex, subunit 3, 21kDa
ATP6V0D1	ATPase, H+ transporting, lysosomal 38kDa, V0 subunit d1
BAIAP2	BAI1-associated protein 2
CALB1	Calbindin 1
CAMK2A	Calcium/calmodulin-dependent protein kinase II alpha
CAMK2B	Calcium/calmodulin-dependent protein kinase II beta
CAMK2D	Calcium/calmoudlin-dependent protein kinase II delta
CAMK2G	Calcium/calmoudlin-dependent protein kinase II gamma

CHUK	Conserved helix-loop-helix ubiquitous kinase
CKMT1A/CKMT1B	Creatine kinase, mitochondrial 1B
CLTA	Clathrin, light chain A
COPS4	COP9 constitutive photomorphogenic homolog subunit 4
CRYM	Crystallin
CS	Citrate synthase
CTSD	Cathepsin D
DCC	Deleted in colorectal carcinoma
DLG4	Discs, large homolog 4
EEF1B2	Eukaryotic translation elongation factor 1 beta 2
FABP4	Fatty acid binding protein 4
FABP5	Fatty acid binding protein 5
FASN	Fatty acid synthase
FKBP1A	FK506 binding protein 1A
GAD2	Glutamate decarboxylase 2
GANAB	Glucosinide, alpha; neutral AB
GAP43	Growth associated protein 43
GLI2	GLI family zinc finger 2
GPT	Glutamic-pyruvate transaminase (alanine aminotransferase)
GSR	Glutathione reductase
Gtsp1	Glutathione S-transferase pi 1
HARS	Histidine-tRNA synthetase
HBB	Hemoglobin, beta
HBD	Hemoglobin, delta
Hmg1l1	High-mobility group (nonhistone chromosomal) protein 1-like 1
HNRNPK	Heterogenous nuclear ribonucleoprotein K
HSD17B4	Hydroxysteroid (17-beta) dehydrogenase 4
HSPA5	Heat shock 70kDa protein 5
HSPE1	Heat shock 10kDa protein 1
IMPA1	Inositol(myo)-1(or 4)-monophosphatase 1
IMPACT	Impact homolog
KHSRP	KH-type splicing regulatory protein
LAP3	Prolyl aminopeptidase
MAP1LC3A	Microtubule-associated protein 1 light chain 3 alpha
MAPRE3	Microtubule-associated protein, RP/EB family, member 3
MAPT	Microtubule-associated protein tau
MAT2A	Methionine adenosyltransferase II, alpha
MT1E	Metallothionein 1E
NEFL	Neurofilament, light polypeptide
NEFM	Neurofilament, medium polypeptide
NPHP1	Nephronophthisis 1
NR2C2	Nuclear receptor subfamily 2, group C, member 2
PACSIN1	Protein kinase C and casein kinase substrate in neurons 1
PCP4	Purkinje cell protein 4
PDHB	Pyruvate dehydrogenase (lipoamide) beta
PEA15	Phosphoprotein enriched in astrocytes 15
PIK3CB	Phosphoinositide-3-kinase, catalytic, beta polypeptide
PIN1	Peptidyl cis/trans isomerase, NIMA-interacting 1

PPP1R1B	Protein phosphatase inhibitor 1, regulatory (inhibitor) subunit 1B
PPP3R1	Protein phosphatase 3, regulatory subunit B, alpha
PRKACA	Protein kinase, cAMP-dependent catalytic, alpha
PRKAR2A	Protein kinase, cAMP-dependent, regulatory, type II, alpha
PSMA2	Proteasome (prosome, macropain) subunit, alpha type, 2
PSMA6	Proteasome (prosome, macropain) subunit, alpha type, 6
PTK2B	Protein tyrosine kinase 2 beta
RAB1A	Member RAS oncogene family
RASSF5	Ras association (RalGDS/AF-6) domain family member 5
RELB	V-rel reticuloendotheliosis viral oncogene homolog B
RHOC	Ras homolog family member C
ROCK2	Rho-associated, coiled-coil containing protein kinase 2
RTN1	Reticulon 1
RTN4	Reticulon 4
SEPT5	Septin 5
SKP1/SKP1P2	S-phase kinase-associated protein 1
SLC9A3	Solute carrier family 9, subfamily A (NHE3, cation proton antiporter 3), member 3
SRGAP3	SLIT-ROBO Rho GTPase activating protein 3
SST	Somatostatin
STX1B	Syntaxin 1B
THY1	Thy-1 cell surface antigen
TPM3	Tropomyosin 3
VAMP1	Vesicle-associated membrane protein 1
VAMP2	Vesicle-associated membrane protein 2 (synaptobrevin 2)
VARS	Valyl-tRNA synthetase
VIM	Vimentin
WASF1	WAS protein family, member 1
YARS	Tyrosyl-tRNA synthetase

CD40 signaling by CD40L is an important regulator of immune response, vital to class immunoglobulin (Ig) class switching and microglial activation in response to amyloid (Kawabe et al., 1994, Suo et al., 1998, Tan et al., 1999, Jabara et al., 2002, Tan et al., 2002, Townsend et al., 2005). I used CD40 and CD40L as seed molecules to generate a custom pathway of proteins present in the datasets that are related to CD40 or CD40L. The greatest level of overlap with this pathway occurred in the severely injured cortex hippocampus at 3 months with 56% and 46% of the molecules present in those dataset participating, respectively, indicating that it is of ongoing importance in the differential response of APOE3 and APOE4 transgenic mice to TBI (figure 3-1, table 3-2 and table 3-3).

Nuclear factor kappa B (NF-kB) is also a molecule of central importance in regulating the transcription of many inflammatory cytokines, and NF-kB activation is induced by molecules like IL-1, whose pathway was seen to be significantly regulated in our dataset 1 month after mild injury (Malinin et al., 1997, Takeuchi et al., 2000, Tak and Firestein, 2001). I seeded a network based on NF-kB-related molecules and saw participation at all time points and injury levels (figure 3-2 and table 3-4). 67% of the molecules present in the severely injured cortex at 3 months participated in the NF-kB-related pathway, a remarkable shift from only 18% participation in the severely injured cortex at 24 hours, and 20% in the mildly injured cortex at 24 hours. By contrast, the NF-kB pathway accounted for 42% of the proteins present in the severely injured hippocampus at 24hrs (Table 3-2).

Amyloid Precursor Protein (APP) processing was also significantly modulated as a canonical pathway in our 3 month severe cortical dataset. Generating a custom pathway from APP produced the largest network of participating proteins from all of the custom pathways and showed APP playing a

central role in the pathway. 75% of the proteins from the APP pathway were present in the 3 month severe hippocampus dataset, the highest participation level of any dataset in any pathway studied, and overall APP processing had the highest average participation rate of any pathway examined, in excess of 55%. (figure 3-3, table 3-2 and table 3-5)

In order to further examine the acute inflammatory response of mice in the CCI model we examined IL-6 (figure 3-4), IL-1B (figure 3-5) and MCP-1 (figure 3-6) levels by ELISA at a range of acute timepoints after TBI. For this investigation we used wild type mice of the same background strain as the APOE transgenic mice (C57BL/6J). ELISA data for IL-6 and MCP-1 shows the acute response to CCI TBI in these inflammatory cytokines becomes significantly up-regulated compared to sham mice as early as 6 hours after injury, peaking at its highest concentration 12 hours after injury before gradually decreasing. Interestingly, there is no significant effect of TBI on any inflammatory marker at the 1 hour time point. With the CHI injured mice, only IL-6 was significantly up-regulated at 6 hours after injury, and in all cases was less up-regulated than even CCI sham mice, demonstrating that this closed head impact is indeed a very mild injury (as was the intent when it was developed). IL-1B failed to show a significant effect of injury overall.

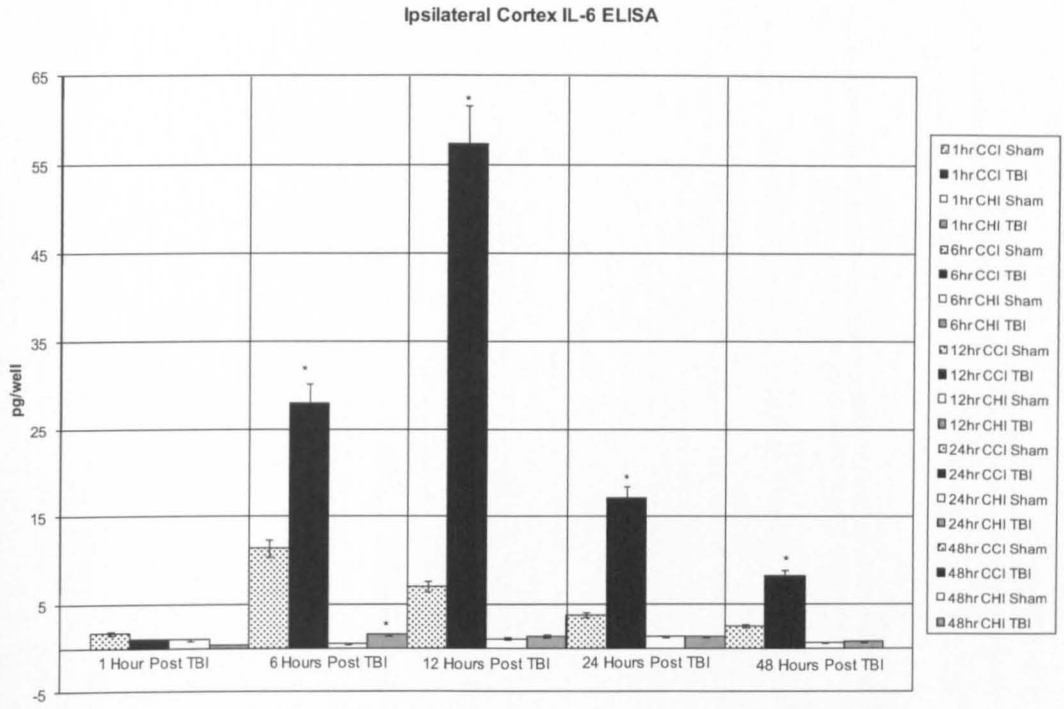

Figure 3 -4. IL-6 ELISA acute timepoint profile in wild type mice. Error bars represent standard error. * indicates significance compared to the corresponding sham ($p<0.05$) by T-test.

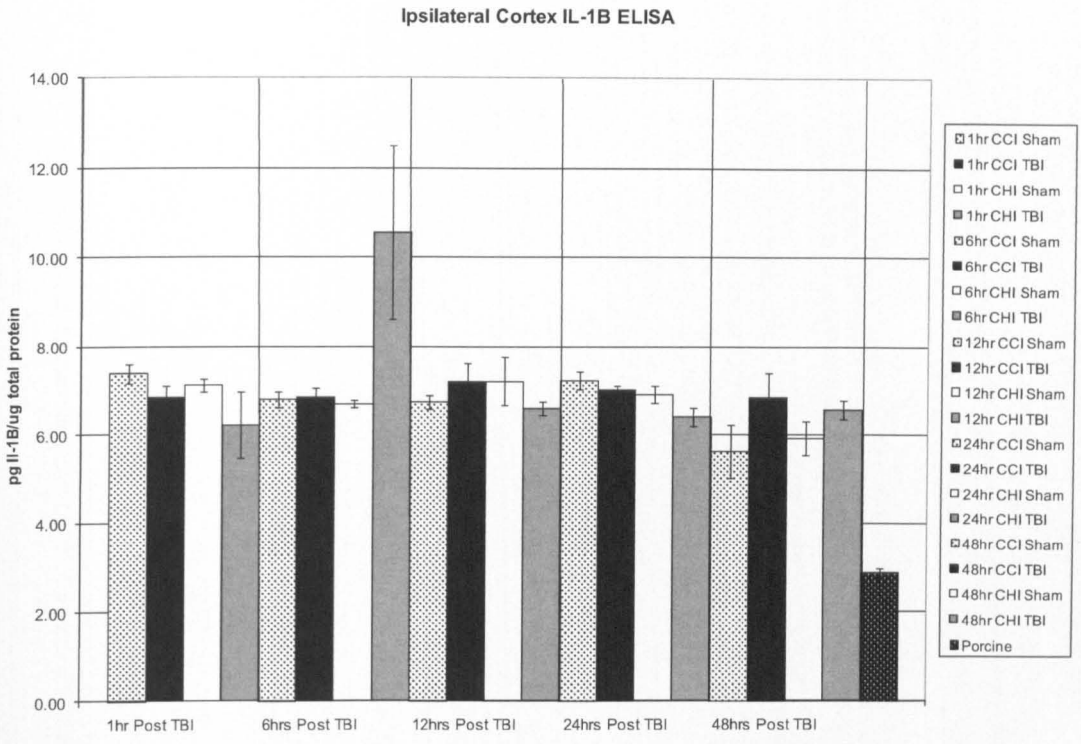

Figure 3-5. IL-1B ELISA acute timepoint profile in wild type mice. Error bars represent standard error. No statistical significance.

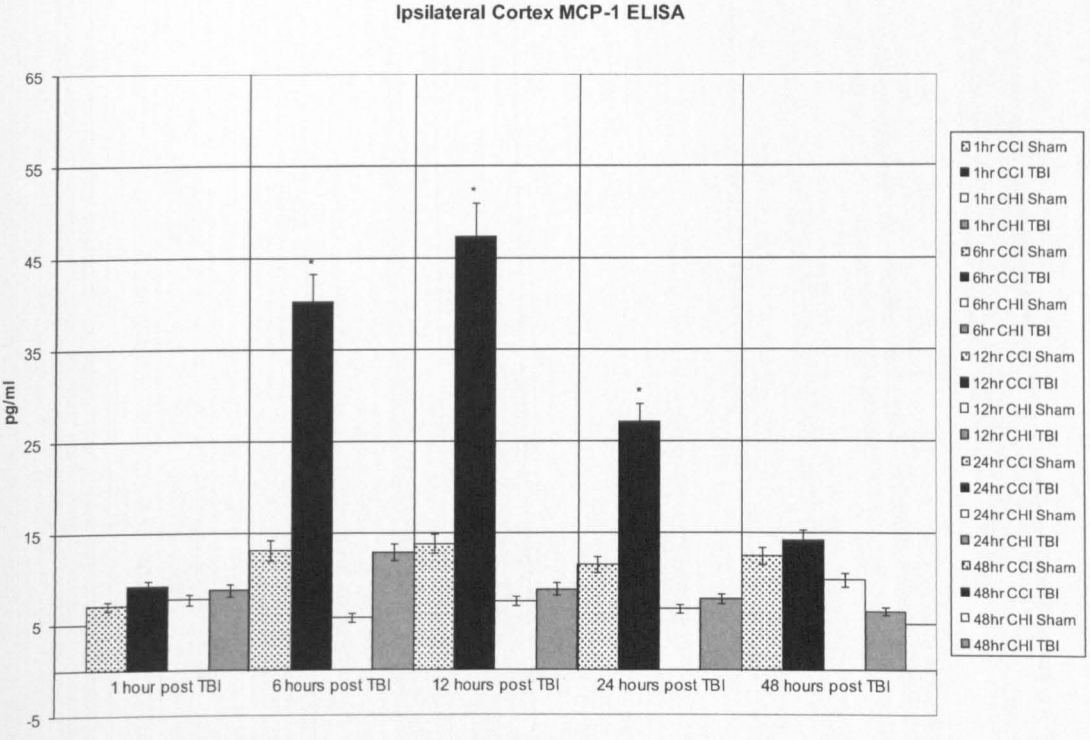

Figure 3-6. MCP-1 ELISA acute timepoint profile in wild type mice. Error bars represent standard error. * indicates significance compared to the corresponding sham ($p<0.05$) by T-test.

Discussion

Delayed secondary injury after TBI may be mitigated by therapeutic intervention, but so far all attempts to intervene in a clinical setting have failed. The molecular analyses and interpretation outlined in this chapter represent our approach to identifying rational targets for new therapeutic approaches. We took a systems biology approach to finding potential therapeutic targets for TBI. LC-MS/MS of iTRAQ-labeled samples gave us the ability to profile the response of a large amount of proteins simultaneously. In order to focus on protein changes that are associated with differential outcome from TBI, we utilized APOE3 and APOE4 transgenic mice at 24 hours, 1 month, and 3 months after injury. As previously discussed in the first two chapters, E4 carriers are predisposed to a worse long-term outcome after TBI than non-carriers, therefore we focused on changes that occurred differentially in E3 and E4 mice after TBI across multiple timepoints up to three months after injury.

Datasets were generated using only the proteins shown to be changing significantly by the interactive effect of injury x genotype. Functional analysis of these datasets using IPA revealed molecular pathway changes over time, not just individual protein changes. This gave a big picture view of the changes occurring after TBI – although individual protein changes in a mouse may not correlate directly to a human situation, we anticipate overlap in terms of the molecular pathways and functions that are modulated in response to injury, thus mouse analyses can provide insight into these common processes of secondary brain injury. For example, cellular immune response was of importance in nearly all cases and time points. IL-1 was also significantly regulated at the one month timepoint in the mildly injured cortex. The significant modulation of these pathways a month or longer after TBI indicates an important role for chronic

inflammatory processes in determining the long term outcome from TBI. The concept of an important role for inflammation after TBI is not a new one (Utagawa et al., 2008, Lu et al., 2009, Amor et al., 2010, Ramlackhansingh et al., 2011) and this provides validation of our approach, but our data also shows its importance in determining the differential outcome in APOE transgenic mice as well as showing the modulation of other functional pathways such as "Regulation of actin based motility by Rho" and "Actin cytoskeleton signaling" for which there is little or no prior indication after TBI.

Inflammation has been shown to be associated with functional deficits after TBI (Cernak et al., 2001, Cernak et al., 2002, Nimmo et al., 2004). Our data show that inflammation plays an important role in the differential response of APOE3 and APOE4 mice to TBI as well, further supporting the importance of inflammatory responses in secondary brain injury. It is known that in glial cells, the apoE protein can act as an inducer of inflammation with apoE4 inducing a greater amount of IL-1B than apoE3 (Guo et al., 2004). ApoE isoforms also differentially affect the oxidative status of macrophages (Jofre-Monseny et al., 2007). ApoE isoforms are known to differentially impact the amount of amyloidogenic processing of APP (Ye et al., 2005). The possibility that the influence of APOE genotype after injury is through its effect on APP metabolism was examined by Ezra and colleagues (Ezra et al., 2003), who used targeted replacement APOE3 and APOE4 transgenic mice to study the levels of secreted APP after a closed head injury (CHI). Their results showed ApoE isoform-specific metabolism of APP following TBI. Specifically, APOE4 transgenic mice produce less secreted APPsα in the hippocampus following TBI than APOE3 transgenic mice, while sham APOE4 transgenics start with a higher basal level than APOE3. Secreted APP enhances neuronal survival (Yamamoto et al., 1994), therefore a lack of it may play a role in the APOE-

genotype dependent outcome from TBI. The converse effect of increased production of amyloid β after TBI (see chapter 1) can lead to microglial activation (Rogers and Lue, 2001) and may also contribute to the differential outcome of APOE3 and APOE4 transgenic mice.

Given the in-house expertise at the Roskamp Institute, and the availability of relevant potential modulators and genetic models, we selected CD40/CD40L, NF-kB and APP as seed molecules with which to interrogate the datasets and determine if they were appropriate targets for efforts to manipulate outcome after TBI. CD40 signaling also increases cytokine production in the presence of amyloid β and induces the activation of microglia (Suo et al., 1998, Townsend et al., 2005). NF-kB is a transcription factor that regulates the transcription of many inflammatory cytokines (Matsusaka et al., 1993, Tak and Firestein, 2001). APP processing is impacted by TBI and leads to the production of Aβ after TBI (Loane et al., 2009, Loane et al., 2011). Based on the effects seen in our data on inflammation and APP processing, we generated custom pathways from the molecules present in the dataset that have relationships to CD40 and the CD40 ligand, NF-kB and APP.

Time Dependent Effects

As discussed above, CD40 signaling is important for Ig class switching as well as inflammatory responses to Aβ (see chapter 4 for more detail). Custom pathway generation for CD40 showed that some CD40-related molecules were present in every one of the datasets, but CD40-related molecules comprised the greatest percentage of the datasets at 3 months after injury. Although CD40-related molecules only comprised 18% of the severely injured cortex dataset at 24 hours, it accounted for 56% of the dataset at 3 months post-TBI. Although the number of molecules present in each dataset at each timepoint change, driving

some of the above percentage changes, this still demonstrates that CD40-related molecules continue to be differentially modulated for long periods of time after TBI even as unrelated molecules become less so over time. A similar situation was true for NF-kB related molecules, which also accounted for only 18% of the severely injured cortex dataset at 24 hours, but by 3 months post-injury accounted for 67% of the cortical dataset. This suggests that inflammatory pathways are part of the initial difference in response between APOE3 and APOE4 transgenic mice following TBI, but in the long term become increasingly important in the process of secondary injury in the cortex after TBI. APP-related molecules, by contrast, were consistently involved in each dataset at a high percentage regardless of time after injury.

Regional Dependent Effects

Regional specific differences were also important in understanding the differential response of APOE transgenic mice. Within severely injured mice, there were consistently greater numbers of proteins significant for interaction in the hippocampus than in the cortex, outweighing the cortical differences by more than 2-to-1 at three months after injury (Table 3-2). Three months after severe injury, 24 proteins were significant for interaction in the hippocampus compared to only 9 in the cortex. Only the mildly injured cortex at the 1 month timepoint showed a greater number of protein significant for interaction compared to the corresponding hippocampus. This is particularly fascinating since the injury itself occurs in the cortex, but the differential response of APOE transgenic mice is distant from that. This may be due in part to the large size of the cortex and the fact that the pericontusional region was not specifically extracted, whereas the hippocampus is directly beneath the site of injury. Nonetheless, it still shows that the differences in

secondary injury in APOE transgenic mice are not isolated to the site of injury itself.

Severity Dependent Effects

Injury severity was also examined; mild injury is the most common form of TBI and is currently under-reported. Differential responses seen in our APOE transgenic mice even a month after our milder form of CCI injury show that injury processes may be ongoing and targets may still be available for therapeutic intervention. In the mild injury, the CD40 and NF-kB pathways accounted for less than half of the amount of the dataset than in the severe injury. This may be due to a difference in the time course of a mild injury; while there were 23 proteins significant for the interactive term of injury*genotype at 24 hours in the hippocampus of the mild injury, only 19 were significant in the severe. At one month after injury, however, 40 proteins in the hippocampus were significant for injury*genotype in the severe injury compared to only 18 in the mild injury. At those timepoints, CD40 and NF-kB related molecules make up less of the hippocampus datasets, though both become important once again at three months after injury in the severe dataset. This may indicate that the differences between the genotypes during the mild injury begin to resolve themselves faster than in the severe injury, and the CD40 and NF-kB pathways appear to become increasingly important as these injuries start to reach that point. Even as the total number of proteins that are significant for genotype*injury decrease in the severely injured hippocampus, the number of proteins that are related to CD40 signaling and NF-kB begin to increase. This same shift was true in the mild injury as well, but occurred from 24 hours to 1 month instead of 1 month to 3 months.

APP Specific Differences

As previously discussed, Aβ is known to be increased after TBI (Roberts et al., 1994, Smith et al., 2003, Ikonomovic et al., 2004, Loane et al., 2009, Loane et al., 2011). In our study APP-related molecules made up large portions of each dataset across all of the time points, both in severe and mild injury. The lowest percentage involvement was 30% in the cortex of mice with mild injury at 24 hours, but on average APP-related molecules accounted for more than 55% of each dataset. At 3 months after TBI, APP-related molecules accounted for 75% of the proteins changing differently in response to injury in the APOE3 vs APOE4 hippocampus, showing that APP processing may be one of the primary processes driving the long-term differences between the APOE3 and APOE4 genotype. Although an acute amyloid beta spike is known to occur after TBI (Raby et al., 1998, Olsson et al., 2004), APP processing may be differentially affected in APOE4 carriers over a much longer period of time and may be responsible for their poorer outcome. Mice that are transgenic for both human APOE and mutated APP showed accelerated neurodegeneration and increased amyloid beta accumulation after TBI if they possessed an APOE4 allele (Laskowitz et al., 2010). APOE genotype also influences the rate of clearance of amyloid beta, with APOE4 transgenic mice showing significantly slower clearance than either APOE2 or APOE3 transgenics (Deane et al., 2008). Therapeutic strategies that target APP processing and clearance may reduce secondary damage and improve the outcome from injury.

We also investigated the acute inflammatory response after TBI, both in a closed mild head injury model (CHI), and in our severe CCI model. Mild TBI is more common than severe, and patients may not even be aware of the injury initially, even in the presence of other injuries (Tolonen et al., 2007). We profiled

the acute inflammatory response in CHI and CCI at 1, 6, 12, 24, and 48 hours after injury and compared each to an appropriate sham (craniectomy for CCI and anesthesia-only for CHI) which showed that IL-6 and MCP-1 were significantly up-regulated at 6 hours after injury and peaked by 12 hours. Interestingly, there was no significant effect of injury at the 1 hour timepoint for any inflammatory marker, thus there may still be time overt inflammatory reactions that result in macrophage accumulation, astrogliosis, and progressive expansion of the lesion volume (Sandhir et al., 2004, Semple et al., 2009). This agrees with previous research showing no significant increase in IL-6 or MCP-1 at 1 hour, and some studies showing even no increase at 4 hours after TBI compared to sham (Lloyd et al., 2008). Others do show a significant increase in MCP-1, but not IL-6, 4 hours after injury (Semple et al., 2009). We also witnessed a significant increase in the CCI sham levels of IL-6 and MCP-1 over time, supporting previous findings that the craniectomy itself induces a mild injury to the brain (Cole et al., 2011). Our severe CCI model, however, is generally a more severe form of TBI than many other groups utilize for their studies, so it is of interest that even in a model that has been optimized for maximum injury without mortality, there is still at least a one hour window before any significant increases in inflammatory markers are seen. In summary we conclude that since IL-6 and MCP-1 both show significant effects of injury and are easily profiled within the first 24 hours, they may be good markers to screen potential therapeutic compounds at acute timepoints after injury.

Detailed investigation of the custom networks for CD40, APP, and NF-kB thus support each of these as potential areas to target for therapeutic intervention. Many other potential targets are suggested by our proteomic analyses, but were beyond the scope of my research for this thesis, including lipid metabolism and cellular metabolic pathways. Though these other targets may well be important in

determining the differential outcome in APOE3 and APOE4 transgenic mice after TBI, they did not provide easily accessible targets for therapeutic intervention. It is intended these additional targets will be investigated in future studies. One of the justifications supporting further analyses of all three of the targets selected was the in-house expertise at the Roskamp Institute; another was the fact that approaches to modulating all of these targets were available and thus enabled me to implement my neurobehavioral paradigms for target validation.

The next three chapters each describe modulation of one of these targets in mouse models of head injury and the consequences on neurobehavioral outcome. The results of these analyses confirm that this overall strategy is an effective pre-clinical approach to the identification and development of novel therapeutics for TBI.

CHAPTER 4
EFFECTS OF CD40 SIGNALING INHIBITION ON OUTCOME FROM TBI

Introduction

As described in chapter 3, we previously analyzed the proteomic profiles of APOE3 and APOE4 transgenic mice following injury in a CCI model of TBI. One of the pathways found to be modulated in an APOE isoform-dependent manner involved CD40-related molecules. CD40-related molecules appeared to become increasingly important over time in determining the differential response of APOE to TBI, up to at least three months after injury. CD40 signaling may therefore be important to determining the long-term outcome from secondary injury after TBI.

CD40 is a member of the TNF-receptor superfamily found on antigen presenting cells (APCs) and is essential for T-cell dependent immunoglobulin class switching as well as Aβ induced microglial activation (Kawabe et al., 1994, Suo et al., 1998, Tan et al., 1999, Jabara et al., 2002, Tan et al., 2002, Townsend et al., 2005). Activation of CD40 by the CD40 ligand (CD40L (CD154)) increases the production of inflammatory cytokines including IL-6, TNF-α, and MCP-1, thus inhibiting CD40 signaling can be expected to have anti-inflammatory effects (Chen et al., 2006). CD40 is expressed not only on B cells, but also on monocytes, dendritic cells, endothelial and epithelial cells. The CD40L ligand is also expressed on more than just activated T lymphocytes; it can also be found on B cells, natural killer cells, monocytes, macrophages, and even dendritic cells in some cases (Kooten, Banchereau 2000). CD40 is also expressed by neurons and its activation results in p44/42 MAPK activation and the opposition of JNK activation (Tan, Town et al. 2002). CD40 and CD40L knockout mice both suffer from a deficiency in immunoglobulin class switching known as hyper-IgM

syndrome (Strom et al., 1999). CD40 is also vital in the maturation of dendritic cells into antigen-presenting cells, thus these mice also have deficiencies in priming naïve CD4+ T cells, but also show improved outcome in models of transplantation rejection and autoimmune disorders (van Kooten and Banchereau, 2000, Ponomarev et al., 2006). This may be advantageous in reducing the immune response after TBI where it has been shown that activated CD4+ T cells can increase the amount of damage acutely after brain injury (Fee et al., 2003). Involvement of CD40 in brain injury or dysfunction is already known, including work from our own team that demonstrated that disruption of CD40 signaling mitigated AD pathology in mouse models of the disease (Tan et al., 1999). CD40 and its ligand have been previously shown to be upregulated following cerebral ischemia (Garlichs et al., 2003), and a study by Ishikawa et al (2004) also showed that CD40 deficient and CD40 ligand deficient mice have reduced infarct volume in a mouse model of ischemia.

Given the interrelationship of AD and TBI (see Chapter 1), and that ischemic conditions are known to occur in the brain following TBI (Coles et al., 2000), and given the APOE isoform-dependent modulation of CD40-related molecules seen at multiple timepoints following TBI (Chapter 3, Figure 3-1A-J), we targeted CD40 signaling in order to modulate the response to TBI and reduce inflammation. Other work has shown that CD40 signaling mediates nuclear factor kappa B (NF-kB) activation through TNF receptor-associated factor 2 (TRAF2) (Rothe et al., 1995), thus the inhibition of downstream signaling from CD40 may also reduce NF-kB activation, (also identified by the work described in chapter 3), and may be important in determining differential outcome from secondary injury.

We first attempted to use an antibody-based therapeutic approach to inhibit CD40 signaling, hoping to take advantage of blood-brain barrier permeability

immediately after TBI in order for the antibody to reach the injured tissue. Others have shown that treating with an anti-CD40L antibody may produce a therapeutic inhibition of CD40 signaling in some disease states such as multiple sclerosis, atherosclerosis and lupus (Mach et al., 1998, Howard et al., 1999, Wang et al., 2003). Our failure to detect any trace of the antibody penetrating into the brain led us to an alternative approach of using mice genetically knocked out for CD40L to disrupt CD40 signaling. CD40L knockout mice (Jackson Laboratories) were used to study the effect of CD40 signaling in our CCI model of severe TBI in order to observe the maximum effect of injury. We evaluated CD40L knockout mice in our CCI model of TBI using the methodology described in chapter 2 for Rotarod and Barnes maze testing of motor coordination and spatial memory.

Materials and Methods

Animals and Injury

For the administration of TBI the same protocol was followed as described in chapter 2. Briefly, all mice (details of numbers and characteristics below) were anesthetized with isofluorane; once anesthetized, animals were mounted in a stereotaxic frame in a prone position secured by ear and incisor bars. Following a midline incision and reflection of the soft tissues, a 5mm craniectomy was performed adjacent to the central suture, midway between lambda and bregma. Severe injury was administered as previously described (Crawford et al., 2009) by impacting the right cortex with a 2 mm diameter tip at a rate of 5 m/s and depth of 1.8 mm. Sham mice for the CCI procedure received craniectomy without injury.

All procedures involving mice were carried out under Institutional Animal Care and Use Committee (IACUC) approval and in accordance with the National Institute of Health Guide for the Care and Use of Laboratory Animals.

Modulation of CD40 signaling

Our initial plan was for a therapeutic approach using an anti-CD40L antibody to interrupt CD40 signaling. We performed a pilot anti-CD40L antibody experiment. It has been shown that TBI in mice induces blood-brain barrier permeability in the peri-contusional area, allowing Evans blue staining to infiltrate the brain in that region (Habgood et al., 2007). Two mice (60 week old male APOE knockout) received a CCI injury followed 30 minutes later by a 100 µl intraperitoneal (IP) injection of either PBS (placebo control) or 100 µl of 1 µg/µl of anti-CD40L (100 µg) (Abcam ab-65854 rabbit polyclonal). 24 hours after injury the mice were euthanized and the brain fixed in paraffin. Coronal sections were examined for intrusion of anti-CD40L into the pericontusional area using an anti-rabbit HRP secondary antibody.

For the CD40 ligand knockout experiment, male CD40L knockout (on a C57BL/6J background strain) and C57BL/6J wild type mice (Jackson Laboratories) between 8 and 9 weeks old were given a CCI at a rate of 5m/s and depth of 1.8mm while sham control mice received only the craniotomy (n = 12 per group). Naive CD40L knockout mice exhibit symptoms similar to humans with hyper-IgM syndrome, with impaired immune responses including a failure to undergo IgG class-switching in response to immunization and a failure to produce germinal centers (Xu et al., 1994).

Neurobehavioral Testing

As described in chapter 2, Rotarod (Med Associates) was used to measure motor coordination. Briefly summarized, baseline testing for Rotarod occurred one day prior to surgery with initial acclimation trials at a fixed speed of 5 rpm for 3 minutes followed by 3 minutes of rest in the home cage for 3 trials. Baseline testing was performed in the afternoon at an accelerating speed of 5-50 rpm over

a period of 5 minutes followed by 3 minutes of rest in the home cage. Each mouse was given 3 trials per day. Post-surgery testing occurred in the afternoons on days 1, 3, 5, and 7 after surgery using the same protocol.

The Barnes maze was used to measure spatial memory and learning as described in chapter 2. Briefly summarized, all mice were given 6 days of acquisition trials starting on the day following the conclusion of Rotarod testing, and a probe trial was administered on the 7th day, as well as at 3 months following surgery. Two flood lamps were aimed at opposite corners of the room to provide bright indirect lighting as a motivator for the mice to find the escape box. For the acquisition trials a black box was hidden beneath a target hole in the north east quadrant of the board. Mice were given 90 seconds to locate and enter the target box, and they were required to remain in the target box for 30 seconds prior to retrieval. After the 30 second dwell time the target box was removed and the mice were returned from the target box into the home cage. 4 trials were given per day (with an inter-trial time of 1.5 hours) starting from 4 randomized cardinal points for a period of 6 days. On the 7th day the target box was removed and a single probe trial was given starting from the center of the maze. The probe trial lasted 60 seconds and the target box was absent. The probe trial was repeated 3 months after injury (Figure 4-1). After completion of the final probe trial mice were euthanized and tissue was paraffinized for pathological analysis.

Immunohistochemistry

Pathological analyses were carried out by the Roskamp Institute Core Pathology lab. All animals were deeply anesthetized with isofluorane before being intracardially perfused by gravity drip with a heparinized PBS solution pH-7.4 for 3 min, followed by an overnight fixation of brain samples in 4% paraformaldehyde and paraffin embedding. Separate series of 5-6 µm-thick

sections were cut throughout the extent of the cortex and hippocampus and associated areas using a microtome (2030 Biocut, Reichert/Leica) and mounted on positively charged glass slides (Fisher, Superfrost Plus). Sections were stained in entire batches with antibodies (cell markers) raised against: Glial Fibrillary Acid Protein (GFAP) (rabbit anti-GFAP, 1:10,000, Dako) for astrocytosis and Myelin Basic Protein (MBP) for myelin (goat anti-MBP, 1:2,000, Santa Cruz Biotechnology). As a general principle, sections were deparaffinized in xylene and rehydrated in a decreasing gradient of ethanol before the immunohistochemical procedure. Sections were then rinsed in water, treated with endogenous peroxidase blocking solution, containing 0.3% hydrogen peroxide diluted in phosphate buffer solution (PBS) for 30 minutes. After rinsing, sections were treated with target retrieval solution for 8 minutes in the microwave, to induce heat mediated antigen retrieval. After overnight incubation with the primary antibodies, sections were rinsed with PBS, transferred to a solution containing the complimentary secondary antibody (from the Vecatastain Elite ABC Kit) for 1hr and further incubated with avidin-biotin-horseradish peroxidase solution (Vectastain Elite ABC kit; Vector Laboratories) for a further hour.

Immunoreactivity was visualised with 3, 3'-diaminobenzidine (DAB) chromogen and hydrogen peroxide. Development with the chromogen was timed and applied as a constant across batches to limit technical variability (in immunodetection) before progressing to quantitative image analysis. For the anti-CD40L antibody pilot study, the chromogen reaction was used to test for the presence of the antibody within the brain. The reaction was terminated by rinsing sections in distilled water. Finally, mounted sections were progressed through a graded series of alcohols (dehydrated), cleared in xylene and coverslipped with permanent mounting medium. Immunoreacted sections were viewed using an

Olympus (BX60) light microscope and photos were taken using an Olympus MagnaFire SP camera.

Immunoreactivity for cell markers was measured by quantitative image analysis (optical segmentation). Rigorous staining protocols were applied, to ensure consistency of immunostaining, and accuracy of image analysis. This procedure was performed by blind assessment (with each slide analysed blind with respect to marker or animal group). Immunoreactivity for each cell marker was assessed within the cortex, hippocampus and/or associated regions. Optical segmentation of immunoreacted profiles were analysed using Image-Pro Plus morphometric image analysis software (Media Cybernetics). A semi-automated RGB histogram-based protocol (specified in the image analysis program) was employed to determine the optimal segmentation (threshold setting) for immunoreactivity for each antibody.

Statistical Methods

All datasets were assessed for normality using the Shapiro-Wilk test. If a given dataset was normally distributed, mixed model ANOVA (single time point) or repeated measures ANOVA (multiple timepoints) were used to assess significant changes due to injury. Pairwise group comparisons were evaluated using t-test. If a given dataset failed the Shapiro-Wilk test, data was transformed (ln, log, square root). When transformation did not yield a normally distributed data set, we used the non-parametric Kruskal-Wallis test. . Pairwise contrasts were calculated using the Wilcoxon rank sums test. A given effect was considered significant at $p<0.05$. Statistical analyses were performed using JMP 8.02 (SAS).

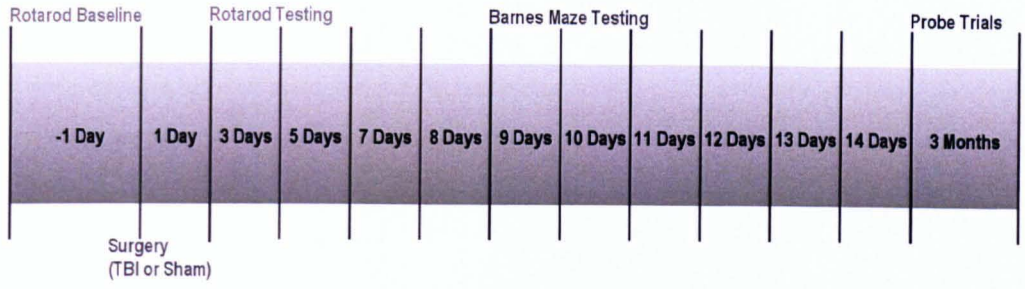

Figure 4-1 Timeline of CD40L KO TBI neurobehavioral testing

Results

Antibody Treatment Approach

Intraperitoneal (IP) injection with anti-CD40L failed to show any signal within the coronal slices of the brain, either at the site of injury or diffusely throughout the brain. Given that 100 ug of antibody cost $337, we had initially tested only 1 mouse to determine if the approach was valid. Based on these results, we concluded that either IP injection of anti-CD40L, even immediately after CCI, was not capable of infiltrating the brain and was therefore not a viable option to inhibit CD40 signaling within the brain; or that significant cost would be expended in optimizing the experiment, not to mention the cost of the experiment itself. Instead we opted to use a genetic knockout model of CD40L to examine the effects of disrupted CD40 signaling on TBI outcome.

Rotarod

Rotarod fall latencies were expressed as a percentage of each mouse's baseline performance (3 trials averaged over each day) since the baseline performance was not significantly different when the groups were compared. CD40L knockout mice showed a significantly higher percentage of baseline performance, as compared to wild type mice, within the injury status category. Repeated measures ANOVA showed a significant effect of both genotype and

injury ($p<0.02$ and $p<0.001$ respectively) with a mean of 147% on day 7 for CD40L knockout sham vs 142% for wild type sham, and 136% for CD40L knockout TBI vs 116% for wild type TBI, indicating that CD40L knockout mice show improved motor coordination compared to wild type controls, and that TBI injured mice performed worse than sham injured mice (figure 4-2).

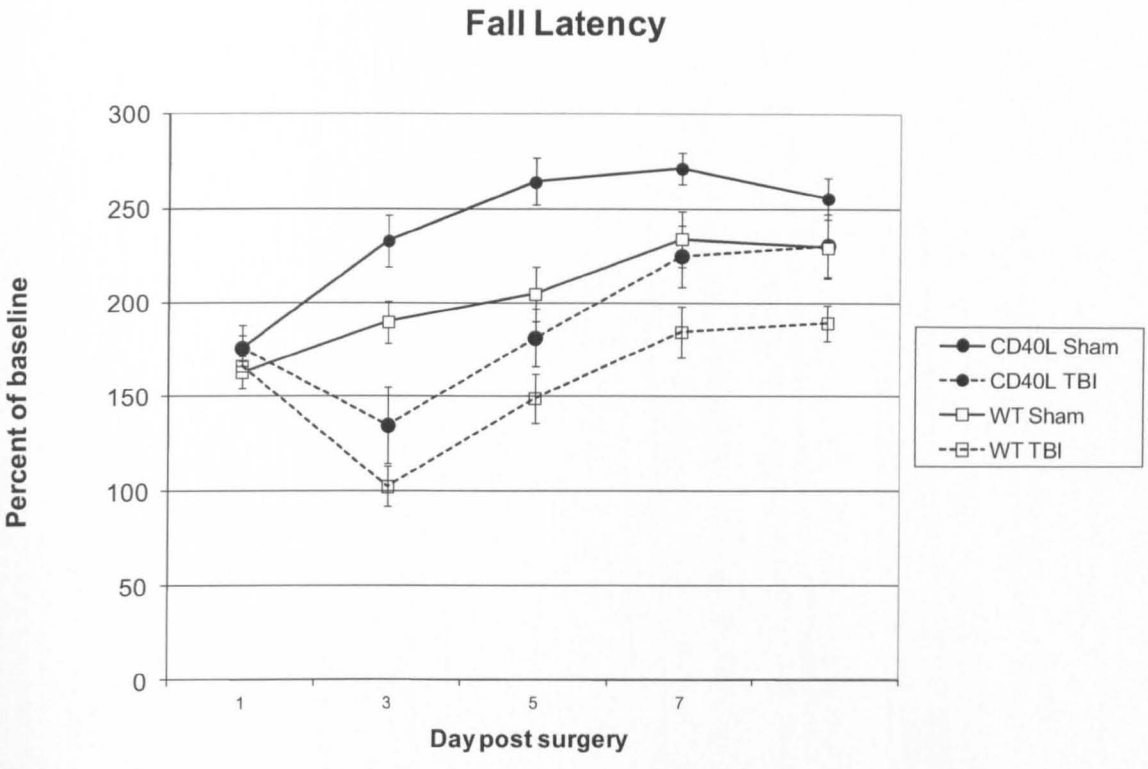

Figure 4-2 Rotarod fall latency in the CD40L knockout cohort. Error bars represent standard error. CD40L knockout genotype was a significant factor by ANOVA repeat measures ($p<0.05$) as was injury ($p<0.01$).

Barnes Maze

Barnes maze acquisition trials were analyzed by measuring the total distance of the Ethovision-determined mouse center point (30 times per second) from the target hole throughout the course of each trial. The distance of the mouse at every sample point was summed and then averaged by day to produce the cumulative distance measurement. Repeated measures ANOVA showed a significant effect of genotype as well as an interactive effect of time x injury (figure 4-3), with a cumulative distance of 66,279 cm for CD40L knockout sham vs 111,360 cm for wild type sham on day 6 ($p<0.05$), and 99,612 cm for CD40L knockout TBI vs 128,555 cm for wild type TBI on day 6 ($p<0.05$), demonstrating improved spatial learning of CD40L knockout mice (108,417 cm mean cumulative distance across all days) compared to wild type mice (134,226 cm mean cumulative distance across all days), and reduced spatial learning in TBI injured mice (132,252 cm mean cumulative distance across all days) compared to sham injured mice (108,951 cm mean cumulative distance across all days).

A probe trial was administered at two weeks after surgery, and again at three months after surgery. At the two week time point a Student's t-test showed CD40L knockout mice had a significantly reduced latency to the target hole compared to wild type sham mice (figure 4-4). CD40L knockout mice experienced extinction to wild type levels by 3 months after surgery (figure 4-5).

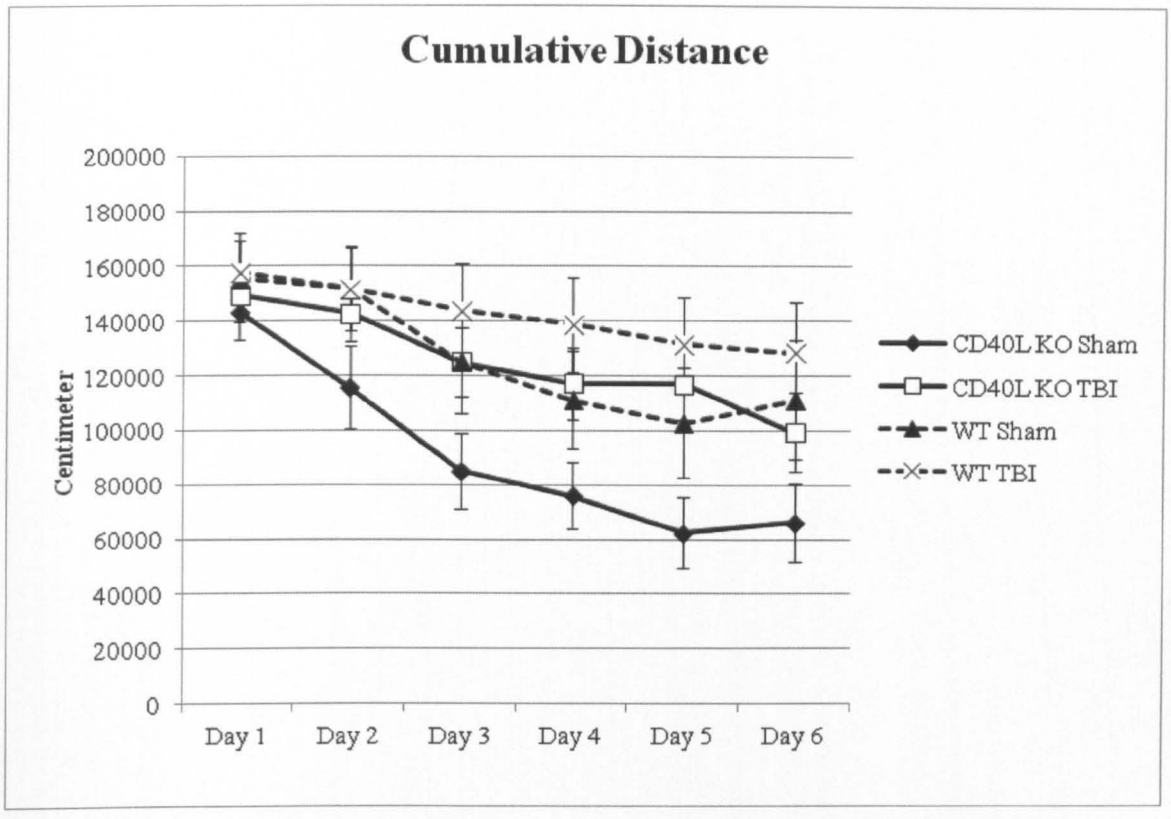

Figure 4-3. Cumulative distance to target hole during the CD40L knockout cohort. Error bars represent standard error. Genotype ($p<0.01$) and time*injury ($p<0.05$) were significant factors by ANOVA. T-tests did not show significance..

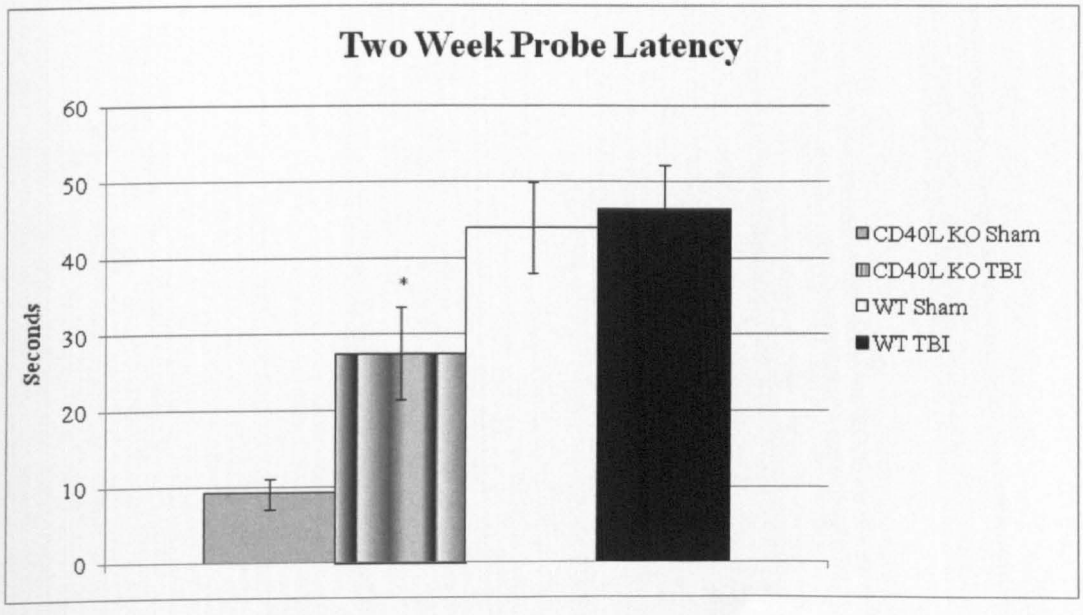

Figure 4-4. Latency to the target hole during the 2 week post-surgery probe trial.CD40L knockout TBI mice had a significantly higher latency than their corresponding shams ($p<0.05$). Error bars represent standard error.

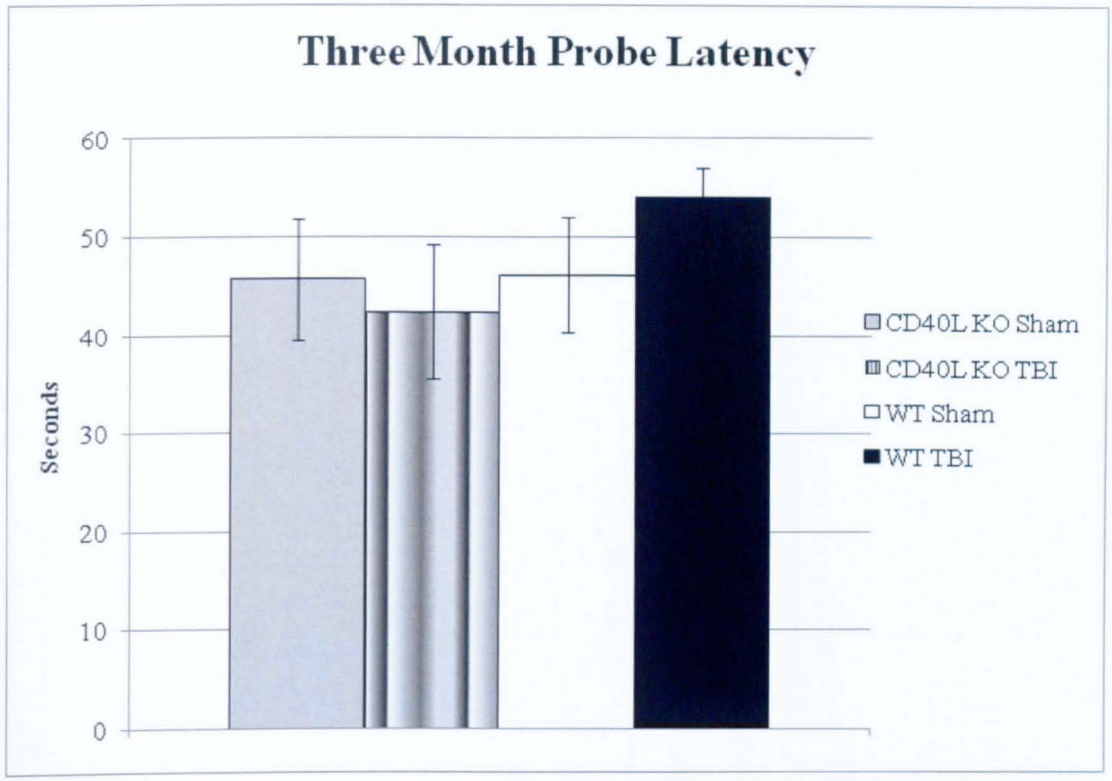

Figure 4-5. Latency to Barnes Maze target hole in CD40L cohort at the 3 month probe trial. Error bars represent standard error. No statistical significance.

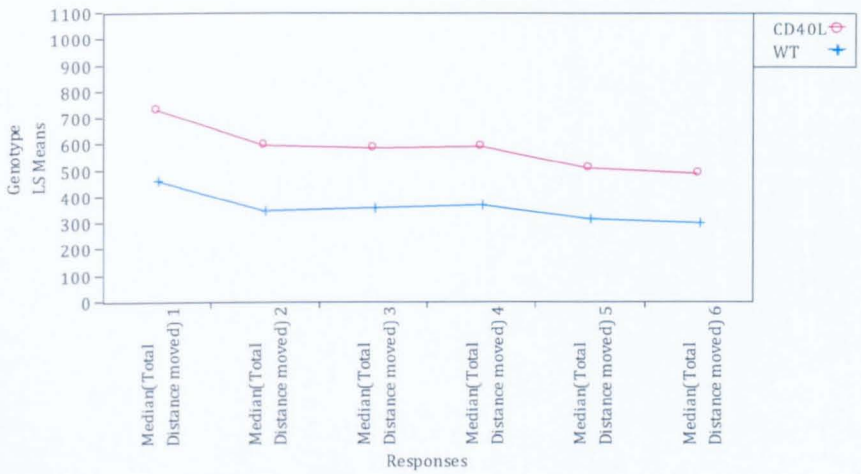

Figure 4-6 Velocity of CD40L knockout mice were significantly higher than that of wild type mice throughout the acquisition testing of the Barnes maze ($p<0.01$).

Immunohistochemistry

GFAP staining showed a highly significant increase in astrocytic activation within the cortex of wild type TBI mice ($p<0.001$), which was completely absent in the CD40L knockout mice (figure 4-7). MBP reactivity showed a significantly higher level in wild type sham mice than wild type TBI ($p<0.001$) but no differences were seen between CD40L knockout sham and TBI mice (figure 4-8). Interestingly, the level of MBP was 4.5 times greater in wild type sham mice than CD40L knockout sham mice.

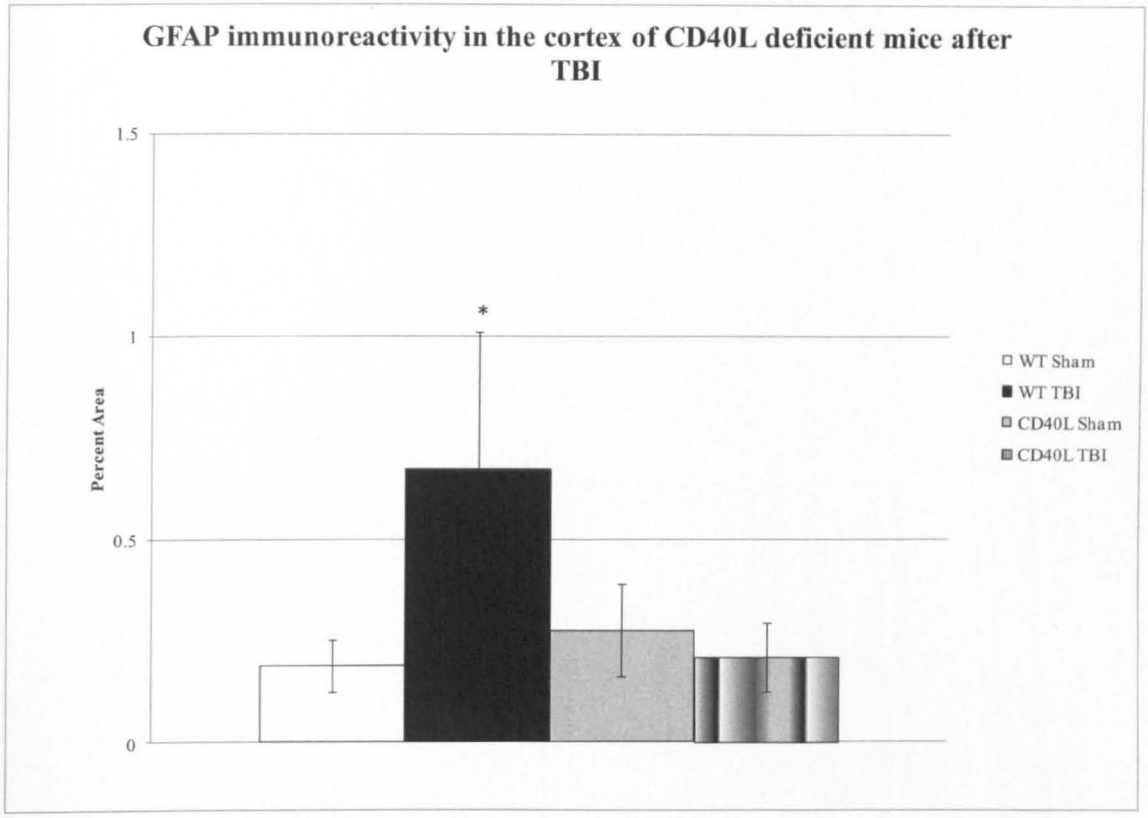

Figure 4-7. Pathological analysis of GFAP in CD40L cohort mouse cortical tissue GFAP showed a significant increase in astroglial activation in wild type TBI mice ($p<0.001$), but not in CD40L knockout TBI. Error bars represent standard error.

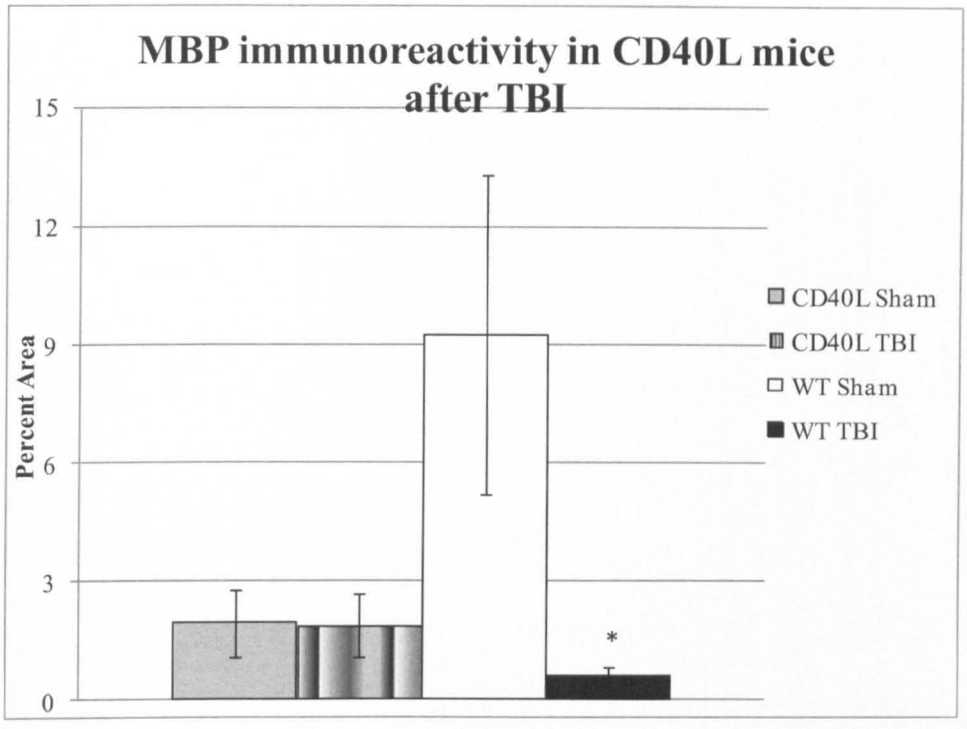

Figure 4-8. Pathological analysis of MBP in CD40L cohort mouse cortical tissue. MBP staining showed a significantly lower amount of myelin ($p<0.001$) after TBI in wild type mice, but not after TBI in CD40L knockout mice. Error bars represent standard error.

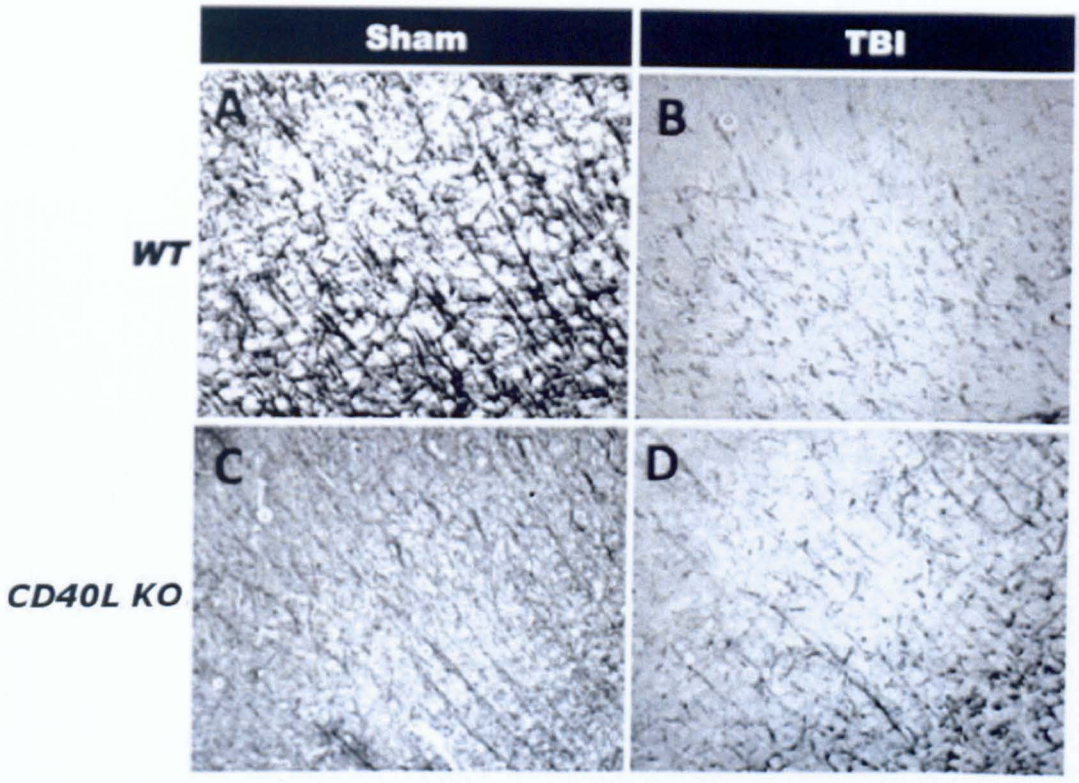

Figure 4-9 Myelin basic protein (MBP) in wild type sham (A), wild type TBI (B), CD40L KO sham (C), and CD40L KO TBI mice (D).

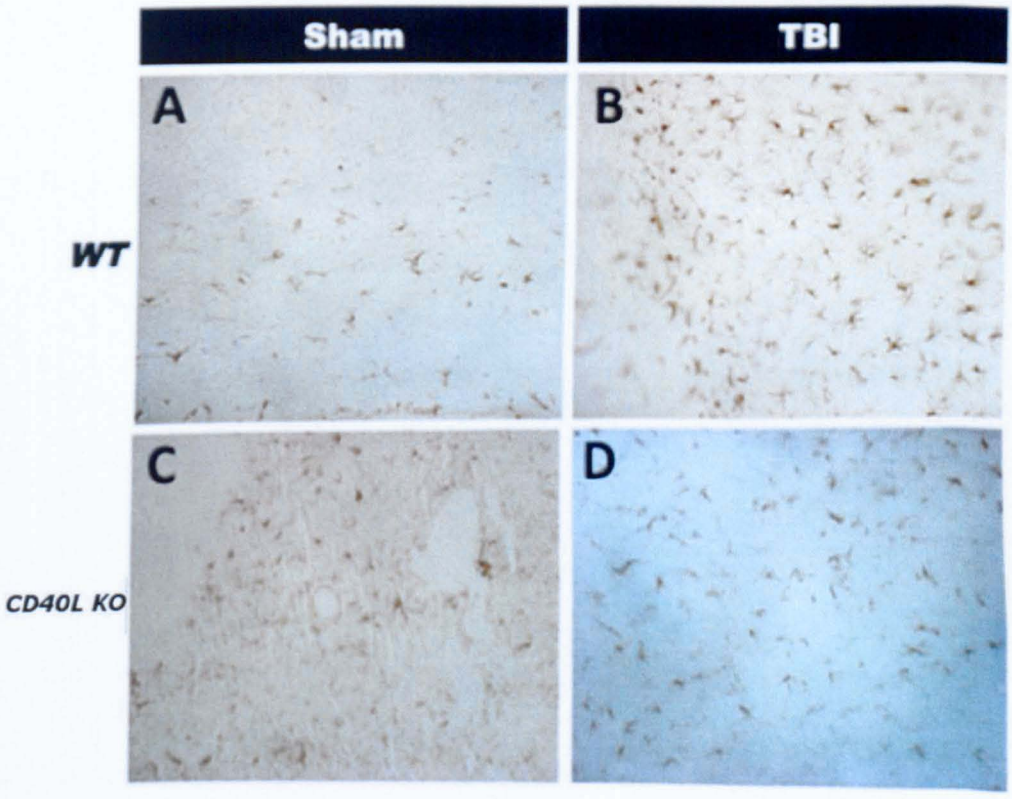

Figure 4-10 GFAP in wild type sham (A), wild type TBI (B), CD40L KO sham (C), and CD40L KO TBI mice (D).

Discussion

CD40 is a costimulatory receptor essential for a variety of immune responses including immunoglobulin class switching (Strom et al., 1999) and memory B cell development (Banchereau et al., 1994). Recently, studies have suggested that CD40 and its ligand CD40L are upregulated after acute cerebral ischemia (Garlichs et al., 2003, Klohs et al., 2008) and that inhibition of CD40/CD40L signaling reduces leukocyte adhesion and blood-brain barrier permeability following middle cerebral artery occlusion (MCAO) in mice (Ishikawa et al., 2004). Given the presence of ischemia-like conditions following TBI, and the differential regulation of proteins related to CD40 signaling in our APOE transgenic mice following TBI, we targeted CD40 signaling in TBI.

Inhibiting CD40 signaling may reduce inflammation after TBI, so we first administered an anti-CD40L antibody immediately after injury. Immunohistochemistry failed to show any sign of infiltration of the antibody into the brain. Previous studies have shown the potential for thromboembolic events when treating with anti-CD40L antibodies, as was the case with failed phase II clinical trials conducted by Biogen to treat multiple sclerosis, Factor VIII inhibitor syndrome, and islet cell transplantation (Biogen press release, 1999). Others that have attempted to treat animal models of multiple sclerosis have failed to show clinical benefits (Kawai et al., 2000, Hart et al., 2005). Our attempt to use an antibody approach to inhibit CD40 signaling was based on a desire for the inhibition to begin after the administration of TBI, not with the intention to take an antibody approach to human testing but with the intent to validate the pathway's importance in secondary injury. Given the extreme cost of this approach and the failure to demonstrate brain penetration, we sought an alternative approach. We proceeded to use CD40L knockout mice as an alternative approach to disruption

of CD40 signaling in TBI. Future studies could employ a conditional knockout model (if such was available) in order to study the effect of inhibiting CD40 signaling at various timepoints after TBI.

Rotarod results showed CD40L knockout mice performing significantly better than their wild type counterparts as measured by the percentage of their baseline fall latency, with CD40L knockout mice returning to sham performance levels by day 7 after TBI. This was true regardless of injury status and may indicate that CD40L knockout mice experience a better outcome even from the sham surgery itself. This may be due to the global effect that the CD40L knockout has on inflammation and thus the reduced susceptibility of CD40L knockout mice to chronic inflammation (Gavins et al., 2011). As discussed previously in chapter 3, sham CCI mice (craniectomy only) are not free from inflammation after TBI; our acute time point cytokine study suggests that a craniectomy alone is a mild injury of greater severity than a single mild closed head injury. The apparent rate of recovery of CD40L knockouts appears to be faster than wild type mice. This is consistent with previous experiments showing superior performance of CD40L knockout mice relative to wild type controls (Ait-Ghezala pers. comm.).

During the Barnes maze, CD40L knockout mice once again showed superior performance than wild type controls over the course of the testing. During the six day acquisition period, genotype and injury were both significant factors on the cumulative distance of the mouse from the target hole showing that TBI mice performed significantly worse than shams, but CD40L knockout mice show significantly better spatial learning. This appears to have been mostly driven by differences in sham performance; in contrast with our other studies the wild type sham mice did not significantly differ from the corresponding wild type TBI mice on any individual day, and did not show nearly as much spatial learning as CD40L

knockout sham mice. It is unknown why this cohort performed in this manner. No other wild type controls tested on the Barnes maze using this protocol showed this small of a degree of separation between sham and TBI. Because the acquisition trials involved 4 trials per day, long term spatial memory is only important for the first trial of acquisition testing and only contributes to one quarter of each day's testing. Whether mice find and enter the target hole successfully or not during that first trial, the target hole's position is re-enforced by guiding mice to the target hole after the end of the trial. Time*injury showed a significant interaction, indicating that sham mice learned the task faster over time, even though the target hole's position was being re-enforced on each trial, thus TBI did have a significant effect on short term spatial learning and memory.

The probe trial also showed CD40L knockout mice performing significantly better than wild type controls. Both the CD40L knockout sham and TBI mice showed a significantly lower latency to the target hole than wild type sham mice, possibly due to minor effects of the sham injury which were mitigated in the CD40L knockout sham mice by the inhibition of CD40 signaling, similar to the effect we see in the CD40L knockout TBI mice. CD40L knockout TBI mice did have a significantly higher latency to the target hole than knockout sham mice, thus injury did result in impairments that were not averted by inhibiting CD40 signaling. Velocity was significantly higher in the knockouts than in the wild type mice, and this was also true during the acquisition testing (figure 4-6). This may account for much of the differences in performance between the two genotypes in the Barnes maze. Although it is primarily a test of spatial memory, motor performance can still be an important factor in determining outcome. A reduced velocity on the test will affect not only the latency to the target hole, but cumulative distance as well since the distance is summed over time. Clearly the Barnes maze is not as demanding

a task on motor performance, but in cases of extreme differences in motor coordination, there may be effects seen as we saw in this cohort. Future studies may examine a cued version of this task in order to discriminate between spatial and nonspatial contributors to performance as previous groups have done (Fox et al., 1998b).

In order to determine if the significant differences seen in the Barnes maze between CD40L knockout mice and wild type mice were entirely due to motor differences, or if there were significant spatial memory differences, mice were re-tested on the probe trial 3 months after surgery. As discussed in chapter 3, CD40 signaling appears to become increasingly important to determining the differential outcome from injury out to 3 months after TBI. By 3 months after surgery, CD40L knockout mice showed extinction to wild type levels; however they also retained their significantly higher velocity during this delayed probe trial, showing that the differences seen during the first probe were not entirely due to differences in motor performance but did likely reflect improved spatial memory. These differences in spatial memory performance may be due to the lessened amount of inflammation within the CD40L knockouts.

The differences in velocity and in the Rotarod are primarily consistent with improved cortical function. CD40L knockout mice are less prone to necrotic pathology (Belkaid et al., 2000) and this may lead to a slower spreading of the necrosis in the pericontusional area of the cortex. In our pathology analysis we witnessed reduced astrocytic activation in the CD40L knockout mice (figure 4-9), as well as no effect of TBI on myelin within the brain, consistent with the hypothesis that reduced inflammation within CD40L knockout mice improved the outcome by reducing the amount of secondary injury. Unexpectedly, however, CD40L knockout mice showed very little myelin by the MBP stain in either the

sham or injured group compared to wild type sham mice (figure 4-10). We currently do not have an explanation for this difference in baseline expression of myelin, and it is clear that the motor and cognitive performance of these mice is not impaired. Inhibition of CD40 signaling effectively halts the progression of experimental autoimmune encephalomyelitis (Howard et al., 1999), showing how important this pathway is to central nervous system (CNS) inflammatory pathology.

These results show that CD40L knockout mice may have superior motor function as assessed by Rotarod, though the spatial learning and memory effects seen by Barnes maze remain unclear due to aberrant performance by the wild type controls. The improvement seen in Rotarod performance carried over to their velocity on the Barnes maze, but cannot fully account for the differences seen in Barnes maze performance. This may be due to reduced cytokine production in the CD40L knockout mice (Henn et al., 1998, Monaco et al., 2002, Omari and Dorovini-Zis, 2003). Pathology shows that the brains of these mice experience significantly reduced inflammation as a result of TBI, which may be reducing secondary injury leading to their improved results on the Rotarod and Barnes maze tasks. Our previous analysis of inflammatory cytokines at acute timpoints after injury shows that even sham mice are not spared from inflammation after surgery, which may be partly why they also show improvements in this cohort compared to wild type controls. CD40 signaling is known to be involved with cytokine production as well as NF-kB activation, thus additional therapies that seek to target both may also be useful in the treatment of TBI. As seen here, CD40 signaling appears to be important in the downstream consequences of TBI and modulation of CD40 signaling may be a potential therapeutic target for the treatment of TBI.

BLANK IN ORIGINAL

CHAPTER 5
IN VIVO INVESTIGATION OF ARC031'S EFFECT ON OUTCOME FROM TBI

Introduction

Chapter 3 describes the proteomic identification of the impact of TBI in mice transgenic for human APOE3 and APOE4. Within those datasets we see significant effects on NF-kB and APP related pathways, suggesting that they may be important in determining outcome after TBI. Both of these pathways have been previously reported in TBI (Murakami et al., 1998, Nonaka et al., 1999a, Sanz et al., 2002, Long et al., 2009, Johnson et al., 2012), but it is the significant interaction between APOE genotype and injury that drew our interest. The participation of these pathways in determining the differential response of E3 and E4 mice to TBI indicates that they may be important for determining outcome from injury. The Roskamp Institute has worked for many years on APP processing and inflammatory mechanisms, specifically with a focus on Alzheimer's Disease (AD), and so both of these areas were prime candidates for us to target with potential therapeutic strategies.

As part of our AD drug discovery program the Institute has a lead compound – Nilvadipine - that impacts both APP processing and NF-kB signaling. Nilvadipine is a dihydropyridine that has been used to treat hypertension in Japan and Europe since 1996. Work from our laboratories has shown that nilvadipine promotes the clearance of amyloid beta across the blood brain barrier (Paris et al. 2011; Bachmeier et al. 2011). Other work has shown that it is capable of inhibiting NF-kB-dependent transcription (Iwasaki et al., 2004). NF-kB inhibitors have also been shown to decrease the production of both Aβ 1-40 and 1-42 production (Paris et al., 2007). Given the role played by NF-kB pathways in post-TBI inflammation and secondary damage, inhibition of NF-kB pathways may prove effective for limiting the damage posed by secondary injury in TBI. Nilvadipine

also decreases the beta cleavage of APP *in vitro*, but without inhibiting the activity of BACE-1 or gamma secretase, and without stimulating additional alpha cleavage of APP (Paris et al., 2011). Our extensive preclinical data in vitro and in vivo in transgenic mouse models of AD, as well as positive results from pilot human clinical trials, have resulted in a Phase III trial (NILVAD) for nilvadipine in Alzheimer's disease, which will begin in Europe in 2012.

Nilvadipine and related compounds have been explored in brain injury models. Nilvadipine has been shown to reduce the infarction area after ischemic injury in rats (Shiino et al., 1991, Takakura et al., 1994). Tissue loss is also an important factor in traumatic brain injury, and loss of synaptophysin expression may indicate a concordant decrease in synaptogenesis as well (Millerot-Serrurot, et al. 2007). Other groups have shown that some dihydropyridines such as nimodipine may be effective in improving the outcome from head injury (Langham et al., 2003, Aslan et al., 2009); but the data are inconsistent (Vergouwen et al., 2006). In particular, Vergouwen and colleagues suggest that although the mortality and poor outcome statistics were no worse than placebo, nimodipine may be deleterious after traumatic subarachnoid hemorrhage due to its profibrinolytic effects which are shared with other dihydropyridine calcium channel blockers. Due to the threat of hypotension and hypoxia in the wake of TBI, administration of an anti-hypertensive may also be extremely detrimental (Stahel et al., 2007).

Nilvadipine is a racemic compound and enantiomers of chiral compounds can have biologically distinct effects from their parent racemic mixture. For example, racemic Equol shares the anti-cancer properties of its S-(-)-equol enantiomer, but the racemic mixture also possesses strong anti-genotoxic activity not present in the S-(-) enantiomer (Magee et al., 2006). In exploring the effects of each nilvadipine enantiomer we discovered that the (-) enantiomer of nilvadipine

retains the anti-amyloidogenic and NF-kB inhibitory effects of its parent molecule, but without the anti-hypertensive effects of racemic nilvadipine. This suggests that higher doses, which may be necessary for APP and NFkB targeting efficacy in humans, could be achieved using the enantiomer, without causing adverse events related to blood pressure lowering. We therefore administered (-)- nilvadipine (termed ARC031 in our laboratories) following TBI in wild type mice to examine its effects on outcome as measured by motor coordination and neurobehavioral analyses.

A pilot study using only CCI injured mice with or without ARC031 treatment (i.e. no sham controls) suggested improved outcome on the Rotarod and MWM. Following the optimization of the Barnes maze, we conducted a full study with all appropriate control groups and used Rotarod and Barnes maze to evaluate the effects of ARC031. These data further supported the use of ARC031 for the treatment of TBI to prevent motor coordination dysfunction and spatial memory loss.

Materials and Methods

Animals and Injury

All mice were wild type C57BL/6J male mice. For the pilot study of ARC031, mice were between 18 and 82 weeks of age. Groups were matched for average and range of age to within 2 weeks. ARC031 (10mg/kg) (n = 12) or vehicle only (DMSO) (100µl) (n = 13) was administered to each group via intraperitoneal injection starting at 30 minutes post surgery and continuing each day at 9am for 7 days. CCI surgery was performed as previously described (see chapter 2). Briefly described, mice were anaesthetized with isofluorane and mounted in a stereotaxic frame. Following a midline incision and reflection of the soft tissues, a 5mm craniectomy was performed adjacent to the central suture. Severe injury was administered as previously described (Crawford et al., 2009) by impacting the right

cortex with a 2 mm diameter tip at a rate of 5 m/s and depth of 1.8 mm by an electromagnetic impactor. No sham controls were used for this study.

For the full study of ARC031, mice were all male C57BL/6J between 11 and 12 weeks old at the time of injury. Mice were divided into 6 groups of naïve, sham, and injured mice with treatment or vehicle control. Within each injury group, mice received ARC031 (20mg/kg, dissolved in 100% DMSO) or vehicle only (100% DMSO) (n = 12 per group) administered via intraperitoneal injection starting at 30 minutes post surgery and continuing for 7 days post-surgery at 9am each morning. The dose was increased from the pilot study in order to maximize the effects and because it lacks the anti-hypertensive effect of its parent molecule, no side effects were anticipated. Mice received either a CCI or sham surgery (craniectomy only) as previously described, or only received the injections in the case of the naïve group.

Based on our acute inflammatory cytokine data from chapter 3, we decided to examine the effect of ARC031 at 6 hours after TBI using both the CCI and CHI injury models, to study ARC031's effectiveness at reducing acute inflammation after both a severe and a mild TBI. This timepoint was selected because it demonstrated a significant effect of CCI and was the only timepoint for which any marker was significantly increased in CHI (IL-6). Mice were divided into groups of TBI and sham, CCI or CHI, with ARC031 or DMSO administered 30 minutes after injury (n = 3 per group). For details on the CHI injury see chapter 3. The same parameters as described above were utilized once again for the CCI injury and the following parameters were used for the mTBI CHI model: a 5.0mm diameter flat face tip, 5m/s strike velocity, 1.0mm strike depth, and a 200msec dwell time. At the end of the procedure, mice were allowed to recover on a heating pad set at 37°C and, upon becoming ambulatory, returned to their cages.

All procedures involving mice were carried out under IACUC approval and in accordance with the National Institute of Health Guide for the Care and Use of Laboratory Animals.

Therapeutic Administration

Synthesis of ARC031 and analytical specifications were carried out in-house at the Roskamp Institute (Dr. Chao Jin and J. Reed). ARC031 was dissolved in DMSO and administered via intraperitoneal injection at a dose of 20mg/kg starting 30 minutes after surgery (or by itself in the case of the naïve group) and once each day at 9:00 AM for a period of 7 days to each of the groups. Control mice received DMSO alone. Naïve, sham, and injured groups all received injection with either ARC031 or DMSO. For the 6 hour acute timepoint study, only one injection was administered 30 minutes after surgery (Figure 5-1).

Rotarod Testing

Rotarod testing was performed as described in chapter 2. One day of baseline testing was administered on the day prior to surgery, followed by post-surgery testing on days 1, 3, 5 and 7 after surgery at a speed of 5-50 rpm over 5 minutes.

Morris Water Maze Testing

Spatial memory and learning of mice in the pilot ARC031 study (n=12 ARC031, n=13 DMSO, all having received CCI) were analyzed using the Morris Water Maze as previously described in chapter 2.

Barnes Maze Testing

For the full ARC031 study the Barnes maze was used to measure spatial memory and learning as described in chapter 2. This cohort was tested after I had established the benefits of Barnes Maze over Morris Water Maze for evaluation of TBI in mice. All mice were given 6 days of acquisition trials starting on the day

following the conclusion of Rotarod testing (day 8 post-surgery), and a probe trial was administered on the 7th day of Barnes maze testing (day 14 post-surgery). All Barnes maze trials were both videotaped and recorded with the Ethovision XT tracking system for analysis.

Acute Timepoint ELISA Analysis

IL-6 and MCP-1 ELISA kits (Invitrogen) were run as described in chapter 3. 150 ug of protein were loaded into each well for each ELISA. Samples were run in triplicate. We did not assay Aβ levels within these mice due to the difficulty in assaying endogenous mouse amyloid.

Tissue collection

For the pilot study, mice were euthanized one month after TBI. For the full study, mice were euthanized two weeks post-procedure.

For the full study, 4 mice from each group were fixed for pathological analysis. These animals were also deeply anesthetized with isofluorane before being intracardially perfused by gravity drip with a heparinized PBS solution pH-7.4 for 3 min, followed by an overnight fixation of brain samples in 4% paraformaldehyde and paraffin embedding. Separate series of 5-6 μm-thick sections were cut throughout the extent of the cortex and hippocampus and associated areas using a microtome (2030 Biocut, Reichert/Leica) and mounted on positively charged glass slides (Fisher, Superfrost Plus). The remaining mice from each group were perfused with heparinized PBS solution (pH 7.4). The ipsilateral and contralateral hemispheres were dissected for the hippocampus, cortex, and cerebellum on ice and frozen at -80 C.

For the six hour acute time point study, mice were euthanized 6 hours after the procedure. Euthanasia was performed by deep anesthesia with isofluorane followed by gravity drip with a heparinized PBS solution pH-7.4. The ipsilateral

and contralateral hippocampus, cortex, and cerebellum were then rapidly dissected on ice and frozen at -80 C.

Immunohistochemistry

Pathological analyses were carried out by the Roskamp Institute Core Pathology lab as described in chapter 3. Sections were stained in entire batches with antibodies (cell markers) raised against: GFAP (rabbit anti-GFAP, 1:10,000, Dako) for astrocytosis and synaptophysin (rabbit anti-synaptophysin, 1:500, Abcam) for synaptic density. For Nissl staining, sections were deparaffinized and cleared in a solution of 0.005% lithium carbonate with 70% ethanol and counterstained with 0.25% Cresyl Violet for 20 minutes.

All animals were deeply anesthetized with isofluorane before being intracardially perfused by gravity drip with a heparinized PBS solution pH-7.4 for 3 min, followed by an overnight fixation of brain samples in 4% paraformaldehyde and paraffin embedding. Separate series of 5-6 µm-thick sections were cut throughout the extent of the cortex and hippocampus and associated areas using a microtome (2030 Biocut, Reichert/Leica) and mounted on positively charged glass slides (Fisher, Superfrost Plus). As a general principle, sections were deparaffinized in xylene and rehydrated in a decreasing gradient of ethanol before the immunohistochemical procedure. Sections were then rinsed in water, treated with endogenous peroxidase blocking solution, containing 0.3% hydrogen peroxide diluted in phosphate buffer solution (PBS) for 30 minutes. After rinsing, sections were treated with target retrieval solution for 8 minutes in the microwave, to induce heat mediated antigen retrieval. After overnight incubation with the primary antibodies, sections were rinsed with PBS, transferred to a solution containing the complimentary secondary antibody (from the Vecatastain Elite ABC

Kit) for 1hr and further incubated with avidin-biotin-horseradish peroxidase solution (Vectastain Elite ABC kit; Vector Laboratories) for a further hour.

Immunoreactivity was visualised with 3, 3'-diaminobenzidine (DAB) chromogen and hydrogen peroxide. Development with the chromogen was timed and applied as a constant across batches to limit technical variability (in immunodetection) before progressing to quantitative image analysis. Finally, mounted sections were progressed through a graded series of alcohols (dehydrated), cleared in xylene and coverslipped with permanent mounting medium. Immunoreacted sections were viewed using an Olympus (BX60) light microscope and photos were taken using an Olympus MagnaFire SP camera.

Immunoreactivity for cell markers was measured by quantitative image analysis (optical segmentation). Rigorous staining protocols were applied, to ensure consistency of immunostaining, and accuracy of image analysis. This procedure was performed by blind assessment (with each slide analysed blind with respect to marker or animal group). Immunoreactivity for each cell marker was assessed within the cortex, hippocampus and/or associated regions. Optical segmentation of immunoreacted profiles were analysed using Image-Pro Plus morphometric image analysis software (Media Cybernetics). A semi-automated RGB histogram-based protocol (specified in the image analysis program) was employed to determine the optimal segmentation (threshold setting) for immunoreactivity for each antibody.

Image Analysis

Photos of Nissl sections stained by the Roskamp Institute Core Pathology lab were taken using an Olympus MagnaFire SP camera. In order to assess any effects of treatment on contusion volume, I measured the peri-contusional area

(1-3 slides per mouse, 4 mice per group) using the Nissl stained slides in coronal sections in an area spanning from the cortex retrosplenialis to the neocortex and from the neocortex across the dentate gyrus to the brachium colliculi superioris. This was compared to the corresponding region of the contra-lateral side of each mouse (3-6 biological replications). The area of this region divided by the area of the contralateral side was used to determine the extent of the lesion volume.

Statistical Methods

All datasets were assessed for normality using the Shapiro-Wilk test. If a given dataset was normally distributed, mixed model ANOVA (single time point) or repeated measures ANOVA (multiple timepoints) were used to assess significant changes due to injury. Pairwise group comparisons were evaluated using t-test. If a given dataset failed the Shapiro-Wilk test, data was transformed (ln, log, square root). When transformation did not yield a normally distributed data set, we used the non-parametric Kruskal-Wallis test. . Pairwise contrasts were calculated using the Wilcoxon rank sums test. A given effect was considered significant at $p<0.05$. Statistical analyses were performed using JMP 8.02 (SAS).

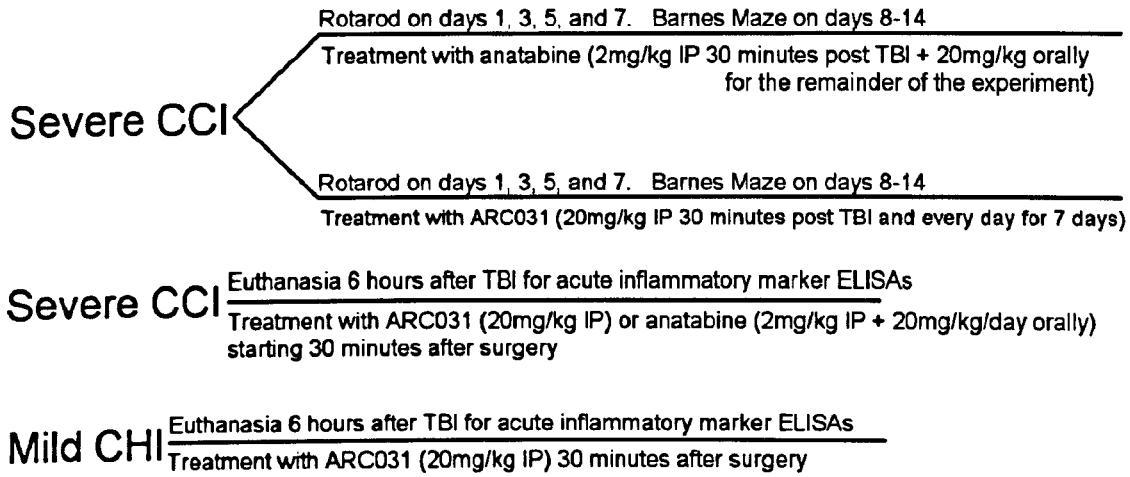

Figure 5-1 Timeline of Therapeutic Administration Experiments for Chapter 5 and Chapter 6.

Rotarod

Our pilot study showed ARC031 mice improving to 120% of their baseline average by day 7 on the Rotarod, whereas DMSO treated mice failed to return to their baseline levels, reaching an average of 88% of baseline performance on day 7. Although their initial starting point after the injury was similar, ARC031 mice returned to baseline performance by day 5, though differences were not significant (figure 5-2).

During the full ARC031 study, baseline testing on the rotarod showed a significant effect of intraday learning between trials; however there were no significant differences between cohorts (Figure 5-3). Testing 1, 3, 5, and 7 days post-surgery showed a significant effect of intraday trial ($p<0.05$), injury ($p<0.0001$), and ARC031 treatment ($p<0.01$), however, the difference between TBI injured mice who received ARC031 vs mice that received DMSO alone were not significant. The average ARC031 TBI latency to fall exceeded the DMSO Sham level by day 7 post-surgery, whereas the DMSO TBI mice did not, though ARC031 TBI and DMSO TBI were still not significantly different by t-test ($p>0.2$). Excluding TBI mice from the analysis, there was no statistically significant effect of sham injury compared to naïve mice who received no craniectomy or anesthesia ($p=0.4907$). Treatment with ARC031 was still a significant factor in the sham and naïve groups ($p<0.05$) with ARC031 treated sham and naïve mice having a higher average fall latency than DMSO treated mice on days 3, 5, and 7.

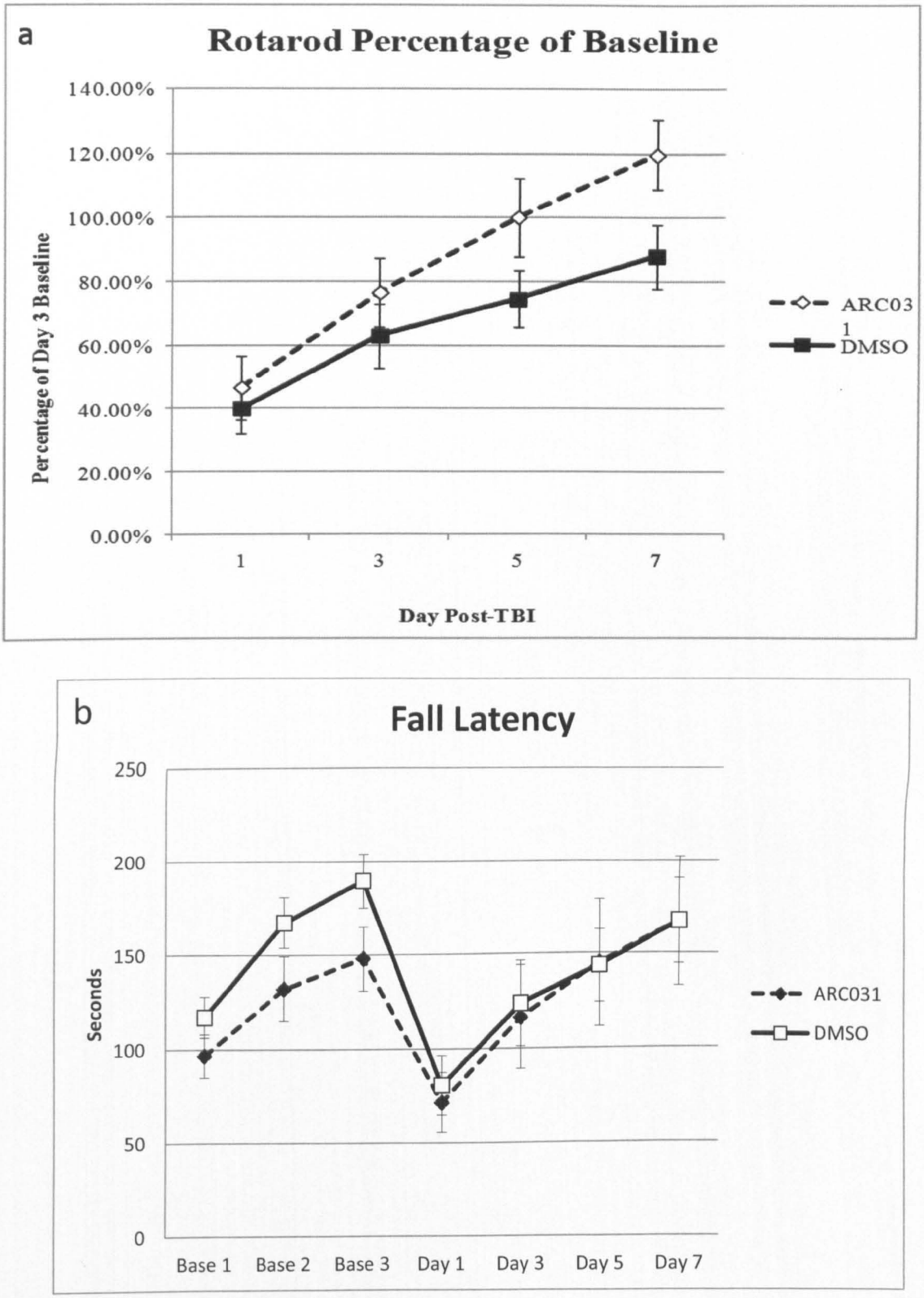

Figure 5-2. Percentage of baseline fall latency (a) and raw fall latency (b) during the ARC031 pilot study. Error bars represent standard error. Differences between groups were not significant by T-test.

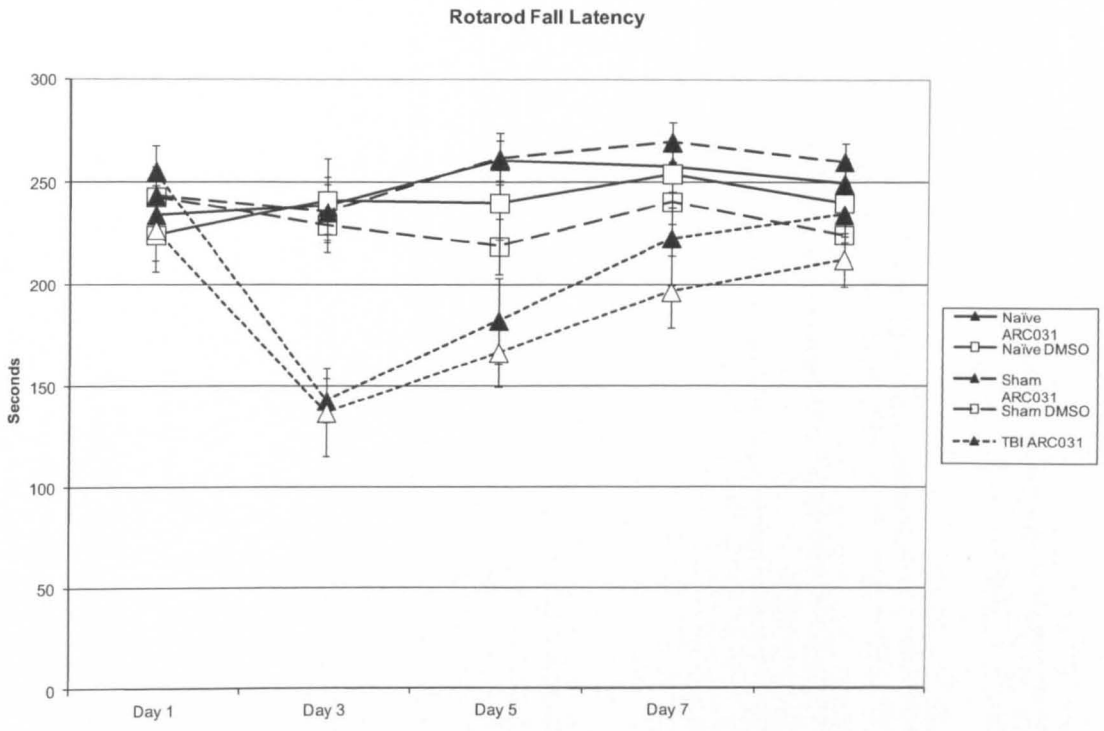

Figure 5-3. Rotarod fall latency in the full ARC031 study. Error bars represent standard error. ARC031 treatment did not produce significant differences by T-test.

Morris Water Maze

Morris water maze was only utilized for the pilot study, which did not include sham mice. Mice in the pilot study treated with ARC031 showed a 20 second improvement in their latency to the target platform from day 1 to day 9, whereas mice treated with DMSO showed only a 10 second improvement in latency over the same time period. Latencies were similar on all prior days of water maze testing (figure 5-4).

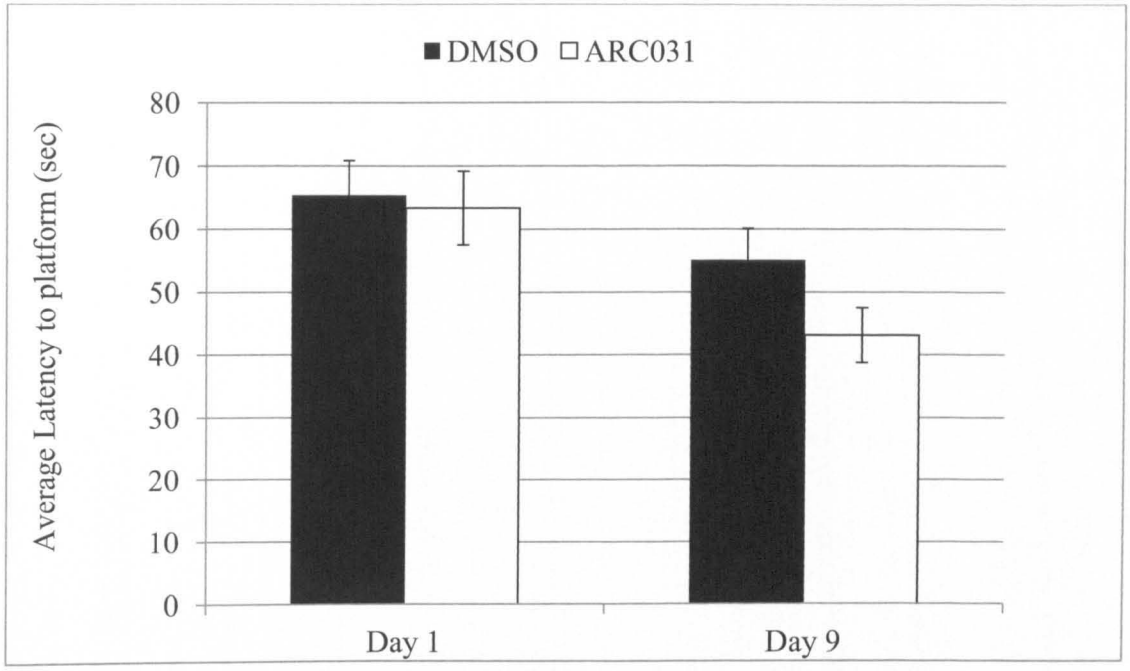

Figure 5-4. Average latency to the hidden platform during MWM testing of the ARC031 pilot cohort. Error bars represent standard error. Treatment with ARC031 did not produce statistical significance by T-test.

Barnes Maze

Acquisition tests were measured by total distance, which we defined as the sum of the distance from the mouse center point to the target hole at each sample point at a rate of 30 samples per second for the entire trial. Acquisition testing showed a statistically significant effect of starting point, block, injury, group*injury, and group*treatment. On day 2 ARC031 treated TBI mice had a significantly lower cumulative distance from the target hole than DMSO treated TBI mice ($p<0.0092$). The treatment effect became insignificant by day 3 and remained an insignificant factor for the duration of the acquisition period (figure 5-4).

A single probe trial was conducted on day 7. ARC031 sham mice unexpectedly showed a higher average distance than DMSO sham mice and analysis of the amount of time each mouse spent with its nose in the target hole similarly showed a greater time spent by DMSO sham mice than ARC031 shams (Figure 5-6a and b). To explore whether or not this discrepancy in the sham data (not seen in the naïve group) was due to a failure of ARC031 treated sham mice to remember the location of the target hole, or due to increased exploratory behavior in an attempt to relocate the target box after initially discovering its disappearance from the arena, we measured their travel time. This was defined as the latency from the first walking motion of each mouse to the first nose poke into either the target or an adjacent hole. Failure to find either the target or adjacent hole was recorded as a time of 60 seconds (trial length). 3 mice that remained stationary for the entire probe trial were excluded from the analysis. ARC031 sham mice travel time was not statistically different from DMSO sham mice ($p<0.5692$) or ARC031 sham mice ($p<0.2128$), whereas DMSO TBI mice had a significantly longer travel

time than DMSO sham mice ($p<0.023$). Figure 5-7. There were no significant differences between TBI mice treated with ARC031 or DMSO.

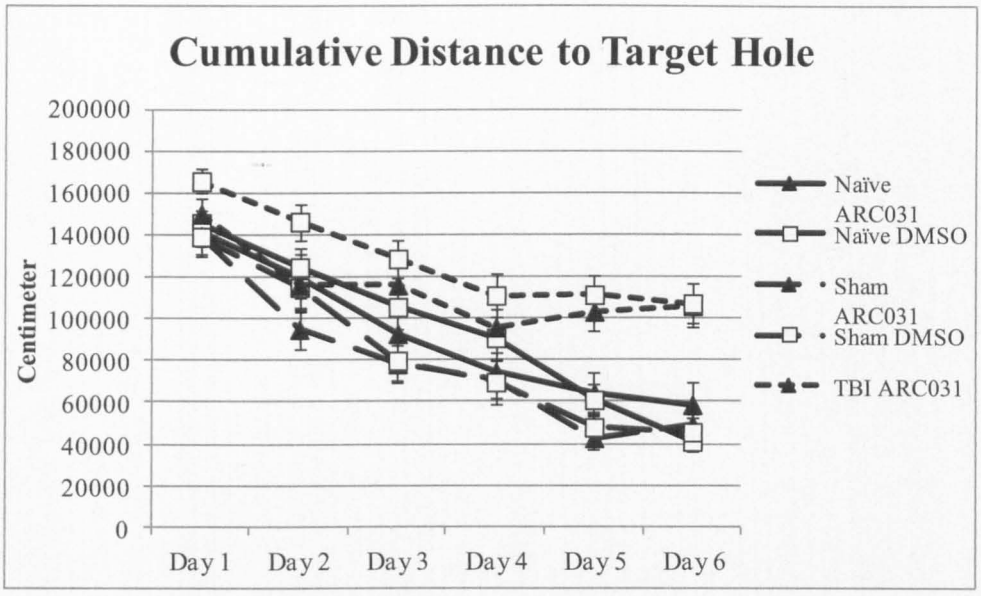

Figure 5-5. Cumulative distance to the target hole during acquisition testing of the ARC031 full cohort on the Barnes maze. Error bars represent standard error. Treatment with ARC031 did not produce statistical significance by T-test.

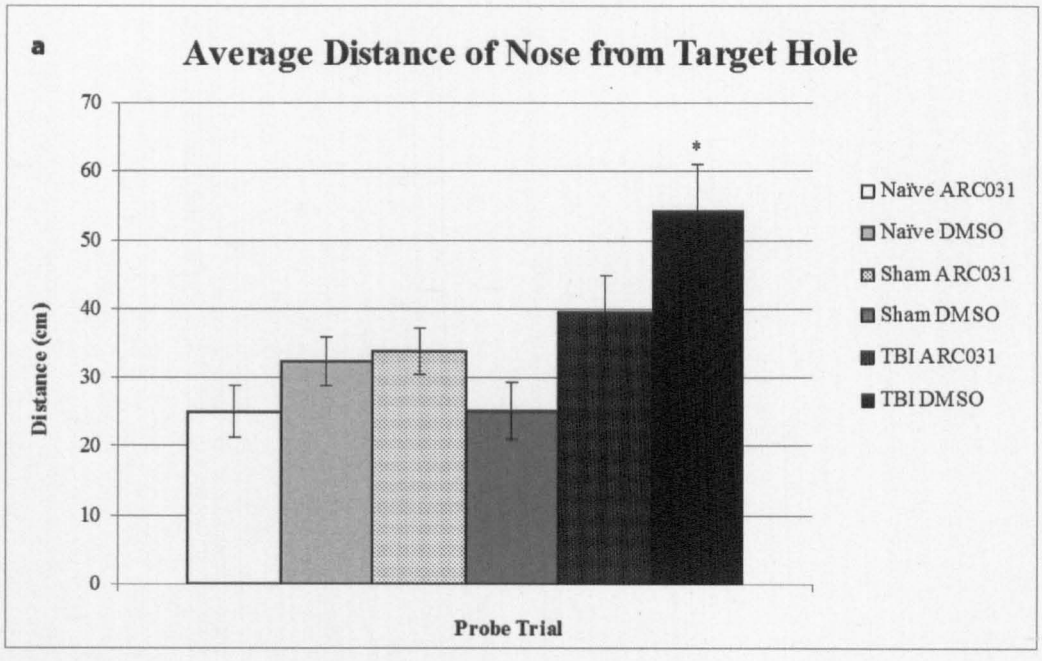

Figure 5-6a.

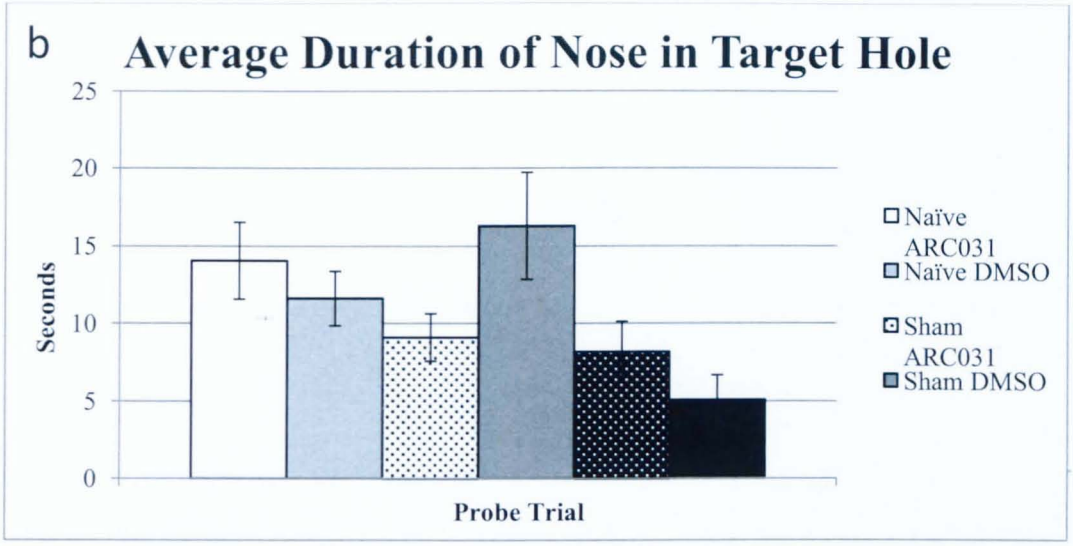

Figure 5-6. a) Average distance from the target hole during the probe trial of the ARC031 full study on day 7 and b) average duration in the target hole during the probe trial of the ARC031 full study on day 7. Error bars represent standard error. * indicates significance ($p<0.05$) by T-test compared to the corresponding sham.

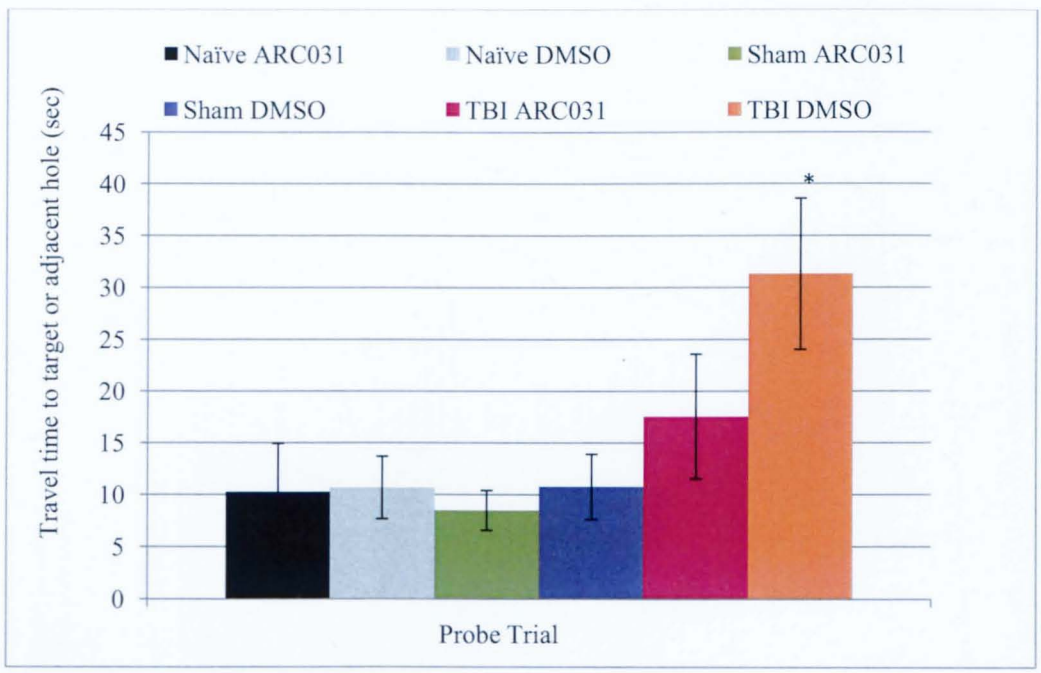

Figure 5-7. Travel time to the target hole during the probe trial ofthe ARC031 full study at day 7 probe trialError bars represent standard error. * indicates statistical significance compared to corresponding sham ($p<0.05$).

IL-6 and MCP-1 were assayed in the tissue of the right cortex 6 hours after CHI or CCI or sham surgery. As before, ARC031 (20 mg/kg) or DMSO was injected by IP injection 30 minutes after surgery. A clear effect of injury was noted in the CCI model, with a highly significant increase in MCP-1 in DMSO treated CCI TBI compared to CCI sham (or CHI sham) by t-test ($p<0.01$). However in the CHI model there was no effect of injury, with a non-significant trend towards greater MCP-1 in DMSO treated CHI TBI than CHI sham. Although ARC031 did not prevent the injury-induced increases in MCP-1, it did show a consistent but non-significant decrease in MCP-1 in every treated group, both in sham and TBI, in both the CHI and CCI models (figure 5-8). IL-6 was significantly increased in both DMSO and ARC031 treated CCI mice compared to shams. In this cohort, a significant increase was not seen in the CHI TBI mice at 6 hours, either in the DMSO and ARC031 treatment groups. The values for the IL-6 within the CHI groups are interpolated because IL-6 levels were below detection limits in every CHI group (Figure 5-9). ARC031 treated CHI mice showed slightly less IL-6 expression than DMSO treated CHI mice, however the difference was once again non-significant.

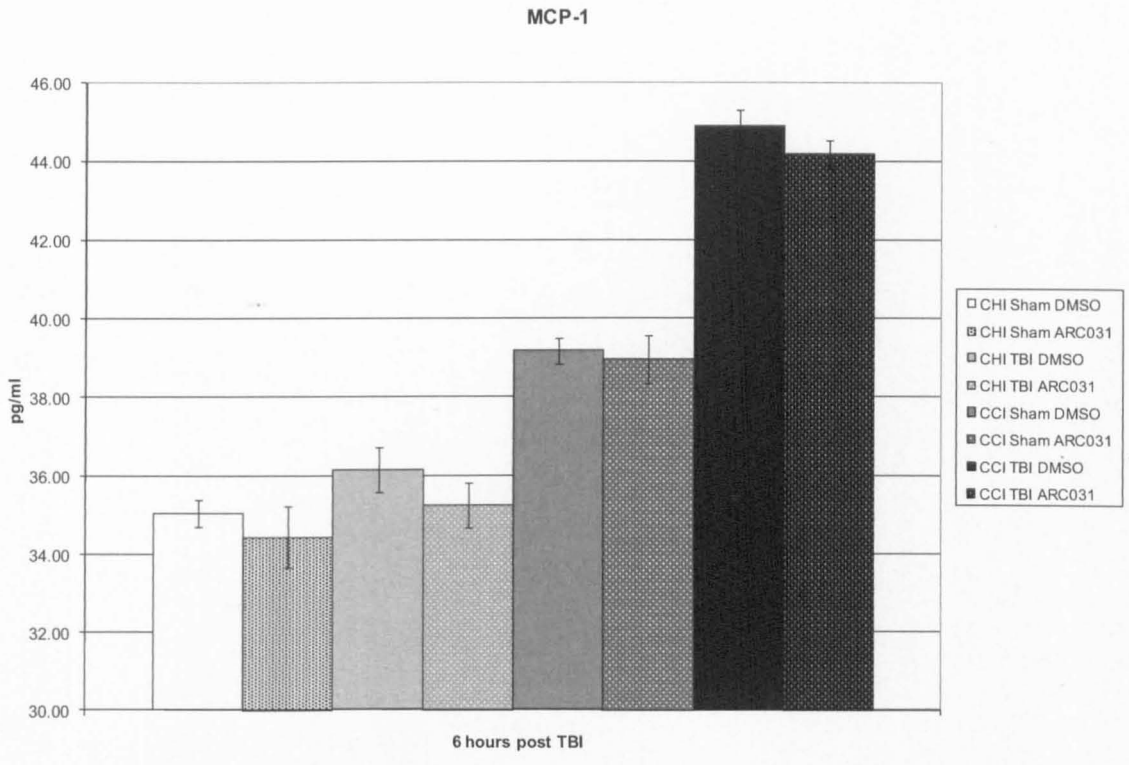

Figure 5-8. MCP-1 ELISA of the ARC031 6hr acute timepoint study. Error bars represent standard error. Treatment with ARC031 did not produce statistical significance by T-test.

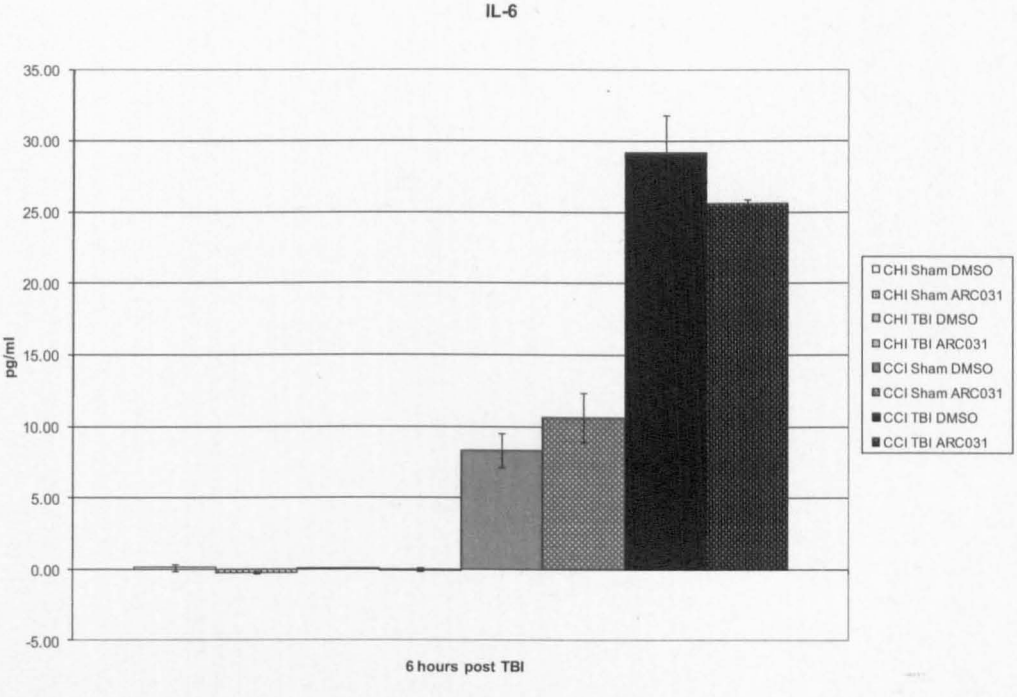

Figure 5-9. IL-6 ELISA of the ARC031 6hr acute timepoint study. Error bars represent standard error. Treatment with ARC031 did not produce statistical significance by T-test.

Pathology

Nissl stained sections were used to measure the peri-contusional area. The data show a significant amount of tissue loss in the ipsilateral cortex of ARC031 TBI and DMSO TBI mice compared to their respective shams (figure 5-10), with an insignificant trend towards a smaller amount of tissue loss in ARC031 treated TBI mice compared to DMSO treated TBI mice.

GFAP immunoreactivity showed only a slight increase in CCI and sham mice compared to naïve mice, but without any statistical significance (figure 5-11). ARC031 failed to show an effect on astrocytic activation in either TBI or control animals.

Synaptophysin staining showed no effect of injury in the DMSO treated mice, but a decrease of 20-40% in ARC031 treated mice compared to their respective DMSO controls. Naïve mice treated with ARC031 showed the smallest decrease while TBI mice treated with ARC031 showed the largest (figure 5-12).

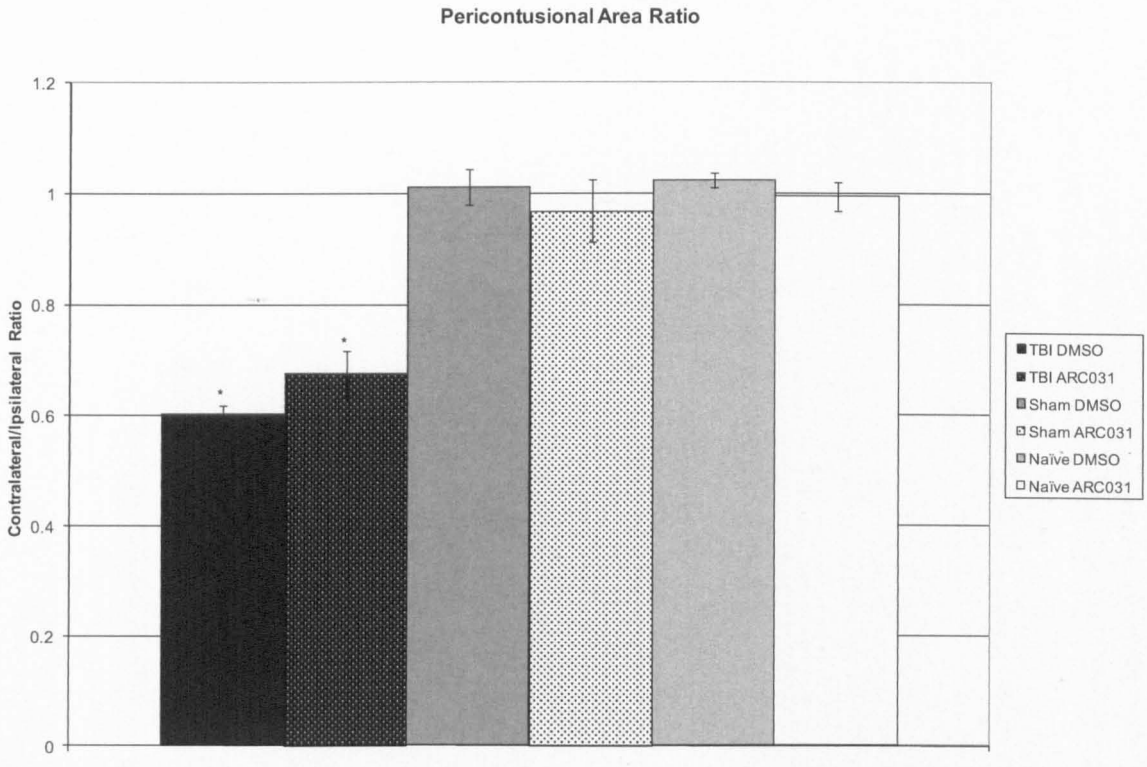

Figure 5-10. Tissue loss as measure by Nissl staining of ipsilateral cortex compared to the contralateral cortex of the ARC031 full study. Error bars represent standard error. * indicates significance relative to corresponding sham by T-test ($p<0.05$).

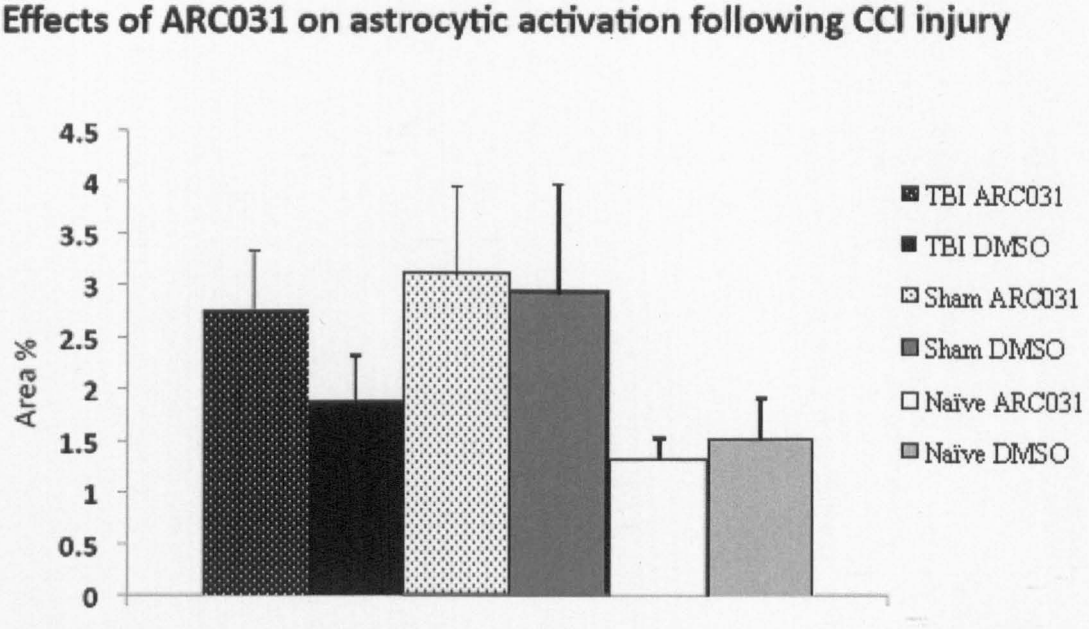

Figure 5-11. Pathological analysis of GFAP in ARC031 full cohort mouse cortical tissue. Error bars represent standard error. Treatment with ARC031 did not produce statistical significance by T-test.

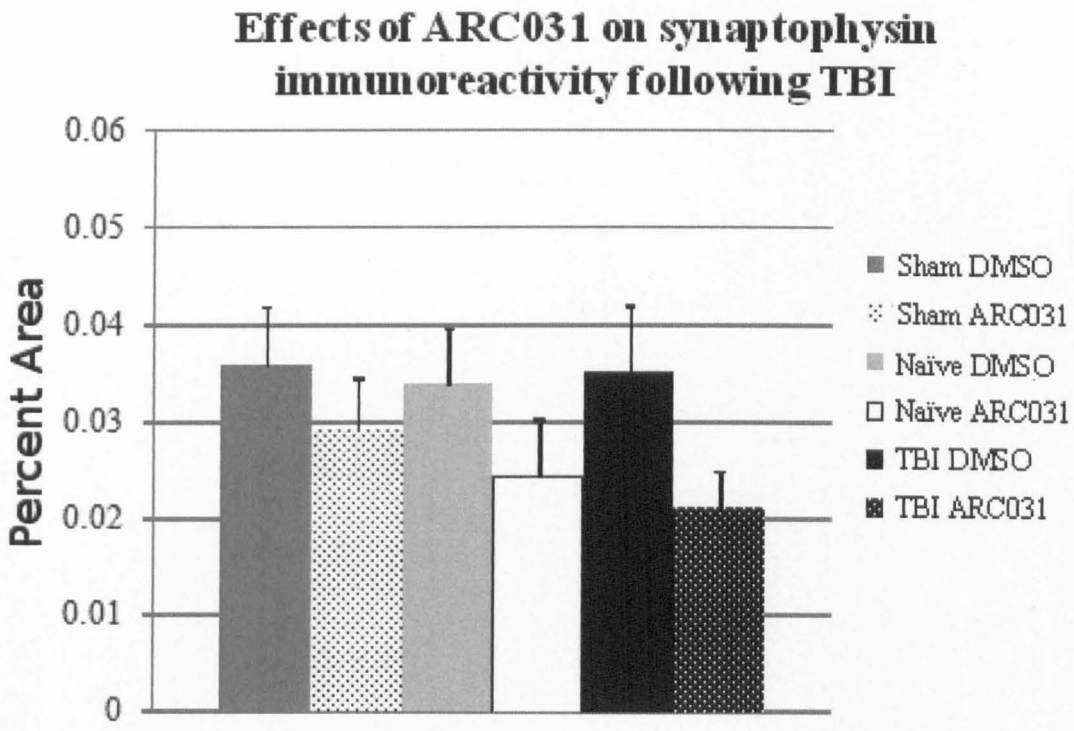

Figure 5-12. Pathological analysis of Synaptophysin in cortex of mice from the ARC031 full study. Error bars represent standard error. Treatment with ARC031 did not produce statistical significance by T-test.

Discussion

As discussed in chapter 1, there are currently no approved therapeutics designed to combat secondary injury after TBI. Our proteomic data from APOE transgenic mice discussed in chapter 3 suggests NF-kB and APP related changes may be important in determining outcome from injury. ARC031 is an inhibitor of NF-kB dependent transcription and is also an inhibitor of amyloidogenic processing, and thus presented itself as a potential therapeutic to explore in our TBI and neurobehavioral testing paradigms (Iwasaki et al., 2004, Paris et al., 2007) (Paris personal communication). We conducted a pilot ARC031 study in wild type mice who received a severe CCI, but as numbers of available mice were limited for this study we did not include sham controls in this group. Our pilot utilized Rotarod and Morris water maze testing, and the data suggested that ARC031 might be effective for treating TBI. This prompted a full study with appropriate sham and naïve controls. This full study utilized the Rotarod but used the Barnes maze to evaluate memory and learning (as per our conclusions from chapter 2) and the results from these neurobehavioral tests confirm that ARC031 may be effective for improving motor function and spatial memory following TBI. Our choice of NFkB related pathways as targets is supported by research from other groups which have shown an immediate increase in NF-kB translocation in humans (Stegmaier et al., 2008) and a prolonged increase in NF-kB binding activity following TBI in rodents (Nonaka et al., 1999b, Sanz et al., 2002, Hang et al., 2005, Zhang, 2005, Chen et al., 2008). This increased activity is known to co-localize with the injured cortex and expanding ventricle for up to at least one year following injury. Mice that have sustained chemical injury to the hippocampus have similarly shown increases in NF-kB activity 4 and 21 days after injury (Kassed et al., 2004). With regard to APP processing, amyloidogenic processing

has been shown to be an important part of secondary injury in transgenic mouse models (Uryu et al., 2002) which correlates with a large burst of amyloid beta seen in the CSF after head injury in humans (Raby et al., 1998, Olsson et al., 2004) and diffuse Aβ plaques that form within the first hours after brain injury (Smith et al., 2003, Ikonomovic et al., 2004). Previous research has shown that some NF-kB inhibitors also reduce Aβ40 and Aβ42 production (Paris et al., 2007).

Mice who received ARC031 showed significantly improved fall latency in the Rotarod task, regardless of injury group. ARC031 treatment was a statistically significant factor for improved fall latency, even in sham and naïve groups, but there was no statistically significant interactive effect of ARC031 treatment with injury, suggesting an overall positive benefit of treatment on motor skills not specific to TBI mechanisms. Other groups have previously shown a positive effect of NF-kB inhibitors on the Rotarod performance of otherwise untreated and uninjured mice (McCall et al., 2009). In humans, DMSO can also cause headaches and dizziness, and the extent to which this is true in mice is not well studied and may provide either enhance or diminish the effectiveness of ARC031 on Rotarod performance.

In the Barnes maze we saw no significant effect of ARC031 treatment on spatial learning over the course of 6 days of acquisition trials as measured by the total distance of the mouse from the target hole, except on day 2 where ARC031 treatment gave a statistically significant effect regardless of injury. This may be due in part to the cessation of treatment on the day prior to the start of Barnes maze testing. ARC031 treated TBI mice did not show significant improvement compared to DMSO treated TBI mice during acquisition, but both groups had a significantly increased average cumulative distance to the target hole compared to sham and naïve groups.

Despite the lack of a significant treatment effect during the acquisition trials, treatment by injury was a significant factor during the probe trial on day 7 as measured by average distance from the target hole. Additionally, ARC031 treated TBI mice did not have a statistically significantly higher average distance from the target hole than their corresponding sham, whereas the DMSO TBI group showed strong statistical significance compared to DMSO sham. This suggests that treatment with ARC031 may enable mice to better remember the location of the target hole despite the severe TBI, and untreated mice either lack the motivation to find the target box or lack the spatial memory required to locate its previous position. To discriminate between these possibilities, we analyzed the probe trial in greater depth by measuring the time it took for each mouse to travel to the target hole from the time they began walking ("travel time"). If the deficit seen in the placebo treated mice were only one of motivation as opposed to memory, travel time should show a low latency for DMSO TBI mice as well. To further exclude motivation as a factor, we excluded any non-participatory mice that failed to register a minimum of one nose poke in any hole. During the probe trial of the Barnes maze we measured the travel time of each mouse in order to measure their spatial memory independent of motivation to participate in the task. The short travel time of ARC031 treated sham mice compared to their higher average distance from the target hole compared to DMSO treated shams shows that they took a more direct route to the target during the probe trial, but continued exploring in order to relocate the target box. A reversal experiment where the position of the target box is reversed at the end of the initial acquisition period may show superior performance by ARC031 treated mice, indicative of superior synaptic plasticity.

Although treatment with ARC031 was only a significant effect on the 2nd day of acquisition testing, the memory involved in acquisition trials differs from that of

the probe trial; all trials during acquisition except for the initial trial of each day occur after re-enforcement of the target hole's position. Therefore, the probe trial involves longer term memory than the acquisition testing.

Examination of the tissue from these mice showed a non-significant trend of decreased lesion volume in TBI mice treated with ARC031. Both TBI groups showed a significant loss of tissue compared to sham controls, but since the mice were euthanized two weeks after injury, it is possible that even a small difference in lesion volume between ARC031 and DMSO treated mice could diverge into a larger significant difference at later timepoints as the necrotic area expands. GFAP staining also showed a non-significant effect of treatment with ARC031 in the TBI mice compared to the sham mice, but its failure to show an injury effect may again be due to the two week timepoint after injury as well as treatment with DMSO which as previously mentioned is known to be neuroprotective. Synaptophysin data showed an effect of treatment with ARC031, but not of TBI. Treatment with ARC031 appeared to decrease the amount of synaptophysin in both injured and uninjured mice. This is in stark contrast to our neurobehavioral data which seems to suggest that ARC031 treated mice may exhibit superior synaptic plasticity, since synaptophysin is essential to synaptic plasticity and is involved in synaptic vesicle recycling(Janz, Sandhof et al. 1999). The decreases seen in ARC031 mice may be part of a denervation and reinnervation process during synaptic remodeling and may indicate an ongoing reparative process rather than degenerative processes (Masliah et al., 2004). Future studies should examine the synaptic plasticity of ARC031 treated TBI mice compared to untreated controls and re-examined synaptophysin across multiple timepoints and brain regions in order to clarify these results.

In the acute treatment study we examined the levels of IL-6 and MCP-1 6 hours after both severe (CCI) and mild (CHI) injury. IL-6 and MCP-1 are both inflammatory cytokines downstream of NF-kB, and we therefore selected them to study ARC031's effect on NF-kB dependent inflammation. As discussed in chapter 3, profiling the acute inflammatory response of untreated wild type mice by ELISA after both CCI and CHI injuries we saw both IL-6 and MCP-1 significantly up-regulated in the CCI model. Although we saw IL-6 significantly up-regulated at 6 hours in the untreated CHI study discussed in chapter 3, in the acute treatment study with ARC031, CHI levels of IL-6 were below detection limits of the kit. Though at first this would seem to suggest a lack of reproducibility, it is important to note that the placebo treated mice in this study were given DMSO, which is known to be neuroprotective (Di Giorgio et al., 2008). This may have masked the signal in the CHI mice in this experiment. Treatment with ARC031 at 6 hours after injury showed a non-significant trend towards reduced IL-6 in CHI sham and TBI mice (according to interpolated values) as well as CCI TBI mice, but not in CCI sham. ARC031 treatment also produced a non-significant decrease in MCP-1 in every group 6 hours after surgery. Such a slight and non-significant reduction does not appear to be a likely mechanism of action for ARC031's significant effects on the Rotarod and Barnes maze, so it may be acting through a different mechanism. Alternatively, it is possible that the slight non-significant decreases seen after treatment with ARC031 at this timepoint become much larger differences after continued treatment at later timepoints.

Our data show only non-significant effects of ARC031 treatment on acute inflammatory markers. Others have shown that cytokine levels correlate with astrocyte activation in inflammatory conditions (Hunter et al., 1992), thus this may help explain why no significant effects of ARC031 on GFAP staining were seen.

TBI also failed to produce a robust activation of astrocytes compared to sham mice, but showed a trend of increase compared to naïve. This further suggests that CCI sham injury is at least a mild injury to the brain and may not provide sufficient discrimination from TBI in all cases (Olesen, 1987, Cole et al., 2011).

Given that ARC031 may assist in recovering a non-injured phenotype in the probe trial of the Barnes maze as well as motor coordination improvements seen by Rotarod, this drug shows potential as a treatment for TBI. Its parent molecule is currently in phase III clinical trials in Europe for the treatment of Alzheimer's disease and it is known to have an excellent safety profile. This greatly enhances the likelihood that this enantiomer can move forward as a potential treatment for TBI as well, at least in Europe where the racemate has a history and thus the enantiomer is not regarded as a new chemical entity. Though the parent molecule has anti-hypertensive effects that may not be desirable after a TBI, ARC031 lacks these effects and should enable increased doses (as compared to the racemate) without blood-pressure lowering side effects that could be adverse. This may allow us to reach a therapeutic dose that could not be reached by Nilvadipine without inducing an excessive loss of blood pressure.

Based on our ELISA data, it appears likely that the mechanism of action of ARC031 is not through any acute action on inflammatory pathways following TBI, though we have demonstrated anti-inflammatory activities of ARC031 in our other pre-clinical research into the effectiveness of ARC031 for the treatment of Alzheimer's disease. There may also be additional inflammatory markers such as TNF-α that do show the effect of ARC031 but were not examined here. Alternatively, it is possible that the slight trends showing a possible decrease of these acute markers leads to improved outcome at latent timepoints, possible through downstream effects not seen here. The effects of ARC031 treatment

noted both by Rotarod and Barnes Maze tasks occur many hours after this acute timepoint. The acute inflammatory profile established in chapter 3 continues to show a significant effect of CCI and sham surgeries, thus it may still have utility in examining the effectiveness of other treatment paradigms. With regard to ARC031 we may simply not be examining the correct markers in order to discern its acute effect after TBI, but the motor and cognitive outcomes are the most important factors in determining a potential therapeutic's efficacy. Thus we consider that ARC031 still warrants further preclinical evaluation as a potential treatment for TBI.

CHAPTER 6
IN VIVO INVESTIGATION OF ANATABINE'S EFFECT ON OUTCOME FROM TBI

Introduction

Previous results discussed in chapter 5 targeting NF-kB activation and Aβ production with ARC031 showed effectiveness at improving spatial memory in a CCI model of TBI using the Barnes maze task, and improved Rotarod fall latency regardless of injury status. After profiling the acute response of NF-kB dependent cytokine activation after CCI, and identifying a 6-hour timepoint as a peak time for response by IL-6 and MCP-1 (Chapter 3) we examined the effect of ARC031 treatment at six hours after TBI on these cytokines. Although treatment with ARC031 showed effectiveness in neurobehavioral testing, it did not produce a significant decrease in inflammatory markers downstream of NF-kB. In order to validate neurobehavioral improvement by targeting NF-kB and Aβ, we sought an alternative inhibitor of NF-kB activation and/or Aβ production to administer in the CCI model of TBI and evaluate with neurobehavioral testing.

Anatabine is a naturally occurring minor alkaloid whose structure is closely related to nicotine. It is an MAO inhibitor and nicotinic receptor and cholinergic agonist. Anatabine is less potent than nicotine, possessing 4.55 times less affinity in the rat frontal cortex, and 2.67 times less affinity in the hippocampus. Partial MAO inhibition occurs in the rat liver at concentrations above 100 μg/kg (Rock Creek Pharmaceuticals). Research at Roskamp Institute on the effects of anatabine showed it to be capable of inhibiting NF-kB activation and Aβ production in vivo and in vitro (Paris et al., 2011). In vitro experiments show that anatabine inhibits Aβ production of human APP overexpressing 7W CHO cells in a concentration-dependent manner and also inhibits NF-kB activation stimulated by TNF-alpha in HEK293 and SH-SY5Y cells in a concentration-dependent manner. Basal levels of NF-kB were also lowered by anatabine in APP over-expressing 7W

CHO cells. Since NF-kB regulates expression of the β-site APP cleavage enzyme (BACE-1), Paris and colleagues also tested anatabine's effect on BACE-1 transcription when stimulated by TNF-alpha. Anatabine completely attenuated the increase in BACE-1 mRNA levels. Anatabine is highly concentrated in the brain 20 minutes after injection, reaching a concentration 3.5 times higher in the brain than in the plasma (Paris et al., 2011). Given the excellent bioavailability and NF-kB and Aβ inhibitory effects of anatabine, we decided to apply it in our CCI model of TBI to further validate those pathways as therapeutic targets.

Anatabine is a nutraceutical, defined as a food or naturally occurring food supplement that has medical or health benefits (Andlauer and Fürst 2002). Because nutraceuticals are naturally found in foods and are not pharmaceutical drugs, they do not require extensive clinical trials and possess a much faster path to clinical application and use than traditional pharmaceuticals. Nutraceuticals do not require long and expensive clinical trials and FDA approval as a drug, and as such they can be employed in a clinical setting almost immediately (Hanninen and Sen, 2008). Within the European Union, substances which can be shown to have physiological effects can be considered medicinal substances, though classification of a particular product can vary from country to country and depend on the nature of the product (Coppens et al., 2006, Gulati and Berry Ottaway, 2006). Glucosamine salts and chondroitin sulfate have enjoyed great success in the United States as dietary supplements since the mid-1990s (Bagchi, 2008). Plant sterols supplemented to orange juice have also shown efficacy at lowering cholesterol levels in hypercholesterolemic individuals (Devaraj et al., 2004).

In order to evaluate anatabine's effectiveness as a TBI treatment, we administered either anatabine or PBS to mice after CCI or sham injury, and performed the same battery of neurobehavioral testing previously used in our

study of ARC031 (Rotarod and Barnes maze). In a second cohort of mice, with the same treatment and injury groups, mice were euthanized six hours after surgery in order to examine the acute inflammatory profile and the impact of anatabine treatment (Figure 5-1).

Materials and Methods

Animals and Injury

All mice were male wild type C57BL/6J male mice between 11 and 12 weeks old at the time of injury. 48 mice were divided into groups of sham and injured with and without treatment (12 mice per group). CCI was administered as described in chapter 2, with a 2 mm diameter tip at a rate of 5 m/s and depth of 1.8 mm. Sham mice for the CCI procedure received craniectomy without injury. Animals were housed singly after the surgical procedure.

Two weeks after surgery, at the completion of behavioral testing (the final day of Barnes maze testing), a subset of mice were euthanized for pathological analyses (not carried out yet). 3 mice from each group (treated only, sham and CCI) are being kept alive and are continuing to consume anatabine for later pathological examination at an extended timepoint after injury (yet to be determined). We anticipate that these mice will be euthanized in the timeframe of 3 months to 1 year after injury, but this will be influenced by our observations of the pathological analyses at the 2 week timepoint. Our proteomic data suggests that the NF-kB pathway becomes increasingly important with time after injury to at least 3 months post-injury, and our previous observations have found that the necrotic area surrounding the impact continues to expand during that time. Latent pathological examinations at that timepoint or beyond may reveal larger differences between treated and untreated groups than at a more acute 2 week timepoint.

For the acute timepoint study all mice were male wild type C57BL/6J male mice 11 weeks old at the time of injury. 12 mice were divided into groups of sham and injured with and without treatment (3 mice per group). CCI was administered as described above. Mice were euthanized 6 hours post-surgery and the hippocampus, cortex, and cerebellum were rapidly dissected on ice and then frozen at -80 C.

All procedures involving mice were carried out under IACUC approval and in accordance with the National Institute of Health Guide for the Care and Use of Laboratory Animals.

Therapeutic Administration

Anatabine (Star Scientific) was dissolved in PBS and administered via intraperitoneal injection at a dose of 2mg/kg starting 30 minutes after surgery. The first dose was administered via IP in order to control the timing and dose of the first administration after injury as the mice do not immediately return to drinking from their water bottles after surgery. Since anatabine has excellent bioavailability when taken orally, for the treatment groups, normal water was substituted with Anatabine treated water, which provided a continuous administration for the duration of the experiment without the need for further intraperitoneal injections. Given that mice of this age consume approximately 5 ml of water per day (Daniel Paris, pers. comm.), and our mice were all approximately 25g in weight, we added anatabine to their water to a concentration of 0.1 mg/ml for a daily dose of 20 mg/kg. I chose this dose based on work that is currently ongoing with this compound in other laboratories of the Roskamp Institute. Control mice received PBS alone (by IP) at 30 minutes, and normal drinking water.

For the 6 hour acute timepoint study, either 2mg/kg of anatabine or PBS was administered by IP injection 30 minutes after surgery. Additionally, mice were

provided with a dish filled with either regular water or water treated with anatabine at the same concentration as in their water bottle (0.1 mg/ml). This was to ensure ease of access to the water and maximize intake during the short six hour survival period.

Rotarod Testing

The Rotarod (Med Associates) was used to measure motor coordination as described in chapter 2. Briefly, all mice were given one day of baseline testing at an accelerating speed of 5 to 50 rpm over a period of 5 minutes. The day after baseline testing, mice were given a sham or TBI, as described above. At day 1 after the surgery, testing resumed using the same criteria as the baseline tests. Testing was repeated on every second day through day 7.

Barnes Maze Testing

The Barnes maze was used to measure spatial memory and learning as described in chapter 2. Briefly, all mice were given 6 days of acquisition trials starting on the day following the conclusion of Rotarod testing, and a probe trial was administered on the 7th day. The cumulative distance from the target hole was measured for each trial and averaged over each day. A probe trial was conducted on the final day of testing. The average distance of the nose from the target hole as well as the latency was recorded. If a mouse failed to complete the task the latency was recorded as 60 seconds. The table and target box were cleaned and disinfected after each trial on all days. All Barnes maze trials were both videotaped and recorded with the Ethovision XT tracking system for analysis.

Acute Timepoint ELISA Analysis

As described in chapter 3, we assessed inflammatory cytokines IL-6 and MCP-1 using ELISA (Invitrogen). Tissue for the ELISA analyses were rapidly dissected on ice and frozen at -80 degrees. ELISAs were run on cortical tissue

homogenate prepared using M-PER and Halt Protease Inhibitors (Pierce) according to manufacturer's directions, with the exception that each of the primary incubations of the samples for the ELISA were performed overnight at 4 degrees Celsius to minimize non-specific binding. A porcine sample was run to validate the specificity of the kit. 150 µg of protein from brain homogenate were loaded into each well for each ELISA. Samples were run in triplicate. ELISA data are expressed in pg/ml.

Statistical Methods

All datasets were assessed for normality using the Shapiro-Wilk test. If a given dataset was normally distributed, mixed model ANOVA (single time point) or repeated measures ANOVA (multiple timepoints) were used to assess significant changes due to injury. Pairwise group comparisons were evaluated using t-test. If a given dataset failed the Shapiro-Wilk test, data was transformed (ln, log, square root). When transformation did not yield a normally distributed data set, we used the non-parametric Kruskal-Wallis test. . Pairwise contrasts were calculated using the Wilcoxon rank sums test. A given effect was considered significant at $p<0.05$. Statistical analyses were performed using JMP 8.02 (SAS).

Results

Rotarod

A number of mice assigned to the anatabine treatment neurobehavioral testing group showed artificially deflated performance during the baseline testing of the rotarod due to a propensity to walk backwards on the bar. As a result, we used the raw fall latency values to evaluate the outcome. Since the data were not normally distributed, instead of ANOVA we employed the Wilcoxon signed rank test to analyze these results. Anatabine treated TBI mice had significantly shorter fall latency times compared to their respective shams on days 1 ($p<0.01$), 3

($p<0.04$), and 7 ($p<0.02$) after surgery whereas PBS treated controls had significantly shorter fall latencies compared to their shams on days 1($p<0.01$), 3($p<0.01$), and 5 ($p<0.03$) after surgery (Figure 6-1). The differences between the anatabine and PBS treated TBI mice were not significant. Anatabine did not appear to have an effect on TBI mice, but did seem to significantly decrease the fall latency of sham mice when expressed as a percentage of the baseline. Raw fall latency were not significantly different between treated and untreated shams or treated and untreated TBI mice for any day after surgery (figure 6-2).

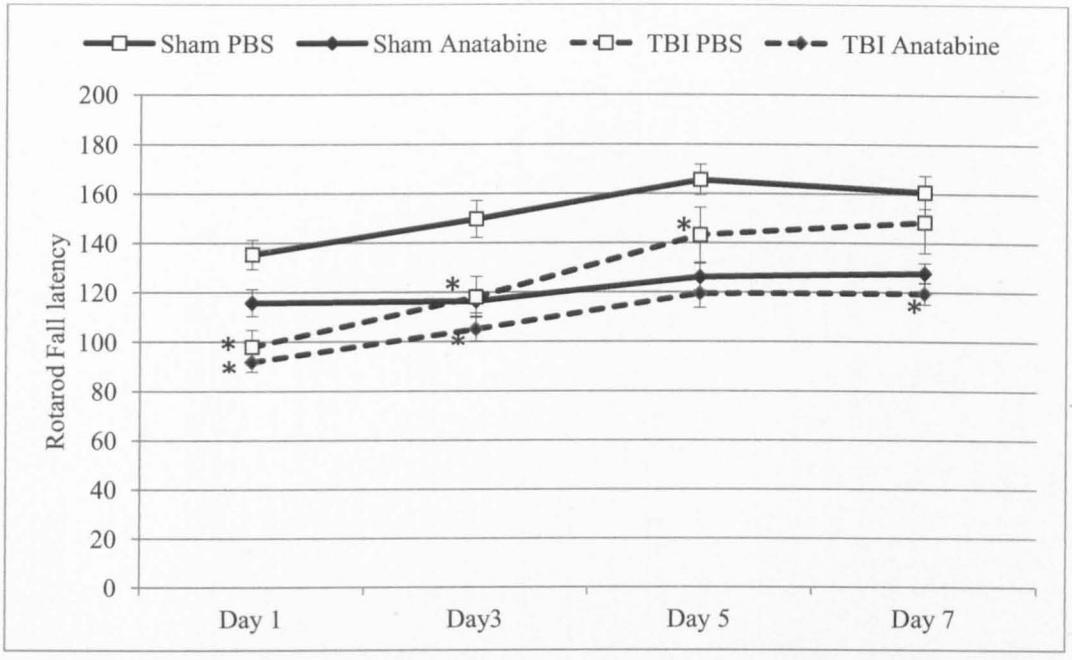

Figure 6-1. Percent of baseline fall latency in the Anatabine study. Error bars represent standard error. * indicates statistical significance relative to the corresponding sham by Wilcoxon signed rank test ($p<0.05$).

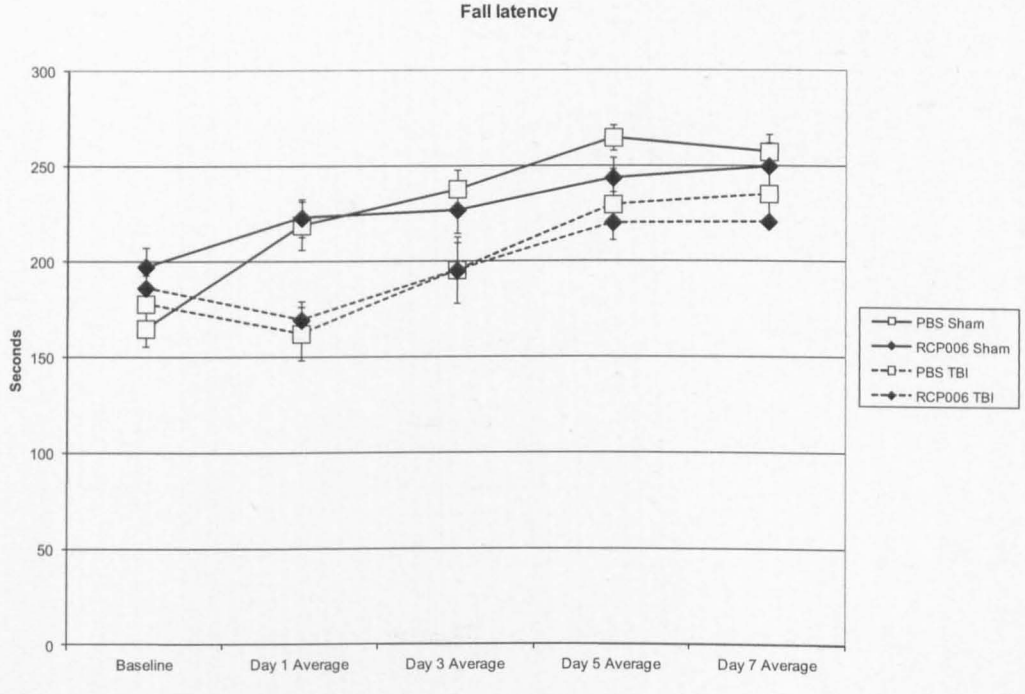

Figure 6-2 Raw fall latency values during Rotarod testing. No significant differences were seen between treatment groups and the data was not normally distributed. Error bars represent standard error.

Barnes Maze

The trial duration shows the length of time the mice spent locating and entering the target box during the acquisition testing in order to end the trial (figure 6-3). The data were not normally distributed thus we couldn't use repeated measures ANOVA, however non parametric tests also did not yield any statistically significant comparison between the pairs. Although no significant differences were seen between any groups, a consistent trend indicated that TBI mice required more time than sham mice, regardless of treatment status. Treatment with anatabine did not produce any detectable trends in the data.

Cumulative distance was normally distributed and the starting point and time were significant factors by ANOVA, the latter of which indicates learning (figure 6-4). PBS treated sham and TBI mice showed the greatest difference during the acquisition trials, and therefore have the largest amount of an injury effect, but anatabine treated sham mice had a higher cumulative distance than PBS sham mice (though the difference was non-significant). Anatabine treatment had a greater effect on sham mice than TBI mice in terms of velocity. As seen in figure 6-5, sham mice treated with anatabine generally had a lower velocity than PBS treated sham mice, while both the anatabine treated and untreated TBI mice performed at a similar velocity, therefore injury*treatment was a significant interactive term ($p<0.05$) by ANOVA. During the probe trial, PBS treated TBI mice had a higher latency to the target hole than PBS sham mice ($p<0.01$) (figure 6-6) and had a lower duration spent with their nose in the target hole ($p<0.05$) (figure 6-7). Anatabine treated TBI mice showed no difference in latency to the target hole compared to sham mice, and no significant differences were seen between anatabine treated TBI mice and shams in duration in the target hole. Treatment *injury was a significant interactive effect by ANOVA ($p<0.05$). Neither latency nor

duration were significantly different between anatabine and PBS treated sham mice. Velocity did not show any significant differences between groups during the probe trial (figure 6-8).

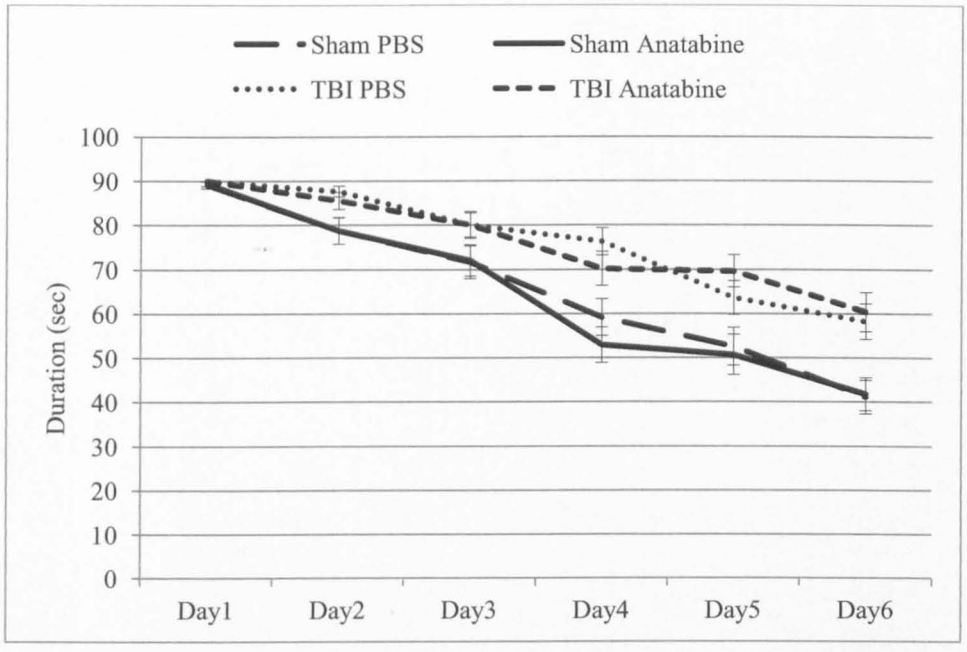

Figure 6-3. Acquisition trial duration during Barnes maze testing of the Anatabine study. Error bars represent standard error. No statistical significance was seen by Wilcoxon signed-rank test.

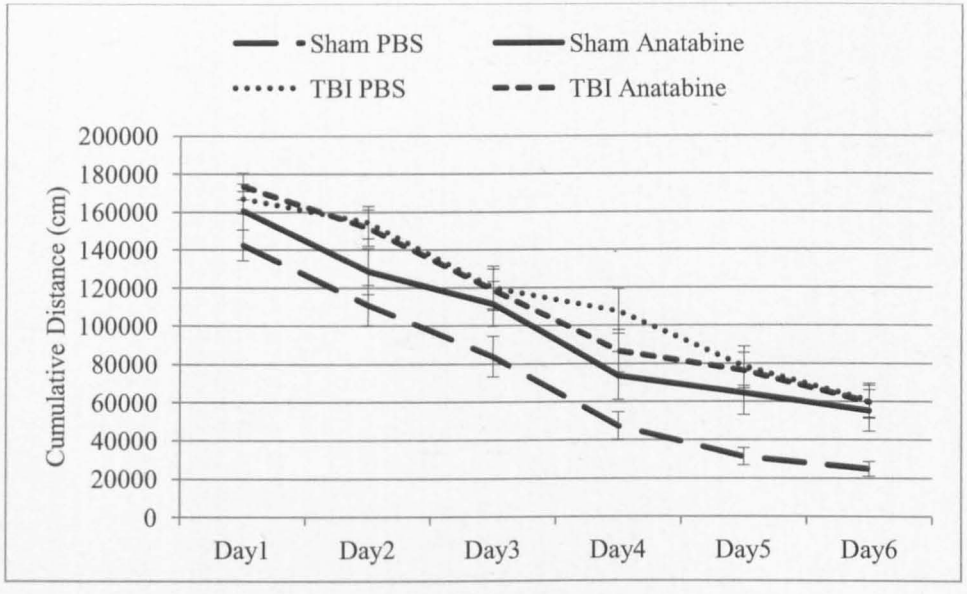

Figure 6-4. Cumulative distance during Barnes Maze acquisition testing of the Anatabine cohort. Error bars represent standard error. No statistical significance was seen by ANOVA repeated measures with the exception of the start point as a significant factor.

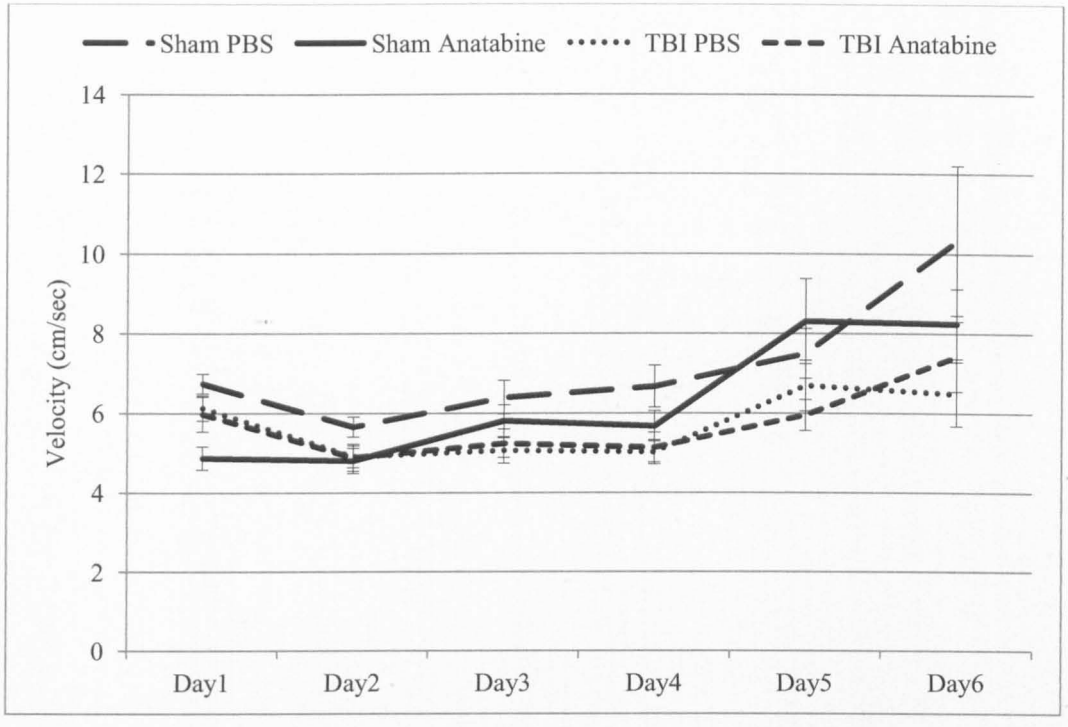

Figure 6-5. Average velocity during the acquisition trials of Barnes maze testing. Error bars represent standard error. No statistical significance by T-test.

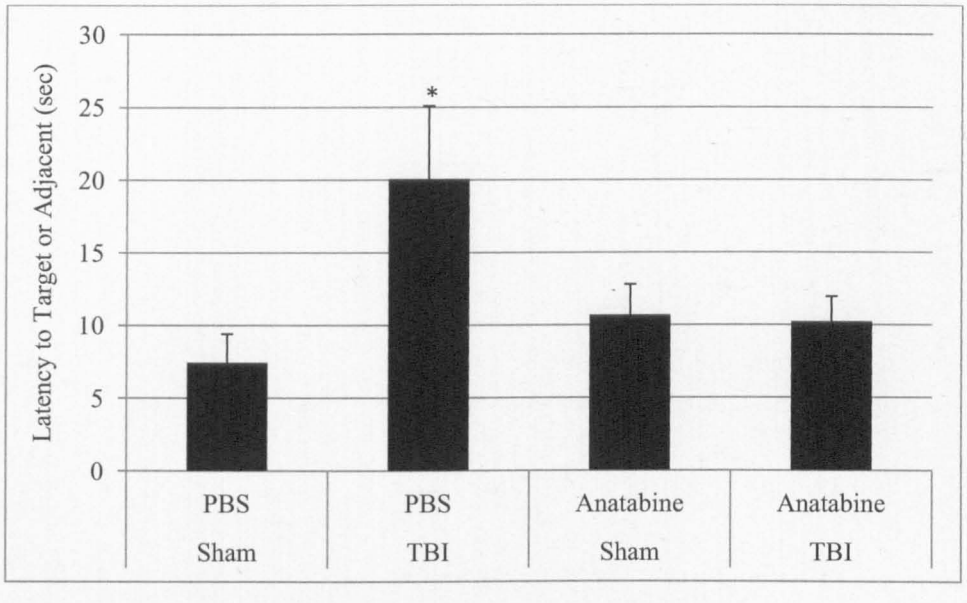

Figure 6-6. Latency to the target hole during the Barnes maze probe trial of the anatabine study. Error bars represent standard error. * indicates significance by T-test ($p<0.05$) compared to the corresponding sham. .

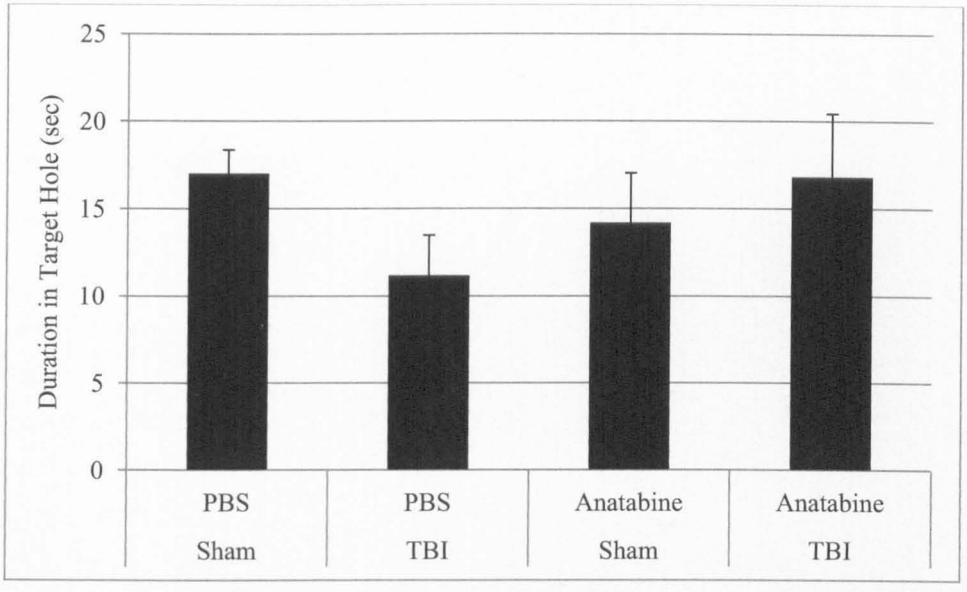

Figure 6-7. Average Duration of the nose point in the target hole of the Barnes Maze during the probe trial of the anatabine study. Error bars represent standard error. No statistical significance.

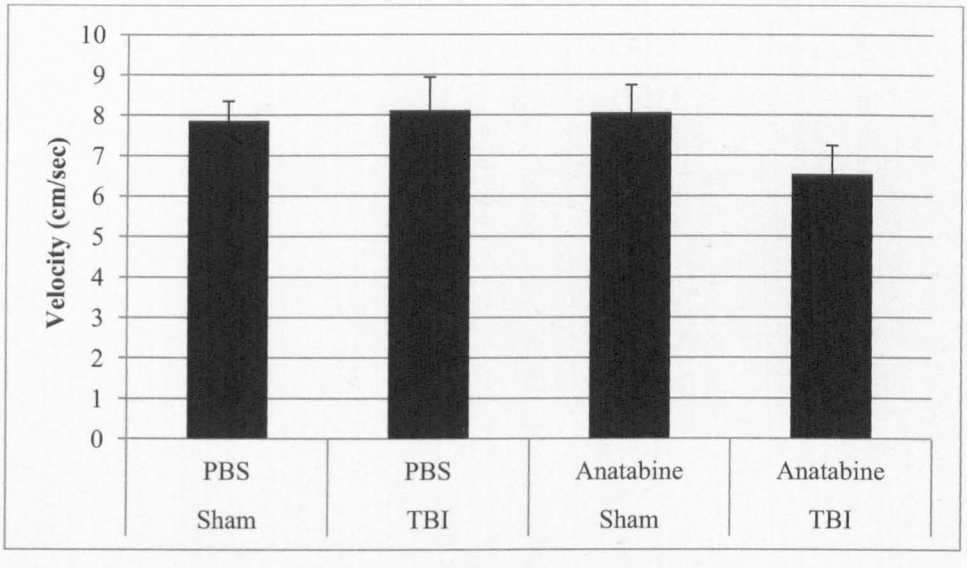

Figure 6-8. Barnes Maze mean velocity during the probe trial. Error bars represent standard error. No statistical significance.

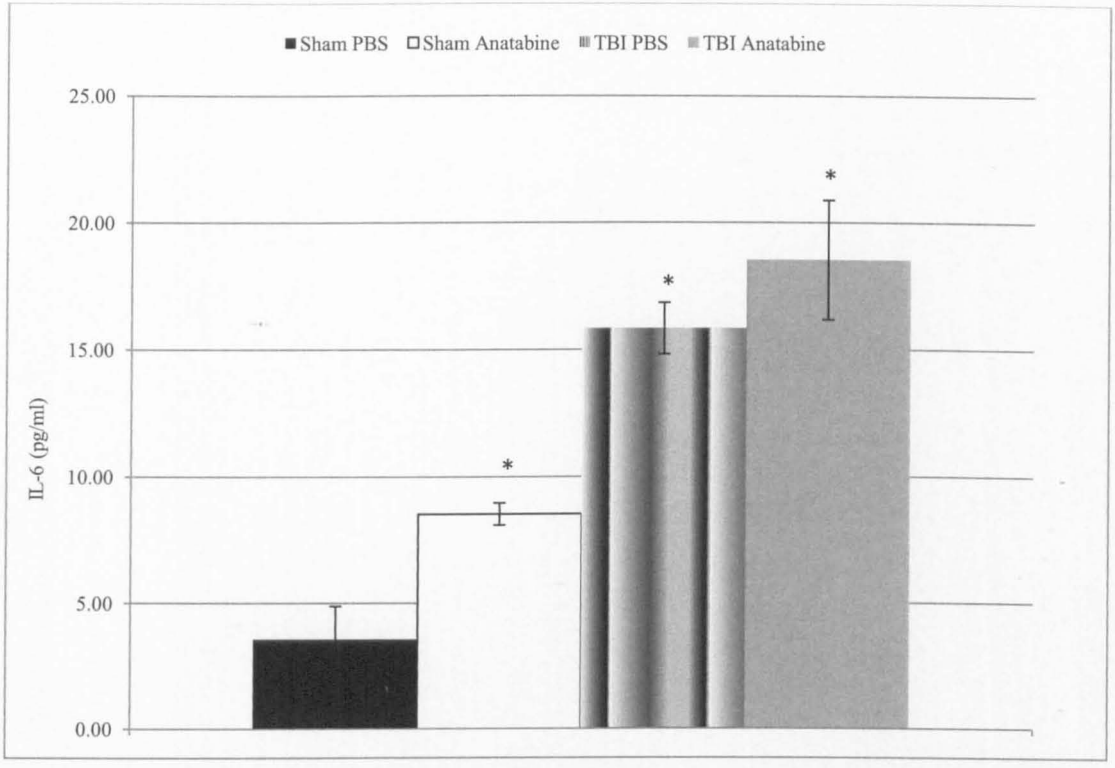

Figure 6-9. IL-6 ELISA 6 hour acute timepoint ELISA with Anatabine treatment. Error bars represent standard error. * indicates statistical significance by T-test ($p<0.05$) compared to PBS sham.

Acute Timepoint ELISA Assay

Both IL-6 and MCP-1 showed a significant effect of injury 6 hours after TBI ($p<0.01$). Unexpectedly, anatabine treated sham mice showed a significantly higher level of IL-6 than untreated sham mice ($p<0.05$), but less than either TBI group (figure 6-9). Treatment was also a significant factor by ANOVA within IL-6 ($p<0.05$), largely because of the aforementioned sham effect. MCP-1 did not show any difference between the treated and untreated shams, and no significant differences were seen between the treated and untreated TBI mice with either marker (figure 6-10).

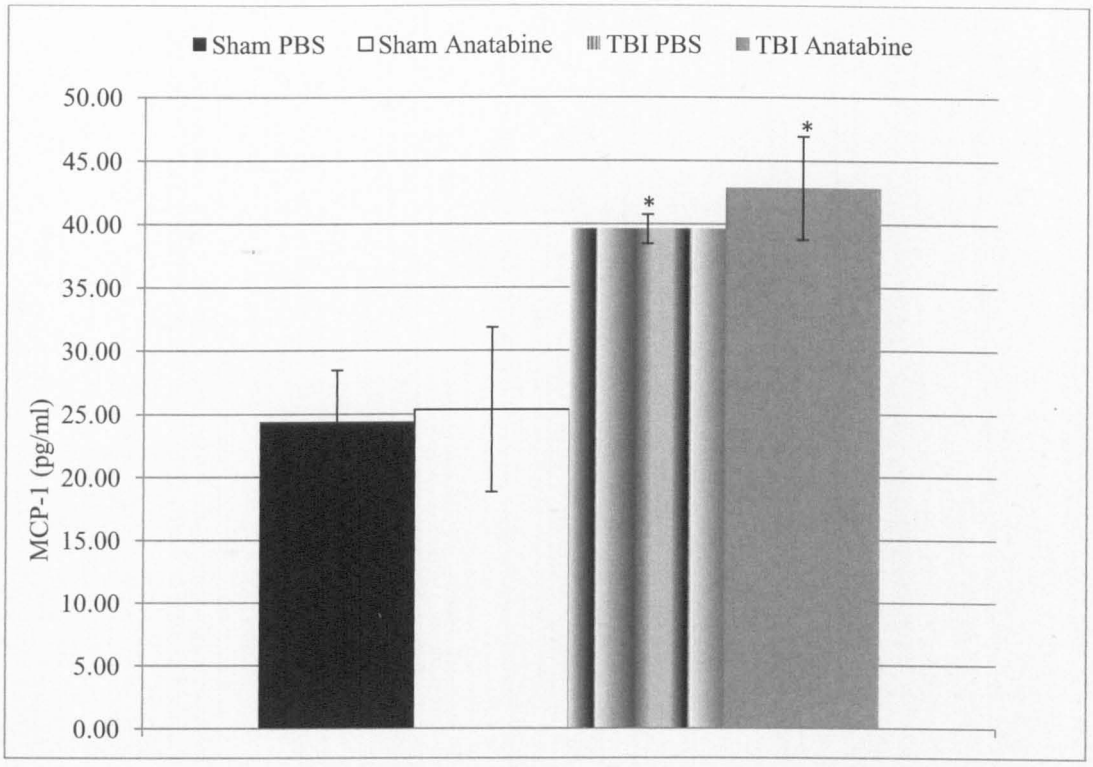

Figure 6-10. MCP-1 ELISA 6 hour acute timepoint ELISA with Anatabine treatment. Error bars represent standard error. * indicates statistical significance by T-test ($p<0.05$) compared to PBS sham.

Discussion

Our results show that treatment with anatabine prevents a loss of spatial memory two weeks after severe TBI as demonstrated during a probe trial of the Barnes maze. Similar to other studies with anatabine conducted at the Roskamp Institute (Daniel Paris, pers. comm.), no improvement was seen during rotarod testing; anatabine does not appear to improve motor function after TBI in the manner seen after treatment with ARC031. This suggests that the effects of ARC031 on motor performance likely occur via mechanisms that are not impacted by anatabine. The results in the Barnes maze resemble the results from our ARC031 treatment experiment. Although no improvement was seen during the learning phase, a probe trial test of longer term spatial memory shows dramatic improvement after treatment. This is consistent with previous research which has shown the ability of probe trials of spatial memory tests to discriminate spatial memory differences not seen during acquisition testing (Petitto et al., 2002, Lin et al., 2009).

During acquisition testing, PBS and anatabine treated sham mice had an identical trial duration, even though treatment with anatabine resulted in significantly decreased velocity. Anatabine treated shams also had a consistent trend for higher cumulative distance, suggesting that anatabine treated sham mice spent slightly more time farther from the target hole due to their lower velocity, but did not hesitate to enter the escape box as much as PBS treated shams. The end result was an identical trial length in spite of anatabine treated sham mice accumulating a greater cumulative distance from the target hole over the course of the trial.

This also suggests a lower stress level in the treated mice and resulting superior performance in the goal-oriented learning portion of the task (entering the

escape box after locating the target hole). Harrison and colleagues (Harrison et al., 2006) suggest that verification of the escape hole's location lowers the stress level of the mice and allows them to continue exploring the rest of the maze once they are assured of their ability to escape, but in our observations the escape box itself causes hesitation and apprehension of the mice who spend a great deal of time examining the escape box from the edge of the hole without entering before they are finally confident enough to enter without being prompted at the end of the trial. Over a few days of testing we see that mice begin to properly associate the target hole with escape from the maze and do not hesitate to enter the box, but the above data suggest that anatabine treated mice form the association faster. The differences seen in our experiment versus others such as the aforementioned Harrison study may be due to the construction of our Barnes maze, which places the black escape box directly under the hole, as opposed to separating the escape box from the target hole by way of an acrylic ramp.

The probe trial showed no impairment in the spatial memory of the anatabine treated sham mice in spite of their trend for a higher cumulative distance, thus their spatial memory is equivalent to PBS treated shams. Treatment with anatabine did not significantly alter the velocity of the mice during the probe trial, most likely due to the novel starting location and the absence of the escape box. These provided new stimuli to the mice and encouraged fresh exploratory behavior. The disappearance of this velocity difference in the probe trial suggests that it is not being driven by motor impairment, but rather by overall differences in stress; the groups equivalent performance in the time to escape the arena during acquisition shows an equivalent motivation to complete the task.

Treatment with anatabine completely prevented any deficit of spatial memory during the probe trial. As was noted before, acquisition testing involves re-

enforcement of the target hole's location and is mostly a test of short-term memory. The longer term task of the probe trial and the novel starting location revealed a significant effect of treatment x injury, showing that although anatabine does not change the performance of sham mice, it significantly improved the performance of TBI mice. Although anatabine did not show beneficial effects in improving motor coordination on the Rotarod, it does show significant effects at improving long term spatial memory in the Barnes maze in a manner similar to ARC031 .

ELISA analysis of acute markers of inflammation showed no significant effect of anatabine treatment on TBI mice, either on IL-6 or MCP-1. Sham mice showed a greater amount of IL-6 after treatment with anatabine, though MCP-1 levels were equal in both sham groups. The failure of anatabine to reduce the acute inflammatory response may indicate that like ARC031, it is acting through some other mechanism to protect spatial memory, such as a reduction in delayed inflammatory response, which we did not profile by ELISA. Alternatively, the therapeutic effect may be specific to the hippocampus and may require profiling the hippocampal response to injury as well as how anatabine modulates that response. Due to the comparatively small amount of tissue recovered from the hippocampus and the large amounts of protein consumed by our ELISA assays, we have thus far focused on the cortical tissue with the aim of later assaying the tissue from the hippocampus using the most responsive and consistent marker found during our cortical investigations. Based on our results from these acute timepoint studies, future investigations will profile the IL-6 response in the hippocampal tissue and we may then be able to discriminate the treatment effect.

Previous studies have shown a differential response of cytokines in the ipsilateral hippocampus compared to the ipsilateral cortex in mice after CCI

(Harting et al., 2008). It may also be necessary to examine the entire timepoint profile previously established in chapter 3 (1, 6, 12, 24, and 48 hours after injury) in order to contextualize the results of these treatment paradigms. Treated mice may exhibit a steeper decline in cytokine levels despite high initial inflammation, which itself may be beneficial while the blood-brain barrier is compromised. Others have shown that mice with genetic knockdown or knockout of various cytokines may have a higher mortality rate than wild type controls, though the extent of blood-brain barrier compromise and intracranial cell death is not directly impacted (Stahel et al., 2000). It is therefore not desirable to completely inhibit cytokine activation, but rather simply attenuate it. It is possible that moderation of the acute inflammatory response is occurring with timepoints or brain regions that have yet to be explored in these anatabine treated mice.

Currently unpublished data generated by Roskamp Institute staff shows an effect of anatabine on spatial memory in mouse models of Alzheimer's disease (Daniel Paris pers. comm.), but we believe the work described in this chapter represents the first exploration of the effects of anatabine on spatial memory in a mouse model of TBI. Previous animal studies have examined the effect of related alkaloids like nicotine for treating brain injury. A study by Hralová et al (2011) showed no effect of a single administration of nicotine at 0.75 mg/kg or 1.0 m/kg on spatial learning and memory in rats. Nicotine, however, has a much shorter half life than anatabine. Our study also involved continuous oral administration rather than a single IP injection alone. Chronic administration of nicotine is known to improve spatial discrimination in rats with septal lesion-induced deficits (Decker et al., 1992). Chronic administration was also studied in a paradigm of pre- and post-treatment following CCI resulting in improved spatial learning and memory on the Morris water maze (Verbois et al., 2003). A study of human patients of

subarachnoid hemorrhage who were receiving nicotine replacement therapy versus those who did not suggested a neuroprotective effect for nicotine as seen by a lower mortality rate at 3 months, however further study is needed (Seder et al., 2011).

Future studies of anatabine will examine its effectiveness at preventing spatial memory loss in a new repetitive mild (mTBI) model of closed head injury (CHI) being developed and characterized by Roskamp Institute staff. This model is a repetitive form of the CHI injury utilized in chapter 3 during our acute inflammatory timepoint profile. If anatabine shows effectiveness at reducing or preventing deficits in the repetitive mTBI model, then it could find immediate application; for example as a supplement in sports drinks to help offset cognitive impairments induced by chronic head injury in high contact athletics such as American football, boxing, and other activities where head injury is common and risk of head injury can be anticipated. Other nutraceuticals such as rosiglitazone and curcumin have been shown to be neuroprotective after TBI (Wu et al., 2006, Yi et al., 2008), so there is support for the idea that dietary supplementation can provide neuroprotection. Anatabine provides an exciting alternative that is non-addictive and has excellent bio-availability when administered orally, and it offers a faster prospect for clinical application than pharmacological alternatives. Dietary supplementation may be a safe and simple method to reduce cognitive deficits after TBI.

CHAPTER 7
CONCLUSIONS

Traumatic brain injury is now recognized to be a major problem for both military and civilian populations. The devastating consequences of head injuries in sports (American football, boxing, rugby, etc) have become the subject of increasingly frequent news and health reports.Additionally, the current conflict in Afghanistan has named TBI "the signature wound" of that war (Martin et al 2008). In the US, the number of emergency department visits increased from 1.25 million in 2002 to 1.43 million in 2006 (Faul et al., 2010). The survival rate increased 20% from 1980 to 1994 (Thurman, 1999), and with the overall incidence of TBI currently increasing, many more patients are now living with the long term consequences of TBI (more than 3 million people in the US alone) (Zaloshnja et al., 2008).

TBI involves a diverse set of events that regulate secondary injury, for which there is currently no treatment (Faden, 2001). Mechanisms of this secondary injury include excitotoxicity (Palmer et al., 1993) and inflammation (Morganti-Kossmann et al., 2002) and within these complex molecular pathways may lie appropriate targets for therapeutic intervention. In order to dissect the molecular pathways important to the pathogenesis of secondary injury after TBI, we utilized a laboratory animal model combined with state-of-the-art proteomic technology in order to reveal the global protein changes occurring in response to injury. Moreover, to further hone in on proteomic changes that correspond to differential outcome from injury we used APOE transgenic mice to reveal changes after TBI that are occurring in a APOE genotype dependent manner. Given that apolipoprotein E isoforms are associated with differential outcome from injury in humans (with E4 genotype conferring poorer outcome than E3), we hypothesized that the proteomic response of mice transgenic for different human APOE isoforms may reveal molecular pathways that specifically contribute to this differential

outcome after TBI and which are amenable to therapeutic intervention. In order to effectively evaluate outcome after injury in our mouse models, I refined and implemented neurobehavioral tests of cognitive and motor function (Chapter 2). We generated datasets of the proteins significant for the interactive effect of genotype*injury and analyzed these to determine the pathways critical to determining differential outcome from injury (Chapter 3). Using this approach, I targeted three pathways whose response to injury was APOE genotype dependent; CD40 signaling, APP metabolism, and NF-kB signaling. These pathways were targeted using three different intervention strategies, genetic manipulation, novel drug administration, and dietary supplementation (Chapters 4-6). Neurobehavioral testing shows that each of the strategies provide benefits specific to the treatment used. However some treatments provide an easier approach to clinical translation than others.

Proteomic profiling of the APOE genotype dependent response to TBI revealed the differential modulation of many pathways and networks of related proteins. In clinical applications, to date proteomics has most frequently been employed in the study of cancer, where it is often used to find potential biomarkers (Chang et al., 2001, Zhang et al., 2004, Bai et al., 2011). Recently, proteomic approaches have been applied to begin to identify therapeutic targets for cancer in addition to biomarkers (Skvortsov et al., 2011, Wu et al., 2011). For example, Wu et al. (2011) used kinase-centric chemical proteomics of 34 head and neck squamous cell carcinoma (HNSCC) cell lines and found significant intercell line differences in a number of kinases involved in cell survival and proliferation. Inhibiting EGFR and EPHA2 kinases reduced the viability of cell lines that showed high expression of these kinases, pointing to the possibility of using kinase inhibitors capable of inhibiting those kinases as a possible treatment.

The research presented here is a very early demonstration of applying state of the art global profiling technology combined with neurobehavioral validation to the identification of pathogenic mechanisms and therapeutic targets of TBI. To identify targets for therapeutic intervention, particularly in a condition as complex as TBI, a systems biology approach is desirable to highlight groups of related proteins involved with the disease process rather than focus on individual protein changes which would be a more suitable approach for a biomarker search. Ingenuity Pathway Analysis provided an excellent tool for arranging the datasets into groups of related proteins and for examining the functional significance of the data (Abdullah et al., 2009, Crawford et al., 2009, Baraibar et al., 2011, Julien et al., 2011, Sandberg et al., 2012). It also allowed for the creation of custom networks of proteins present in the dataset that are known to be interact with each other directly or indirectly. These relationships are derived directly from a curated search of the literature. Custom networks were created using the proteins present in each dataset. This allowed us to isolate specific groups of related proteins that were changing differently in response to injury in APOE3 and APOE4 transgenic mice at multiple timepoints after TBI, indicating prolonged differences in response that presumably correlate with outcome.

Being able to view the patterns of response in large proteomic datasets allowed us to find potential targets for intervention that may not have been revealed by more narrow molecular approaches. Often when such functional groupings or networks are examined there is an evident nidus (or several nidi) whose modulation would obviously impact the entire grouping. Using multiple time points spanning one day to three months after injury allowed us to focus on specific pathways which showed changes occurring over long periods of time, possibly indicating that intervention at an acute timepoint after injury could have

long lasting effects that would otherwise result in long term deleterious processes. The data also indicated that even at extended timepoints post-injury (3 months in a mouse) there was significant APOE-genotype dependent cellular response, suggesting that later interventions might yet prove valuable. Proteomic studies that examine the broad array of protein changes occurring after TBI give us insight into molecular pathways that may not have been previously anticipated to be of importance to head injury, such as CD40 signaling, Rho signaling, and metabolic pathways such as alanine and aspartate metabolism and butanoate metabolism. For this research we focused on pathways that appeared to be easily targetable with therapeutic strategies that could be implemented in-house such as CD40 signaling, APP metabolism, and NF-kB signaling.

To validate whether or not these pathways play a central role in determining the degree of secondary injury or are peripheral consequences of secondary injury, it is necessary to modulate these pathways and observe the outcome. *In vitro* models cannot capture the full complexity of the *in vivo* situation. *In vitro* models of TBI such as the axonal stretch model are excellent examining a specific aspect of injury in detail. The axonal stretch model itself has revealed the importance of calpain proteolysis of voltage gated sodium channels in causing calcium influx in axonal injury (von Reyn et al., 2012). *In vitro* hippocampal slice models have also shown how chemokine up-regulation precedes the spreading of tissue injury during secondary brain damage (Fahlenkamp et al., 2012). Traumatic brain injury induces a wide array of changes, not all of which can be anticipated, as seen in our datasets. A cell culture model cannot replicate this level of complex and ongoing interaction; neurodegenerative processes that begin in the cortex near the site of injury at a 24 hour timepoint may lead to downstream effects in the hippocampus that are not seen until 1 month after injury or longer. In order to test

our therapeutic strategies properly, we need to utilize an *in vivo* animal model of TBI which recreates the full complexity of the TBI process.

We applied a variety of intervention strategies in order to modulate each of the three target pathways selected from our proteomic data; knockout of CD40L to modulate CD40 signaling; treatment with an Aβ inhibitor/Aβ clearance/anti-inflammatory chemical to impact APP and NF-kB signaling; treatment with an anti-inflammatory dietary supplement to impact NF-kB and other inflammatory mechanisms. I evaluated the consequences of each of these strategies with the neurobehavioral paradigms that I optimized, in order to examine both the motor and memory outcomes after TBI. I have focused on neurobehavioral outcome as the most critical outcome measure for these studies, and to that end refined and implemented tests of cognitive and motor function for their specific application to these mouse models of TBI. Future studies should naturally seek to understand the molecular and pathological outcomes of treatment, but if the neurobehavioral outcome is no better or worse than that of an untreated animal, then its clinical utility is extremely questionable. Both motor and cognitive impairments are primary problems facing victims of TBI (Caeyenberghs et al., 2011, Kinnunen et al., 2011, Leunissen et al., 2012), so we tested both.

The Rotarod is a test of motor coordination and balance, and in our experience it provides a more sensitive measurement of impairment than the traditional balance beam combined with grip strength testing. The latter primarily reveal impairments in balance and neuromuscular health, but does not depend on motor coordination as much as Rotarod does. Rotarod testing repeated on alternating days after injury shows an immediate and dramatic impairment due to injury followed by gradual recovery within the week after injury as the mice adapt to the task. Though their gait on the Rotarod appears to remain altered, CCI

injured mice learn to adapt to the impairment and remain walking on the bar for increasingly longer periods of time in spite of it.

Rotarod performance varies with age, and as the experiments performed here were all conducted with young mice around 10-12 weeks of age, the task was optimized to provide a challenge with a minimum of baseline testing time in order to minimize ceiling effects. Rotarod provided excellent discrimination of the initial injury, with large deficits seen at the first day within injury groups followed by a gradual return to sham levels. The ability of the Rotarod task to produce such a large degree of separation between sham and injured mice allows treatment effects to become readily visible over the recovery period. A large number of trials can be conducted in a short period of time, which allows for many technical as well as biological replicates within the data, minimizing uncertainty and maximizing statistical power. Rotarod discrimination of motor skill does not necessarily translate to differential movement velocity in less strenuous conditions. However, if differences in velocity are noted in other tests, for example the Barnes maze, then we can consider that in our evaluation of the Rotarod results.

Mice improved in their performance in the Rotarod over time, particularly after a severe TBI which induces large deficits. In my observations of Rotarod testing, I have noted that some mice have an altered gait while performing the task the day after surgery. Though I am blind to group assignment while testing, these mice invariably are ultimately revealed to have received a severe TBI. Though they improve over time through compensation using their contralateral side, their altered gait remains and this may affect their velocity even in less strenuous conditions like the Barnes maze. Although CD40L knockout mice showed superior performance to wild type mice on the Rotarod as well as increased velocity on the Barnes maze and though wild type controls showed abnormal results in spatial

memory, their motor performance on the Rotarod was consistent with previous results. ARC031 treated mice showed a significant effect on the Rotarod without a corresponding increase in velocity on the Barnes maze. Conversely as we saw during treatment with anatabine, significant velocity differences during Barnes maze testing do not necessarily correlate to a significant increase in fall latency during Rotarod testing. Rotarod is therefore a vital test to unambiguously determine the presence or absence of motor impairment. Spatial memory tests, though they involve the use of motor functions, do not always correlate with Rotarod performance.

Spatial memory is a hippocampal dependent neurobehavioral function. Loss of spatial memory is associated with secondary injury after traumatic brain injury. Although controlled cortical impacts cause primary injury to the cortex, in the weeks that follow the lesion volume will expand and hippocampal volume will decrease. In testing spatial memory we found the Barnes maze to be a superior test to the Morris water maze for our C57BL/6J mouse strain, consistent with previous reports (Patil et al., 2009). All three of our treatment strategies showed effectiveness in various measures during the probe trial compared to wild type untreated mice. Acquisition testing relies heavily on short term memory and goal-oriented learning, whereas the probe trial is a more specific test of long term spatial memory. During the probe trial, CCI injured mice typically perform significantly worse than sham or naïve mice, whereas sham mice showed no significant difference from naïve. Inexplicably, in the CD40L study, the injury effect was only evident in the CD40L knockout mice, which also showed superior latency to the target hole than wild type mice regardless of injury. However, with both of the actual "treatment" studies, (ARC031 and anatabine), we observed that untreated mice did show the effects of injury and treated injured mice did not differ

significantly from uninjured mice. Mice treated with ARC031 had a travel time to the target hole that was not significantly different from sham mice. Anatabine treated TBI mice showed no difference compared to their corresponding shams at all during the probe trial, indicating that long term spatial memory was rescued by its use.

Although neurobehavioral testing effectively distinguished injured and uninjured groups, as well as treated and untreated groups, it requires large group sizes and time to conduct. Although pathological examination of outcome from TBI does not require as many mice to conduct, it may require examining long timepoints after injury to see significant differences with some markers. For instance, within this body of research some of the clearest pathology data showing significant differences between treated and untreated groups with an injury effect present was within the CD40L knockout experiment. For that cohort, the brains of the mice were analyzed months after the TBI and we see a significant effect of injury on astroglial activation by GFAP in the wild type mice not seen in the CD40L knockout mice. In our ARC031 and anatabine cohorts where the brains were extracted at a two week timepoint, we failed to detect an unambiguous effect of injury. These analyses carried out by the Roskamp Institute Pathology Core team are essential to fully understanding TBI and the effects of treatment as well as validating our TBI models' clinical relevance, but do not provide a rapid method for assessing outcome.

Given the time and mice required to conduct neurobehavioral and pathological testing, and focusing on the inflammatory responses that were evident from our proteomic datasets, I explored the acute cytokine response to TBI, correlating profiles with injury severity and time post injury. The idea behind this approach was that by characterizing an acute profile of response to injury that

correlated with later demonstration of neurobehavioral dysfunction, this profile could be used as a surrogate biomarker of "response to treatment". Thus additional therapeutics could be screened in future studies by this rapid test, avoiding the necessity for the time, labor and mouse-intensive neurobehavioral studies for all but the top therapeutic candidates.

Acute mediators of inflammation after TBI may suggest a potential strategy for therapy and a time window for such therapy. We examined IL-6, IL-1B, and MCP-1 in cortical tissue at an array of acute timepoints after TBI using ELISA. IL-6 and MCP-1 showed significant effects of time after surgery, even sham surgery produced an up-regulation, though to a lesser extent than with TBI mice. A closed head injury model produced less up-regulation than sham surgery, only showing significance in one cohort at 6 hrs after injury by IL-6. These cytokines distinguish not only time after injury but injury severity as well. This suggests that the CHI model may involve distinct mechanisms of injury from CCI, and different forms and severities of head injury may require different therapeutic strategies. The results also suggest that the craniectomy administered to "sham" mice in the CCI procedure is itself a mild form of injury, consistent with previous results from other groups reporting sham surgery as a distinct brain injury (Cole et al., 2011, Xing et al., 2011). Though neurobehavioral testing is still necessary to truly validate the effectiveness of a potential therapeutic at reducing the neurobehavioral sequelae from TBI, the ability to pre-screen compounds and select the leads will accelerate the drug discovery process. Profiling the acute inflammatory response after injury may also indicate the maximum window of time available for the administration of any treatment designed to pacify this response.

Inflammatory cytokine levels peaked within 6-12 hours after injury, showing that some of the first signs of inflammation after TBI still only appear after a delay

greater than at least one hour. ARC031 and anatabine treatments showed effectiveness in neurobehavioral paradigms when applied 30 minutes after surgery, though they were apparently not acting on these markers of inflammation. Future studies may look at more latent timepoints to explore the window of time where these treatments show efficacy. Alternatively, we may also look at applying anatabine as a prophylactic. Anatabine supplementation is viable for individuals at-risk for head injury, as it is a nutraceutical. In our study, even administration 30 minutes after injury shows efficacy but previous studies of potential neuroprotective compounds have employed pre-administration schemes (Marklund et al., 2001, Noh et al., 2005).

New chemical entities (NCE) face a long, difficult route to clinical application involving large expenses that smaller organizations cannot afford on their own (Claeys and Dodd, 2011). A wealth of supporting pre-clinical data and toxicology has to be carried out, together with application submission and approval by the appropriate regulatory authority (FDA, EMEA) before entering human clinical trials; in order to pass all three phases of clinical trials, a drug must prove not only its safety, but also its efficacy in a human population (Friedman et al., 2010). ARC031's parent molecule, Nilvadipine, is known to be safe for human use as an anti-hypertensive and is currently beginning phase III clinical trials in Europe for use in Alzheimer's disease. ARC031 did show efficacy at improving motor coordination during Rotarod testing regardless of injury status, and in the Barnes maze, showed improved spatial memory in injured mice, but it failed to show a significant reduction in any cytokine response. A trend towards reduced inflammation was visible in IL-6 and MCP-1, but this did not reach statistical significance and was less pronounced than expected, thus we conclude that ARC031 may be acting through a mechanism other than NF-kB inhibition. It

remains a promising potential treatment for TBI, however, especially given that the clinical history with Nilvadipine would likely expedite ARC031's path to clinical application. More potent inhibitors of NF-kB dependent transcription and Aβ production may also offer therapeutic benefits after TBI. The dietary supplement anatabine is not burdened by the same restrictions as pharmacological compounds. Rigorous scientific study of the effects of treatment with dietary supplementation can lead to beneficial breakthroughs with immediate public access (Hu and Cassano, 2000, Reginster et al., 2001, Shah and Shah, 2007). We have shown that treatment with anatabine starting 30 minutes after injury effectively prevents any loss of spatial memory two weeks after severe TBI. Future studies will examine the long term pathogenesis of severe TBI with and without anatabine supplementation. We will also examine the effectiveness of continuous anatabine supplementation in a model of repetitive mild head injury. Our mouse model of mild TBI demonstrates sustained neurobehavioral deficits in repetitively vs singly injured mice (Crawford pers. comm.) and other work has shown that repetitive injuries produce cumulative consequences including accelerated amyloid beta deposition and cognitive impairment in APP transgenic mice (Tg2576) (Uryu et al., 2002). Demonstrating effectiveness in our model of mild TBI would open up the possibility for application of this supplement in a wide array of situations as mild TBI is the most prevalent form of TBI and some individuals have a persistent risk of head injury (e.g. soldiers and certain athletes). Dietary modification provides a simple, safe, direct route to improving outcome that can be initiated even prior to the primary injury, if it can be anticipated. The benefit to risk ratio is very high in this situation. Just as efforts are made with improvements in helmets and safety equipment to prevent or reduce primary injury both in athletics and on the

battlefield, efforts can potentially be made to reduce second injury preemptively with dietary supplementation and modification.

These results collectively show the effectiveness of adopting a systems biology approach to finding therapeutic targets after TBI. The differential response to injury within an APOE transgenic model of TBI over timepoints spanning one day to three months provided insight to potential targets for therapeutic intervention, some of which have now been validated using neurobehavioral testing. Molecular characterization of the acute response to injury now provides markers that are known to correlate with the extent of injury and can be used to screen potential therapies at timepoints that are measured in hours instead of weeks. Future studies may examine the effects seen on lipid metabolism within our proteomic dataset, and work is currently underway at the Roskamp Institute to study the lipidomic response after TBI. The lipid content of the brain is extremely high, and disrupted lipid metabolism is implicated or involved in a host of CNS disease states ranging from Niemann-Pick diseases to bipolar disorder (Adibhatla and Hatcher, 2008). ApoE itself is a cholesterol transporter, and since outcome from brain injury is ApoE isoform-dependent, lipid metabolism is likely to be a key factor in the secondary injury process. Another likely target is Tau; as mentioned in chapter 1, phosphorylation of Tau is now known to be key in TBI pathogenesis (Liliang et al., 2010, Johnson et al., 2012) and we observed evidence of modulation of Tau related pathways in our proteomic datasets. Other possibilities include finding therapies to reduce mitochondrial damage after TBI; within our mild TBI dataset, energy metabolism was significantly modulated in both the cortex and hippocampus and glycolysis/glucogenesis was also significantly affected by injury. Previous research has shown that mitochondrial damage can result in oxidative stress and neurodegeneration after TBI (Mazzeo et al., 2009, Mustafa et al.,

2010). Our proteomic results suggest a role cellular mechanisms and functions that are supported by previous research, but also identify novel areas and provide new insights into possible targets for therapeutic intervention of TBI that have not been previously attempted. The therapeutic strategies attempted here based on our proteomic data have all shown improved outcome from TBI by various measures. Thus this work provides a foundation of pre-clinical research upon which a translational TBI program will be built.

APPENDIX A
MORRIS WATER MAZE AND BARNES MAZE VIDEOS

Chapter 1

https://vimeo.com/45337069

Password: roskamp

Chapter 2

https://vimeo.com/45337068

Password: roskamp

Abdullah L, Crynen G, Reed J, Bishop A, Phillips J, Ferguson S, Mouzon B, Mullan M, Mathura V, Mullan M (2011) Proteomic CNS Profile of Delayed Cognitive Impairment in Mice Exposed to Gulf War Agents. Neuromolecular medicine 1-14.

Abdullah L, Reed J, Kayihan G, Mathura V, Mouzon B, Mullan M, Crawford F (2009) Proteomic Analysis of Human Neuronal Cells Treated with the Gulf War Agent Pyridostigmine Bromide. J Proteomics Bioinform 2:439-444.

Adibhatla RM, Hatcher JF (2008) Altered lipid metabolism in brain injury and disorders. Subcell Biochem 49:241-268.

Aebersold R, Mann M (2003) Mass spectrometry-based proteomics. Nature 422:198-207.

Albers GW, Goldstein LB, Hall D, Lesko LM (2001) Aptiganel hydrochloride in acute ischemic stroke: a randomized controlled trial. Jama 286:2673-2682.

Allain P, Etcharry-Bouyx F, Le Gall D (2001) A case study of selective impairment of the central executive component of working memory after a focal frontal lobe damage. Brain Cogn 45:21-43.

Amor S, Puentes F, Baker D, Van Der Valk P (2010) Inflammation in neurodegenerative diseases. Immunology 129:154-169.

Ashman TA, Cantor JB, Gordon WA, Sacks A, Spielman L, Egan M, Hibbard MR (2008) A comparison of cognitive functioning in older adults with and without traumatic brain injury. J Head Trauma Rehabil 23:139-148.

Aslan A, Gurelik M, Cemek M, Goksel HM, Buyukokuroglu ME (2009) Nimodipine can improve cerebral metabolism and outcome in patients with severe head trauma. Pharmacological Research 59:120-124.

Ates O, Cayli S, Gurses I, Yucel N, Iraz M, Altinoz E, Kocak A, Yologlu S (2006) Effect of pinealectomy and melatonin replacement on morphological and biochemical recovery after traumatic brain injury. Int J Dev Neurosci 24:357-363.

Bachmeier C, Beaulieu-Abdelahad D, Mullan M, Paris D (2011) Selective dihydropyiridine compounds facilitate the clearance of beta-amyloid across the blood-brain barrier. Eur J Pharmacol 659:124-129.

Bagchi D (2008) Nutraceutical and functional food regulations in the United States and around the world: Academic Press.

Bai Z, Ye Y, Liang B, Xu F, Zhang H, Zhang Y, Peng J, Shen D, Cui Z, Zhang Z (2011) Proteomics-based identification of a group of apoptosis-related

proteins and biomarkers in gastric cancer. International journal of oncology 38:375-383.

Banchereau J, Bazan F, Blanchard D, Briere F, Galizzi JP, van Kooten C, Liu YJ, Rousset F, Saeland S (1994) The CD40 antigen and its ligand. Annu Rev Immunol 12:881-922.

Baraibar MA, Hyzewicz J, Rogowska-Wresinska A, Ladouce R, Roepstorff P, Mouly V, Friguet B (2011) Oxidative stress induced proteome alterations target different cellular pathways in human myoblasts. Free Radical Biology and Medicine.

Belkaid Y, Mendez S, Lira R, Kadambi N, Milon G, Sacks D (2000) A natural model of Leishmania major infection reveals a prolonged "silent" phase of parasite amplification in the skin before the onset of lesion formation and immunity. J Immunol 165:969-977.

Bergem AL, Lannfelt L (1997) Apolipoprotein E type epsilon4 allele, heritability and age at onset in twins with Alzheimer disease and vascular dementia. Clin Genet 52:408-413.

Bigler ED, Blatter DD, Anderson CV, Johnson SC, Gale SD, Hopkins RO, Burnett B (1997) Hippocampal volume in normal aging and traumatic brain injury. AJNR Am J Neuroradiol 18:11-23.

Brain T (1999) Rehabilitation of persons with traumatic brain injury. JAMA 282:974-983.

Brody DL, Mac Donald C, Kessens CC, Yuede C, Parsadanian M, Spinner M, Kim E, Schwetye KE, Holtzman DM, Bayly PV (2007) Electromagnetic controlled cortical impact device for precise, graded experimental traumatic brain injury. J Neurotrauma 24:657-673.

Brooks CA, Gabella B, Hoffman R, Sosin D, Whiteneck G (1997) Traumatic brain injury: designing and implementing a population-based follow-up system. Arch Phys Med Rehabil 78:S26-30.

Brouwer WH, Ponds RW, Van Wolffelaar PC, Van Zomeren AH (1989) Divided attention 5 to 10 years after severe closed head injury. Cortex 25:219-230.

Cacabelos R (2007) Pharmacogenetic basis for therapeutic optimization in Alzheimer's disease. Mol Diagn Ther 11:385-405.

Cacabelos R (2008) Influence of pharmacogenetic factors on Alzheimer's disease therapeutics. Neurodegener Dis 5:176-178.

Cacabelos R, Martinez-Bouza R (2011) Genomics and pharmacogenomics of dementia. CNS Neurosci Ther 17:566-576.

Caeyenberghs K, Leemans A, Geurts M, Vander Linden C, Smits-Engelsman BCM, Sunaert S, Swinnen SP (2011) Correlations between white matter integrity and motor function in traumatic brain injury patients. Neurorehabilitation and Neural Repair 25:492-502.

Cantu RC (2001) Posttraumatic Retrograde and Anterograde Amnesia: Pathophysiology and Implications in Grading and Safe Return to Play. J Athl Train 36:244-248.

Carbonell WS, Maris DO, McCall T, Grady MS (1998) Adaptation of the fluid percussion injury model to the mouse. J Neurotrauma 15:217-229.

Cernak I (2005) Animal models of head trauma. NeuroRx 2:410-422.

Cernak I, Merklė AC, Koliatsos VE, Bilik JM, Luong QT, Mahota TM, Xu L, Slack N, Windle D, Ahmed FA (2011) The pathobiology of blast injuries and blast-induced neurotrauma as identified using a new experimental model of injury in mice. Neurobiol Dis 41:538-551.

Cernak I, O'Connor C, Vink R (2002) Inhibition of cyclooxygenase 2 by nimesulide improves cognitive outcome more than motor outcome following diffuse traumatic brain injury in rats. Experimental brain research 147:193-199.

Cernak I, Savic J, Ignjatovic D, Jevtic M (1999) Blast injury from explosive munitions. J Trauma 47:96-103; discussion 103-104.

Cernak I, Wang Z, Jiang J, Bian X, Savic J (2001) Ultrastructural and functional characteristics of blast injury-induced neurotrauma. J Trauma 50:695-706.

Chang JW, Jeon HB, Lee JH, Yoo JS, Chun JS, Kim JH, Yoo YJ (2001) Augmented expression of peroxiredoxin I in lung cancer. Biochemical and biophysical research communications 289:507-512.

Chen G, Shi J, Qi M, Yin H, Hang C (2008) Glutamine decreases intestinal nuclear factor kappa B activity and pro-inflammatory cytokine expression after traumatic brain injury in rats. Inflammation Research 57:57-64.

Chen K, Huang J, Gong W, Zhang L, Yu P, Wang JM (2006) CD40/CD40L dyad in the inflammatory and immune responses in the central nervous system. Cell Mol Immunol 3:163-169.

Chen Y, Lomnitski L, Michaelson DM, Shohami E (1997) Motor and cognitive deficits in apolipoprotein E-deficient mice after closed head injury. Neuroscience 80:1255-1262.

Christensen DZ, Schneider-Axmann T, Lucassen PJ, Bayer TA, Wirths O (2010) Accumulation of intraneuronal Abeta correlates with ApoE4 genotype. Acta Neuropathol 119:555-566.

Claeys K, Dodd P (2011) New and Notable Medications Approved in 2010 and 2011.

Clausen F, Hanell A, Israelsson C, Hedin J, Ebendal T, Mir AK, Gram H, Marklund N (2011) Neutralization of interleukin IL-1B reduces cerebral edema and tissue loss and improves late cognitive outcome following traumatic brain injury in mice. European Journal of Neuroscience.

Cogswell JP, Godlevski MM, Wisely GB, Clay WC, Leesnitzer LM, Ways JP, Gray JG (1994) NF-kappa B regulates IL-1 beta transcription through a

consensus NF-kappa B binding site and a nonconsensus CRE-like site. The Journal of immunology 153:712-723.

Cole JT, Yarnell A, Kean WS, Gold E, Lewis B, Ren M, McMullen DC, Jacobowitz DM, Pollard HB, O'Neill JT (2011) Craniotomy: true sham for traumatic brain injury, or a sham of a sham? Journal of Neurotrauma 28:359-369.

Colicos MA, Dixon CE, Dash PK (1996) Delayed, selective neuronal death following experimental cortical impact injury in rats: possible role in memory deficits. Brain Res 739:111-119.

Coon KD, Myers AJ, Craig DW, Webster JA, Pearson JV, Lince DH, Zismann VL, Beach TG, Leung D, Bryden L, Halperin RF, Marlowe L, Kaleem M, Walker DG, Ravid R, Heward CB, Rogers J, Papassotiropoulos A, Reiman EM, Hardy J, Stephan DA (2007) A high-density whole-genome association study reveals that APOE is the major susceptibility gene for sporadic late-onset Alzheimer's disease. J Clin Psychiatry 68:613-618.

Coppens P, Delmulle L, Gulati O, Richardson D, Ruthsatz M, Sievers H, Sidani S (2006) Use of botanicals in food supplements. Annals of nutrition and metabolism 50:538-554.

Corder EH, Saunders AM, Strittmatter WJ, Schmechel DE, Gaskell PC, Small GW, Roses AD, Haines JL, Pericak-Vance MA (1993) Gene dose of apolipoprotein E type 4 allele and the risk of Alzheimer's disease in late onset families. Science 261:921-923.

Crack PJ, Gould J, Bye N, Ross S, Ali U, Habgood MD, Morganti-Kossman C, Saunders NR, Hertzog PJ (2009) The genomic profile of the cerebral cortex after closed head injury in mice: effects of minocycline. J Neural Transm 116:1-12.

Crawford F, Wood M, Ferguson S, Mathura V, Gupta P, Humphrey J, Mouzon B, Laporte V, Margenthaler E, O'Steen B, Hayes R, Roses A, Mullan M (2009) Apolipoprotein E-genotype dependent hippocampal and cortical responses to traumatic brain injury. Neuroscience 159:1349-1362.

Crawford FC, Crynen G, Reed J, Mouzon B, Bishop A, Katz B, Ferguson S, Phillips J, Ganapathi V, Mathura V (2012) Identification of plasma biomarkers of TBI outcome using proteomic approaches in an APOE mouse model. Journal of neurotrauma.

Crawford FC, Vanderploeg RD, Freeman MJ, Singh S, Waisman M, Michaels L, Abdullah L, Warden D, Lipsky R, Salazar A, Mullan MJ (2002) APOE genotype influences acquisition and recall following traumatic brain injury. Neurology 58:1115-1118.

Crawford FC, Wood M, Ferguson S, Mathura VS, Faza B, Wilson S, Fan T, O'Steen B, Ait-Ghezala G, Hayes R, Mullan MJ (2007) Genomic analysis of response to traumatic brain injury in a mouse model of Alzheimer's disease (APPsw). Brain Res 1185:45-58.

Cruz-Sanchez FF, Durany N, Thome J, Riederer P, Zambon D (2000) Correlation between Apolipoprotein-E polymorphism and Alzheimer's disease pathology. J Alzheimers Dis 2:223-229.

Cui T, Zhou X, Jin W, Zheng F, Cao X (2000) Gene polymorphism in apolipoprotein E and presenilin-1 in patients with late-onset Alzheimer's disease. Chin Med J (Engl) 113:340-344.

Deane R, Sagare A, Hamm K, Parisi M, Lane S, Finn MB, Holtzman DM, Zlokovic BV (2008) apoE isoform specific disruption of amyloid B peptide clearance from mouse brain. The Journal of clinical investigation 118:4002.

Decker MW, Majchrzak MJ, Anderson DJ (1992) Effects of nicotine on spatial memory deficits in rats with septal lesions. Brain research 572:281-285.

DeKosky ST, Abrahamson EE, Ciallella JR, Paljug WR, Wisniewski SR, Clark RS, Ikonomovic MD (2007) Association of increased cortical soluble abeta42 levels with diffuse plaques after severe brain injury in humans. Arch Neurol 64:541-544.

Demery JA, Hanlon RE, Bauer RM (2001) Profound amnesia and confabulation following traumatic brain injury. Neurocase 7:295-302.

Devaraj S, Jialal I, Vega-LÃ³pez S (2004) Plant sterol-fortified orange juice effectively lowers cholesterol levels in mildly hypercholesterolemic healthy individuals. Arteriosclerosis, thrombosis, and vascular biology 24:e25-e28.

Di Giorgio AM, Hou Y, Zhao X, Zhang B, Lyeth BG, Russell MJ (2008) Dimethyl sulfoxide provides neuroprotection in a traumatic brain injury model. Restorative neurology and neuroscience 26:501-507.

Dixon CE, Clifton GL, Lighthall JW, Yaghmai AA, Hayes RL (1991) A controlled cortical impact model of traumatic brain injury in the rat. J Neurosci Methods 39:253-262.

Dixon CE, Lyeth BG, Povlishock JT, Findling RL, Hamm RJ, Marmarou A, Young HF, Hayes RL (1987) A fluid percussion model of experimental brain injury in the rat. J Neurosurg 67:110-119.

Donadelli R, Abbate M, Zanchi C, Corna D, Tomasoni S, Benigni A, Remuzzi G, Zoja C (2000) Protein traffic activates NF-kB gene signaling and promotes MCP-1-dependent interstitial inflammation. American journal of kidney diseases 36:1226-1241.

Evans P, Persinger MA (2010) Erythropoietin and mild traumatic brain injury: Neuroprotective potential and dangerous side-effects. Journal of Biological Sciences 10:739-746.

Ezra Y, Oron L, Moskovich L, Roses AD, Beni SM, Shohami E, Michaelson DM (2003) Apolipoprotein E4 decreases whereas apolipoprotein E3 increases the level of secreted amyloid precursor protein after closed head injury. Neuroscience 121:315-325.

Fabricius M, Fuhr S, Bhatia R, Boutelle M, Hashemi P, Strong AJ, Lauritzen M (2006) Cortical spreading depression and peri-infarct depolarization in acutely injured human cerebral cortex. Brain 129:778-790.

Faden AI (2001) Neuroprotection and traumatic brain injury: the search continues. Archives of neurology 58:1553.

Faden AI, Demediuk P, Panter SS, Vink R (1989) The role of excitatory amino acids and NMDA receptors in traumatic brain injury. Science 244:798-800.

Fahlenkamp AV, Coburn M, Czaplik M, Ryang YM, Kipp M, Rossaint R, Beyer C (2012) Expression analysis of the early chemokine response 4 h after in vitro traumatic brain injury. Inflammation Research 60:379-387.

Faul M, Xu L, Wald MM, Coronado VG (2010) Traumatic brain injury in the United States: Emergency department visits, hospitalizations and deaths 2002-2006. Atlanta, GA: Centers for Disease Control and Prevention, National Center for Injury Prevention and Control.

Fee D, Crumbaugh A, Jacques T, Herdrich B, Sewell D, Auerbach D, Piaskowski S, Hart MN, Sandor M, Fabry Z (2003) Activated/effector CD4+ T cells exacerbate acute damage in the central nervous system following traumatic injury. J Neuroimmunol 136:54-66.

Ferguson S, Mouzon B, Kayihan G, Wood M, Poon F, Doore S, Mathura V, Humphrey J, O'Steen B, Hayes R, Roses A, Mullan M, Crawford F (2010) Apolipoprotein E genotype and oxidative stress response to traumatic brain injury. Neuroscience 168:811-819.

Finkelstein E, Corso PS, Miller TR (2006) The incidence and economic burden of injuries in the United States: Oxford University Press, USA.

Fischer H (2010) U.S. Military Casualty Statistics: Operation New Dawn, Operation Iraqi Freedom, and Operation Enduring Freedom In: CRS Report for Congress: Congressional Research Service.

Foda MA, Marmarou A (1994) A new model of diffuse brain injury in rats. Part II: Morphological characterization. J Neurosurg 80:301-313.

Fox GB, Fan L, Levasseur RA, Faden AI (1998a) Sustained sensory/motor and cognitive deficits with neuronal apoptosis following controlled cortical impact brain injury in the mouse. J Neurotrauma 15:599-614.

Fox GB, Fan L, LeVasseur RA, Faden AI (1998b) Effect of traumatic brain injury on mouse spatial and nonspatial learning in the Barnes circular maze. J Neurotrauma 15:1037-1046.

Franz G, Beer R, Kampfl A, Engelhardt K, Schmutzhard E, Ulmer H, Deisenhammer F (2003) Amyloid beta 1-42 and tau in cerebrospinal fluid after severe traumatic brain injury. Neurology 60:1457-1461.

Friedman G, Froom P, Sazbon L, Grinblatt I, Shochina M, Tsenter J, Babaey S, Yehuda B, Groswasser Z (1999) Apolipoprotein E-epsilon4 genotype

predicts a poor outcome in survivors of traumatic brain injury. Neurology 52:244-248.

Friedman LM, Furberg CD, DeMets DL (2010) Fundamentals of clinical trials: Springer Verlag.

Garlichs CD, Kozina S, Fateh-Moghadam S, Handschu R, Tomandl B, Stumpf C, Eskafi S, Raaz D, Schmeisser A, Yilmaz A, Ludwig J, Neundorfer B, Daniel WG (2003) Upregulation of CD40-CD40 ligand (CD154) in patients with acute cerebral ischemia. Stroke 34:1412-1418.

Gavett BE, Stern RA, Cantu RC, Nowinski CJ, McKee AC (2010) Mild traumatic brain injury: a risk factor for neurodegeneration. Alzheimers Res Ther 2:18.

Gavins FN, Li G, Russell J, Perretti M, Granger DN (2011) Microvascular thrombosis and CD40/CD40L signaling. J Thromb Haemost 9:574-581.

Gehrmann J, Mies G, Bonnekoh P, Banati R, Iijima T, Kreutzberg GW, Hossmann KA (1993) Microglial reaction in the rat cerebral cortex induced by cortical spreading depression. Brain Pathol 3:11-17.

Genis L, Chen Y, Shohami E, Michaelson DM (2000) Tau hyperphosphorylation in apolipoprotein E-deficient and control mice after closed head injury. J Neurosci Res 60:559-564.

Giovannini MG, Scali C, Prosperi C, Bellucci A, Vannucchi MG, Rosi S, Pepeu G, Casamenti F (2002) Beta-amyloid-induced inflammation and cholinergic hypofunction in the rat brain in vivo: involvement of the p38MAPK pathway. Neurobiol Dis 11:257-274.

Giza CC, Hovda DA (2001) The Neurometabolic Cascade of Concussion. J Athl Train 36:228-235.

Gohar M, Yang W, Strong W, Volkening K, Leystra-Lantz C, Strong MJ (2009) Tau phosphorylation at threonine-175 leads to fibril formation and enhanced cell death: implications for amyotrophic lateral sclerosis with cognitive impairment. J Neurochem 108:634-643.

Goldman SM, Tanner CM, Oakes D, Bhudhikanok GS, Gupta A, Langston JW (2006) Head injury and Parkinson's disease risk in twins. Ann Neurol 60:65-72.

Gong QZ, Delahunty TM, Hamm RJ, Lyeth BG (1995) Metabotropic glutamate antagonist, MCPG, treatment of traumatic brain injury in rats. Brain research 700:299-302.

Gouvier WD, Blanton PD, LaPorte KK, Nepomuceno C (1987) Reliability and validity of the Disability Rating Scale and the Levels of Cognitive Functioning Scale in monitoring recovery from severe head injury. Arch Phys Med Rehabil 68:94-97.

Graham DI, Gentleman SM, Lynch A, Roberts GW (1995) Distribution of beta-amyloid protein in the brain following severe head injury. Neuropathol Appl Neurobiol 21:27-34.

Guerrero JL, Thurman DJ, Sniezek JE (2000) Emergency department visits associated with traumatic brain injury: United States, 1995-1996. Brain Inj 14:181-186.

Gulati OP, Berry Ottaway P (2006) Legislation relating to nutraceuticals in the European Union with a particular focus on botanical-sourced products. Toxicology 221:75-87.

Guo L, LaDu MJ, Van Eldik LJ (2004) A dual role for apolipoprotein E in neuroinflammation. Journal of Molecular Neuroscience 23:205-212.

Gygi SP, Corthals GL, Zhang Y, Rochon Y, Aebersold R (2000) Evaluation of two-dimensional gel electrophoresis-based proteome analysis technology. Proceedings of the National Academy of Sciences 97:9390.

Habgood MD, Bye N, Dziegielewska KM, Ek CJ, Lane MA, Potter A, Morganti-Kossmann C, Saunders NR (2007) Changes in blood-brain barrier permeability to large and small molecules following traumatic brain injury in mice. Eur J Neurosci 25:231-238.

Hall ED, Sullivan PG, Gibson TR, Pavel KM, Thompson BM, Scheff SW (2005) Spatial and temporal characteristics of neurodegeneration after controlled cortical impact in mice: more than a focal brain injury. J Neurotrauma 22:252-265.

Hamm RJ, Dixon CE, Gbadebo DM, Singha AK, Jenkins LW, Lyeth BG, Hayes RL (1992) Cognitive deficits following traumatic brain injury produced by controlled cortical impact. J Neurotrauma 9:11-20.

Hamm RJ, Pike BR, O'Dell DM, Lyeth BG, Jenkins LW (1994) The rotarod test: an evaluation of its effectiveness in assessing motor deficits following traumatic brain injury. J Neurotrauma 11:187-196.

Hanell A, Clausen F, Bjork M, Jansson K, Philipson O, Nilsson LN, Hillered L, Weinreb PH, Lee D, McIntosh TK, Gimbel DA, Strittmatter SM, Marklund N (2010) Genetic deletion and pharmacological inhibition of Nogo-66 receptor impairs cognitive outcome after traumatic brain injury in mice. J Neurotrauma 27:1297-1309.

Hang CH, Shi J, Li J, Wu W, Yin HX (2005) Concomitant upregulation of nuclear factor-kB activity, proinflammatory cytokines and ICAM-1 in the injured brain after cortical contusion trauma in a rat model. Neurology India 53:312.

Hanninen OH, Sen OCKS (2008) Nutritional Supplements and Functional Foods: Functional Significance and Global Regulations: Academic Press.

Harrison FE, Hosseini AH, McDonald MP (2009) Endogenous anxiety and stress responses in water maze and Barnes maze spatial memory tasks. Behav Brain Res 198:247-251.

Harrison FE, Reiserer RS, Tomarken AJ, McDonald MP (2006) Spatial and nonspatial escape strategies in the Barnes maze. Learning & Memory 13:809-819.

Hart S, Fonareva I, Merluzzi N, Mohr DC (2005) Treatment for depression and its relationship to improvement in quality of life and psychological well-being in multiple sclerosis patients. Quality of life research 14:695-703.

Harting MT, Jimenez F, Adams SD, Mercer DW, Cox CS (2008) Acute, regional inflammatory response after traumatic brain injury: Implications for cellular therapy. Surgery 144:803-813.

Hartman RE, Laurer H, Longhi L, Bales KR, Paul SM, McIntosh TK, Holtzman DM (2002) Apolipoprotein E4 influences amyloid deposition but not cell loss after traumatic brain injury in a mouse model of Alzheimer's disease. J Neurosci 22:10083-10087.

Hawley CA, Ward AB, Magnay AR, Long J (2002) Children's brain injury: a postal follow-up of 525 children from one health region in the UK. Brain Inj 16:969-985.

Henn V, Slupsky JR, Grafe M, Anagnostopoulos I, Forster R, Muller-Berghaus G, Kroczek RA (1998) CD40 ligand on activated platelets triggers an inflammatory reaction of endothelial cells. Nature 391:591-594.

Hiekkanen H, Kurki T, Brandstack N, Kairisto V, Tenovuo O (2009) Association of injury severity, MRI-results and ApoE genotype with 1-year outcome in mainly mild TBI: a preliminary study. Brain Inj 23:396-402.

Hill EG, Schwacke JH, Comte-Walters S, Slate EH, Oberg AL, Eckel-Passow JE, Therneau TM, Schey KL (2008) A statistical model for iTRAQ data analysis. Journal of proteome research 7:3091-3101.

Himanen L, Portin R, Isoniemi H, Helenius H, Kurki T, Tenovuo O (2005) Cognitive functions in relation to MRI findings 30 years after traumatic brain injury. Brain Inj 19:93-100.

Hoe HS, Freeman J, Rebeck GW (2006) Apolipoprotein E decreases tau kinases and phospho-tau levels in primary neurons. Mol Neurodegener 1:18.

Horn LJ, Zasler ND (1996) Medical rehabilitation of traumatic brain injury: Hanley & Belfus.

Howard LM, Miga AJ, Vanderlugt CL, Dal Canto MC, Laman JD, Noelle RJ, Miller SD (1999) Mechanisms of immunotherapeutic intervention by anti-CD40L (CD154) antibody in an animal model of multiple sclerosis. J Clin Invest 103:281-290.

Hralova M, Mareova D, Riljak V (2011) Is Learning Ability and Spatial Memory in Rats Influenced by Single Dose of Nicotine? Prague Medical Report 112:193-204.

Hu G, Cassano PA (2000) Antioxidant nutrients and pulmonary function: the Third National Health and Nutrition Examination Survey (NHANES III). Am J Epidemiol 151:975-981.

Hunter CA, Jennings FW, Kennedy PG, Murray M (1992) Astrocyte activation correlates with cytokine production in central nervous system of

Trypanosoma brucei brucei-infected mice. Laboratory investigation; a journal of technical methods and pathology 67:635.

Ikonomidou C, Turski L (2002) Why did NMDA receptor antagonists fail clinical trials for stroke and traumatic brain injury? Lancet Neurol 1:383-386.

Ikonomovic MD, Uryu K, Abrahamson EE, Ciallella JR, Trojanowski JQ, Lee VM, Clark RS, Marion DW, Wisniewski SR, DeKosky ST (2004) Alzheimer's pathology in human temporal cortex surgically excised after severe brain injury. Exp Neurol 190:192-203.

Ishikawa M, Cooper D, Arumugam TV, Zhang JH, Nanda A, Granger DN (2004) Platelet-leukocyte-endothelial cell interactions after middle cerebral artery occlusion and reperfusion. J Cereb Blood Flow Metab 24:907-915.

Isoniemi H, Tenovuo O, Portin R, Himanen L, Kairisto V (2006) Outcome of traumatic brain injury after three decades--relationship to ApoE genotype. J Neurotrauma 23:1600-1608.

Iwasaki Y, Asai M, Yoshida M, Nigawara T, Kambayashi M, Oiso Y, Nakashima N (2004) Nilvadipine inhibits nuclear factor-Î°B-dependent transcription in hepatic cells. Clinica chimica acta 350:151-157.

Jabara H, Laouini D, Tsitsikov E, Mizoguchi E, Bhan A, Castigli E, Dedeoglu F, Pivniouk V, Brodeur S, Geha R (2002) The binding site for TRAF2 and TRAF3 but not for TRAF6 is essential for CD40-mediated immunoglobulin class switching. Immunity 17:265-276.

Jellinger KA, Paulus W, Wrocklage C, Litvan I (2001) Effects of closed traumatic brain injury and genetic factors on the development of Alzheimer's disease. Eur J Neurol 8:707-710.

Jennett B, Bond M (1975) Assessment of outcome after severe brain damage. Lancet 1:480-484.

Jiang YH, Pan Y, Zhu L, Landa L, Yoo J, Spencer C, Lorenzo I, Brilliant M, Noebels J, Beaudet AL (2010) Altered ultrasonic vocalization and impaired learning and memory in Angelman syndrome mouse model with a large maternal deletion from Ube3a to Gabrb3. PLoS One 5:e12278.

Jofre-Monseny L, de Pascual-Teresa S, Plonka E, Huebbe P, Boesch-Saadatmandi C, Minihane AM, Rimbach G (2007) Differential effects of apolipoprotein E3 and E4 on markers of oxidative status in macrophages. British Journal of Nutrition 97:864-871.

Johnson VE, Stewart W, Smith DH (2012) Widespread tau and amyloid-Beta pathology many years after a single traumatic brain injury in humans. Brain Pathol 22:142-149.

Julien R, Vinzenz G, Marybeth MF, Paige RC, Jiri A, June S, Laurent C (2011) Comparison of genomic and proteomic data in recurrent airway obstruction affected horses using ingenuity pathway analysis. BMC Veterinary Research 7:48.

Kalabalikis P, Papazoglou K, Gouriotis D, Papadopoulos N, Kardara M, Papageorgiou F, Papadatos J (1999) Correlation between serum IL-6 and CRP levels and severity of head injury in children. Intensive care medicine 25:288-292.

Kassed CA, Butler TL, Pennypacker K (2004) NF-kB and Neurotoxicity. Molecular neurotoxicology: environmental agents and transcription-transduction coupling 68.

Kawabe T, Naka T, Yoshida K, Tanaka T, Fujiwara H, Suematsu S, Yoshida N, Kishimoto T, Kikutani H (1994) The immune responses in CD40-deficient mice: impaired immunoglobulin class switching and germinal center formation. Immunity 1:167.

Kawai T, Andrews D, Colvin RB, Sachs DH, Cosimi AB (2000) Thromboembolic complications after treatment with monoclonal antibody against CD40 ligand. Nat Med 6:114.

Kay AD, Petzold A, Kerr M, Keir G, Thompson EJ, Nicoll JA (2003) Cerebrospinal fluid apolipoprotein E concentration decreases after traumatic brain injury. J Neurotrauma 20:243-250.

Kim J, Whyte J, Patel S, Avants B, Europa E, Wang J, Slattery J, Gee JC, Coslett HB, Detre JA (2010) Resting cerebral blood flow alterations in chronic traumatic brain injury: an arterial spin labeling perfusion FMRI study. J Neurotrauma 27:1399-1411.

Kinnunen KM, Greenwood R, Powell JH, Leech R, Hawkins PC, Bonnelle V, Patel MC, Counsell SJ, Sharp DJ (2011) White matter damage and cognitive impairment after traumatic brain injury. Brain 134:449-463.

Klohs J, Grafe M, Graf K, Steinbrink J, Dietrich T, Stibenz D, Bahmani P, Kronenberg G, Harms C, Endres M, Lindauer U, Greger K, Stelzer EH, Dirnagl U, Wunder A (2008) In vivo imaging of the inflammatory receptor CD40 after cerebral ischemia using a fluorescent antibody. Stroke 39:2845-2852.

Kochanek PM, Bauman RA, Long JB, Dixon CR, Jenkins LW (2009) A critical problem begging for new insight and new therapies. J Neurotrauma 26:813-814.

Koopmans G, Blokland A, van Nieuwenhuijzen P, Prickaerts J (2003) Assessment of spatial learning abilities of mice in a new circular maze. Physiol Behav 79:683-693.

Kypreos KE, van Dijk KW, van Der Zee A, Havekes LM, Zannis VI (2001) Domains of apolipoprotein E contributing to triglyceride and cholesterol homeostasis in vivo. Carboxyl-terminal region 203-299 promotes hepatic very low density lipoprotein-triglyceride secretion. J Biol Chem 276:19778-19786.

Langham J, Goldfrad C, Teasdale G, Shaw D, Rowan K (2003) Calcium channel blockers for acute traumatic brain injury. Cochrane Database Syst Rev 4.

Langlois JA, Rutland-Brown W, Wald MM (2006) The epidemiology and impact of traumatic brain injury: a brief overview. J Head Trauma Rehabil 21:375-378.

Laskowitz D, Song P, Wang H, Vitek M, Dawson HN (2010) Traumatic brain injury exacerbates neurodegenerative pathology: improvement with an apolipoprotein E-based therapeutic. Journal of neurotrauma 27:1983-1995.

Leunissen I, Coxon JP, Geurts M, Caeyenberghs K, Michiels K, Sunaert S, Swinnen SP (2012) Disturbed cortico subcortical interactions during motor task switching in traumatic brain injury. Human Brain Mapping.

Levin HS, O'Donnell VM, Grossman RG (1979) The Galveston Orientation and Amnesia Test. A practical scale to assess cognition after head injury. The Journal of nervous and mental disease 167:675.

Levine B, Black SE, Cabeza R, Sinden M, McIntosh AR, Toth JP, Tulving E, Stuss DT (1998) Episodic memory and the self in a case of isolated retrograde amnesia. Brain 121 (Pt 10):1951-1973.

Levita L, Muzzio IA (2010) Role of the hippocampus in goal-oriented tasks requiring retrieval of spatial versus non-spatial information. Neurobiol Learn Mem 93:581-588.

Lewin ICF (1992) The cost of disorders of the brain. Washington, DC: The National Foundation for the Brain.

Lighthall JW (1988) Controlled cortical impact: a new experimental brain injury model. J Neurotrauma 5:1-15.

Liliang PC, Liang CL, Lu K, Wang KW, Weng HC, Hsieh CH, Tsai YD, Chen HJ (2010) Relationship between injury severity and serum tau protein levels in traumatic brain injured rats. Resuscitation 81:1205-1208.

Lin HB, Yang XM, Li TJ, Cheng YF, Zhang HT, Xu JP (2009) Memory deficits and neurochemical changes induced by C-reactive protein in rats: implication in Alzheimerâ€™s disease. Psychopharmacology 204:705-714.

Link AJ, Eng J, Schieltz DM, Carmack E, Mize GJ, Morris DR, Garvik BM, Yates Iii JR (1999) Direct analysis of protein complexes using mass spectrometry. Nature biotechnology 17:676-682.

Lloyd E, Somera-Molina K, Van Eldik LJ, Watterson DM, Wainwright MS (2008) Suppression of acute proinflammatory cytokine and chemokine upregulation by post-injury administration of a novel small molecule improves long-term neurologic outcome in a mouse model of traumatic brain injury. J Neuroinflammation 5:28-41.

Loane DJ, Pocivavsek A, Moussa CEH, Thompson R, Matsuoka Y, Faden AI, Rebeck GW, Burns MP (2009) Amyloid precursor protein secretases as therapeutic targets for traumatic brain injury. Nature medicine 15:377-379.

Loane DJ, Washington PM, Vardanian L, Pocivavsek A, Hoe HS, Duff KE, Cernak I, Rebeck GW, Faden AI, Burns MP (2011) Modulation of ABCA1 by an

LXR agonist reduces beta-amyloid levels and improves outcome after traumatic brain injury. Journal of Neurotrauma 28:225-236.

Long JB, Bentley TL, Wessner KA, Cerone C, Sweeney S, Bauman RA (2009) Blast overpressure in rats: recreating a battlefield injury in the laboratory. J Neurotrauma 26:827-840.

Lu D, Mahmood A, Qu C, Goussev A, Schallert T, Chopp M (2005) Erythropoietin enhances neurogenesis and restores spatial memory in rats after traumatic brain injury. J Neurotrauma 22:1011-1017.

Lu J, Goh SJ, Tng PY, Deng YY, Ling EA, Moochhala S (2009) Systemic inflammatory response following acute traumatic brain injury. Frontiers in bioscience: a journal and virtual library 14:3795.

Maas AI, Stocchetti N, Bullock R (2008) Moderate and severe traumatic brain injury in adults. Lancet Neurol 7:728-741.

Mach F, Schonbeck U, Sukhova GK, Atkinson E, Libby P (1998) Reduction of atherosclerosis in mice by inhibition of CD40 signalling. Nature 394:200-203.

Magee PJ, Raschke M, Steiner C, Duffin JG, Pool-Zobel BL, Jokela T, Wahala K, Rowland IR (2006) Equol: a comparison of the effects of the racemic compound with that of the purified S-enantiomer on the growth, invasion, and DNA integrity of breast and prostate cells in vitro. Nutrition and cancer 54:232-242.

Malinin NL, Boldin MP, Kovalenko AV, Wallach D (1997) MAP3K-related kinase involved in NF-kB induction by TNF, CD95 and IL-1.

Mangels JA, Craik FI, Levine B, Schwartz ML, Stuss DT (2002) Effects of divided attention on episodic memory in chronic traumatic brain injury: a function of severity and strategy. Neuropsychologia 40:2369-2385.

Marchione M (2012.) High cost of care becomes cancer's burden. In: USA Today.

Marklund N, Clausen F, Lewen A, Hovda DA, Olsson Y, Hillered L (2001) alpha±-phenyl-tert-N-butyl nitrone (PBN) improves functional and morphological outcome after cortical contusion injury in the rat. Acta neurochirurgica 143:73-81.

Markowitsch HJ, Calabrese P, Liess J, Haupts M, Durwen HF, Gehlen W (1993) Retrograde amnesia after traumatic injury of the fronto-temporal cortex. J Neurol Neurosurg Psychiatry 56:988-992.

Masliah E, Roberts ES, Langford D, Everall I, Crews L, Adame A, Rockenstein E, Fox HS (2004) Patterns of gene dysregulation in the frontal cortex of patients with HIV encephalitis. Journal of neuroimmunology 157:163-175.

Matsusaka T, Fujikawa K, Nishio Y, Mukaida N, Matsushima K, Kishimoto T, Akira S (1993) Transcription factors NF-IL6 and NF-kappa B synergistically activate transcription of the inflammatory cytokines, interleukin 6 and interleukin 8. Proceedings of the National Academy of Sciences 90:10193.

Mazzeo AT, Beat A, Singh A, Bullock MR (2009) The role of mitochondrial transition pore, and its modulation, in traumatic brain injury and delayed neurodegeneration after TBI. Exp Neurol 218:363-370.

McCall JM, Hoffman E, Nagaraju K (2009) Non-hormonal steroid modulators on NF-kB for treatment of disease. (USPTO, ed) USA: WO/2009/155,056.

McDowell S, Whyte J, D'Esposito M (1997) Working memory impairments in traumatic brain injury: evidence from a dual-task paradigm. Neuropsychologia 35:1341-1353.

McIntosh TK, Garde E, Saatman KE, Smith DH (1997) Central nervous system resuscitation. Emerg Med Clin North Am 15:527-550.

McIntosh TK, Vink R, Noble L, Yamakami I, Fernyak S, Soares H, Faden AL (1989) Traumatic brain injury in the rat: characterization of a lateral fluid-percussion model. Neuroscience 28:233-244.

McKee AC, Cantu RC, Nowinski CJ, Hedley-Whyte ET, Gavett BE, Budson AE, Santini VE, Lee HS, Kubilus CA, Stern RA (2009) Chronic traumatic encephalopathy in athletes: progressive tauopathy after repetitive head injury. J Neuropathol Exp Neurol 68:709-735.

Methia N, Andre P, Hafezi-Moghadam A, Economopoulos M, Thomas KL, Wagner DD (2001) ApoE deficiency compromises the blood brain barrier especially after injury. Mol Med 7:810-815.

Monaco C, Andreakos E, Young S, Feldmann M, Paleolog E (2002) T cell-mediated signaling to vascular endothelium: induction of cytokines, chemokines, and tissue factor. J Leukoc Biol 71:659-668.

Millerot-Serrurot E, Chausset A, Mossiat C, Prigent-Tessier A, Bertrand N, Garnier P, Beley A, Marie C (2007) Effect of early decrease in the lesion size on late brain tissue loss, synaptophysin expression and functionality after a focal brain lesion in rats. Neurochem Int 50:328-335.

Morganti-Kossmann MC, Rancan M, Otto VI, Stahel PF, Kossmann T (2001) Role of cerebral inflammation after traumatic brain injury: a revisited concept. Shock 16:165-177.

Morganti-Kossmann MC, Rancan M, Stahel PF, Kossmann T (2002) Inflammatory response in acute traumatic brain injury: a double-edged sword. Current opinion in critical care 8:101.

Morris R (1984) Developments of a water-maze procedure for studying spatial learning in the rat. J Neurosci Methods 11:47-60.

Morris S, Ridley S, Lecky FE, Munro V, Christensen MC (2008) Determinants of hospital costs associated with traumatic brain injury in England and Wales. Anaesthesia 63:499-508.

Muir KW, Teal PA (2005) Why have neuroprotectants failed? Journal of neurology 252:1011-1020.

Murakami N, Yamaki T, Iwamoto Y, Sakakibara T, Kobori N, Fushiki S, Ueda S (1998) Experimental brain injury induces expression of amyloid precursor protein, which may be related to neuronal loss in the hippocampus. J Neurotrauma 15:993-1003.

Mustafa AG, Singh IN, Wang J, Carrico KM, Hall ED (2010) Mitochondrial protection after traumatic brain injury by scavenging lipid peroxyl radicals. J Neurochem 114:271-280.

Narayan RK, Michel ME, Ansell B, Baethmann A, Biegon A, Bracken MB, Bullock MR, Choi SC, Clifton GL, Contant CF, Coplin WM, Dietrich WD, Ghajar J, Grady SM, Grossman RG, Hall ED, Heetderks W, Hovda DA, Jallo J, Katz RL, Knoller N, Kochanek PM, Maas AI, Majde J, Marion DW, Marmarou A, Marshall LF, McIntosh TK, Miller E, Mohberg N, Muizelaar JP, Pitts LH, Quinn P, Riesenfeld G, Robertson CS, Strauss KI, Teasdale G, Temkin N, Tuma R, Wade C, Walker MD, Weinrich M, Whyte J, Wilberger J, Young AB, Yurkewicz L (2002) Clinical trials in head injury. J Neurotrauma 19:503-557.

Neistadt ME (1994) The effects of different treatment activities on functional fine motor coordination in adults with brain injury. Am J Occup Ther 48:877-882.

Nemetz PN, Leibson C, Naessens JM, Beard M, Kokmen E, Annegers JF, Kurland LT (1999) Traumatic brain injury and time to onset of Alzheimer's disease: a population-based study. Am J Epidemiol 149:32-40.

Nimmo AJ, Cernak I, Heath DL, Hu X, Bennett CJ, Vink R (2004) Neurogenic inflammation is associated with development of edema and functional deficits following traumatic brain injury in rats. Neuropeptides 38:40-47.

Noh HS, Kang SS, Kim DW, Kim YH, Park CH, Han JY, Cho GJ, Choi WS (2005) Ketogenic diet increases calbindin-D< sub> 28k</sub> in the hippocampi of male ICR mice with kainic acid seizures. Epilepsy research 65:153-159.

Nonaka M, Chen XH, Pierce JE, Leoni MJ, McIntosh TK, Wolf JA, Smith DH (1999a) Prolonged activation of NF-kappaB following traumatic brain injury in rats. J Neurotrauma 16:1023-1034.

Nonaka M, Chen XHAN, Pierce JES, Leoni MJ, McIntosh TK, Wolf JA, Smith DH (1999b) Prolonged activation of NF-Î°B following traumatic brain injury in rats. Journal of Neurotrauma 16:1023-1034.

Obrenovitch TP, Urenjak J (1997) Is high extracellular glutamate the key to excitotoxicity in traumatic brain injury? Journal of neurotrauma 14:677-698.

Olesen SP (1987) Leakiness of rat brain microvessels to fluorescent probes following craniotomy. Acta physiologica scandinavica 130:63-68.

Olsson A, Csajbok L, Ost M, Hoglund K, Nylen K, Rosengren L, Nellgard B, Blennow K (2004) Marked increase of beta-amyloid(1-42) and amyloid precursor protein in ventricular cerebrospinal fluid after severe traumatic brain injury. Journal of neurology 251:870-876.

Omari KM, Dorovini-Zis K (2003) CD40 expressed by human brain endothelial cells regulates CD4+ T cell adhesion to endothelium. J Neuroimmunol 134:166-178.

Ost M, Nylen K, Csajbok L, Ohrfelt AO, Tullberg M, Wikkelso C, Nellgard P, Rosengren L, Blennow K, Nellgard B (2006) Initial CSF total tau correlates with 1-year outcome in patients with traumatic brain injury. Neurology 67:1600-1604.

Palmer AM, Marion DW, Botscheller ML, Swedlow PE, Styren SD, DeKosky ST (1993) Traumatic Brain Injury• Induced Excitotoxicity Assessed in a Controlled Cortical Impact Model. Journal of neurochemistry 61:2015-2024.

Paris D, Beaulieu-Abdelahad D, Bachmeier C, Reed J, Ait-Ghezala G, Bishop A, Chao J, Mathura V, Crawford F, Mullan M (2011) Anatabine lowers Alzheimer's Ab production in vitro and in vivo. European journal of pharmacology.

Paris D, Bachmeier C, Patel N, Quadros A, Volmar CH, Laporte V, Ganey J, Beaulieu-Abdelahad D, Ait-Ghezala G, Crawford F, Mullan MJ (2011) Selective antihypertensive dihydropyridines lower Abeta accumulation by targeting both the production and the clearance of Abeta across the blood-brain barrier. Molecular medicine 17:149-162.

Paris D, Patel N, Quadros A, Linan M, Bakshi P, Ait-Ghezala G, Mullan M (2007) Inhibition of A [beta] production by NF-[kappa] B inhibitors. Neuroscience letters 415:11-16.

Park NW, Moscovitch M, Robertson IH (1999) Divided attention impairments after traumatic brain injury. Neuropsychologia 37:1119-1133.

Patil SS, Sunyer B, Hoger H, Lubec G (2009) Evaluation of spatial memory of C57BL/6J and CD1 mice in the Barnes maze, the Multiple T-maze and in the Morris water maze. Behav Brain Res 198:58-68.

Petitto JM, Huang Z, Hartemink DA, Beck R (2002) IL-2/15 receptor-[beta] gene deletion alters neurobehavioral performance. Brain research 929:218-225.

Ponomarev ED, Shriver LP, Dittel BN (2006) CD40 expression by microglial cells is required for their completion of a two-step activation process during central nervous system autoimmune inflammation. J Immunol 176:1402-1410.

Ponsford J, McLaren A, Schonberger M, Burke R, Rudzki D, Olver J, Ponsford M (2011) The association between apolipoprotein E and traumatic brain injury severity and functional outcome in a rehabilitation sample. J Neurotrauma 28:1683-1692.

Raby CA, Morganti-Kossmann MC, Kossmann T, Stahel PF, Watson MD, Evans LM, Mehta PD, Spiegel K, Kuo YM, Roher AE (1998) Traumatic Brain Injury Increases beta• Amyloid Peptide 1-42 in Cerebrospinal Fluid. Journal of neurochemistry 71:2505-2509.

Raghavendra Rao VL, Dogan A, Todd KG, Bowen KK, Dempsey RJ (2001) Neuroprotection by memantine, a non-competitive NMDA receptor antagonist after traumatic brain injury in rats. Brain research 911:96-100.

Ramlackhansingh AF, Brooks DJ, Greenwood RJ, Bose SK, Turkheimer FE, Kinnunen KM, Gentleman S, Heckemann RA, Gunanayagam K, Gelosa G (2011) Inflammation after trauma: microglial activation and traumatic brain injury. Annals of neurology.

Rapoport M, Wolf U, Herrmann N, Kiss A, Shammi P, Reis M, Phillips A, Feinstein A (2008) Traumatic Brain Injury, Apolipoprotein E-4, and Cognition in Older Adults: A Two-Year Longitudinal Study. The Journal of neuropsychiatry and clinical neurosciences 20:68-73.

Rasmusson DX, Brandt J, Martin DB, Folstein MF (1995) Head injury as a risk factor in Alzheimer's disease. Brain Inj 9:213-219.

Reginster JY, Deroisy R, Rovati LC, Lee RL, Lejeune E, Bruyere O, Giacovelli G, Henrotin Y, Dacre JE, Gossett C (2001) Long-term effects of glucosamine sulphate on osteoarthritis progression: a randomised, placebo-controlled clinical trial. Lancet 357:251-256.

Roberts GW, Gentleman SM, Lynch A, Murray L, Landon M, Graham DI (1994) Beta amyloid protein deposition in the brain after severe head injury: implications for the pathogenesis of Alzheimer's disease. Journal of Neurology, Neurosurgery & Psychiatry 57:419-425.

Rogers J, Lue LF (2001) Microglial chemotaxis, activation, and phagocytosis of amyloid [beta]-peptide as linked phenomena in Alzheimer's disease. Neurochemistry international 39:333-340.

Ross PL, Huang YN, Marchese JN, Williamson B, Parker K, Hattan S, Khainovski N, Pillai S, Dey S, Daniels S (2004) Multiplexed protein quantitation in Saccharomyces cerevisiae using amine-reactive isobaric tagging reagents. Molecular & Cellular Proteomics 3:1154-1169.

Rothe M, Sarma V, Dixit VM, Goeddel DV (1995) TRAF2-mediated activation of NF-kappa B by TNF receptor 2 and CD40. Science 269:1424-1427.

Sabo T, Lomnitski L, Nyska A, Beni S, Maronpot RR, Shohami E, Roses AD, Michaelson DM (2000) Susceptibility of transgenic mice expressing human apolipoprotein E to closed head injury: the allele E3 is neuroprotective whereas E4 increases fatalities. Neuroscience 101:879-884.

Saljo A, Bao F, Haglid KG, Hansson HA (2000) Blast exposure causes redistribution of phosphorylated neurofilament subunits in neurons of the adult rat brain. J Neurotrauma 17:719-726.

Salloway S, Sperling R, Gilman S, Fox NC, Blennow K, Raskind M, Sabbagh M, Honig LS, Doody R, van Dyck CH, Mulnard R, Barakos J, Gregg KM, Liu E, Lieberburg I, Schenk D, Black R, Grundman M (2009) A phase 2 multiple ascending dose trial of bapineuzumab in mild to moderate Alzheimer disease. Neurology 73:2061-2070.

Sandberg AS, Lindell G, Nordstrom-Kallstrom B, Branca RM, Danielsson KG, Dahlberg M, Larson B, Forshed J, Lehtio J (2012) Tumor proteomics by multivariate analysis on individual pathway data for characterization of vulvar cancer phenotypes. Molecular & Cellular Proteomics.

Sandhir R, Puri V, Klein RM, Berman NEJ (2004) Differential expression of cytokines and chemokines during secondary neuron death following brain injury in old and young mice. Neuroscience letters 369:28-32.

Sanz O, Acarin L, GonzÃ¡lez B, Castellano B (2002) NFkB and IkB-alpha expression following traumatic brain injury to the immature rat brain. Journal of neuroscience research 67:772-780.

Scheff SW, Baldwin SA, Brown RW, Kraemer PJ (1997) Morris water maze deficits in rats following traumatic brain injury: lateral controlled cortical impact. J Neurotrauma 14:615-627.

Seder DB, Schmidt JM, Badjatia N, Fernandez L, Rincon F, Claassen J, Gordon E, Carrera E, Kurtz P, Lee K (2011) Transdermal nicotine replacement therapy in cigarette smokers with acute subarachnoid hemorrhage. Neurocritical care 14:77-83.

Semple BD, Bye N, Rancan M, Ziebell JM, Morganti-Kossmann MC (2009) Role of CCL2 (MCP-1) in traumatic brain injury (TBI): evidence from severe TBI patients and CCL2â^'/â^' mice. Journal of Cerebral Blood Flow & Metabolism 30:769-782.

Serradj N, Jamon M (2007) Age-related changes in the motricity of the inbred mice strains 129/sv and C57BL/6j. Behav Brain Res 177:80-89.

Shah P, Shah V (2007) Arginine supplementation for prevention of necrotising enterocolitis in preterm infants. Cochrane Database Syst Rev CD004339.

Shanker T (2007) Iraqi bombers thwart efforts to shield G.I.s. In: New York Times, p 1.

Shiino A, Matsuda M, Susumu T, Handa J (1991) Effects of the calcium antagonist nilvadipine on focal cerebral ischemia in spontaneously hypertensive rats. Surgical neurology 35:105-110.

Singleton RH, Yan HQ, Fellows-Mayle W, Dixon CE (2010) Resveratrol attenuates behavioral impairments and reduces cortical and hippocampal loss in a rat controlled cortical impact model of traumatic brain injury. J Neurotrauma 27:1091-1099.

Skvortsov S, Jimenez CR, Knol JC, Eichberger P, Schiestl B, Debbage P, Skvortsova I, Lukas P (2011) Radioresistant head and neck squamous cell carcinoma cells: Intracellular signaling, putative biomarkers for tumor recurrences and possible therapeutic targets. Radiotherapy and Oncology.

Small BJ, Rosnick CB, Fratiglioni L, Backman L (2004) Apolipoprotein E and cognitive performance: a meta-analysis. Psychol Aging 19:592-600.

Smith C, Graham DI, Murray LS, Stewart J, Nicoll JA (2006) Association of APOE e4 and cerebrovascular pathology in traumatic brain injury. J Neurol Neurosurg Psychiatry 77:363-366.

Smith DH, Chen XH, Iwata A, Graham DI (2003) Amyloid beta accumulation in axons after traumatic brain injury in humans. J Neurosurg 98:1072-1077.

Smith DH, Nakamura M, McIntosh TK, Wang J, Rodriguez A, Chen XH, Raghupathi R, Saatman KE, Clemens J, Schmidt ML, Lee VM, Trojanowski JQ (1998) Brain trauma induces massive hippocampal neuron death linked to a surge in beta-amyloid levels in mice overexpressing mutant amyloid precursor protein. Am J Pathol 153:1005-1010.

Sosnoff JJ, Broglio SP, Ferrara MS (2008) Cognitive and motor function are associated following mild traumatic brain injury. Exp Brain Res 187:563-571.

Stahel PF, Shohami E, Younis FM, Kariya K, Otto VI, Lenzlinger PM, Grosjean MB, Eugster HP, Trentz O, Kossmann T (2000) Experimental Closed Head Injury: Analysis of Neurological Outcome, Blood-Brain Barrier Dysfunction, Intracranial Neutrophil Infiltration, and Neuronal Cell Death in Mice Deficient in Genes for Pro-Inflammatory Cytokines. Journal of Cerebral Blood Flow & Metabolism 20:369-380.

Stahel PF, Smith WR, Moore EE (2007) Role of biological modifiers regulating the immune response after trauma. Injury 38:1409-1422.

Stegmaier JC, Kirchhoff C, Bogner V, Matz M, Kanz KG, Mutschler W, Biberthaler P (2008) Dynamics of neutrophilic NF-kB translocation in relation to IL-8 mRNA expression after major trauma. Inflammation Research 57:547-554.

Strom L, Laurencikiene J, Miskiniene A, Severinson E (1999) Characterization of CD40-dependent immunoglobulin class switching. Scand J Immunol 49:523-532.

Sun SC, Ganchi PA, Ballard DW, Greene WC (1993) NF-kappa B controls expression of inhibitor I kappa B alpha: evidence for an inducible autoregulatory pathway. Science 259:1912-1915.

Suo Z, Tan J, Placzek A, Crawford F, Fang C, Mullan M (1998) Alzheimer's beta-amyloid peptides induce inflammatory cascade in human vascular cells: the roles of cytokines and CD40. Brain Res 807:110-117.

Tagliaferri F, Compagnone C, Korsic M, Servadei F, Kraus J (2006) A systematic review of brain injury epidemiology in Europe. Acta Neurochir (Wien) 148:255-268; discussion 268.

Tak PP, Firestein GS (2001) NF-kappaB: a key role in inflammatory diseases. J Clin Invest 107:7-11.

Takakura S, Furuichi Y, Yamamoto T, Ogawa T, Satoh H, Mori J (1994) Effect of nilvadipine on the development of neurological deficits in stroke-prone spontaneously hypertensive rats. Stroke 25:677-682.

Takeuchi J, Hirota K, Itoh T, Shinkura R, Kitada K, Yodoi J, Namba T, Fukuda K (2000) Thioredoxin Inhibits Tumor Necrosis Factor-or Interleukin-1-Induced NF-kB Activation at a Level Upstream of NF-kB-Inducing Kinase. Antioxidants & redox signaling 2:83-92.

Talving P, Lustenberger T, Kobayashi L, Inaba K, Barmparas G, Schnuriger B, Lam L, Chan LS, Demetriades D (2010) Erythropoiesis stimulating agent administration improves survival after severe traumatic brain injury: a matched case control study. Ann Surg 251:1-4.

Tan J, Town T, Crawford F, Mori T, DelleDonne A, Crescentini R, Obregon D, Flavell RA, Mullan MJ (2002) Role of CD40 ligand in amyloidosis in transgenic Alzheimer's mice. Nat Neurosci 5:1288-1293.

Tan J, Town T, Paris D, Mori T, Suo Z, Crawford F, Mattson MP, Flavell RA, Mullan M (1999) Microglial activation resulting from CD40-CD40L interaction after beta-amyloid stimulation. Science 286:2352-2355.

Tasker RC, Salmond CH, Westland AG, Pena A, Gillard JH, Sahakian BJ, Pickard JD (2005) Head circumference and brain and hippocampal volume after severe traumatic brain injury in childhood. Pediatr Res 58:302-308.

Teasdale G, Jennett B (1976) Assessment and prognosis of coma after head injury. Acta Neurochir (Wien) 34:45-55.

Tennant A (2005) Admission to hospital following head injury in England: incidence and socio-economic associations. BMC Public Health 5:21.

Thurman DJ (1999) Traumatic brain injury in the United States: A report to Congress: Centers for Disease Control and Prevention.

To AWM, Ribe EM, Chuang TT, Schroeder JE, Lovestone S (2011) The E3 and E4 Alleles of Human APOE Differentially Affect Tau Phosphorylation in Hyperinsulinemic and Pioglitazone Treated Mice. PloS one 6:e16991.

Tolonen A, Turkka J, Salonen O, Ahoniemi E, Alaranta H (2007) Traumatic brain injury is under-diagnosed in patients with spinal cord injury. Journal of Rehabilitation Medicine 39:622-626.

Tortarolo M, Veglianese P, Calvaresi N, Botturi A, Rossi C, Giorgini A, Migheli A, Bendotti C (2003) Persistent activation of p38 mitogen-activated protein kinase in a mouse model of familial amyotrophic lateral sclerosis correlates with disease progression. Mol Cell Neurosci 23:180-192.

Townsend KP, Town T, Mori T, Lue LF, Shytle D, Sanberg PR, Morgan D, Fernandez F, Flavell RA, Tan J (2005) CD40 signaling regulates innate and adaptive activation of microglia in response to amyloid beta-peptide. Eur J Immunol 35:901-910.

Tran HT, LaFerla FM, Holtzman DM, Brody DL (2011) Controlled cortical impact traumatic brain injury in 3xTg-AD mice causes acute intra-axonal amyloid-beta accumulation and independently accelerates the development of tau abnormalities. J Neurosci 31:9513-9525.

Uryu K, Laurer H, McIntosh T, Pratico D, Martinez D, Leight S, Lee VM, Trojanowski JQ (2002) Repetitive mild brain trauma accelerates Abeta deposition, lipid peroxidation, and cognitive impairment in a transgenic mouse model of Alzheimer amyloidosis. J Neurosci 22:446-454.

Utagawa A, Truettner JS, Dietrich WD, Bramlett HM (2008) Systemic inflammation exacerbates behavioral and histopathological consequences of isolated traumatic brain injury in rats. Experimental neurology 211:283-291.

Valadka AB, Gopinath SP, Robertson CS (2000) Midline shift after severe head injury: pathophysiologic implications. J Trauma 49:1-8; discussion 8-10.

Van der Linden M, Coyette F, Seron X (1992) Selective impairment of the â€œcentral executiveâ€• component of working memory: A single case study. Cognitive Neuropsychology 9:301-326.

van Kooten C, Banchereau J (2000) CD40-CD40 ligand. J Leukoc Biol 67:2-17.

Veltman JA, Gaillard AW (1996) Physiological indices of workload in a simulated flight task. Biol Psychol 42:323-342.

Verbois SL, Hopkins DM, Scheff SW, Pauly JR (2003) Chronic intermittent nicotine administration attenuates traumatic brain injury-induced cognitive dysfunction. Neuroscience 119:1199-1208.

Vergouwen MDI, Vermeulen M, Roos YB (2006) Effect of nimodipine on outcome in patients with traumatic subarachnoid haemorrhage: a systematic review. The Lancet Neurology 5:1029-1032.

von Reyn CR, Mott RE, Siman R, Smith DH, Meaney DF (2012) Mechanisms of calpain mediated proteolysis of voltage gated sodium channel Î±â€• subunits following in vitro dynamic stretch injury. Journal of Neurochemistry.

Wang X, Huang W, Schiffer LE, Mihara M, Akkerman A, Hiromatsu K, Davidson A (2003) Effects of anti-CD154 treatment on B cells in murine systemic lupus erythematosus. Arthritis Rheum 48:495-506.

Werner C, Engelhard K (2007) Pathophysiology of traumatic brain injury. Br J Anaesth 99:4-9.

Whiting MD, Baranova AI, Hamm RJ (2006) Cognitive Impairment following Traumatic Brain Injury.

Williams AJ, Wei HH, Dave JR, Tortella FC (2007) Acute and delayed neuroinflammatory response following experimental penetrating ballistic brain injury in the rat. J Neuroinflammation 4:17.

Wu A, Ying Z, Gomez-Pinilla F (2006) Dietary curcumin counteracts the outcome of traumatic brain injury on oxidative stress, synaptic plasticity, and cognition. Experimental neurology 197:309-317.

Wu T, Zhao H, Spratt H, Kurosky A, Wu B, Williams K (2005) Proteomics and the analysis of proteomic data: an overview of current protein-profiling technologies. Current Protocols in Bioinformatics 13:1-13.11.

Wu Z, Doondeea JB, Gholami AM, Janning MC, Lemeer S, Kramer K, Eccles SA, Gollin SM, Grenman R, Walch A (2011) Quantitative chemical proteomics reveals new potential drug targets in head and neck cancer. Molecular & Cellular Proteomics 10.

Xing G, Ren M, O'Neill JT, Watson WD, Verma A (2011) Controlled cortical impact injury and craniotomy result in divergent alterations of pyruvate metabolizing enzymes in rat brain. Experimental Neurology.

Xiong Y, Gu Q, Peterson PL, Muizelaar JP, Lee CP (1997) Mitochondrial dysfunction and calcium perturbation induced by traumatic brain injury. J Neurotrauma 14:23-34.

Xu J, Foy TM, Laman JD, Elliott EA, Dunn JJ, Waldschmidt TJ, Elsemore J, Noelle RJ, Flavell RA (1994) Mice deficient for the CD40 ligand. Immunity 1:423-431.

Xu PT, Schmechel D, Rothrock-Christian T, Burkhart DS, Qiu HL, Popko B, Sullivan P, Maeda N, Saunders AM, Roses AD, Gilbert JR (1996) Human apolipoprotein E2, E3, and E4 isoform-specific transgenic mice: human-like pattern of glial and neuronal immunoreactivity in central nervous system not observed in wild-type mice. Neurobiol Dis 3:229-245.

Yamamoto K, Miyoshi T, Yae T, Kawashima K, Araki H, Hanada K, Otero DAC, Roch JM, Saitoh T (1994) The survival of rat cerebral cortical neurons in the presence of trophic APP peptides. Journal of neurobiology 25:585-594.

Yao Y, Bennett BJ, Wang X, Rosenfeld ME, Giachelli C, Lusis AJ, Bostrom KI (2010) Inhibition of bone morphogenetic proteins protects against atherosclerosis and vascular calcification. Circ Res 107:485-494.

Ye S, Huang Y, Mullendorff K, Dong L, Giedt G, Meng EC, Cohen FE, Kuntz ID, Weisgraber KH, Mahley RW (2005) Apolipoprotein (apo) E4 enhances amyloid b peptide production in cultured neuronal cells: ApoE structure as a potential therapeutic target. Proceedings of the National Academy of Sciences of the United States of America 102:18700.

Yi JH, Park SW, Brooks N, Lang BT, Vemuganti R (2008) PPAR [gamma] agonist rosiglitazone is neuroprotective after traumatic brain injury via anti-inflammatory and anti-oxidative mechanisms. Brain research 1244:164-172.

Zaloshnja E, Miller T, Langlois JA, Selassie AW (2008) Prevalence of long-term disability from traumatic brain injury in the civilian population of the United States, 2005. The Journal of head trauma rehabilitation 23:394.

Zhang J (2005) Experimental therapies for cerebral vascular diseases. Neurological Research 27:227-228.

Zhang J, Li Q, Nguyen TD, Tremblay TL, Stone E, To R, Kelly J, Roger MacKenzie C (2004) A pentavalent single-domain antibody approach to

tumor antigen discovery and the development of novel proteomics reagents. Journal of molecular biology 341:161-169.

Zhou W, Xu D, Peng X, Zhang Q, Jia J, Crutcher KA (2008) Meta-analysis of APOE4 allele and outcome after traumatic brain injury. J Neurotrauma 25:279-290.

Zhu ZF, Wang QG, Han BJ, William CP (2010) Neuroprotective effect and cognitive outcome of chronic lithium on traumatic brain injury in mice. Brain Res Bull 83:272-277.